On the expression, function and regulation of the murine Ifit family of antiviral RNA-binding proteins.

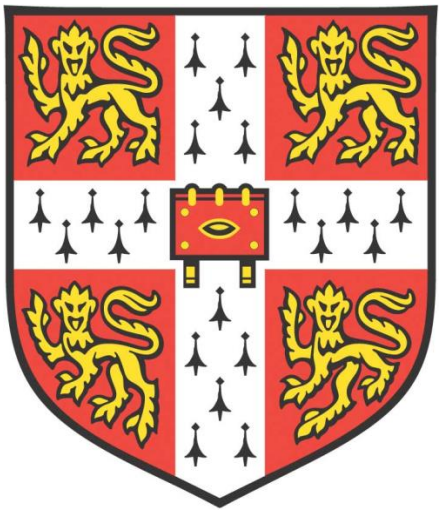

Harriet Victoria Mears

Clare College

Division of Virology

Department of Pathology

University of Cambridge

This dissertation is submitted for the degree of Doctor of Philosophy

September 2019

This thesis is dedicated to my mum, Helen

DECLARATION

This thesis is the result of my own work and includes nothing which is the outcome of work done in collaboration except as declared in the Preface and specified in the text. It is not substantially the same as any that I have submitted, or, is being concurrently submitted for a degree or diploma or other qualification at the University of Cambridge or any other University or similar institution except as declared in the Preface and specified in the text. I further state that no substantial part of my dissertation has already been submitted, or, is being concurrently submitted for any such degree, diploma or other qualification at the University of Cambridge or any other University or similar institution except as declared in the Preface and specified in the text.

The work on human IFIT complexes presented in Chapter 3 was performed in collaboration with Dr Renata Fleith, with some experiments performed by Dr Trevor Sweeney and Xin Yun Leong. Their data are included as appendices. Only experiments performed by myself are included in the main text. Chapter 3 forms the basis of the following publication:

Renata C. Fleith*, Harriet V. Mears*, Xin Yun Leong, Thomas J. Sanford, Edward Emmott, Stephen C. Graham, Daniel S. Mansur, Trevor R. Sweeney. (2018) IFIT3 and IFIT2/3 promote IFIT1-mediated translation inhibition by enhancing binding to non-self RNAs. *Nucleic Acids Res*, 46(10):5269-5285. *Co-first author.

This thesis consists of approximately 51,000 words and 55 display items. It does not exceed the prescribed word limit for the relevant Degree Committee.

ABSTRACT

IFIT proteins are highly expressed as part of the cell-intrinsic immune response following viral infection. In humans, IFIT1 inhibits translation at the initiation stage by binding directly to the 5' terminus of foreign RNA, precluding the recruitment of the cap-binding translation initiation factor complex, eIF4F. IFIT1 is highly specific for 'non-self' RNA, which lacks methylation on the first and second cap-proximal nucleotides (cap0), but at high concentrations may also restrict 'self' cap1 translation. Knock-out mouse models have been extensively used to study IFIT antiviral activity and, more recently, vaccines based on the antiviral activity of IFIT1 have been trialled for efficacy in mice. However, it is becoming clear that there are differences in murine and human IFIT function and regulation, which impacts the interpretation of these models. Mice lack a true orthologue of IFIT1 and instead the closely-related Ifit1b has been duplicated twice, yielding three paralogues: Ifit1, Ifit1b and Ifit1c. Murine Ifit1, like human IFIT1, can bind to cap0 RNA and inhibit its translation, but lacks cap1 binding activity. Ifit1b and Ifit1c are closely related to Ifit1 and share many of the residues critical for RNA-binding, but their precise functions are unknown.

In this thesis, the expression of the entire murine Ifit family was examined in different mouse cell lines, validating expression of Ifit1b and Ifit1c following interferon stimulation. The murine Ifit family was then recombinantly expressed and purified, allowing biochemical characterisation. It was discovered that Ifit1b, a previously uncharacterised protein, preferentially inhibited the translation of cap1 mRNA, while cap0 and cap2 mRNAs were inhibited to a much lesser extent. Specific cap1 binding allows Ifit1b to inhibit a proportion of cellular translation and block translation of murine hepatitis virus, a cap1 coronavirus. However, both Ifit1 and Ifit1b were incapable of inhibiting translation from a more structured Zika virus reporter mRNA. The same reporter was effectively inhibited by human IFIT1, highlighting a key difference between the activities of human and murine IFIT proteins.

IFIT proteins are known to form both homo- and hetero-oligomers, but the functional significance of these interactions is unclear. Here, interaction between human IFIT1 and IFIT3 was shown to increase the stability of both proteins and stimulate translation inhibition by IFIT1. IFIT1 and IFIT3 interacted via a C-terminal YxxxL motif, and disruption of this motif in either protein abolished the cofactor activity of IFIT3, both *in vitro* and in

cells. In mice, Ifit3 is truncated and lacks the YxxxL motif, thus precluding interaction with murine Ifit1. However, this motif is maintained in Ifit1, Ifit1b and Ifit1c, which were found to interact with one-another *in vitro*. Interaction between murine Ifit proteins increased their stability and Ifit1c enhanced translation inhibition by Ifit1 and Ifit1b *in vitro*, thereby acting analogously to human IFIT3.

Together this work provides a better understanding of the function and regulation of murine Ifit proteins, to aid interpretation and improvement of mouse models in studying the role of IFIT proteins in the antiviral response.

ACKNOWLEDGEMENTS

I would first like to thank my supervisor Trevor Sweeney for his support and guidance over the last four years. It's been a real adventure.

The Sweeney lab and the division of Virology have been amazing places to work. I have made so many friends here, who were always happy to discuss both the scientific and the silly, and generally make my life better. I especially need to acknowledge Thomas Sanford, who started his PhD at the same time as me in Trevor's lab and has been there for me throughout. I'm so lucky to have such a good friend to accompany me on this journey and I will miss our tea and biscuits keenly. Likewise Renata Fleith, who lived and worked with me for a full year, continues to be a great source of support and friendship.

Thanks go to everyone else who has contributed to this work. Ed Emmott took me under his wing when I first started and continues to be one of the most generous and kind people I know. I am especially thankful to Stephen Graham for all his guidance and his endless patience with me in my ventures into biophysics. Chris, Laura, Hazel and Yaz were always happy to give me advice and they made the difficult times seem a lot easier. Many other members of the division have helped me with different techniques, reagents and friendships, and I'm very grateful to them as well. I also need to thank the Department of Pathology for funding my studentship and giving me this opportunity.

Finally, I wouldn't be anywhere without the support of my family. I've had so many ups and downs and could always rely on my big sisters to pick me up. My partner Dave has kept me going, made me smile and reminded me that, no matter how hard things seem, his job is definitely tougher than mine. Special thanks go to my mum, Helen, for gifting me my curiosity and for always believing in me.

CONTENTS

LIST OF TABLES

List of Figures

List of Abbreviations and Acronyms

ARE, adenylate-uridylate-rich element

Bcl-2, B cell lymphoma 2

CBC, cap-binding complex

CCL, chemokine ligand

CT, cycle threshold

CTD, C-terminal domain

DENV, dengue virus

DHX, DEAH-box helicase

DNA, deoxyribonucleic acid

ds, double-stranded

eIF, eukaryotic translation initiation factor

EMCV, encephalomyocarditis virus

Fluc, firefly luciferase

GAS, gamma-interferon activation sites

GTP, guanosine triphosphate

HCV, hepatitis C virus

HuCoV, human coronavirus

IFIT, interferon-induced protein with tetratricopeptide repeats

IFN, interferon

IFNAR, interferon alpha receptor

IL, interleukin

IRES, internal ribosome entry site

IRF, interferon regulatory factor

ISG, interferon stimulated gene

ISGF3, interferon stimulated gene factor 3

ISRE, interferon simulated response element

JAK1, Janus kinase 1

LPS, lipopolysaccharide

MAVS, mitochondrial activator of viral signalling

MBP, maltose binding protein

MDA5, melanoma differentiation-associated 5

MERS, Middle East respiratory syndrome virus

MHV, mouse hepatitis virus

NF-κB, nuclear factor kappa-light-chain-enhancer of activated B cells

Ni-NTA, nickel-nitrilotriacetic acid

Nluc, Nanoluciferase

PAMP, pathogen-associated molecular patterns

PDB, protein data bank

PIV, parainfluenza virus

PKR, protein kinase R

pol, polymerase

polyI:C, polyinosinic:polycytidylic acid

qPCR, quantitative polymerase chain reaction

RIG, retinoic acid inducible gene

RIP, receptor interacting protein

RLR, RIG-like receptor

RNA, ribonucleic acid

RNase, ribonuclease

RRL, rabbit reticulocyte lysate

RT, reverse transcription/transcriptase

SARS, severe acute respiratory syndrome virus

SCR, scrambled DNA sequence

SDS-PAGE, sodium dodecyl sulphate polyacrylamide gel electrophoresis

SEC, size exclusion chromatography

SEC-MALS, SEC coupled with multi angle light scattering

SILAC, stable isotope labelling of amino acids in cell culture

ss, single-stranded

STAT, signal transducer and activator of transcription

TANK, TRAF family member associated NF-κB activator

TBK1, TANK-binding kinase

TLR, Toll-like receptor

TNF, tumour necrosis factor

TPR, tetratricopeptide repeats

TRAF, TNF receptor associated factor

TRIF, TIR-domain containing adapter-inducing interferon-beta

TSS, transcription start site

TYK2, tyrosine kinase 2

UTR, untranslated region

VSV, vesicular stomatitis virus

WNV, West Nile virus

ZIKV, Zika virus

List of Appendices

1 INTRODUCTION

An effective immune response to pathogens relies on rapid and accurate discrimination of self and non-self. Before an antigen-specific response is raised, the innate immune system must control infection by recognising molecular signatures which are unique to pathogens.

Viruses are obligate intracellular pathogens, which rely on the host translation machinery for their protein synthesis. Viral genomes are diverse in their length and composition, and can be broadly categorised by their nucleic acid (RNA or DNA) and strandedness (double- or single-stranded, positive or negative sense) *(Baltimore, 1971)*. These genomes, or derivatives thereof generated during replication, often include distinctive molecular signatures which can be recognised and targeted by the cell. Their detection leads to the induction of both cell-intrinsic factors to restrict infection and chemical messengers to recruit the immune system and clear infection. As such, viruses must hide their genomes from the cellular sensing machinery, or else find ways of convincingly mimicking cellular nucleic acids to escape recognition.

Among the highest expressed proteins during the innate immune response are the interferon-induced protein with tetratricopeptide repeats (IFIT). These are a conserved protein family with orthologues found in all major vertebrate clades *(Liu et al., 2013)*. IFIT proteins have numerous described antiviral activities, including binding to non-self RNA in the cytoplasm of infected cells, to prevent the translation and replication of invading viruses. IFITs have also been described to regulate innate and inflammatory immune

responses, to control cell proliferation and to regulate cell death *(reviewed in Fensterl and Sen, 2011, 2015; Diamond and Farzan, 2013; Zhou et al., 2013)*.

1.1 Eukaryotic RNA

In eukaryotic cells there are three major RNA species: ribosomal RNA (rRNA), transfer RNA (tRNA) and messenger RNA (mRNA), whose major function is to facilitate protein synthesis, with the former two serving to catalyse the translation of the latter. Transcription of these RNAs is performed by cellular DNA-dependent RNA polymerases: polI, polII and polIII. PolI is responsible for synthesis of the large pre-rRNA transcript. PolII transcribes mRNA, small nuclear RNA and micro RNA. PolIII transcribes short RNAs, including tRNA and the small 5S rRNA. These polymerases are recruited to genetic promoters through the concerted actions of various transcription factors, regulated by DNA and chromatin modifications, which govern cell-specific gene programmes *(Roeder, 1991)*.

Transcribed RNA undergoes considerable processing both co- and post-transcriptionally, including splicing, chemical modification and nucleotidylation. Transcripts are typically synthesised with a triphosphate moiety at the 5' end (5'ppp), which is rapidly processed. Pre-tRNAs are trimmed by RNase P, which removes the 5' leader oligonucleotide leaving a 5'-monophosphate *(Phizicky and Hopper, 2015)*, while the 13.7 kb pre-rRNA primary transcript is endonucleolytically cleaved into 28S, 18S and 5.8S rRNAs *(Henras et al., 2015)*. tRNAs are additionally processed at the 3' end, then extended with a uniform 3' CCA end necessary for aminoacylation. These RNAs also can undergo extensive nucleotide modification as they mature, including methylation, isoprentenylation and pseudouridylation *(Phizicky and Hopper, 2015)*.

1.1.1 mRNA capping

Messenger RNAs are uniquely processed by co-transcriptional capping with an inverted guanosine residue, via a 5'-5' triphosphate bridge *(Perry et al., 1975; Wei et al., 1975)*. The capping enzyme complex associated with RNA polII consists of a 5' phosphatase, guanylyl transferase and 7-methyltransferase *(McCracken et al., 1997; Cowling, 2010)*. The RNA 5'-triphosphate moiety is trimmed to diphosphate then ligated to GMP (capG, GpppNN),

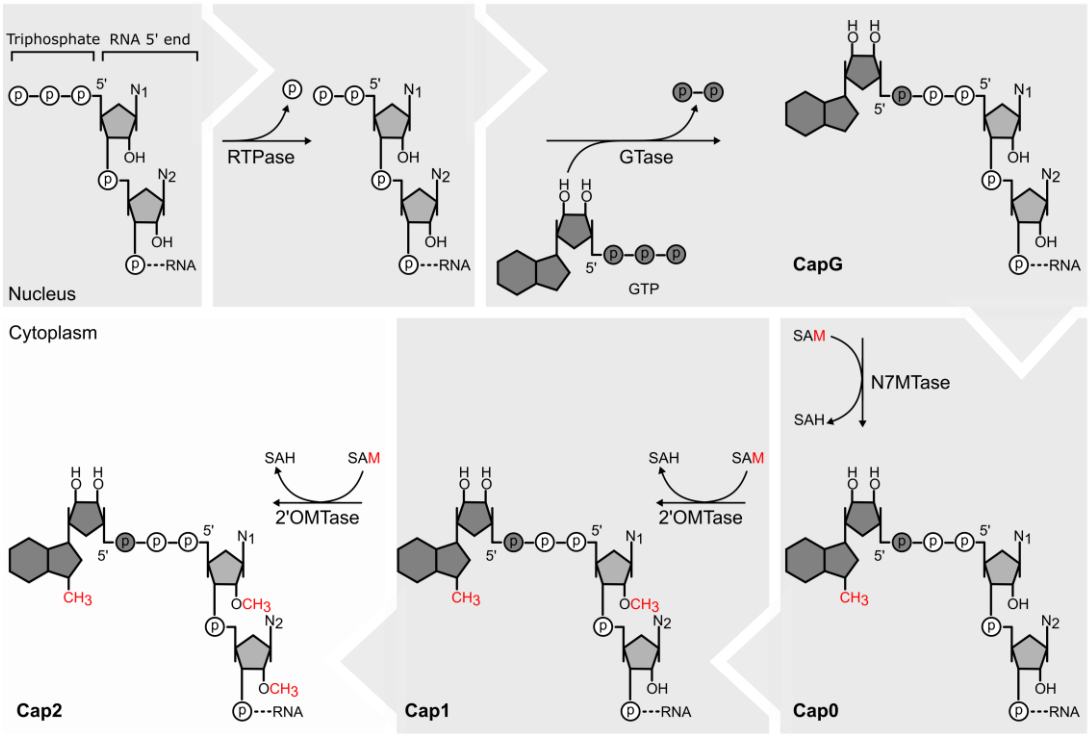

Figure 1-1 Capping of eukaryotic mRNA.

Clockwise; in the nucleus, nascent triphosphate polII transcripts are trimmed by RNA 5' triphosphatase (RTPase). GTP is cleaved to GMP, then ligated to the diphosphate RNA by guanylyl transferase (GTase), yielding capG RNA. The cap is methylated on the 7 position by N-7 methyltransferase (N7MTase), yielding cap0 RNA. S-adenosyl methionine (SAM) acts as the methyl donor, producing S-adenosyl homocysteine (SAH) as a by-product. The 2'-hydroxyl on the first ribonucleotide is methylated by 2'-O-methyltransferase (2'OMTase), yielding cap1 RNA. Finally, once in the cytoplasm, a proportion of transcripts are further modified to cap2 by the action of a cytoplasmic 2'OMTase.

which is subsequently methylated at the 7 position on the guanylate ring (cap0, m^7GpppNN) (Figure 1-1).

The 5' cap promotes 5' intron splicing *(Konarska et al., 1984)* and nuclear export of mature mRNA *(Lewis and Izaurralde, 1997)*, via the action of the nuclear cap-binding complex (CBC). The CBC is a heterodimer of cap-binding protein (CBP) 20 and CBP80, which binds to the 5' cap of immature pre-mRNA *(Mazza et al., 2001)* and recruits the nuclear RNA processing machinery *(Izaurralde et al., 1994)*. Mature, CBC-bound mRNAs are exported to the cytoplasm where they undergo a pioneer round of translation, facilitated by interactions between the CBC and the translation initiation machinery *(Maquat et al.,*

2010). This round of translation serves as a quality control gateway for cellular mRNAs: CBC binds to nonsense-mediated mRNA decay factors and senses ribosomes terminating on internal stop codons, indicative of incorrect splicing *(Hwang et al., 2010)*. The defective message is degraded and the translation machinery is recycled, to maintain the integrity of the cellular proteome.

Following pioneer translation, the CBC is displaced by the eukaryotic translation initiation factor (eIF) 4F. eIF4F comprises eIF4A, a DEAD-box RNA helicase; eIF4G, a large scaffold protein related to Cbp80 *(Marintchev and Wagner, 2005)*; and eIF4E, a small cap-binding protein. eIF4E specifically recognises capped mRNA by stacking the methylguanosine residue between two conserved tryptophans on its concave surface, mediated by an extensive water-bridge network *(Brown et al., 2009; Lama et al., 2017)*. The affinity of this interaction is enhanced by eIF4G, which wraps around the N-terminus of eIF4E *(Gross et al., 2003; Brown et al., 2009; Grüner et al., 2016)*.

Recognition of capped mRNA by eIF4F allows recruitment of the rest of the translation initiation machinery *(Jackson et al., 2010)*. The 40S small ribosomal subunit is associated with eIF3, a large multisubunit scaffolding complex which regulates the association of other initiation factors. eIF1 and eIF1A are associated with the 40S mRNA decoding centre, and stimulate the recruitment of the eIF2-GTP-Met-tRNA$^{Met}_{i}$ ternary complex, forming the 43S preinitiation complex. The 43S complex is loaded onto capped mRNA via interactions between eIF3 and eIF4G, where it scans the mRNA 5' untranslated region (UTR) *(Korneeva et al., 2000; Hinnebusch, 2017)*. Scanning is facilitated by RNA helicases, principally eIF4A, which unwind RNA secondary structure. eIF1 and eIF1A control the fidelity of scanning by modulating the conformation of the mRNA binding channel, allowing stable codon-anticodon base-pairing only on AUG start codons in good nucleotide context. Hydrolysis of GTP then stabilises the 48S preinitiation complex on the AUG start codon, allowing eIF5B-mediated 60S subunit recruitment, ready for polypeptide elongation *(Jackson et al., 2010)*.

In higher eukaryotes, including insects and vertebrates, mRNA is further modified by 2'-O-methylation on the first and second cap-proximal nucleotides (cap1, m^{7}GpppNmN and cap2, m^{7}GpppNmNm) *(Liu and Jia, 2014)*. *In vivo* labelling experiments demonstrated that cap1 modification occurs first on nuclear mRNAs, while cap2 modification is found only

on cytoplasmic transcripts *(Perry and Kelley, 1976)*. Two human 2'-O-methyltransferases were later isolated from HeLa lysates *(Langberg and Moss, 1981)*. The cap1 methyltransferase was shown to be exclusively nuclear, while the cap2 methyltransferase is present in both the nucleus and the cytoplasm *(Werner et al., 2011)*.

Cap-proximal 2'-O-methylation has been linked to translational efficiency in kinetoplastid parasites *(Zamudio et al., 2009)*, but its significance in multicellular eukaryotes remains unclear. In polysome profiling experiments from mouse cells, cap2 mRNAs were more abundant in the actively-translated polyribosome fraction and were suggested to be more stable *(Perry and Kelley, 1976)*. Cap2-modified messages were found to be a non-random subset of the transcriptome: cap2 modification preferentially occurred on pyrimidine nucleotides, in particular cytidine *(Perry and Kelley, 1976)*. Several transcripts have been identified which typically possess cap2 termini, including the globin mRNA *(Perry and Scherrer, 1975; Heckle et al., 1977; Cho et al., 1978)* and the Bombyx mori silk fibroin mRNA *(Yang et al., 1976)*, both of which are highly translated, stable messages.

Early experiments examining cap modification in mammalian cells relied on radioactive labelling of modified RNA followed by shearing and separation of oligonucleotides by chromatography. However, these methods do not lend themselves to high throughput analysis of cap modifications in infected cells and, since the mRNA is hydrolysed, do not allow identification of particular transcripts from an mRNA pool. Similarly, sequencing-based approaches which have been used to determine the role of RNA base methylation in the body of the RNA or 2'-O-methylation in the 3'UTRs of certain messages are not able to identify modifications so close to the 5'-terminus *(Dai et al., 2017)*. As such, the identity of transcripts which are preferentially cap2 modified, and thus the functional significance of this modification, is still unknown.

1.1.2 Viral RNA

While some viruses bypass the need for mRNA capping by employing non-canonical mechanisms of translation initiation, the majority of viruses produce capped mRNA. These therefore must convincingly mimic the host cell cap to avoid detection.

Those which replicate in the nucleus can co-opt the host capping machinery. mRNAs from retroviruses, whose genomes are integrated into the host cell chromosomes, are transcribed, spliced and capped by the host, resulting in authentic-looking messages. Similarly some DNA viruses, including herpes-, papilloma- and polyomaviruses, recruit cellular RNA polII to direct their transcription *(Harwig et al., 2017)*. To the same end, influenza virus cleaves the mature 5' end of nascent host transcripts and uses those fragments to prime viral transcription, thereby producing mRNAs with a properly-modified host cap *(Plotch et al., 1979; Walker and Fodor, 2019)*.

Cytoplasm-resident viruses must supply their own capping machinery. Capping and 2'-O-methyltransferase enzymes have evolved in diverse viral lineages, such as the dsDNA poxviruses *(Wei and Moss, 1974; Kyrieleis et al., 2014)*, as well as negative sense RNA rhabdoviruses *(Ogino and Green, 2019)*, large positive sense RNA coronaviruses *(Menachery et al., 2017)* and many of the small positive sense RNA viruses. These enzymes share little sequence or structural homology, and often utilise unique biochemical pathways to achieve the same goal *(Koonin and Moss, 2010)*.

Within the genus *Flavivirus*, the viral RNA-dependent RNA polymerase has an N-terminal 2'-O-methyltransferase domain which, in concert with the viral helicase/RNA triphosphatase protein, is responsible for capping and methylation of the viral genomic RNA *(Egloff et al., 2007)*. Both Dengue virus and West Nile virus (WNV) have been shown to possess exclusively cap1 genomic RNA *(Cleaves and Dubin, 1979; Ray et al., 2006)*. By contrast, a small fraction of messages produced by adenovirus and the rhabdovirus vesicular stomatitis virus (VSV) are modified to cap2 *(Rose, 1975; Hashimoto and Green, 1976)*. This may be by low efficiency cap2 activity of the viral methyltransferase or through the action of host cap2 methyltransferases. Conversely, the 5' end of sindbis virus genomic *(Hefti et al., 1975)* and subgenomic *(Dubin and Stollar, 1975)* RNA is not 2'-O-methylated at all. Indeed, while alphaviruses, like sindbis, encode a unique m7G-guanylyltransferase to cap their RNAs, they do not possess a 2'-O-methyltransferase and are thus exclusively cap0 *(Pietilä et al., 2017)*. These viruses instead have highly structured 5'UTRs, which shields them from innate immune defences; this will be discussed in detail below.

1.2 Sensing non-self RNA

Host cells have evolved several families of invariant receptors to recognise pathogen-associated molecular patterns (PAMPs) to sense viral infection. These pattern recognition receptors (PRRs) include, but are not limited to, the cytoplasmic RIG-like-receptors (RLRs) and the membrane-bound Toll-like receptors (TLRs). Many of these specialise in discriminating non-self RNA molecules *(Kondili et al., 2016)*.

TLRs are a family of 11 transmembrane proteins in humans, whose large leucine-rich repeat domains are responsible for ligand binding in the extracellular space and in endocytosed vesicles *(Kawasaki and Kawai, 2014)*. TLRs are largely expressed by myeloid-lineage cells of the innate immune system, including macrophages and dendritic cells, which patrol the skin and mucosa. TLR3, TLR7, TLR8 and TLR9 have been well characterised to recognise non-self nucleic acids in the endosomal compartment. TLR3, for example, is a key receptor involved in the sensing of rotavirus, a gastrointestinal pathogen with a double-stranded RNA (dsRNA) genome which enters the cell via endosomes *(Uchiyama et al., 2015)*.

Upon PAMP recognition, TLR3 homodimerises and recruits the TIR domain-containing adaptor protein, TRIF *(Ullah et al., 2013; Kawasaki and Kawai, 2014)*. TRIF can signal via the TNF-associated factor (TRAF) 3 to promote the activation of TANK-binding kinase 1 (TBK1) by stimulating autophosphorylation *(Ma et al., 2012)*. Phospho-TBK1 is then capable of recruiting and phosphorylating interferon regulatory factor (IRF) 3 and IRF7, which can homo- or hetero-dimerise, prompting their translocation to the nucleus. IRF3/7 stimulate expression of different subsets of type I interferon (IFN). IRF3 homodimers primarily stimulate expression of IFNβ, as well as a subset of antiviral effector proteins *(Grandvaux et al., 2002)*. Alternatively, TRIF may signal via the Ripl-TRAF6 complex, which ultimately results in derepression of the nuclear factor kappa B (NF-κB) transcription factor complex, allowing it to translocate to the nucleus (Figure 1-2). NF-κB drives the expression of proinflammatory cytokines and pro-survival signals, which promote immune cell recruitment and proliferation.

RLRs are a small family of cytoplasmic RNA helicase-like proteins which are expressed in a large number of cell types, and comprise only three prototype members: retinoic acid-inducible gene I (RIG-I), melanoma differentiation-associated protein 5 (MDA5) and LGP2

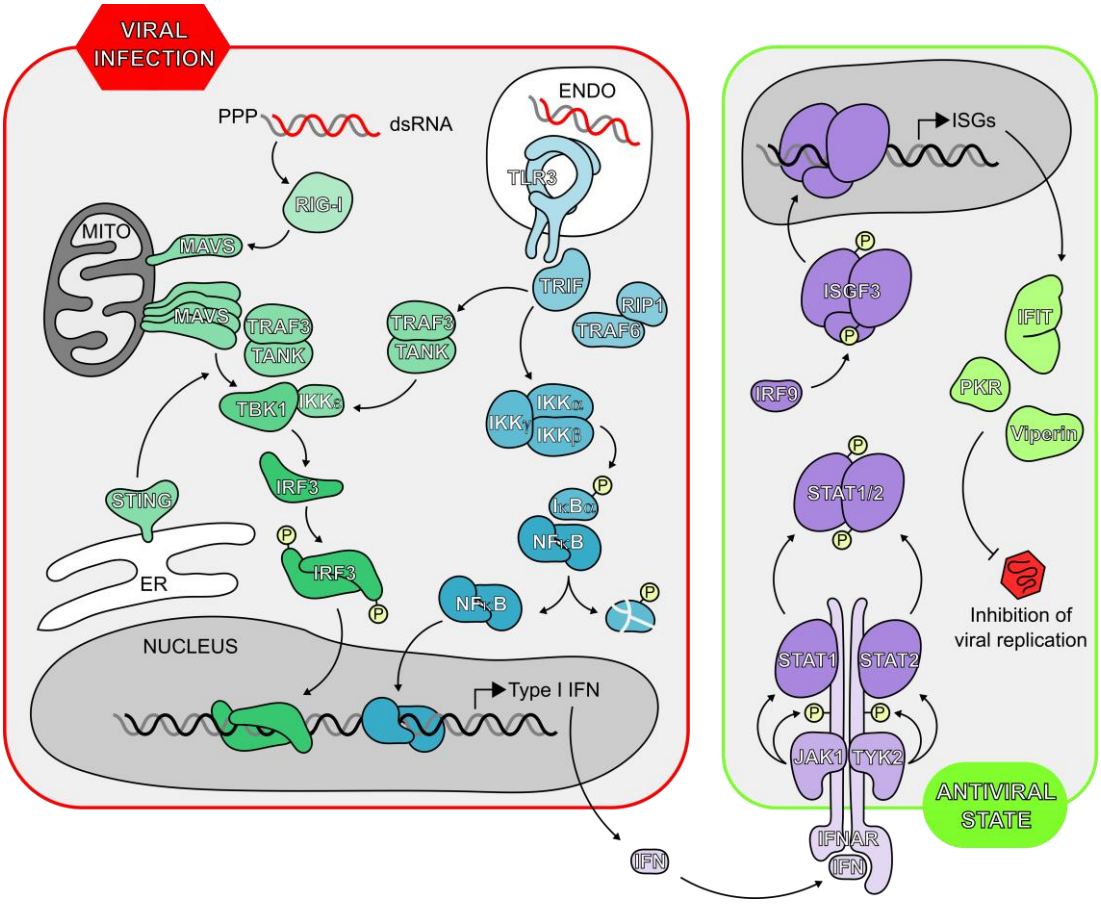

Figure 1-2 Innate immune signalling.

Left; pathogen-associated molecular patterns, such as double-stranded RNA (dsRNA), are sensed by cytoplasmic and endosomal receptors during viral infection. Signalling pathways activate cytoplasm-resident transcription factor complexes, which translocate into the nucleus and promote the expression of proinflammatory cytokines including type I interferons (IFN). Right; secreted IFN signals back to the infected cell and to neighbouring cells by engaging the type I IFN receptor (IFNAR), which signals via the JAK-STAT pathway to activate the interferon stimulated growth factor 3 (ISGF3) transcription factor complex. ISGF3 translocates to the nucleus where it promotes the expression of hundreds of interferon stimulated genes (ISG), such as the interferon-induced proteins with tetratricopeptide repeats (IFIT). These ISGs inhibit viral replication by targeting various stages of the viral lifecycle and recruiting the cellular immune system to clear infection.

(also known as DHX58). These receptors bind to dsRNA with differing specificity and affinity *(Loo and Gale, 2011)*. RIG-I preferentially binds short dsRNA substrates with non-self 5' ends, particularly uncapped 5'ppp RNA *(Pichlmair et al., 2006; Kowalinski et al., 2011)*. As a result, RIG-I is the principle receptor responsible for sensing defective RNA genomes generated as a result of polymerase slippage during influenza A virus infection, which have a 5'ppp dsRNA panhandle structure *(te Velthuis et al., 2018)*. More recently,

RIG-I was shown to bind cap0 RNA with comparable affinity to 5'ppp RNA *(Devarkar et al., 2016)* and mediated sensing of a mutant of yellow fever virus with a defective 2'-O-methyltransferase *(Schuberth-Wagner et al., 2015)*.

MDA5 binds to dsRNAs over 2 kb in length and is primarily responsible for sensing dsRNA intermediates made during RNA virus replication. Consistently, MDA5 has been identified as the principal receptor responsible for sensing infection with small positive sense RNA viruses like picornaviruses *(Feng et al., 2012)* and caliciviruses *(McCartney et al., 2008)*. MDA5 has also been implicated in sensing cap0 RNA in the context of coronavirus infection *(Züst et al., 2011)*, suggesting it may also play a role in scrutinising RNA 5' ends.

Upon PAMP recognition, RIG-I or MDA5 bind to the membrane-associated mitochondrial activator of viral signalling (MAVS) complex, causing it to polymerise. Oligomeric MAVS can then recruit TBK1, via the actions of TANK and TRAF3, promoting IRF3 activation and IFN expression as described above (Figure 1-2). MAVS, acting as a large molecular scaffold, may also bind to other signalling components such as TRAF6 to activate NF-κB signalling *(Scott, 2010)*.

1.2.1 Interferon

Interferons (IFN) are a conserved family of around 20 cytokines found in almost all vertebrates, which were first identified for their ability to 'interfere' with viral infection *(Isaacs and Lindenmann, 1957)*. There are three classes of IFN: type I, type II and type III. Type I IFN is expressed by almost all cells in response to viral infection, and is comprised of two major subtypes, alpha and beta, and a number of minor subtypes *(McNab et al., 2015)*. IFNβ in particular is produced in large quantities upon infection of fibroblast tissues. Type II IFN is expressed by immune cells and promotes a pro-inflammatory environment for the activation and proliferation of immune cells during infection. Finally, type III IFN is predominantly expressed by epithelial cells and has been associated with control of viral infection in alveolar, hepatic and gastrointestinal tissues *(Kotenko et al., 2003; Douam et al., 2017)*.

Type I IFN signals through the IFN-alpha receptor (IFNAR), a heterodimer comprised of IFNAR1 and IFNAR2, which are associated with kinases TYK2 and JAK1 respectively *(Platanias, 2005)*. Upon binding to type I IFN, IFNAR subunits dimerise, activating their receptor-associated kinases, leading to recruitment and tyrosine-phosphorylation of signal transducer and activator of transcription (STAT) proteins. Phosphorylated STAT proteins dimerise and translocate into the nucleus. STAT1 or STAT3 homodimers bind to GAS promoter elements, resulting in activation of an inflammatory response. By contrast, heterodimers of STAT1 and STAT2 associate with IRF9 to form the IFN-stimulated growth factor 3 (ISGF3), a transcription factor complex which recognises IFN-stimulated response elements (ISRE) in target promoters (Figure 1-2), directing the transcription of hundreds of IFN-stimulated genes (ISGs) *(Samarajiwa et al., 2009)* .

Many ISGs have well characterised antiviral function and can inhibit virtually any step of the viral lifecycle. Protein kinase R (PKR), for example, phosphorylates the alpha subunit of eIF2 *(Williams, 1999)*. Phosphorylated eIF2α cannot be recharged by the guanine exchange factor eIF2B, and as such remains in its inactive GDP-bound form. However, phospho-eIF2α has higher affinity for eIF2B, thereby acting as a competitive inhibitor to prevent recycling of further ternary complex *(Bogorad et al., 2017; Kashiwagi et al., 2017)*. This effectively shuts down cellular translation. Viruses, in response, have evolved mechanisms to avoid or counteract these restriction factors. Alphaviruses, for instance, initiate translation of their subgenomic mRNA in a manner independent of eIF2 and are thus impervious to the action of PKR *(Ventoso et al., 2006; Skabkin et al., 2010; Sanz et al., 2017)*.

Alongside antiviral genes, inflammatory cytokines and chemokines are expressed to alert the immune system to the infection *(Zlotnik and Yoshie, 2000)*. Myeloid lineage cells, including macrophages and neutrophils, are recruited early in the response and have numerous antiviral tools at their disposal, including lysis and phagocytosis of virus-infected cells *(Stegelmeier et al., 2019)*. Following presentation of viral antigens to T and B cells, pathogen-specific responses are mounted to initiate clearance of infected cells and the establishment of long-term pathogen-specific immunity *(Dörner and Radbruch, 2007; Pennock et al., 2013; Kumar et al., 2018)*.

1.3 Interferon-induced proteins with tetratricopeptide repeats

Among the highest expressed of the interferon-stimulated genes are the IFN-induced proteins with tetratricopeptide repeats (IFIT) family. IFIT-like genes are found in all vertebrate lineages (see Figure 1-6). They are thought to have co-evolved with the interferon system *(Liu et al., 2013)*, implying an absolute requirement for IFIT-like genes in the innate immune response.

Mammals have a conserved complement of IFIT proteins (IFIT1, IFIT1B, IFIT2, IFIT3 and IFIT5). These have undergone duplication, deletion and recombination events in a number of phyla, presumably in response to evolutionary pressure from lineage-specific pathogens *(Fensterl and Sen, 2011; Liu et al., 2013; Daugherty et al., 2016)*. IFIT-like genes have also been identified in non-mammalian vertebrates, including reptiles, amphibians and fish. Zebrafish, for example, have been shown to express at least seven IFITs *(Liu et al., 2013; Varela et al., 2014)*. By contrast in birds almost all IFIT genes have been lost except for IFIT5, which appears to maintain the antiviral functions of its human counterpart *(Magor et al., 2013; Li et al., 2017; Santhakumar et al., 2018)*.

IFIT proteins were first observed nearly 40 years ago. Translation of mRNA extracted from IFN-stimulated human fibroblasts produced distinct protein products between 50-60 kDa, when translated in a cell-free system *(Colonno and Pang, 1982)*. A particularly prominent band was observed at ~56 kDa, the molecular weight of IFIT1 (also named ISG56). IFIT1 was partially *(Chebath et al., 1983)*, then fully *(Wathelet et al., 1986)*, cloned and sequenced, allowing analysis of its induction kinetics. IFIT1 mRNA was shown to be strongly and rapidly induced by type I IFN in various primary and immortalised human cell lines *(Kusari and Sen, 1986; Wathelet et al., 1986; Bandyopadhyay et al., 1990; Der et al., 1998)*. A similar sequence was then identified for a 54 kDa protein, IFIT2, with type I IFN-dependent induction kinetics and ISRE sequences in its promoter region *(Levy et al., 1986; Bluyssen et al., 1994b)*. Homologues of IFIT1 and IFIT2 were later identified in mice *(Bluyssen et al., 1994a)*, followed by identification of two further human IFIT family members, IFIT3 (also named IFIT4) *(Smith and Herschman, 1996; Yu et al., 1997; de Veer et al., 1998)* and IFIT5 *(Niikura et al., 1997)*. Since the nomenclature of IFIT proteins has changed multiple times since their discovery, a summary of IFIT aliases is provided in Table 1-1.

Table 1-1 IFIT aliases.

A summary of known aliases for human (uppercase) and murine (lowercase) IFIT genes and proteins. GARG, glucocorticoid-attenuated response gene; IFI, interferon-induced; ISG, interferon-stimulated gene; RIG, retinoic acid inducible gene.

IFIT	Accession number	Alternative names
IFIT1	NP_001539.3	C56, G10P1, IFI-56, IFI-56K, IFI56, IFIT-1, IFNAI1, ISG56, P56
IFIT1B	NP_001010987.1	IFIT1L
IFIT2	NP_001538.4	G10P2, GARG-39, IFI-54, IFI-54K, IFI54, IFIT-2, ISG-54 K, ISG-54K, ISG54, P54
IFIT3	NP_001540.2	GARG-49, IFI60, IFIT4, ISG60, P60, RIG-G
IFIT5	NP_036552.1	ISG58, P58
Ifit1	NP_032357.2	Garg16, Isg56, Ifi56, Ifit1b1, p56
Ifit1b	NP_444447.1	Ifit1b2, Ifit1bl2
Ifit1c	NP_001103987.1	Ifit1b3, Ifit1bl1
Ifit2	NP_032358.1	Garg-39, Ifi54, p54
Ifit3	NP_034631.1	Garg-49, Ifi49, p49
Ifit3b	NP_001005858.2	Ifit3-like

1.3.1 IFIT induction

IFIT genes typically have one to two ISREs in their promoter regions. The human IFIT1 promoter was first shown to respond strongly and rapidly to IFNα *(Kusari and Sen, 1986)* and was bound by ISGF3 in gel shift assays *(Bandyopadhyay et al., 1990)*. The ISRE I element in the IFIT1 promoter was later shown to be bound directly by IRF3 *(Grandvaux et al., 2002)*, and forms the basis of the ISG56.1 reporter plasmid frequently used in IRF3 activation assays *(Wathelet et al., 1986; Ferguson et al., 2013; White et al., 2016)*. These elements are conserved within the other human IFIT promoters, save IFIT1B *(Levy et al., 1986; Xiao et al., 2006)*, and the murine Ifit promoters *(Bluyssen et al., 1994a)*. Given their co-evolution with type I IFNs, it is likely that IFIT genes in all vertebrate species have similar IFN-responsive expression patterns, underpinning their vital role in the innate immune response.

1.3.1.1 Human IFIT expression

In human cell lines, IFIT1 *(Kusari and Sen, 1986; Guo et al., 2000a; Terenzi et al., 2006)*, IFIT2 *(Levy et al., 1986; Terenzi et al., 2006)*, IFIT3 *(Yu et al., 1997; de Veer et al., 1998; Xiao et al., 2006)* and IFIT5 *(Niikura et al., 1997)* are induced by type I IFN treatment, in a manner dependent on STAT1. By contrast, IFIT expression is induced to a much lesser extent *(Yu et al., 1997; Guo et al., 2000a)* or not at all *(Kusari and Sen, 1986; de Veer et al., 1998; Der et al., 1998)* by type II IFN. IFITs are also induced directly downstream of dsRNA sensing, in a manner dependent on IRF3 *(Guo et al., 2000a; Grandvaux et al., 2002; Imaizumi et al., 2014, 2016)*. As such, IFIT expression is detectable within a few hours after viral infection *(Guo et al., 2000a)*. Other PAMPs, including bacterial lipopolysaccharide (LPS) *(Imaizumi et al., 2013; John et al., 2018)* and all-trans retinoic acid *(Yu et al., 1997; Xiao et al., 2006)*, are known to induce IFIT expression, typically dependent on the expression of type I IFN.

Expression of IFIT1 *(Buggele and Horvath, 2013)*, IFIT2 *(Feng et al., 2014; Wang et al., 2016)* and IFIT3 *(Hou et al., 2016)* is post-transcriptionally regulated by different IFN-inducible micro RNAs, which attenuate IFIT mRNA expression late in infection. As such, IFITs are only expressed for the duration of the innate immune response and are quickly degraded once the host cell is no longer receiving stimulus *(Kusari and Sen, 1986; Guo et al., 2000a)*. The kinetics and magnitude of this expression also varies according to cell type *(Terenzi et al., 2006)*, likely reflecting differences in innate immune pathways in different cell types. In human cell lines, IFIT1 was detectable at the protein level as early as 2-6 hours post stimulation and expression was maintained 24 to 48 hours after IFN-treatment *(Guo et al., 2000a; Terenzi et al., 2006)*.

IFIT expression is targeted by different viruses. Vaccinia virus was found to induce proteasome-dependent degradation of IFIT1, IFIT2 and IFIT5 *(Soday et al., 2019)*. Similarly, in herpes simplex virus infection, IFIT3 is targeted for proteasomal degradation by the viral protein UL41 *(Jiang et al., 2016)*. During infection with UL41 deletion viruses, IFIT3 is highly expressed and is strongly antiviral. Human foreskin fibroblasts infected with Zika virus (ZIKV) expressed high levels of IFIT1 and IFIT3 but IFIT2 was undetectable; infection of the same cell line with Chikungunya virus induced IFIT2 expression, indicating that ZIKV may selectively downregulate IFIT2 *(Wichit et al., 2019)*.

IFIT expression is also known to be dysregulated in other diseases. IFIT3, for example, is highly expressed in peripheral blood mononuclear cells from patients with the autoimmune disorder systemic lupus erythematosus *(Huang et al., 2008; Wang et al., 2018)*. IFIT3 overexpression drove monocyte differentiation *in vitro* toward the dendritic cell lineage, and enhanced dendritic cell activity. Elevated IFIT3 expression was detected in the spleen, as well myeloid-lineage immune cells, such as monocytes *(Huang et al., 2008)* and M1-polarised macrophages *(Huang et al., 2018)*, supporting a role in myeloid cell regulation.

There is some evidence of differential IFIT expression provided by the human protein atlas, a database which maps RNA and protein expression of human genes in different tissues and cell lines *(Uhlén et al., 2015)*. Of interest, histological sections from this consortium have suggested IFIT1B is expressed in haematopoietic progenitor cells, including myeloid cell precursors, as well as mature splenic lymphocytes and macrophages, suggesting it may play a similar role to IFIT3 in regulating immune cell differentiation. If IFIT1B does indeed have a restricted expression profile in stem-like cells, this may account for its poor detection in standard cell lines.

1.3.1.2 Murine Ifit expression

Murine Ifit1, Ifit2 and Ifit3 follow similar expression patterns to their human counterparts. mRNA is detectable as little as 1-2 hours following type I IFN treatment and 2 hours after type II IFN treatment *(Bluyssen et al., 1994a; Smith and Herschman, 1996; Terenzi et al., 2005)*. Expression following type I IFN is considerably stronger, and is dependent on the activation of STAT1 and STAT2 *(Bluyssen et al., 1994a; Terenzi et al., 2005; Wacher et al., 2007)*. Ifit expression is similarly stimulated by dsRNA and viral infection *(Terenzi et al., 2005; Wacher et al., 2007)*, downstream of IRF3 *(Guinn et al., 2017)*, as well as LPS treatment and bacterial infection *(Smith and Herschman, 1996; John et al., 2018)*.

Ifit1 and Ifit2 expression was strongly stimulated in mice injected with IFNβ or synthetic dsRNA in a number of murine tissues *(Terenzi et al., 2007)*. Treatment with IFNα resulted in tissue-dependent variation in Ifit expression: Ifit1 was moderately expressed in all tissues except kidney and heart, while Ifit2 was only expressed in lung, spleen and, to a lesser extent, liver. In mice infected with VSV, Ifit1 expression was detectable in most

tissues, while Ifit2 expression was only detectable in lung, spleen and intestinal tissues. Ifit expression was dependent on STAT1, but was independent of TLR3 and PKR *(Terenzi et al., 2007)*.

Ifit expression has also been examined in the central nervous system during viral infection. Ifit1, Ifit3 and, to a lesser extent, Ifit2 mRNAs were strongly upregulated 2-6 days post infection in the brains of mice infected with lymphocytic choriomeningitis virus (LCMV) or WNV *(Wacher et al., 2007)*. LCMV and WNV are pathogenic neurotropic viruses of the families Arenaviridae and Flaviviridae, respectively. In LCMV infection, both Ifit1 and Ifit3 mRNA were diffusely expressed throughout the brain and meninges, while Ifit2 was expressed more strongly in the regions of the brain immediately surrounding the sites of infection. Following infection with WNV, Ifit1, Ifit2 and Ifit3 were detectable throughout the entire brain, particularly in the cerebellum. Cell type-specific differences were observed in the expression of Ifit mRNA in infected brains, though the reason for and functional significance of this is unclear. For example, in neurones Ifit expression was completely dependent on STAT1, while in non-neuronal tissue STAT1 knockout only partially decreased Ifit expression *(Wacher et al., 2007)*.

Ifit expression has also been examined in different immune cell subsets. At least 50% of bone marrow-derived cells from mice injected with dsRNA, IFNα or infected with VSV expressed Ifit1 and Ifit2, while up to 90% of T cells and natural killer cells from the spleens of those mice expressed Ifit2 *(Terenzi et al., 2007)*. Similarly, Ifit2 expression was strongly upregulated in murine macrophages following WNV infection *(Daffis et al., 2007)*. Some Ifit2 expression was also detectable in unstimulated macrophages *(Daffis et al., 2007)*. This expression was dependent on IRF3, suggesting some basal level of activation in cultured myeloid cells. By contrast, Ifit1 was only detected in 50% of T cells, and less than 10% of natural killer cells *(Terenzi et al., 2007)*. Ifit1 expression is specifically downregulated in B cells *(White et al., 2016)*. B cells express high levels of IRF8, a repressive transcription factor which was shown to bind the Ifit1 promoter. Ectopic expression of IRF8 in murine fibroblasts strongly inhibited IFN-stimulated Ifit1 expression, while Ifit2 and Ifit3 expression were partially inhibited *(White et al., 2016)*.

While it is clear that murine Ifit1, Ifit2 and Ifit3 expression is dependent on type I IFN and dsRNA sensing in a number of cell lines, a comprehensive analysis of the entire murine Ifit

family has not been carried out. In particular, the expression of Ifit1b, Ifit1c and Ifit3b has not been formally demonstrated and their induction patterns have not been characterised.

1.3.2 eIF3 binding

IFIT1 was first described to inhibit translation by binding to the translation initiation factor eIF3, which is essential for the majority of cap-dependent and cap-independent translation. In mammals, eIF3 consists of 13 subunits (eIF3a-m) and binds across the solvent-exposed surface of the 40S subunit. eIF3 mediates assembly of multiple initiation factors on the 40S subunit, to coordinate translation initiation *(Cate, 2017; Hinnebusch, 2017)*. In particular, eIF3 binds to the middle domain of eIF4G, the large protein scaffold component of eIF4F, via the eIF3c, –d and –e subunits *(LeFebvre et al., 2006; Villa et al., 2013; Kumar et al., 2016)*. This interaction mediates recruitment of the ribosome of the 5' end of mRNAs, to initiate translation. eIF3 is also an RNA binding protein in its own right, and can interact directly with cellular and viral RNAs to promote non-canonical translation initiation *(Sun et al., 2013; Meyer et al., 2015; Lee et al., 2016)*, and may be involved in coordinating or stabilising mRNA exiting the 40S subunit during scanning *(Jackson et al., 2010; Valášek et al., 2017)*.

Human IFIT1 was found to interact with a C-terminal fragment of the eIF3e subunit (originally named Int6/p48) in a yeast two-hybrid screen *(Guo and Sen, 2000; Guo et al., 2000b)*. When overexpressed in human cells, IFIT1 could relocalise eIF3e from the nucleus to the cytoplasm and was shown to co-immunoprecipitate eIF3e, suggesting a direct interaction. A small proportion of IFIT1 also co-migrated with eIF3 when analysed by gel filtration. This interaction was mapped to the C-terminal domain of IFIT1, since C-terminal truncation prevented co-migration during gel filtration.

IFIT1 was shown to inhibit the translation of uncapped *(Hui et al., 2003)* and cap0 *(Guo et al., 2000b)* model RNAs *in vitro*, while truncated IFIT1 did not affect translation. However, IFIT1 did not disrupt interaction between eIF3 and eIF4F *(Hui et al., 2003)*, neither did it affect association of eIF3 and the 40S subunit *(Hui et al., 2003; Kumar et al., 2014)*. The N-terminal two-thirds of eIF3e are necessary for eIF4G binding *(LeFebvre et al., 2006)*, but IFIT1 binds the C-terminal half of eIF3e *(Guo and Sen, 2000)*, which may explain why IFIT1 does not interfere with eIF4F binding+. Instead, IFIT1 was proposed to inhibit eIF3-

mediated enhancement of ternary complex formation *(Hui et al., 2003)*. eIF3 binding to the ternary complex is suggested to stabilise the complex *(Valášek et al., 2002)*, thereby encouraging more complex to form by shifting the equilibrium of the reaction to the product side. Translation was partially restored on addition of exogenous eIF2, to counteract the proposed decrease in ternary complex concentration mediated by the IFIT1-eIF3 interaction. However, translation driven by the encephalomyocarditis virus (EMCV) internal ribosome entry site (IRES) was unaffected by IFIT1 addition *(Hui et al., 2003)*, despite reliance on both eIF3 and ternary complex *(Pestova et al., 1996)*.

This mechanism of translation inhibition was suggested to account for the restriction of hepatitis C virus (HCV) replication in human hepatocytes upon overexpression of IFIT1 *(Raychoudhuri et al., 2011)*. The HCV IRES is directly engaged by eIF3 *(Kieft et al., 2001; Sun et al., 2013)* and is modulated by eIF2 for effective translation initiation *(Jaafar et al., 2016)*. Overexpression of IFIT1 inhibited HCV IRES-dependent translation in human hepatocellular carcinoma cells *(Ishida et al., 2019)*. However, in this study, cap-dependent and EMCV IRES-dependent translation was also inhibited to a similar extent; translation inhibition was also observed for overexpressed IFIT2, IFIT3 and IFIT5. Therefore the observed translation inhibition may be a side-effect of cytotoxic protein overexpression, rather than a specific effect of IFIT1. In these cells overexpressed IFIT1, which typically has diffuse cytoplasmic expression *(Guo et al., 2000a)*, was found to co-localise in cytoplasmic puncta with endogenous eIF3 and eIF2 *(Ishida et al., 2019)*, reminiscent of stress granules. Therefore, overexpression of IFIT1 may induce cellular stress. In cell-free extracts, translation driven by the HCV IRES was not inhibited by up to 5 μM IFIT1 *(Abbas et al., 2017a, 2017b)*. The exact role of IFIT1 in regulating HCV IRES-driven translation still requires clarification.

Murine Ifit1, like human IFIT1, was shown to inhibit the translation of uncapped model RNAs *in vitro (Hui et al., 2005)*. Ifit1 weakly associated with eIF3 in gel filtration experiments and co-precipitated with the eIF3c subunit when both were overexpressed in human cells. Unlike human IFIT1, murine Ifit1 did not have a large effect on eIF3-mediated stabilisation of the ternary complex, nor on the recruitment of the ternary complex to the 40S ribosome. Instead, Ifit1 appeared to prevent eIF4F interaction with the 43S complex, precluding formation of preinitiation complexes *(Hui et al., 2005)*. Along with eIF3e and eIF3d, eIF3c contributes to stable association of eIF3 with eIF4G *(Villa et al., 2013)*. Murine

Ifit2 and Ifit3 were also shown to co-precipitate with eIF3c, but not with eIF3e *(Terenzi et al., 2005; Fensterl et al., 2008)*. Ifit2 inhibited the translation of uncapped model mRNAs *in vitro*, but to a much lesser degree than human IFIT1 or murine Ifit1, while murine Ifit3 had no effect on translation *(Fensterl et al., 2008)*.

A number of studies have failed to recapitulate these results. Peptides corresponding to eIF3 did not co-precipitate with human IFIT1 *(Pichlmair et al., 2011; Habjan et al., 2013)* or murine Ifit1 *(Habjan et al., 2013)* in independent mass-spectrometry pull-down experiments. Human IFIT2 did not co-precipitate with eIF3c when both were overexpressed in HEK293T cells and did not inhibit translation of uncapped RNAs *in vitro (Yang et al., 2012)*. Endogenous Murine Ifit1, Ifit2 and Ifit3 also did not precipitate eIF3c from primary murine cells *(Siegfried et al., 2013)*. Additionally, human IFIT1 was shown to associate with 40S ribosomal subunits independently of eIF3, and the presence of eIF3 did not enhance recruitment *(Kumar et al., 2014)*. Furthermore, in sucrose density gradient centrifugation experiments, addition of IFIT1 was not inhibitory to 43S complex formation *(Kumar et al., 2014)*. Together, this indicates that IFIT proteins may interact weakly or non-specifically with eIF3.

1.3.3 RNA binding

It was later discovered that IFIT proteins could inhibit translation by binding to RNA directly. Pichlmair et al. *(2011)* first described RNA binding activity for human IFIT protein after precipitating IFN-treated HEK293 cell lysates on PPP-RNA-coupled beads, to simulate viral RNA. Binding to single-stranded 5'-triphosphate RNA was then confirmed for IFIT1 and IFIT5, using a number of different techniques *(Pichlmair et al., 2011; Abbas et al., 2013)*. Interaction with 5'ppp-RNA was similarly shown for murine Ifit1, which shares 70% amino acid similarity with human IFIT1.

A putative RNA binding surface was identified, lined with positively-charged residues which could interact with the negatively-charged phosphate backbone of RNA. Indeed mutation of this surface, particularly towards the N-terminus of the protein, disrupted the ability of IFIT1 and IFIT5 to bind 5'-ppp RNA *(Pichlmair et al., 2011; Abbas et al., 2013)*. Many of these residues are conserved among IFIT family members, indicating that RNA binding may be a common function of IFIT family members.

Recombinant IFIT1 was shown to inhibit translation of uncapped RNA at micromolar concentrations, both in rabbit reticulocyte lysate (RRL) and wheat germ extract, but translation inhibition was relieved by mutating RNA binding residues *(Pichlmair et al., 2011)*. This indicates that RNA binding specifically mediates translation inhibition by IFIT1. The authors additionally argued that the evolutionary distance between human and wheat, and thus the divergence between their translation initiation factors, implies eIF3 binding is unlikely to be the major mechanism by which IFIT1 inhibited translation *(Pichlmair et al., 2011)*.

1.3.3.1 IFIT5 RNA binding

The crystal structure of IFIT5 was later solved by three independent groups, in both unbound (apo) *(Abbas et al., 2013; Feng et al., 2013; Katibah et al., 2013)* and RNA-bound (holo) states *(Abbas et al., 2013)* (Figure 1-3). This has revealed a great deal of insight into the mechanism of IFIT-RNA binding. IFIT5 is made up of sequential tetratricopeptide repeats (TPRs), which are a helix-turn-helix structural motif. TPR-containing proteins are typically open superhelical structures, caused by sequential stacking of the helix-turn-helix TPR motifs *(Das et al., 1998; D'Andrea and Regan, 2003)*. In IFIT5, the N-terminal domain is closed off by non-TPR α-helices and loops, which disrupt the expected superhelical topology. The C-terminal domain is joined by a flexible linker, or pivot, domain comprised of two longer α-helices (Figure 1-3A-B). A positively charged channel, approximately 15 Å wide, is formed in the groove between the N- and C-terminal domains (Figure 1-3C).

Positively charged residues within the RNA binding channel interact with single-stranded 5'ppp-RNA, by coordinating the negatively-charged phosphate backbone and 5'-triphosphate moiety (Appendix A). A metallic ion, likely Mg^{2+}, is involved in coordinating the α and γ phosphates. IFIT5 was shown to bind 5'ppp-ssRNA with nanomolar affinity *(Abbas et al., 2013; Kumar et al., 2014)*. Binding was not observed for dsRNA and ssRNA with a stable hairpin at the 5' end *(Abbas et al., 2013)*, or capped RNA *(Abbas et al., 2013; Habjan et al., 2013; Kumar et al., 2014)*. Primer extension inhibition assays revealed that IFIT5 binding results in a truncated cDNA product approximately 6-7 nt shorter than the full length cDNA *(Kumar et al., 2014)*. This corresponds to the depth of the IFIT5 RNA binding pocket, thus directly visualising binding to the 5' end of the RNA. The triphosphate binding cavity is closed at the 5' end,

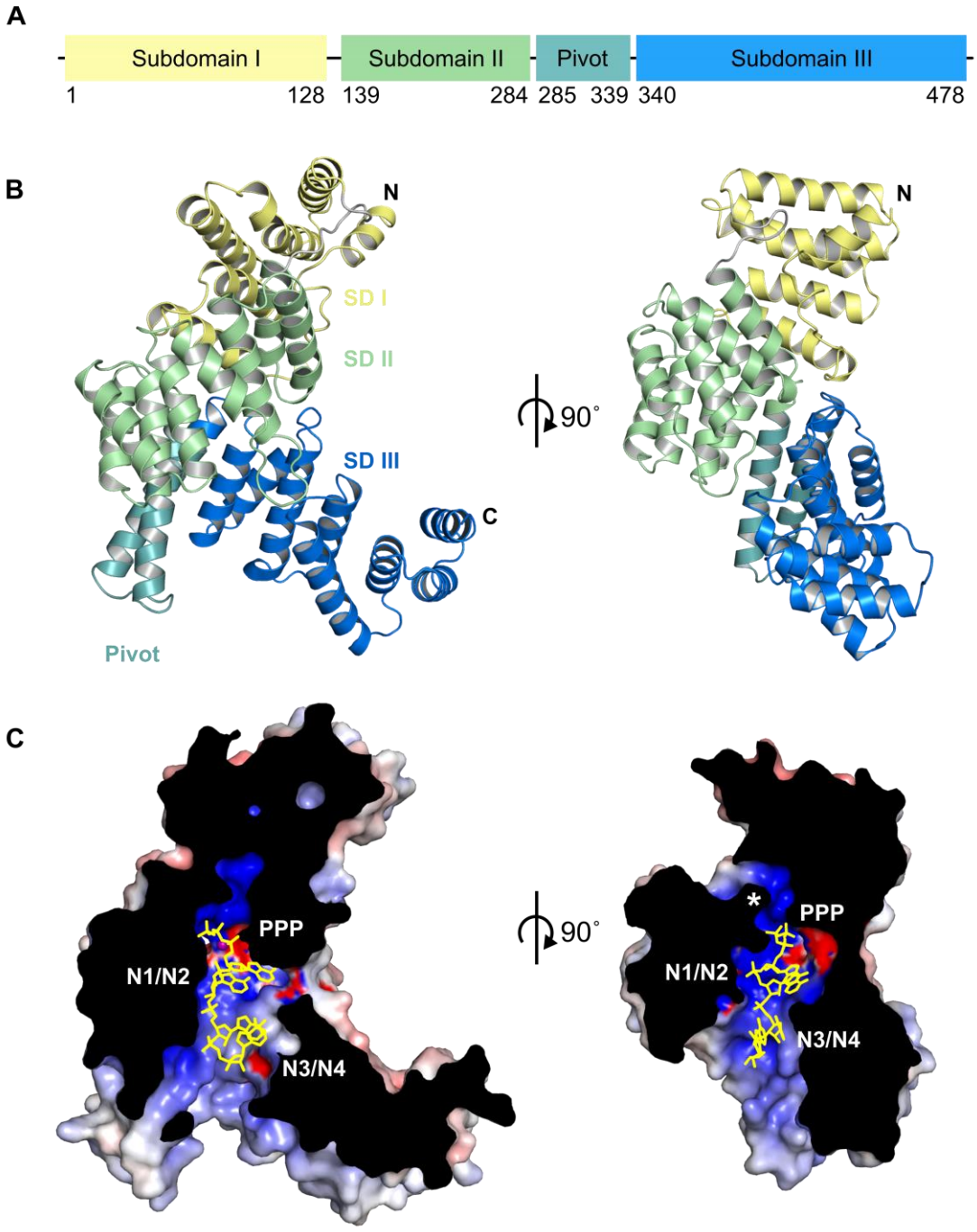

Figure I-3 IFIT5 RNA binding.

A. *Domain diagram of human IFIT5.* ***B.*** *Cartoon representation of IFIT5 in complex with PPP-oligo(A) (PDB: 4HOT), coloured by subdomain (SD).* ***C.*** *Surface Cutaway of IFIT5 coloured by electrostatic potential from negative (-10 kTe^{-1}; red) to positive (+10 kTe^{-1}; blue), via hydrophobic (white), generated with the Adaptive Poisson-Boltzmann Solver (APBS) plugin for Pymol, using PDB2PQR (Dolinsky et al., 2004). Cross-section is indicated by solid black shading and RNA is shown as yellow sticks. Features of the RNA are annotated: PPP, 5′ triphosphate moiety; N1/N2, first two nucleotides; N3/N4, third and fourth nucleotides. Residues which close the RNA binding channel, occluding cap binding, are indicated with an asterisk.*

making it unlikely that IFIT5 could accommodate capped RNA transcripts in this conformation (Appendix A).

However, one report has shown IFIT5 binding to capped RNA in gel shift assays, with comparable affinity to 5'ppp-RNA binding *(Katibah et al., 2014)*. Residues in the N-terminus and RNA binding channel were identified which specifically decreased cap0 binding, while maintaining 5'ppp binding, which are located at the neck of the triphosphate binding channel (Q41 and K150, see Appendix A). Given that the top of the IFIT5 RNA binding channel is closed by a number of flexible loops, including some of these putative cap0 binding residues, remodelling of the N-terminal domain may allow accommodation of cap0 RNA *(Katibah et al., 2014)*. Overexpression of IFIT5 in human cells was shown to inhibit the replication of a mutant of WNV which lacks 2'-O-methyltransferase activity (NS5 E218A), by about 50%, but could not inhibit wildtype virus *(Daffis et al., 2010)*. This may support the supposition that IFIT5 can bind to cap0 RNA but not to cap1 RNA.

A point mutation (E33A) was also identified which could confer cap1 binding to IFIT5 *(Katibah et al., 2014)*. However, given the physical distance between this residue and the first RNA nucleotide in the IFIT5 structure, the mechanism of this is unclear. It is possible that this mutation causes an N-terminal structural rearrangement which alters the local geometry of the RNA binding channel, allowing cap1 substrates to be accommodated. How IFIT5 can accommodate capped RNA, and the consequence of this in infection, remains to be clarified.

A flexible loop from TPR4 allows van der Waals interactions with both pyrimidine and purine bases at the N1 position, indicating that IFIT5 has the capacity to accommodate RNA in a sequence non-specific manner *(Abbas et al., 2017a)*. Indeed, IFIT5 was co-crystallised with ssRNA oligonucleotides of adenosine, uridine and cysteine, which adopted similar conformations within the RNA binding channel (Appendix A), indicating that IFIT5 can bind those substrates equally *(Abbas et al., 2013)*. However, while IFIT5 bound well to poly-A and poly-U ssRNA, it was unable to bind poly-C RNA in gel shift assays *(Feng et al., 2013)*, indicating that IFIT5 may have a nucleotide preference under certain conditions. There is also evidence that IFIT5 is capable of binding AT-rich dsDNA

with comparable affinity to its ssRNA binding *(Feng et al., 2013)*, though this finding has not been elaborated upon.

Comparison of apo and holo structures reveals that IFIT5 undergoes a conformational change upon RNA binding (Appendix A). The C-terminal domain rotates anticlockwise about the pivot domain, towards the RNA binding channel, creating a more closed structure. Small angle X-ray scattering analysis revealed that IFIT5 adopts a more compact structure in solution when bound to RNA *(Abbas et al., 2013)*. Therefore, unliganded IFIT5 exists in an open conformation, presumably to facilitate RNA entry into the narrow RNA-binding channel, which then closes upon binding.

Despite clear evidence for non-self RNA binding by IFIT5, the role of human IFIT5 in controlling infection has not been well studied. Overexpression of IFIT5 was shown to restrict the replication of VSV, which may be due to binding the 5'ppp genome and inhibiting its replication *(Abbas et al., 2013)*. There also is increasing evidence that IFIT5 in bird species can inhibit influenza A virus infection *(Li et al., 2017; Santhakumar et al., 2018)*, presumably by inhibition of viral RNA synthesis. However, more work is needed to determine the exact role of IFIT5 in human infection.

1.3.3.2 IFIT1 RNA binding

IFIT1 was originally shown to bind 5'ppp RNA with sub-micromolar affinity *(Pichlmair et al., 2011)*. IFIT1 is 55% identical to IFIT5 and shares many of the key RNA binding residues identified in IFIT5 *(Abbas et al., 2013; Kumar et al., 2014)*. IFIT1 was capable of precipitating viral RNA from cells infected with VSV or influenza A virus, both of which possess triphosphate (-)ssRNA genomes. Consistently, knockdown of IFIT1 resulted in higher VSV infectious titres in a number of human cell lines *(Guo and Sen, 2000; Pichlmair et al., 2011; Daugherty et al., 2016; Johnson et al., 2018)* in a manner dependent on its RNA binding capacity *(Pichlmair et al., 2011)*. Similarly, Ifit1 knockout mice showed higher mortality *in vivo* and embryonic fibroblasts, derived from those mice, supported higher VSV replication *(Pichlmair et al., 2011)*.

Binding to 5'ppp RNA genomes may allow IFIT1 to inhibit viral RNA polymerase recruitment, this preventing replication. Indeed, in a cell-based assay, IFIT1 was shown to

partially inhibit influenza A virus polymerase activity *(Abbas et al., 2013)*. However, in this system, initial RNA synthesis is driven from a plasmid DNA template driven by a cellular polymerase, presenting a limitation: the RNA 5' end may not immediately be bound and protected by viral polymerase complexes, as would occur in infection, leaving a window of time for IFIT1 to bind. In infected cells, neither human IFIT1 nor murine Ifit1 were able to restrict influenza A virus replication *(Pinto et al., 2015)*. IFIT1 was also incapable of restricting the replication of a number of cytoplasmic (-)ssRNA viruses, including Ebola virus and Rift valley fever virus *(Abbas et al., 2013; Pinto et al., 2015)*. Furthermore, more recent studies have failed to recapitulate the antiviral effect of IFIT1 on VSV replication *(Li et al., 2009; Fensterl et al., 2012; Daugherty et al., 2016)*, indicating that IFIT1 may not efficiently target 5'ppp RNA genomes.

More recent estimates of IFIT1 affinity for 5'ppp-RNA are much lower, in the micromolar range *(Johnson et al., 2018)*. Instead, IFIT1 was found to have considerably higher affinity for cap0 RNA, which was low nanomolar in several different assay systems *(Habjan et al., 2013; Kumar et al., 2014; Johnson et al., 2018)*. Both human IFIT1 and murine Ifit1 precipitated on capG and cap0 beads *(Habjan et al., 2013)* and murine Ifit1 could bind to cap0 RNA in mobility shift and pulldown assays *(Kimura et al., 2013)*. It was then shown that IFIT1 could form a toeprint on cap0 RNA, but not uncapped or cap1 RNA, in primer extension inhibition assays *(Kumar et al., 2014)*. Similar affinities were independently determined by gel shift assay *(Abbas et al., 2013; Kumar et al., 2014)*. IFIT1 was shown to directly compete with eIF4E for binding to cap0 RNA *(Habjan et al., 2013; Kumar et al., 2014)*, inhibited 48S complex formation on bound transcripts *(Kumar et al., 2014)*, and inhibited cap0-mRNA translation *in vitro (Abbas et al., 2013)*. By contrast, IFIT5 could only inhibit the translation of cap0 transcripts at micromolar concentrations, indicating weaker or non-specific binding *(Abbas et al., 2013)*.

The crystal structure of IFIT1 revealed that IFIT1 possesses a similar positively charged RNA binding tunnel to that of IFIT5 *(Abbas et al., 2013)* (Figure 1-4A-C). The RNA backbone largely adopts the same conformation as IFIT5-bound RNA, with only slight changes in the orientation of the bases themselves. The 5'ppp moiety in IFIT1 is held in an extended conformation, which directs the methylguanosine residue into the cap-binding pocket, described below, compared to the bent conformation coordinated by IFIT5 (Appendix A).

Hydrogen-deuterium exchange assays revealed that longer RNA oligonucleotides make additional contacts with the IFIT1 C-terminal domain, which is also lined with positively-charged residues *(Johnson et al., 2018)*. Mutation of residues within the C-terminal domain partially decreases cap0 binding and translation inhibition by IFIT1 *(Kumar et al., 2014)*, suggesting that this domain contributes to stable RNA binding. It was this C-terminal domain which was originally thought to mediate eIF3 interaction. Deletion of this domain prevented translation inhibition by IFIT1 *(Guo et al., 2000b)*. Together, it seems likely that IFIT1 RNA binding relies on an intact C-terminal domain, which clamps onto bound RNA in the same manner as IFIT5, and this binding is primarily responsible for translation [[inhibition. It is also possible that RNA bound by IFIT1 could non-specifically mediate interactions with other RNA-binding proteins, including eIF3.

Within the N-terminus, IFIT1 has a hydrophobic pocket which extends from the end of the 5'ppp-binding channel and accommodates the 5' cap (Figure 1-4C). IFIT1 has a unique mode of cap coordination, in which the 7-methylguanosine is stacked by a tryptophan residue on one surface, and is coordinated by aliphatic residues on the other (Appendix A). In IFIT1, the cap can be accommodated in both syn- and anti-conformations *(Abbas et al., 2017a)*, and is independent of 7-methylation or even cap nucleotide identity *(Kumar et al., 2014; Abbas et al., 2017a)*. This contrasts with canonical cap-binding proteins, such as eIF4E, which typically sandwich the 7mG residue between two aromatic side chains in the anti-conformation, dependent on specific interactions with the 7-methyl group *(Brown et al., 2009)*.

2'-O-methylation of the first or second RNA nucleotide greatly reduces IFIT1-RNA binding, while methylation of both inhibits binding completely *(Abbas et al., 2017a)*. In filter binding assays, IFIT1 bound cap1 RNA with submicromolar affinity *(Johnson et al., 2018)*, and IFIT1 could inhibit translation of cap1 transcripts at micromolar concentrations *(Abbas et al., 2013)*. However, cap2 transcripts were resistant to translation inhibition, even at micromolar concentrations of IFIT1 *(Abbas et al., 2017a)*. In this way, IFIT1 distinguishes non-self RNA from self.

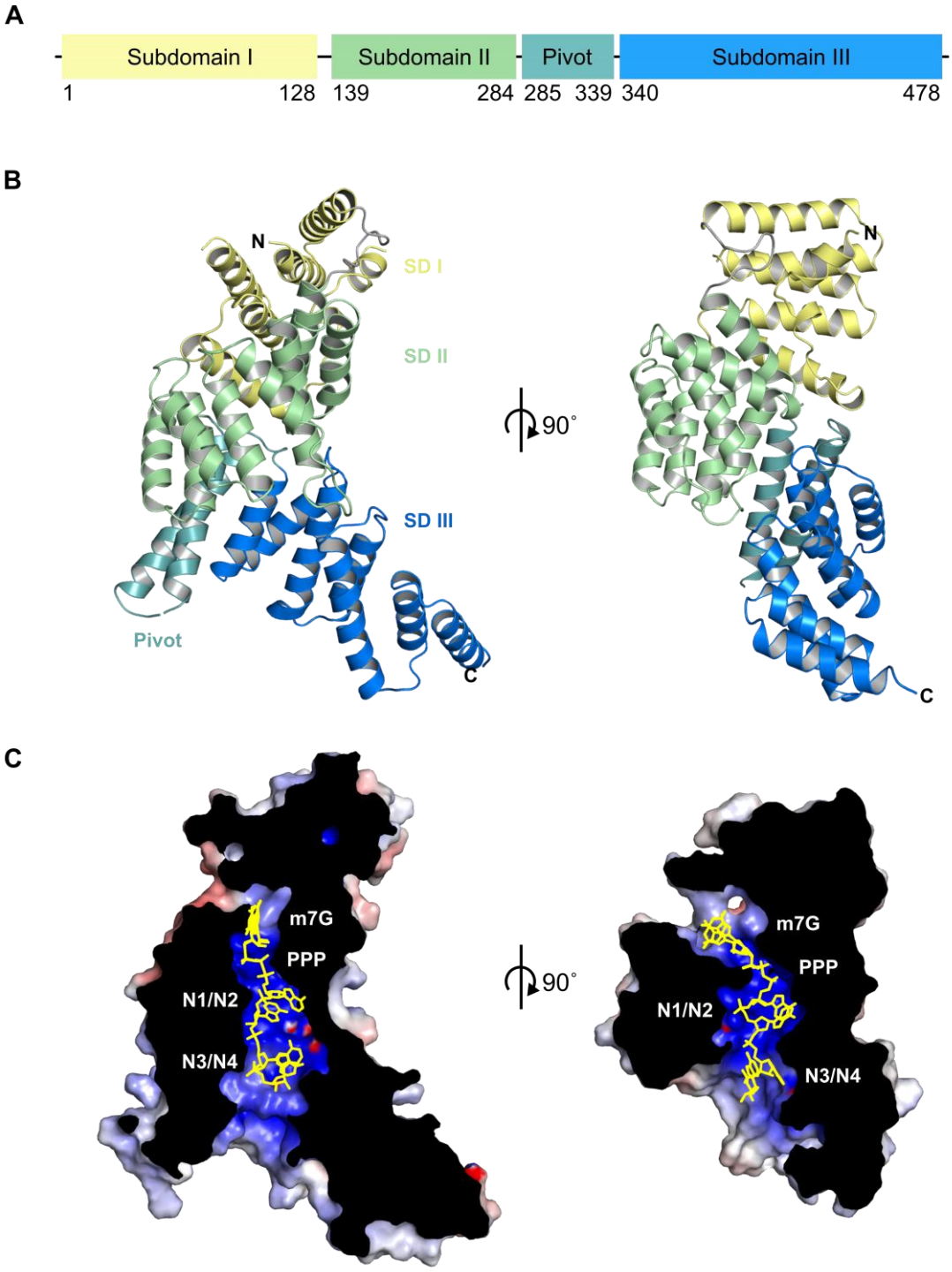

Figure 1-4 IFIT1 RNA binding.

***A**. Domain diagram of human IFIT1. **B**. Cartoon representation of IFIT1 in complex with cap0-oligo(A) (PDB: 5UDI), coloured by subdomain (SD). **C**. Surface cutaway of IFIT1 coloured by electrostatic potential from negative (-10 kTe^{-1}; red) to positive (+10 kTe^{-1}; blue), via hydrophobic (white), generated in APBS using PDB2PQR (Dolinsky et al., 2004). Cross-section is indicated by solid black shading and RNA is shown as yellow sticks. Features of the RNA are annotated: m7G, 7-methylguanosine cap; PPP, 5' triphosphate moiety; N1/N2, first two nucleotides; N3/N4, third and fourth nucleotides.*

Alphaviruses do not encode a 2'-O-methyltransferase and as such have cap0 genomic and subgenomic mRNA *(Dubin and Stollar, 1975; Hefti et al., 1975)*, which should be susceptible to IFIT1 restriction. However, there is a stable stem loop at the very 5' end of the alphavirus genome, which inhibits binding by both human IFIT1 and mouse Ifit1 *(Hyde et al., 2014; Reynaud et al., 2015)*, since it cannot be accommodated in the IFIT ssRNA binding pocket. Inhibition by IFIT1 varies by alphavirus species, according to the stability of the RNA structure in the 5'UTR *(Reynaud et al., 2015)*. Tissue culture-adapted strains, which are typically grown in IFN-deficient cells, contain mutations which destabilise this stem, since less structured 5'UTRs favour RNA replication *(Hyde et al., 2014; Reynaud et al., 2015)*. Therefore mechanisms to avoid recognition by IFIT1 are maintained even at a fitness cost to the virus.

In coronaviruses and flaviviruses, mutation of the virally-encoded 2'-O-methyltransferase has been shown to increase sensitivity to IFIT1. Knockdown of human IFIT1 recovered replication of 2'-O-methyltransferase-deficient human coronavirus (HuCoV) in HeLa cells, while murine Ifit1$^{-/-}$ macrophages supported higher mutant mouse hepatitis virus (MHV) replication, when pre-treated with IFN *(Habjan et al., 2013)*. Pulse labelling experiments demonstrated that viral translation was specifically targeted in 2'-O-methyltransferase mutants *(Habjan et al., 2013)*. Inhibition of these viruses is also influenced by 5' RNA structure, since human IFIT1 inhibited translation of cap0 MHV reporter mRNAs better than HuCoV *(Abbas et al., 2017a)*. MHV possesses a weaker stem-loop (ΔG = -7.8 kCal/mol) with 5 unpaired nucleotides at the 5' end, while HuCoV has a more stable stem (ΔG = -12.1 kCal/mol) with 4 unpaired nucleotides, thereby having a reduced platform for IFIT1 binding.

In murine cells and *in vivo*, a 2'-O-methyltransferase mutant of WNV was attenuated and highly susceptible to type I IFN *(Daffis et al., 2010)*. Murine macrophages lacking Ifit1 rescued replication of 2'-O-methyltransferase mutant of WNV, while knockout of Ifit2 could not *(Daffis et al., 2010; Szretter et al., 2012)*. *In vivo*, 2'-O-methyltransferase-deficient WNV was attenuated in both Ifit1-dependent and –independent manners, subject to differences in cell-type and route of infection *(Szretter et al., 2012)*.

Mouse models have also shown Ifit1-dependent restriction of mutant Japanese encephalitis virus *(Kimura et al., 2013; Li et al., 2013)* and dengue virus *(Züst et al., 2013)*,

both mosquito-borne flaviviruses. Consistently, severe acute respiratory syndrome virus (SARS) *(Menachery et al., 2014)* and Middle East respiratory syndrome virus (MERS) *(Menachery et al., 2017)*, both pathogenic coronaviruses, were attenuated in an Ifit1-dependent manner when the viral 2'-O-methyltransferase was mutated. In one of these studies, this phenotype was also observed in macaques, and provided full protection against homologous challenge after 64 days. Mutation of the viral 2'-O-methyltransferase therefore provides a framework for the development of new live attenuated vaccine strains for high-risk emerging pathogens.

While alpha-, flavi- and coronaviruses typically require mutation for IFIT susceptibility, human IFIT1 was found to restrict replication of wildtype parainfluenza virus 5 (PIV5). PIV5 is a segmented negative-sense ssRNA virus from the family *Paramyxoviridae*, which transcribes, caps and methylates its messages in the cytoplasm. Overexpression of IFIT1 in human cells prevented PIV5 protein expression, and knockdown of IFIT1 rescued IFN-dependent viral restriction *(Andrejeva et al., 2013)*. Interestingly, when total RNA from PIV5-infected cells was translated *in vitro*, IFIT1 selectively inhibited translation of some mRNA segments, particularly the matrix (M) protein *(Young et al., 2016)*, a viral particle budding factor. Knockdown of IFIT1 also disrupted the formation of viral cytoplasmic bodies *(Andrejeva et al., 2013)*, which may be linked to the establishment of viral persistence in infected cells *(Carlos et al., 2009)*. This indicates that PIV5 may direct IFIT1 restriction, to promote the establishment of persistent infection.

It was later shown that other members of the genus *Rubulavirus*, including PIV2 and mumps virus, were similarly sensitive to IFIT1 restriction while non-rubulavirus paramyxoviruses, such as canine distemper virus and PIV3, were resistant *(Young et al., 2016)*. Rubulaviruses have polymorphisms in their 2'-O-methyltransferases which may alter their methylation efficiency, leading to a pool of viral mRNAs with unmethylated caps which are sensitive to IFIT1. Indeed, methylation of mumps virus mRNA extracted from infected cells partially rescued translation in the presence of IFIT1, indicating that the viral transcripts are not efficiently methylated *(Young et al., 2016)*. In an independent study, it was shown that PIV3 could be restricted by overexpression of IFIT1, indicating that IFIT1 may have wider antiviral activity against members of the paramyxoviridae.

1.3.3.3 IFIT2 RNA binding

IFIT2 is homodimeric in solution and interacts via a domain swap in the N-terminus, in which one and a half TPR motifs are exchanged between each monomer *(Yang et al., 2012)* (Figure 1-5A-B). The C-terminal domain is lined with positively charged residues on the inner face, resulting in a wide RNA binding surface formed between both monomeric units of the homodimer (Figure 1-5C). As such IFIT2 binds to RNA in a manner distinct from IFIT1 or IFIT5.

In gel shift assays, IFIT2 bound strongly to short dsRNA templates comprising repetitive AU sequences, but not GC sequences. IFIT2 also did not bind to corresponding poly(AT) dsDNA or annealed oligo(A)-oligo(U) dsRNA *(Yang et al., 2012)*. Binding was shown to be independent of the triphosphate moiety at the 5' end, indicating that IFIT2 binding is internal to the RNA. Consistently, IFIT2 did not produce a 5' toeprint on ssRNA with different 5' ends *(Kumar et al., 2014)* and could not inhibit the translation of uncapped reporter mRNA *in vitro (Yang et al., 2012)*. IFIT2 was shown to reduce infection by Newcastle disease virus, a zoonotic paramyxovirus, in a manner dependent on RNA binding. The exact mechanism of restriction was not determined.

This preference for AU-rich RNA sequences raises the possibility that IFIT2 may play a role in regulating mRNA with AU-rich elements (AREs) in their 3'UTRs. Indeed, IFIT2 was shown to bind a defined ARE, which comprises an AUUUA tandem repeat, in a gel shift assay *(Yang et al., 2012)*. AREs act as degradation signals for labile mRNAs, since they promote rapid deadenylation, as well as directing degradation-independent translation inhibition, through the action of different ARE-binding proteins *(Shaw and Kamen, 1986; Xu et al., 1997; Barreau et al., 2005)*. They are found in genes which require short, regulated bursts of expression, such as cytokines TNFα and IL-6. Murine Ifit2 has been described to both positively *(Siegfried et al., 2013)* and negatively *(Berchtold et al., 2008)* regulate TNFα and IL-6 expression. The message encoding the pro-apoptotic protein Bcl-2 also contains AREs in its 3'UTR. Human IFIT2 has been reported to simulate apoptosis in a Bcl-2 dependent manner *(Stawowczyk et al., 2011; Chen et al., 2017)*. It is therefore possible that

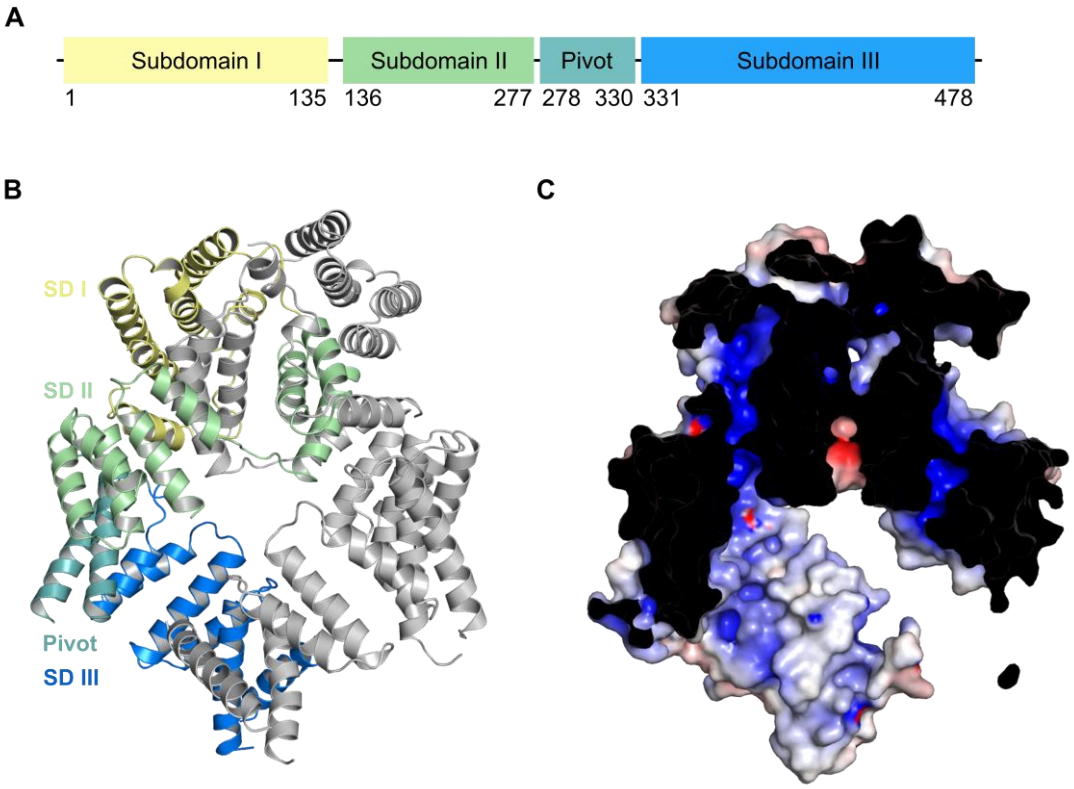

Figure 1-5 IFIT2 RNA binding.

A. *Domain diagram of human IFIT2.* ***B.*** *Cartoon representation of IFIT2 (PDB: 4GIT), coloured by subdomain (SD).* ***C.*** *Surface cutaway of IFIT2, coloured by electrostatic potential from negative (-10 kTe^{-1}; red) to positive (+10 kTe^{-1}; blue), via hydrophobic (white), generated in APBS using PDB2PQR (Dolinsky et al., 2004). Cross-section is indicated by solid black shading.*

IFIT2 may stabilise Bcl2 mRNA or affect its translation to promote apoptosis induction. While stabilisation of mRNA by IFIT2 binding is an intriguing possibility, this has not yet been formally demonstrated.

1.3.3.4 tRNA binding

tRNA is highly structured, consisting of three stem loops and a 5'-3' panhandle, forming a characteristic L-shaped tertiary fold *(Brown et al., 1985)*. Despite the lack of 5' ssRNA, human IFIT1, rabbit IFIT1 and rabbit IFIT1B were shown to bind to $tRNA_i^{Met}$ in gel shift assays. High concentrations of tRNA could even inhibit IFIT1 binding to cap0 RNA, indicating competitive binding. Binding was relatively specific for $tRNA_i^{Met}$, since $tRNA^{His}$, $tRNA^{Leu}$ and $tRNA^{Lys}$ were much less effective at outcompeting cap0 RNA binding *(Kumar et al., 2014)*. IFIT5 was also shown to bind to $tRNA_i^{Met}$ by gel shift analysis, to a greater

extent than IFIT1 *(Katibah et al., 2013; Kumar et al., 2014)*, while neither human IFIT2 nor murine Ifit2 could bind *(Katibah et al., 2013)*.

From human cell lysates, IFIT5 selectively precipitated a distinct pool of tRNA-sized RNA species, including $tRNA_i^{Met}$ *(Katibah et al., 2013)*. Deep sequencing analysis showed that IFIT5 preferentially binds aberrant tRNAs, especially those with poorly trimmed 5' leader sequences, suggesting that IFIT5 may play a role in tRNA quality control and surveillance *(Katibah et al., 2014)*. IFIT5-RNA precipitates included a number of incorrectly-sized $tRNA_i^{Met}$ species, consistent with tRNA base modification and 3' poly-U tailing *(Katibah et al., 2014)*. Polyuridylation is an RNA degradation signal *(Norbury, 2010)*, indicating that IFIT5 may promote turnover of aberrant tRNA in the cytoplasm. However, bound tRNAs were spliced, since intron sequences were not detected in the RNAseq analysis, indicating that IFIT5 binds poorly trimmed tRNAs that have been exported from the nucleus, rather than binding nuclear pre-tRNAs.

Mutation of 5'ppp binding residues in the N-terminus of IFIT5 shifted the RNA binding preference to mature tRNA species *(Katibah et al., 2014)*. As such, IFIT5 probably engages mature tRNA with a different binding surface to ssRNA binding. A large positively charged patch on the C-terminus of IFIT1 and IFIT5, which occludes the entrance to the ssRNA binding channel, has been suggested to mediate this interaction with mature tRNA *(Katibah et al., 2014; Kumar et al., 2014)*. For IFIT5 this interaction was mapped to the last two C-terminal TPRs *(Katibah et al., 2013)*.

1.4 Mouse models

The first murine Ifit family members were described shortly after the discovery of human IFIT1 *(Bluyssen et al., 1994a)*. The mouse Ifit family has six annotated members: Ifit1, Ifit1b, Ifit1c, Ifit2, Ifit3 and Ifit3b which are clustered on chromosome 19C1 *(Fensterl and Sen, 2011)*. Of these, Ifit1, Ifit2 and Ifit3 have been well-studied, owing to their sequence similarity with human IFIT1, IFIT2 and IFIT3. On this basis, these genes have been considered to be homologous, and murine Ifit1 in particular has been used extensively as a model for human IFIT1 function. The contribution of Ifit1b, Ifit1c and Ifit3b to the murine antiviral programme is as yet unknown.

Many studies have focussed on murine Ifit1 to examine its effect on human diseases *(Daffis et al., 2010; Szretter et al., 2012; Kimura et al., 2013; Li et al., 2013; Hyde et al., 2014; Hu et al., 2016)*. A number of other studies have concurrently examined both human IFIT1 and murine Ifit1. While many reported similar phenotypes in both species *(Züst et al., 2013; Menachery et al., 2014, 2017; Pinto et al., 2015; Reynaud et al., 2015; White et al., 2016)*, others have noticed differences in the activity of human IFIT1 and murine Ifit1 *(Habjan et al., 2013; Daugherty et al., 2016)*. Murine Ifit2 has also been used as an *in vitro* model for infectious disease *(Fensterl et al., 2012; Cho et al., 2013; Siegfried et al., 2013; Jia et al., 2017; Stawowczyk et al., 2018)*, despite little biochemical data supporting shared functions of the two proteins. As discussed above, the use of 2'-O-methyltransferase mutant viruses is a promising tool for rational attenuation, in an effort to produce new vaccine strains. Therefore, a complete understanding of the antiviral mechanism of the murine Ifit family is necessary to properly interpret the results from mouse models before trials in humans are pursued.

1.4.1 Differences between human and murine IFIT families

Mice, along with other small rodents including other murids, cricetids (hamsters, voles etc) and squirrels, have lost the gene for IFIT5 *(Liu et al., 2013)*. Recent phylogenetic has revealed that human IFIT1 and murine Ifit1 may not be orthologous, as previously thought *(Daugherty et al., 2016)*. The IFIT1 gene was duplicated approximately 100 million years ago, before the radiation of the placental mammals, generating two paralogous genes: IFIT1 and IFIT1B *(Liu et al., 2013; Daugherty et al., 2016)*. Owing to the high similarity of the two genes, considerable recombination has occurred between IFIT1 and IFIT1B, particularly in the 5' two-thirds of the gene, resulting in homogenised 5' sequences and divergent 3' sequences *(Daugherty et al., 2016)*. When only the divergent 3' end of the gene was analysed, this revealed that genes annotated as 'Ifit1' or 'Ifit1-like' in mice and other rodents actually cluster with Ifit1b genes from other species (Figure 1-6). As such these 'Ifit1' genes are descended from the ancestral IFIT1B, and IFIT1 has been lost entirely. Subsequently, in mice Ifit1b has undergone duplication to yield three paralogous: Ifit1, Ifit1b and Ifit1c (also known as Ifit1b1, Ifit1b2 and Ifit1b3 to reflect their evolutionary origins).

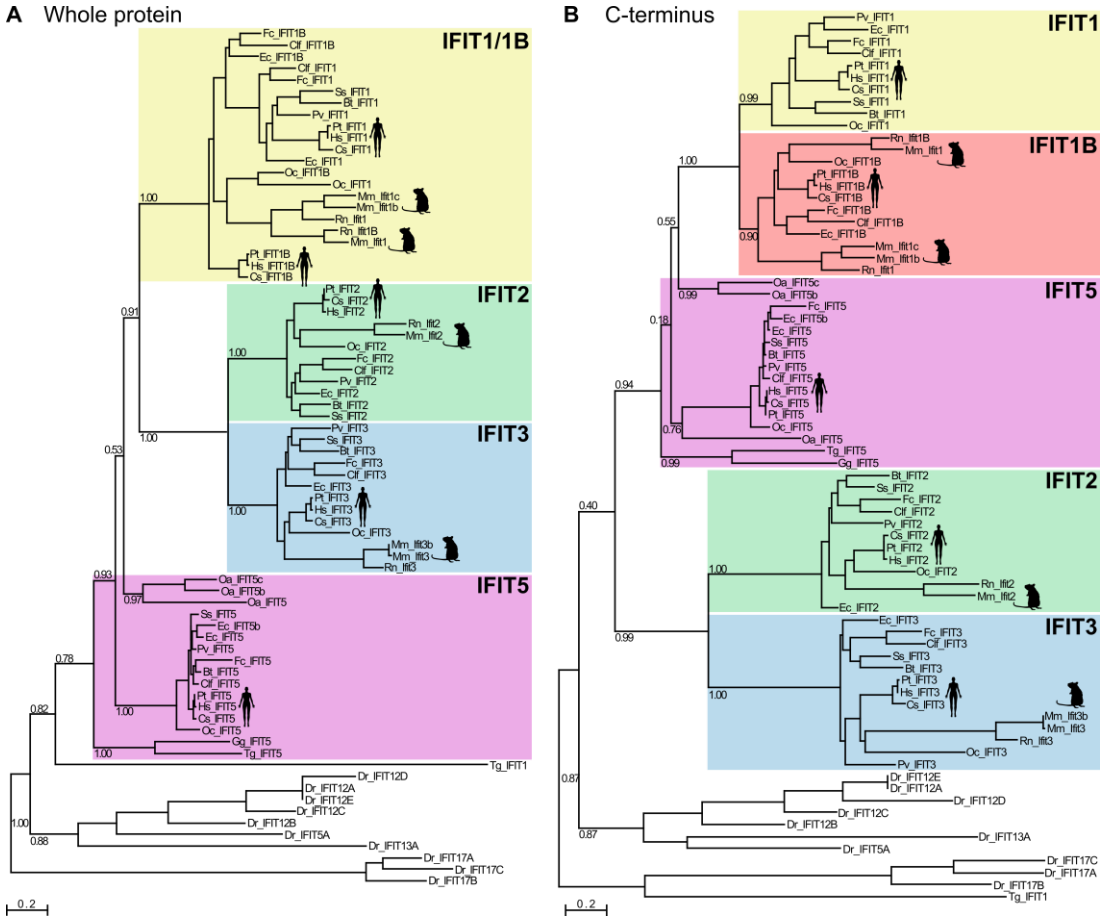

Figure 1-6 The IFIT family.

A maximum-likelihood tree was constructed using PhyML, based on 74 IFIT protein sequences from different mammals (Hs, human; Pt, chimpanzee; Cs, African green monkey; Mm, mouse; Rn, rat; Oc, rabbit; Pv, flying fox; Fc, cat; Clf, dog; Ss, pig; Bt, cow; Ec, horse; Oa, platypus) and representative bird (Gg, chicken; Tg, zebra finch) and fish (Dr, zebrafish) species. Alignments were made in MUSCLE using ***A.*** *whole protein sequences, or* ***B.*** *C-terminal sequences excluding amino acids 1-280 (subdomains I and II), to properly distinguish IFIT clusters. Bootstrap supports are shown for major branches. Scale bars represent amino acid substitutions per position.*

Human IFIT1 and murine Ifit1 have slightly different biochemical activities. Growth of yeast, which does not have 2'-O-methylated mRNA, was completely inhibited by ectopic expression of murine Ifit1, consistent with cap0-RNA binding *(Daugherty et al., 2016)*. Inhibition was completely relieved on expression of human cap1 methyltransferase. While human IFIT1 also potently inhibited yeast growth, consistent with its characterised cap0 binding function *(Habjan et al., 2013; Kumar et al., 2014; Abbas et al., 2017a)*, growth could not be rescued upon overexpression cap1 methyltransferase, indicating that human IFIT1 can also inhibit the translation of cap1 transcripts *(Daugherty et al., 2016)*. This is

consistent with *in vitro* data showing that, at high concentrations, IFIT1 is capable of inhibiting cap1 but not cap2 translation *(Abbas et al., 2017a)*.

There is some confusion in the literature over which viruses can be restricted by human IFIT1 or murine Ifit1 (see Table 1-2). Daugherty et al. *(2016)* found that overexpression of human IFIT1 could inhibit the replication of wild-type VSV, which encodes its own 2'-O-methyltransferase, but murine Ifit1 could not. Consistently, murine Ifit1 was previously shown to have little effect on VSV during sublethal infection in mice *(Fensterl et al., 2012)*. However when infected at a high multiplicity, Ifit1 knockout mice were more susceptible to lethal infection, indicating that murine Ifit1 may also control wildtype VSV *(Pichlmair et al., 2011)*. Other studies have also shown little effect of human IFIT1 alone during VSV infection *(Guo et al., 2000b; Li et al., 2009; Johnson et al., 2018)*, further complicating interpretation of these results.

Similarly, there is confusion over the role of IFIT1 in vaccinia virus infection. In one study, murine Ifit1 was capable of inhibiting the replication of a vaccinia virus strain with mutant 2'-O-methyltransferase, when overexpressed in human cells *(Daugherty et al., 2016)*. However a previous study showed that overexpression of Ifit1 had no effect on vaccinia replication in and ex vivo *(Daffis et al., 2010; Szretter et al., 2012)*. Unexpectedly, overexpressed human IFIT1 was found not to inhibit 2'-O-methyltransferase-deficient vaccinia virus but could inhibit replication of the wildtype cap1 virus *(Daugherty et al., 2016)*, contrary to the described biochemical activity of IFIT1 *(Kumar et al., 2014; Abbas et al., 2017a)*.

There is a lack of data concerning the function of other murine Ifit family members. While human IFIT2 was shown to bind AU-rich dsRNA in a 5'-independent manner *(Yang et al., 2012)* and there is some evidence that murine Ifit2 may also regulate mRNAs with AREs in their 3'UTRs *(Berchtold et al., 2008; Siegfried et al., 2013)*. One study observed that overexpression of murine Ifit2 could restrict wildtype and 2'-O-methyltransferase deficient strains of vaccinia virus, WNV, and MHV *(Daffis et al., 2010)*. Cap0 mutant viruses appeared more susceptible to restriction, suggesting a role in cap0 binding. However, knockout of Ifit2 had no effect on wildtype or mutant WNV replication, indicating that overexpressed Ifit2 may simply be cytotoxic *(Daffis et al., 2010)*. Another study found that murine Ifit2 could protect against WNV infection by promoting type I

IFN signalling, rather than by RNA binding *(Perwitasari et al., 2011)*, a role that has not been ascribed to human IFIT2.

Finally, murine Ifit3 is shorter than its human homologue, having undergone a 3' deletion during rodent evolution, and therefore lacks a significant portion of the C-terminal subdomain. This deletion is found in all rodent clades in which IFIT1 and IFIT5 have been lost, however the consequence of this deletion, and the role of Ifit3 in mice generally, is unknown. Mice also encode a second Ifit3 paralogue, Ifit3b, which differs from Ifit3 by just five amino acids. Why mice need two almost identical copies of Ifit3, when most other species, including closely related rats, only have one, is also unclear.

1.5 Aims and Scope of the Thesis

IFIT proteins are inextricably linked with innate immunity and play extensive and diverse roles not only in antiviral defence, but also in inflammation, cancer and autoimmunity *(reviewed in Mears and Sweeney, 2018)*. Studying their function *in vivo* is invaluable to properly understand their role in modulating such complex diseases. Given the widespread use of animal models, in particular mice, in biomedical research, it is important to understand how their innate immune systems differ to that of humans in order to properly evaluate the usefulness of data generated by animal studies. However, it is clear that the human and murine IFIT families, while superficially similar, differ in key aspects both in terms of their function and their regulation.

This thesis aims to examine the function and regulation of the murine Ifit family. This will involve characterising the expression patterns of the entire murine Ifit family, as well as assaying their biochemical activity *in vitro*, to determine the role of uncharacterised Ifit protein in modulating translation. To examine how IFIT function is regulated, the ability of IFIT proteins to interact with each other, and the functions of IFIT complexes, will be assessed in both human and mouse. Together, this will allow evaluation of the murine model in studying IFIT biology during viral infection and disease, and provide an understanding of how this model can be interpreted or improved. This study also hopes to reveal novel aspects of IFIT biology, which may contribute to the understanding of both innate immunity and translation regulation.

Table I-2 Antiviral activity of IFIT proteins in human and mouse.

A summary of studies investigating the effect of IFIT proteins during viral infection. Human IFITs are given in upper case, while murine Ifits are in lower case. CDV, canine distemper virus; CHIKV, chikungunya virus; DENV, dengue virus; EBOV, Ebola virus; EMCV, encephalomyocarditis virus; HCMV, human cytomegalovirus; HCoV, human coronavirus; HCV, hepatitis C virus; HEV, hepatitis E virus; HPV, human papilloma virus; HSV, herpes simplex virus; IAV, influenza A virus; JEV, Japanese encephalitis virus; LACV, La Crosse encephalitis virus; MERS, Middle East respiratory syndrome; MHV, murine hepatitis virus; MNV, murine norovirus; MuV, mumps virus; NDV, Newcastle disease virus; OROV, Oropouche virus; PIV, parainfluenza virus; SARS, severe acute respiratory syndrome; SeV, Sendai virus; SINV, Sindbis virus; VACV, vaccinia virus; VEEV, Venezuelan equine encephalitis virus; VSV, vesicular stomatitis virus; WNV, West Nile virus; ZIKV, Zika virus. Adapted from Mears and Sweeney *(2018)*.

Virus	IFIT	Species	Effect
Caliciviridae			
MNV	Ifit1	Mouse	**Antiviral** – Ifit1 knockout increased viral titres *(Mears et al., 2019)*
Coronaviridae			
MERS, SARS, HCoV	IFIT1, IFIT2	Human	**Antiviral** – IFIT1 decreased viral replication and titre by inhibiting translation *(Habjan et al., 2013; Menachery et al., 2014; Abbas et al., 2017a)*. IFIT2 significantly decreased viral titres *(Menachery et al., 2014)*. These effects were moderate for WT viruses but severe for cap0 mutant viruses.
MERS, SARS, MHV	Ifit1, Ifit2	Mouse	**Antiviral** – Ifit1 and Ifit2 inhibited replication of cap0 mutant virus *(Daffis et al., 2010; Züst et al., 2011; Habjan et al., 2013)*. Virus is attenuated *in vivo (Menachery et al., 2014, 2017)*.
Filoviridae			
EBOV	Ifit1	Mouse	**No effect** on viral replication *in vitro* (Pinto et al., 2015).
Flaviviridae			
HCV	IFIT1	Human	**Antiviral** – IFIT1 impaired viral replication by inhibiting translation *(Raychoudhuri et al., 2011; Ishida et al., 2019)*.
WNV, ZIKV, DENV	IFIT1, IFIT3	Human	**Antiviral** – IFIT1 reduced translation of cap0 mutant virus, but not WT *(Daffis et al., 2010; Pinto et al., 2015)*, and was enhanced by coexpression with IFIT3 *(Johnson et al., 2018)*. IFIT3 restricted WT DENV replication *(Hsu et al., 2013)*. IFIT1 and IFIT3 restricted WT ZIKV infection *(Wichit et al., 2019)*.
WNV, JEV, DENV	Ifit1, Ifit2	Mouse	**Antiviral** – Ifit1 inhibits translation and replication of cap0 mutant virus *(Daffis et al., 2010; Szretter et al., 2012; Kimura et al., 2013)*, resulting in attenuation *in vivo (Li et al., 2013; Züst et al., 2013)*. Ifit2 decreased WNV replication *in vitro (Daffis et al., 2010)* and neuropathology *in vivo (Cho et al., 2013)*.
Herpesviridae			
HCMV	IFIT1	Human	**Antiviral** – decreased viral titre *(Zhang et al., 2017a)*.
HSV-1	IFIT3	Human	**Antiviral** – viral UL41 protein downregulates IFIT3. IFIT3 impaired replication of UL41 virus *(Jiang et al., 2016)*.

Orthomyxoviridae			
IAV	IFIT1, Ifit1	Human, Mouse	**No effect** – IFIT1 decreased polymerase activity *in vitro (Pichlmair et al., 2011)* but had no effect on viral titres (Pinto et al., 2015). Viral replication and pathology was unaffected *in vivo* (Pinto et al., 2015).
Papillomaviridae			
HPV	IFIT1	Human	**Antiviral** – IFIT1 bound the viral helicase E1 and impaired DNA replication *(Terenzi and Saikia, 2008; Saikia et al., 2010)*.
Paramyxoviridae			
MuV, PIV2, PIV5	IFIT1	Human	**Antiviral** – IFIT1 inhibited translation and replication of WT Rubulaviruses *(Young et al., 2016)*.
CDV, SeV, PIV3	IFIT1, IFIT3	Human	**No effect** on translation or replication of non-Rubulavirus family members *(Young et al., 2016)*. IFIT3 had no effect on SeV replication *(Jiang et al., 2016)*.
PIV3	IFIT1	Human	**Antiviral** – IFIT1 and IFIT3 inhibited viral protein expression and infectivity *(Rabbani et al., 2016)*.
NDV	IFIT2, IFIT3, IFIT5	Human	**Antiviral** – IFIT2 *(Yang et al., 2012)*, IFIT3 *(Liu et al., 2011; Zhang et al., 2013)* and IFIT5 *(Zhang et al., 2013)* inhibited viral replication.
Peribunyaviridae			
LACV, OROV	Ifit1	Mouse	**No effect** on viral replication *in vitro* and *in vivo* (Pinto et al., 2015).
Picornaviridae			
EMCV	IFIT1, Ifit1, Ifit2	Human, Mouse	**No effect** on viral translation *(Hui et al., 2003)* or replication *in vitro* and *in vivo (Guo et al., 2000a; Daffis et al., 2010; Pichlmair et al., 2011; Fensterl et al., 2012).*
EMCV	IFIT3	Human	**Antiviral** – slightly decreased viral titres *(Schmeisser et al., 2010)*.
HEV	IFIT1	Human	**Antiviral** – slightly decreased viral replicon replication *(Pingale et al., 2019)*.
Poxviridae			
VACV	IFIT1, Ifit1	Human, Mouse	**No effect** on viral translation or replication *in vitro* and *in vivo (Daffis et al., 2010; Daugherty et al., 2016)*.
VACV	Ifit1, Ifit2	Mouse	**Antiviral** – Ifit1 and Ifit2 restricted replication of cap0 mutant virus *(Daffis et al., 2010; Daugherty et al., 2016)*
Rhabdoviridae			
VSV	IFIT1, IFIT2, IFIT3, IFIT5	Human	**Antiviral** – decreased viral replication *(Guo et al., 2000a; Pichlmair et al., 2011; Feng et al., 2013; Daugherty et al., 2016)*. IFIT1 restriction was enhanced by coexpression with IFIT3 *(Johnson et al., 2018)*.
VSV	Ifit1, Ifit2	Mouse	**Antiviral** – decreased viral titres *in vitro* and reduced disease pathology *in vivo* during fatal infection *(Pichlmair et al., 2011)*. Ifit2 protected mice from viral neuroinvasion and disease pathology *(Fensterl et al., 2012)*.
VSV	Ifit1	Mouse	**No effect** on viral replication *in vitro (Daugherty et al., 2016)* and no effect on pathology or replication during sublethal infection *in vivo (Fensterl et al., 2012)*.
VSV	IFIT1, IFIT2	Human	**Proviral** – slight increase in viral titres *(Li et al., 2009)*.
Togaviridae			
CHIKV	IFIT1, IFIT2, IFIT3	Human	**Antiviral** – IFIT1, IFIT2 and IFIT3 decreased viral replication and virion production *(Wichit et al., 2019)*.

VEEV	IFIT1	Human	**Antiviral** – TC83 strain was susceptible to translation inhibition by IFIT1 *(Reynaud et al., 2015)*. Effect was enhanced by coexpression with IFIT3 *(Johnson et al., 2018)*.
VEEV, CHIKV, SINV	Ifit1	Mouse	**Antiviral** – inhibited translation and replication of viruses with unstable 5'UTR RNA structure *(Hyde et al., 2014; Reynaud et al., 2015)*.
VEEV	Ifit2	Mouse	**No effect** on viral replication *(Reynaud et al., 2015)*.

2 MATERIALS AND METHODS

2.1 Plasmids

Plasmids used in this study, including restriction sites used for cloning and any tags or other features, are listed in Table 2-1. Accession numbers for insert sequences are listed in Table 2-2.

2.2 Cell lines

Human embryonic kidney (HEK293T), murine macrophage-like (RAW264.7) and murine embryonic fibroblast (MEF) cell lines were maintained in Dulbecco's modified Eagle's medium (DMEM) with 4.5 mg/mL glucose supplemented with 10% foetal calf serum, 2 mM L-glutamine, 100 SI units/mL penicillin and 100 μg/mL streptomycin. Murine 17C1 cells, which are derived from spontaneously transformed BALB/c 3T3 fibroblasts *(Sturman and Takemoto, 1972)*, were maintained in DMEM with 1 mg/mL glucose. For stable isotope labelling of amino acids in cell culture (SILAC), HEK293T cells were cultured in Arg/Lys-free DMEM, supplemented with light (R0K0), medium (R6K4) or heavy (R10K8) amino acids, as described *(Emmott and Goodfellow, 2014)*.

2.2.1 Transfection of mammalian cells

Plasmids (Table 2-1) were transfected into HEK293T cells using lipofectamine 2000 (Invitrogen), at 70-90% confluency in antibiotic-free DMEM. Typically, 2 μg plasmid DNA was transfected per well in a 6 well plate, using 2:1 lipofectamine reagent volume to

plasmid mass. For RAW264.7 cells and 17C1 cells, to improve efficiency, transfection was performed in a low volume of Opti-MEM, using lipofectamine 2000 (Invitrogen) at a ratio of 1:1. Media was changed after 3 hours to reduce cytotoxicity.

2.2.1.1 SILAC immunoprecipitation

$1x10^7$ SILAC-labelled HEK293T cells were transfected with 10 μg pCDNA3.1-IFIT plasmid DNA using Lipofectamine 2000 (ThermoFisher). After 24 hours, media was replaced to contain 1000 U/mL human interferon α-2a for a further 16 hours (Roferon-A, Roche). Cells were harvested in lysis buffer (50 mM Tris pH 7.5, 150 mM NaCl, 1 mM EDTA, 1 % Triton-X100) containing 1:200 Protease Inhibitor Cocktail Set III (Merck) and 1:200 Benzonase nuclease (Sigma-Aldrich). Lysates were normalised to 3 mg/mL of protein before incubation with anti-FLAG-M2 affinity gel (Sigma-Aldrich) at 4 °C overnight. Beads were washed 3 times in T-ris-buffered saline, then resuspended in 2x SDS-sample buffer and boiled for 5 minutes to elute bound proteins. Samples were combined, then submitted to the Proteomics Facility of the University of Bristol for liquid chromatography tandem mass spectrometry analysis (LC-MS/MS). Data analysis was performed by Dr Edward Emmott, as described *(Emmott and Goodfellow, 2014; Fleith and Mears et al., 2018)*.

2.2.1.2 RNA transfection

For human IFIT translation inhibition assays, $1x10^6$ HEK293T cells were transfected with FLAG-tagged IFIT1 and IFIT3 expression plasmids as indicated (Table 2-1), in triplicate. After 24 hours, cells were trypsinised and $1.5x10^5$ cells per well were plated into a 48 well plate, in duplicate. After 4 hours, cells were washed into Opti-MEM (Thermofisher) and transfected with 100 fmol each cap0-ZIKV-Fluc and cap1-ZIKV-Nluc RNA using Lipofectamine 2000, or left untreated (mock), for 6 hours before harvesting in passive lysis buffer (Promega). Fluc signal was detected using firefly luciferase reagent and Nluc signal was detected using the Nano-Glo luciferase assay system (Promega) with a Glomax luminometer (Promega). Luciferase values are expressed as a ratio of Fluc (cap0) divided by Nluc (cap1), normalised to the empty vector control.

2.2.1.3 Puromycin labelling

For puromycylation assays, 17C1 cells were transfected with 2 μg per well pCDNA3.1-FLAG-Ifit1, -Ifit1b or Ifit1c, or empty pCDNA3.1, using lipofectamine 2000. After 16 hours, nascent

proteins were labelled using puromycin at 5 μg/ml for 4 hours. Cells were harvested by washing in phosphate-buffered saline (PBS) and lysis in passive lysis buffer. Puromycin signal was detected by immunoblotting, as described below, and was quantified using ImageJ, normalised to total protein signal and/or tubulin.

2.2.1.4 Recombinant interferon production

To generate recombinant murine IFNβ, HEK293T cells were transfected with 10 μg pCDNA3.1-mIFNb using lipofectamine 2000. Supernatant was harvested after 24 hours, aliquoted, and stored at -70 ˚C.

2.2.1.5 Ifit promoter assays

For promoter assays, RAW264.7 cells and 17C1 cells were transfected at 70% confluency with 800 ng pGL3-Ifit promoter plasmid and 200 ng pRLTK Rluc expression plasmid in 24 well plates (Table 2-1). After 6 hours, cells were stimulated with 1:100 recombinant IFNβ in fresh media. Cells were harvested after 24 hours by washing in PBS and lysis in passive lysis buffer (Promega). Promoter activity was measured using the Dual-Glo luciferase assay system (Promega) with a Glomax luminometer (Promega). Fluc signal was normalised to Rluc signal and fold changes were calculated between IFN-treated and mock-treated wells.

2.2.1.6 Ifit co-expression

For Ifit co-expression studies, 17C1 cells were seeded onto glass coverslips to 50% confluency before transfection with 2 μg per well with pCDNA-eGFP-Ifit coexpression plasmids (Table 2-1). After 24 hours, coverslips were fixed and stained for immunofluorescence microscopy, as described below, and surrounding cells from the same well were harvested for immunoblotting in passive lysis buffer.

2.2.2 Ifit induction assays

To examine Ifit expression in murine cell lines, MEFs and RAW264.7 cells were stimulated with 1:100 recombinant IFNβ or transfected with 1 μg/mL polyI:C, using lipofectamine 2000 (Invitrogen). Cells were washed twice in PBS and harvested in passive lysis buffer (Promega), at the indicated time points, for qPCR or immunoblot analysis, described

below. 17C1 cells were stimulated with increasing concentrations of recombinant IFNβ and harvested after 24 hours for immunoblot analysis.

2.2.3 Virus infections

Recombinant mouse hepatitis virus strain A59 (MHV-A59) was a gift from Dr Nerea Irigoyen, derived from a full-length cDNA clone, as described *(Coley et al., 2005; Irigoyen et al., 2016)*. Cells were transfected as described in section 2.2.2.4. After 16 hours, cells were infected at a multiplicity of infection (MOI) of 3 PFU/cell in low glucose DMEM containing 50 μg/mL DEAE-dextran and 0.2% bovine serum albumin (BSA). After 45 minutes at 37 ˚C, inoculum was removed and replaced with media. After the indicated times (Table 2-5) supernatants were harvested by freezing, cells on coverslips were processed for immunofluorescence microscopy and remaining cells in the well were washed twice in PBS and harvested in passive lysis buffer (Promega) for immunoblot analysis, as described below.

2.2.3.1 Plaque assay

MHV titres were determined by plaque assay. 17C1 cells were seeded to 80-90% confluency before infection with ten-fold serial dilutions of supernatants from MHV infection experiments. Virus adsorption was carried out in 200 μL per well of a 12-well plate, in low glucose DMEM containing 50 μg/mL DEAE-dextran and 0.2% BSA, for 45 minutes at 37 ˚C with occasional agitation. Inoculum was then replaced with low glucose DMEM mixed 2:1 with 3 % agarose (1 % agarose final), and left to set. After 16 hours, cells were fixed in formal saline for 2 hours, then agar plugs were removed and cells were stained with 0.1 % toluidine blue for 1 hour. Stained cells were rinsed in water before drying, imaging and counting.

2.3 qPCR primer design and validation

qPCR primers were designed to detect Ifit1b, Ifit1c, Ifit2, Ifit3 and Ifit3b, within the coding sequence of the second exon (Table 2-3). Regions of high nucleotide diversity were chosen to maximise specificity. Primers for Ifit1 have been described *(Tamassia et al., 2008)* targeting sequences within the 5'UTR. GAPDH was used to normalise against and Viperin was included as a positive control for IFN induction.

End-point PCR was performed using Taq polymerase (Invitrogen) on 10 ng pTriEx1.1-Ifit template plasmid to verify primer specificity. pTriEx1.1-Ifit plasmids were then linearised with XhoI and gel extracted for use in a DNA standard curve. Serial dilutions were made from 100 ng (1.5×10^{10} copies) to 10 ag (1.5 copies) of DNA per well and qPCR was performed as described below. Linear regression was performed on CT values plotted against $\log_{10}$-transformed DNA mass, to ensure PCR efficiency was within acceptable parameters (90-110%). Finally, qPCR was performed on cDNA from RAW264.7 cells treated with 1:100 IFNβ for 8 hours, as described below. qPCR products were purified by gel extraction, then sent for Sanger sequencing, using the qPCR primers as sequencing primers, to verify target specificity.

2.3.1 RT-qPCR

RNA was extracted from cell lysates in passive lysis buffer, using 2.5 volumes TRI reagent (Sigma) with 0.75 volumes chloroform, according to the manufacturer's protocol. Care was taken to not disturb the interface when taking the aqueous layer, to avoid genomic DNA contamination. Where RNA was extracted from low cell numbers, 10 μg GlycoBlue and 10 μg heterogeneous yeast tRNA (Ambion) was included to aid precipitation. RNA was resuspended in 40 μL MQW.

5 μL total RNA was annealed to 500 pmol random hexamers by heating to 75 ˚C for 5 minutes before snap-cooling on ice. cDNA was generated using 100 U M-MLV reverse transcriptase (Promega) with 1 mM dNTPs in 25 μL reactions. Reverse transcriptions were incubated at 37 ˚C for 60 minutes before heat inactivation at 95 ˚C for 5 minutes, then diluted 1:4 in water. qPCR was performed on 5 μL cDNA mixed with 100 nM forward and reverse primers, using the qPCR core kit for SYBR green I with low ROX passive reference (Eurogentec), with the manufacturer's recommended parameters: 95 ˚C for 15 seconds then 60 ˚C for 1 minute, for 50 cycles. Data were normalised against GAPDH and expressed as fold change over mock (2^{-ddCq}).

2.4 SDS-PAGE and immunoblotting

Proteins were separated by electrophoresis in 10 %, 12.5 % or 15 % SDS-polyacrylamide gels. Electrophoresis was typically carried out at 180 V for 55 minutes in 0.5x Gringo buffer (12.5 mM Tris, 115 mM glycine, 0.05% w/v SDS, pH 8.3). Where similarly-sized proteins were difficult to resolve (Figure 6-3E and Figure 6-4C-D), proteins were separated on precast 4-12 % NuPAGE Bis-Tris gels (Invitrogen) in MES buffer, at 180V for 110 minutes at 4 ˚C. Gels were stained using coomassie brilliant blue R, destained in 25% ethanol and imaged using a LiCor Odyssey imaging system.

To normalise cell lysates for immunoblotting, protein concentration was determined by BCA assay (Pierce) against a BSA standard curve. Typically 5-15 μg total cellular protein was loaded per well. Separated proteins were transferred to 0.45 μm nitrocellulose membrane (GVS Filter Technology) using a Trans-Blot SD semi-dry electrophoretic cell (BioRad). Where applicable, to visualise total protein, membranes were stained using REVERT (Li-Cor), according to the manufacturer's protocol, imaged on an Odyssey CLx Imaging System (Li-Cor), then destained using the REVERT destain solution (Li-Cor). Membranes were blocked using 5 % milk in PBS with 0.1 % tween-20 (PBST) for 1 hour at room temperature, then rinsed in PBST, before incubation with antibodies as described in Table 2-5. Primary antibodies were typically incubated in 5 % BSA PBST at 4 ˚C overnight while secondary antibodies were incubated in PBST at room temperature for one hour. Membranes were washed three times with PBST after each antibody, then rinsed in PBS and distilled water before imaging on an Odyssey CLx Imaging System. The HRP-conjugated anti-FLAG was visualised by chemiluminescence using 2 mL Westar Sun reagent (Cyanagen) per membrane, with Super RX-N film (Fujifilm).

2.5 Immunofluorescence microscopy

Cells were seeded onto glass coverslips for a final confluency of 50-80 % at the end of the experiment, and transfected or infected, as described above. Cells were fixed in 3 % paraformaldehyde in PBS for 15 minutes, then permeabilised in 0.1 % triton X-100 in PBS, with 50 mM NH_4Cl to quench aldehydes, for a further 15 minutes. Cells were blocked in PBS with 0.2 % fish gelatin, 0.02% NaN_3 and 0.01% triton X-100 (PGAT) for 10 minutes or overnight at 4 ˚C. Cells were stained with antibodies according to Table 2-5, and washed 3 times in PGAT after each antibody. Finally, coverslips were washed in PBS, then water,

before mounting onto slides using ProLong Gold Antifade Reagent with 4′,6-diamidino-2-phenylindole (DAPI) (Invitrogen). Slides were visualised using either a 10x objective or 60x oil immersion objective of an Olympus IX81 wide field microscope, using the Image-Pro Plus software.

2.6 RNA preparation

Plasmids were linearised as indicated in Table 2-1. RNA was transcribed from 0.5 – 2 μg linearised template using 50 ng/μL recombinant T7 RNA polymerase in transcription buffer (40 mM HEPES pH 7.5, 32 mM MgOAc, 40 mM DTT, 2 mM spermidine, 7.5 mM ATP, 7.5 mM CTP, 7.5 mM GTP, 7.5 mM UTP, and 0.2 U/μL RNaseOUT (Invitrogen)). Reactions were incubated for up to 18 hours at 37 ˚C, before treatment with 0.1 U/μL DNaseI (Roche) in the presence of 1x DNaseI buffer (or 1 mM $CaCl_2$). RNA was extracted using 1 volume phenol:chloroform:isoamylalcohol (25:24:1) pH 4.5 and precipitated in 2 volumes 100 % ethanol with 0.1 volumes 3 M NaOAc pH 4.8. Precipitated RNA was washed once with 70 % ethanol before resuspension in MQW. Residual nucleotides were removed using Illustra MicroSpin G-50 columns (GE Healthcare).

2.6.1 Transcription of RNA oligonucleotides

Short RNA transcripts were transcribed from negative strand DNA oligonucleotide templates, containing a 3' negative strand T7 promoter sequence (Table 2-4). These templates were annealed to DNA a oligonucleotide bearing the positive strand T7 promoter sequence by heating together at 75 ˚C for 5 minutes before snap-cooling on ice. RNA was transcribed from 5-10 μM annealed DNA oligos, in modified transcription buffer (500 ng/μL T7 polymerase, 40 mM HEPES pH 7.5, 13.4 mM MgOAc, 40 mM DTT, 2 mM spermidine, 0.6 mM ATP, 4 mM CTP, 6 mM GTP, 0.6 mM UTP, and 0.1 U/μL RNaseOUT (Invitrogen)). Reaction volumes were typically 1-5 mL. Transcription reactions were incubated at 37 ˚C for at least 6 hours before treatment with DNaseI, acidic phenol extraction and ethanol precipitation, as described above. RNA was washed in 95% ethanol before resuspension in MQW. To remove residual nucleotides, RNA was purified by FPLC on a HiLoad Superdex 75 pg 16/600 column (GE healthcare) in MQW at 4 ˚C, at a flow rate of 1 mL/min. Peak fractions were concentrated by ethanol precipitation as described above.

2.6.2 RNA capping

To produce cap0 and cap1 RNA, 40-60 μg RNA was capped using the ScripCap m7G capping system and 2'-O-methyltransferase system (CellScript). Cap2 RNA was generated from cap1 templates using 200 ng/μL recombinant cap2 methyltransferase in cap2 buffer (50 mM Tris pH 7.5, 5 mM DTT, 2 mM S-adenosyl methionine, 0.1 U/μL RNaseOUT), incubated at 20 ˚C for 4 hours before acidic phenol extraction and ethanol precipitation, as described above. Residual nucleotides and SAM were removed using Illustra MicroSpin G-50 columns (GE Healthcare). For oligonucleotide RNA, up to 150 μg (~ 200 μM) was capped in modified capping reactions, containing 1 mM (cap0 reactions) or 2 mM (cap1 reactions) S-adenosyl methionine (NEB). Residual nucleotides were removed by FPLC, as previously.

2.6.3 Denaturing PAGE

Short RNAs were denatured by boiling in 50% formamide loading buffer and separated in 15 % acrylamide 7 M urea gels at 300 V for 35 minutes. Longer RNAs were separated in 6 % acrylamide 7 M urea gels at 300 V for 45 minutes. Gels were stained in 1x TBE containing 2 μg/mL ethidium bromide for 10 minutes, then washed twice in water before imaging using a G:BOX transilluminator under 302 nm ultraviolet light (Syngene).

2.7 Recombinant protein preparation

Recombinant proteins were expressed in Rosetta2 (DE3) pLysS Escherichia coli cells (Novagen). Cells were grown to OD_{600} of between 0.4-1 in 2x TY medium containing 0.8x antibiotics (28 μg/mL chloramphenicol and 40 μg/mL ampicillin or 20 μg/mL kanamycin, as appropriate) at 37 ˚C. Protein expression was induced using 1 mM isopropyl b-D-1-thiogalactopyranoside (IPTG) and incubated at 22 ˚C for 16-24 hours. Cells were harvested by centrifugation at 5000 x g for 20 minutes and cell pellets were stored at -80 ˚C prior to purification.

2.7.1 Recombinant protein extraction

Thawed cell pellets were resuspended in Buffer H (400 mM KCl, 40 mM Tris pH 7.5, 5 % glycerol, 0.1 mM EDTA, 2 mM DTT) supplemented with 1 mg/mL lysozyme (from hen's egg, Invitrogen) and 0.5 mM phenylmethylsulphonyl fluoride (PMSF), on ice. Cell suspensions were lysed by sonication on ice, using 20 second pulses at 8-10 microns, typically 3 times. Lysates were clarified by centrifugation at 40,000 x g for 20 minutes at 4 ˚C. All subsequent purification steps were carried out on ice in the cold room (4-6 ˚C).

2.7.2 Affinity chromatography

Histidine-tagged proteins were isolated using Ni-NTA agarose resin (Qiagen) or PureCube 100 Ni-NTA agarose (Cube Biotech), which had a higher flowrate but equivalent purity to Qiagen resin. Clarified lysates were typically supplemented with 5-10 mM imidazole to reduce nonspecific binding. Lysates were passed over equilibrated Ni-NTA resin and washed with Buffer H + 5-20 mM imidazole before elution in Buffer H + 150 mM imidazole. Proteins were typically dialysed overnight into Buffer I (200 mM KCl, 40 mM Tris pH 7.5, 5 % glycerol, 1 mM DTT).

2.7.3 Fast protein liquid chromatography

Fast protein liquid chromatography (FPLC) was performed on an ÄKTA pure protein purification system (GE Life Sciences) at 4 ˚C. Anion exchange chromatography was carried out on a MonoQ 10/100 GL column (GE Healthcare) in Buffer Q (20 mM Tris pH 7.5, 5 % glycerol, 1 mM DTT, 100-500 mM KCl) at a flow rate of 0.5 mL/min. Cation exchange chromatography was carried out on a MonoS 10/100 GL column (GE Healthcare) in Buffer S (20 mM HEPES pH 7.5, 5 % glycerol, 1 mM DTT, 100-500 mM KCl). Size exclusion chromatography was carried out on a HiLoad Superdex 200 pg 16/600 column in Buffer I, at a flow rate of 1 mL/min.

2.7.4 Protein concentration

Proteins were concentrated using 10 or 30 kDa molecular weight cut-off Amicon Ultra centrifugal filter units (Merck), pre-equilibrated for at least 10 minutes in buffer I, at 4 ˚C.

For use in biochemical assays, proteins were concentrated to 1-10 mg/mL and stored at -70 ˚C without flash-freezing.

2.8 *In vitro* assays

2.8.1 *In vitro* translation

In vitro translation assays were carried out using the Flexi RRL system (Promega). For translation inhibition assays, IFIT proteins were serially diluted BSA buffer in a volume of 2.5 µL (20 mM Tris pH 7.5, 150 mM KCl, 5 % glycerol, 1 mM DTT, 0.5 mg/mL BSA, 10 U/µL RNaseOUT). IFITs were left for up to 5 minutes at room temperature to ensure RNase inhibition. 125 ng Fluc reporter RNA bearing different 5' and 3'UTRs (15-20 nM final) was added to diluted IFITs and incubated at 37 ˚C for 15 minutes for RNA binding. Due to lower thermal stability, mouse Ifits were incubated at 30 ˚C to maintain activity. Rabbit reticulocyte lysate (RRL) was then added to a final reaction volume of 12.5 µL, in a final reaction mixture of 60% v/v RRL, 100 mM KCl, 0.5 mM MgOAc, 2 mM DTT, 10 µM amino acid mixture minus cysteine, 10 µM amino acid mixture minus leucine, 1 U/µL RNaseOUT, 0-1280 nM IFIT, 15-20 nM RNA, and 100 ng/µL BSA. For murine Ifit complexes, 500 nM MBP-Ifit1c$_{CTD}$ or the equivalent volume of Buffer I was included in the RRL master mix. Reactions were incubated at 30 ˚C for 90 minutes, then stopped by addition of 50 µL passive lysis buffer (Promega) on ice. Stopped translation reactions were diluted 1:10 and an equal volume of firefly luciferase assay reagent was added, to a final volume of 50 µL. Luminescence was measured by GloMax for 10 seconds per well. Data were normalised to the no IFIT control for each experiment.

2.8.2 Co-precipitation

For co-precipitation experiments, 2.5 µM MBP-tagged bait protein was incubated with 2.5 µM prey protein at 30 ˚C for 1 hour, in buffer P (20 mM Tris pH 7.5, 200 mM KCl, 5 % glycerol, 0.1 % NP-40, 1 mM EDTA, 5 mM DTT) in a final volume of 40 µL. Proteins were spun down to remove any precipitate, then applied to equilibrated amylose magnetic beads (NEB) for 30 minutes, in a final volume of 200 µL. Beads were washed 3 times for one minute in buffer P, then eluted by incubation for 20 minutes with 100 mM maltose in buffer P. For competition assays, beads were washed once in buffer P, followed by 3 washes

with increasing concentrations of competitor protein (0.5, 1 and 2 μM), for 10 minutes each. Beads were washed once in buffer P before elution. 10 μL samples were taken at each stage for SDS-PAGE analysis.

2.8.3 SEC-MALS

Ifit1b (0.5 or 2 mg/mL in a 150 μL loop) was applied to a Superdex 200 Increase 10/300 GL column at room temperature, at a flow rate of 0.4 mL/min. Multi-angle light scattering (MALS) analysis was performed by inline measurement of static light scattering (DAWN 8+, Wyatt Technology), differential refractive index (Optilan T-rEX, Wyatt Technology) and 280 nm absorbance (Aligent 1260 UV, Aligent Technologies). Molecular mass was calculated using the AS-TRA6 software package (Wyatt Technology). Access to SEC-MALS apparatus was kindly provided by Dr Janet Deane.

2.8.4 Differential scanning fluorimetry

For testing the stability of IFIT proteins and complexes, in an optical 96-well reaction plate (Applied Biosystems), 2.5 μg protein was mixed with 1:500 Protein Thermal Shift dye (Life Technologies) in 20 mM HEPES pH 7.5, 150 mM KCl, 2.5 mM MgOAc, 5% glycerol and 1 mM DTT, in a final volume of 20 μL. To assay RNA binding, dilution series of 25 nt model RNAs (see section 2.6.1) were mixed with 2 μM protein and 1:500 Protein Thermal Shift dye in 20 mM HEPES pH 7.5, 150 mM KCl, 5% glycerol, 1 mM DTT and 20 ng/μL yeast tRNA (Ambion). Emission was measured at 623 nm in a ViiA7 Real-Time PCR system (Applied Biosystems), ramping from 25 to 95 ˚C stepwise at a rate of 1 ˚C per 20S.

2.8.5 Primer extension inhibition

For IFIT binding experiments, RNA was incubated with indicated concentrations of IFIT in 20 μL reactions containing 20 mM Tris pH 7.5, 100 mM KCl, 2.5 mM MgCl2, 1 mM ATP, 0.2 mM GTP, 1 mM DTT, 0.25 mM spermidine, 0.1 U/μL RNaseOUT and 0.5 mg/mL BSA. Reactions were incubated at 37 ˚C for 10 minutes before addition of 2.5 U AMV reverse transcriptase (Promega), 4 mM MgCl2, 0.5 mM dNTPs and labelled primer (see below). Reverse transcription reactions were incubated at 37 ˚C for 30 minutes, then stopped with 100 mM EDTA and 10% SDS. cDNA products were extracted with UltraPure

phenol:chloroform:isoamylalcohol (25:24:1) pH 8 (ThermoFisher) and ethanol precipitated. Pellets were resuspended in 91 % formamide loading dye for PAGE.

For radiolabelled toeprints, 1 μg DNA primer was end-labelled with 32P-α-ATP (Perkin-Elmer) using T4 polynucleotide kinase (NEB). Reactions were incubated at 37 ˚C for 15 minutes and heat inactivated at 75 ˚C for 5 minutes. 50 ng ^{32}P-labelled primer was used in each reverse transcription reaction. cDNA products were separated by 6% denaturing PAGE for up to 2 hours. Dried gels were imaged by autoradiography using an FLA7000 Typhoon Scanner (GE).

For fluorescent toeprints, Cy5-labelled primers were synthesised (Sigma). Prior to IFIT complex assembly, 25 ng primer was annealed to RNA by heating to 75 ˚C for 5 minutes before snap cooling on ice. Reverse transcriptions were incubated at 37 ˚C for 2 hours before extraction and purification of cDNA. cDNA products were separated by 6 % denaturing PAGE for 30-60 minutes, then imaged directly on a FLA7000 Typhoon scanner (GE).

2.8.5.1 2'-O-Me assay

A modified primer extension inhibition assay was used to detect 2'-O-methylation of mRNA. 50 ng Cy5-labelled primer was annealed to 40 nM RNA by heating to 75 ˚C for 5 minutes and snap-cooling on ice. Reverse transcription was carried out using 5 U AMV reverse transcriptase (Promega) in 20 mM Tris pH 7.5, 100 mM KCl, 0.5 mM dNTPs with 0-4 mM MgOAc. cDNA products were separated and imaged as described above.

2.9 In silico analysis

2.9.1 Graphs and statistics

Graphs were generated in GraphPad Prism 7 (Version 7.03) or Microsoft Excel (Micrsosoft Office 2013, Version 15.0.5119.1000). For pairwise comparisons of data means, data were analysed by two-tailed Student's t-test, assuming unequal variance, as indicated in the figure legends. Nonlinear regression was carried out using GraphPad Prism. For interpolation of melting temperatures, data were analysed using the Bolzmann equation

(y = LL +(UL –LL)/(1 + exp(Tm – x)/1)) where LL and UL are the minimum and maximum fluorescence intensities, respectively, and melting temperature (Tm) was interpolated from the 50% intersect of the curve. For translation inhibition assays, 50% inhibitory concentrations (IC_{50}) were derived by fitting to [Inhibitor] versus normalised response curve (Y = 100)/(1 + (XHillSlope)/(IC50HillSlope)) using the least squares method in GraphPad Prism. Confidence intervals were calculated using the likelihood ratio asymmetric method and a replicates test was performed to test for lack of it. Curves were compared by extra sum of squares F-test.

2.9.2 Phylogenetic analysis

Mammalian IFIT mRNA sequences were assembled by Daughtery et al. *(2016)* (Table 2-6). Protein sequences were aligned using MUSCLE *(Edgar, 2004)* and maximum likelihood trees were built and visualised in Seaview *(Gouy et al., 2010)* using PhyML *(Guindon et al., 2010)*, with 100 bootstrap replicates for statistical support.

2.9.3 Structural modelling

Protein structures were visualised using the PyMOL Molecular Graphics System (Version 1.5.0.5, Schrödinger, LLC, www.pymol.org). Surface electrostatic potentials were calculated using Adaptive Poisson-Boltzmann Solver (APBS) with maps generated using PDB2PQR *(Dolinsky et al., 2004)*. Homology models were generated using SWISS-MODEL *(Waterhouse et al., 2018)*, based on known IFIT structures as indicated in the relevant figure legends. RNA secondary structural models and free energy calculations were generated with Mfold *(Zuker, 2003)*.

Table 2-1 Plasmids.

Plasmids used in this study. Where "IFIT" is written, a plasmid was made containing each human IFIT sequence; where "Ifit" is written, a plasmid was made containing each mouse Ifit sequence. Accession numbers for inserts are given in Table 2-2. Abbreviations: His, polyhistidine tag; FLAG, DYKDDDDK tag; GST, Glutathione S-transferase; MBP, maltose binding protein; eGFP, enhanced green fluorescent protein; TEV, tobacco etch virus protease site; Thr, thrombin site; 2A, thosea asigna virus 2A stop-go peptide; AMP, ampicillin; KAN, kanamycin; MHV, mouse hepatitis virus; ZIKV, Zika virus; UTR, untranslated region.

Plasmid	Promoter	Features	5' RS	3' RS	Antibiotic	Notes
Bacterial expression						
pTriEx1.1-Ifit-His	T7	C-8xHis	NcoI	XhoI	AMP	
pTriEx1.1-Ifit-FLAG	T7	C-FLAG	NcoI	XhoI	AMP	
pOPT3G-Ifit-His	T7	N-GST-3C, C-8xHis	NdeI	BamHI	AMP	
pOPTHM-Ifit and pOPTHM-Ifit1cCTD	T7	N-6xHis-MBP-TEV	NdeI	BamHI	AMP	Ifit1cCTD, amino acids 338-470
pOPTH-Ifit1cCTD	T7	N-8xHis			AMP	MBP tag removed from pOPTHM-Ifit1cCTD by mutagenesis
pET28b-Ifit1b	T7	N-6xHis-TEV	NdeI	BamHI	KAN	
pET28a-His-IFIT1	T7	N-6xHis-TEV	NheI	XhoI	KAN	*(Katibah et al., 2013)*
pET28b-His-IFIT2	T7	N-6xHis-Thr	NdeI	XhoI	KAN	*(Fleith and Mears et al., 2018)*
pET28b-His-IFIT3	T7	N-6xHis-Thr	NdeI	XhoI	KAN	*(Fleith and Mears et al., 2018)*
Mammalian expression						
pCDNA3.1-IFIT-FLAG	CMV	C-FLAG	BamHI	XhoI	AMP	*(Fleith and Mears et al., 2018)*
pCDNA3.1-FLAG-Ifit	CMV	N-FLAG			AMP	Purchased from Genscript
pCDNA3.1-eGFP	CMV	N-eGFP	NheI	XbaI	AMP	
pCDNA3.1-eGFP-Ifit1	CMV	N-eGFP	NdeI	BamHI	AMP	
pCDNA3.1-eGFP-Ifit1b	CMV	N-eGFP	NdeI	BamHI	AMP	
pCDNA3.1-eGFP-Ifit1c	CMV	N-eGFP	NdeI	BamHI	AMP	
pCDNA3.1-eGFP-Ifit1-FLAG-Ifit1c	CMV	N-eGFP; N-2A-FLAG	NdeI	BamHI	AMP	
pCDNA3.1-eGFP-Ifit1b-FLAG-Ifit1c	CMV	N-eGFP;N-2A-FLAG	NdeI	BamHI	AMP	
RNA transcription						
pUC57-Globin-Fluc	T7	Human β-globin 5' and 3' UTR	EcoRI	PstI	AMP	Linearise with FspI
pUC57-MHV-Fluc	T7	MHV 5' and 3' UTR	EcoRI	PstI	AMP	Linearise with PmlI
pUC57-ZIKV-Fluc	T7	ZIKV 5' and 3' UTR	EcoRI	PstI	AMP	Linearise with HindIII, *(Chavali et al., 2017)*
pUC57-Globin-Nluc	T7	Human β-globin 5' and 3' UTR	EcoRI	PstI	AMP	Linearise with FspI
pUC57-MHV-Nluc	T7	MHV 5' and 3' UTR	EcoRI	PstI	AMP	Linearise with PmlI
pUC57-ZIKV-Nluc	T7	ZIKV 5' and 3' UTR	EcoRI	PstI	AMP	Linearise with HindIII

Table 2-2 Sequence accession numbers.

Nucleotide accession numbers for insert sequences cloned into plasmids in Table 2-1.

Sequence	Accession number
IFIT1	BC007091.1
IFIT2	NM_001547.4
IFIT3	NM_001549.5
Ifit1	NM_008331.3
Ifit1b	NM_053217.2
Ifit1c	NM_001101605.1
Ifit2	NM_008332.3
Ifit3	NM_010501.2
Ifit3b	NM_001005858.3
β-globin	NM_000518.4
MHV	AY700211.1
ZIKV	NC_035889.1

Table 2-3 qPCR primers.

Target	Forward primer	Reverse primer
Ifit1	CCAAGTGTTCCAATGCTCCT	GGATGGAATTGCCTGCTAGA
Ifit1b	AACCCTGAGTACAACGCTGG	CGAGAGCTTCCTCCACACAA
Ifit1c	CAATGCTGGCTATGCAGTCG	AGACATAGGGCTGCGAGGAT
Ifit2	CTTGACTGTGAGGAGGGGTG	TAGTTCGCAATGGCCCATCC
Ifit3	AGACAGGGTGTGCAACCAGG	CGACGAATTTCTGATTGATC
Ifit3b	AGACAGGGTGTGCAACCAGC	CGGCGAATTTCTGCTTGATC
Viperin	GGTTCAAGGACTATGGGGAGTATTTGGAC	GAAATCTTTCTGCTTCCCTCAGGGCATC
GAPDH	CATGGCCTTCCGTGGTTCCTA	GCGGCACGTCAGATCCA

Table 2-4 RNA oligonucleotide sequences.

Oligonucleotide	DNA sequence	RNA sequence
T7_promoter	TAATACGACTCACTATA	
globin25	CACAGTTGTGTCAGAAGCAAATGTCTATAGTGAGTCGTATTA	GACATTTGCTTCTGACACAACTGTG

Table 2-5 Antibodies.

Antibodies used for immunoblotting and immunofluorescence. Asterisks indicate custom antibodies, for which the batch number is given in place a catalogue number. BSA, bovine serum albumin; PBST, phosphate-buffered saline with 0.1% tween-20; PGAT, PBS with 0.2 % fish gelatin, 0.02% NaN_3 and 0.01% triton X-100.

Target	Dilution	Buffer	Species	Clonality	Supplier	Catalogue number
Immunoblotting: primaries						
Ifit1	1:500	5% BSA PBST	Rabbit	Poly	Santa Cruz	sc-134949
Ifit1b	1:500	5% BSA PBST	Rabbit	Poly	Pierce	PA3-848
Ifit1b*	50 ug/mL	5% BSA PBST	Rat	Poly	Eurogentec	1711946*
Ifit1c*	25 ug/mL	5% BSA PBST	Rat	Poly	Eurogentec	1711948*
Ifit2/3	1:800	5% BSA PBST	Rabbit	Poly	Proteintech	12604-1-AP
IFIT1	1:1000	5% BSA PBST	Rabbit	Poly	Pierce	PA3-848
IFIT2	1:1000	5% milk PBST	Mouse	Poly	ProteinTech	12604-1-AP
IFIT3	1:1000	5% milk PBST	Rabbit	Poly	Sigma	SAB1410691
GAPDH	1:8000	5% BSA PBST	Mouse	Mono	Invitrogen	AM4300
Tubulin	1:1000	5% BSA PBST	Rat	Mono (YL1/2)	Abcam	ab6160
Puromycin	1:20	Odyssey block buffer	Mouse	Mono	Made by Dr Jia Liu	
His	1:2000	3% BSA PBST	Mouse	Mono	Qiagen	34660
FLAG	1:1000	5% BSA PBST	Mouse	Mono	Sigma	F3165
FLAG-HRP	1:1500	5% milk PBST	Mouse	Mono	Sigma	A8592
GFP	1:4000	5% BSA PBST	Rabbit	Poly	Sigma	G1544
MHV N protein	1:1000	5% BSA PBST	Mouse	Mono	*(Irigoyen et al. 2016)*	
Immunoblotting: secondaries						
Goat anti-mouse IgG (IRDye 800CW)	1:10000	PBST	Goat	Mono	Li-Cor	926-32210
Goat anti-mouse IgG (IRDye 680RD)	1:10000	PBST	Goat	Mono	Li-Cor	926-68020
Donkey anti-rabbit IgG (IRDye 800CW)	1:10000	PBST	Donkey	Mono	Li-Cor	926-32213
Donkey anti-rabbit IgG (IRDye 680RD)	1:10000	PBST	Donkey	Mono	Li-Cor	926-68071
Alexa Fluor 680 goat anti-rat IgG	1:10000	PBST	Goat	Mono	Life Technologies	A-21096
Immunofluorescence: primaries						
FLAG	1:1000	PGAT	Mouse IgG1	Mono (M2)	Sigma	F1804
dsRNA	1:1000	PGAT	Mouse IgG2a	Mono (J2)	Scions	10010500
Immunofluorescence: secondaries						
Alexa Fluor 568 donkey anti-mouse IgG	1:1000	PGAT	Donkey	Mono	Life Technologies	A-10037
Alexa Fluor 647 goat anti-mouse IgG2a	1:1000	PGAT	Goat	Mono	Life Technologies	A-21241
Alexa Fluor 568 goat anti-mouse IgG1	1:1000	PGAT	Goat	Mono	Life Technologies	A-21124

Table 2-6 Accession numbers for IFIT phylogenetic trees.

Species	IFIT	Accession number
Bos taurus	Bt_IFIT1	XP_010818066.1
Cow	Bt_IFIT2	XP_001787875.2
	Bt_IFIT3	NP_001068882.1
	Bt_IFIT5	NP_001069166.1
Canis lupus familiaris	Clf_IFIT1	XP_848364.1
Dog	Clf_IFIT1B	XP_848342.2
	Clf_IFIT2	XP_005618815.1
	Clf_IFIT3	XP_005618816.1
	Clf_IFIT5	XP_005637570.1
Chlorocebus sabaeus	Cs_IFIT1	XP_007961691.1
African green monkey	Cs_IFIT1B	XP_007961693.1
	Cs_IFIT2	XP_007961687.1
	Cs_IFIT3	XP_007961688.1
	Cs_IFIT5	XP_007961694.1
Danio rerio	Dr_IFIT5A	AID69083.1
Zebrafish	Dr_IFIT12A	AID69084.1
	Dr_IFIT12B	AID69087.1
	Dr_IFIT12C	AID69086.1
	Dr_IFIT12D	AID69085.1
	Dr_IFIT12E	AID69084.1
	Dr_IFIT13A	NP_001032654.1
	Dr_IFIT17A	AID69090.1
	Dr_IFIT17B	AID69091.1
	Dr_IFIT17C	AID69092.1
Equus caballus	Ec_IFIT1	XP_005602428.2
Horse	Ec_IFIT1B	XP_005613850.1
	Ec_IFIT2	AEH58159.1
	Ec_IFIT3	XP_001501453.3
	Ec_IFIT5	XP_005602426.2
	Ec_IFIT5B	XP_001491865.1
Felis catus	Fc_IFIT1	XP_003993924.2
Cat	Fc_IFIT1B	XP_006937789.2
	Fc_IFIT2	XP_006937780.2
	Fc_IFIT3	XP_011285498.1
	Fc_IFIT5	XP_011285500.1
Gallus gallus / Chicken	Gg_IFIT5	NP_001307351.1
Homo sapiens	Hs_IFIT1	AAH07091.1
Human	Hs_IFIT1B	AAI37369.1
	Hs_IFIT2	NP_001538.4
	Hs_IFIT3	NP_001276688.1
	Hs_IFIT5	AAH25786.1
Ornithorhynchus anatinus	Oa_IFIT5	XP_007664436.1
Platypus	Oa_IFIT5L1	XP_001506422.3
	Oa_IFIT5L2	XP_007669809.1
Oryctolagus cuniculus	Oc_IFIT1	XP_008268395.1
Rabbit	Oc_IFIT1B	XP_008268389.1
	Oc_IFIT2	XP_002718418.1
	Oc_IFIT3	XP_008268388.1
	Oc_IFIT5	XP_008268391.1
Pan troglodytes	Pt_IFIT1	NP_001192276.1
Chimpanzee	Pt_IFIT1B	XP_009457196.1
	Pt_IFIT2	XP_507902.2
	Pt_IFIT3	NP_001182075.1
	Pt_IFIT5	XP_003312804.1
Pteropus vampyrus	Pv_IFIT1	XP_011359939.1
Flying fox	Pv_IFIT2	XP_011359906.1
	Pv_IFIT3	XP_011359904.2
	Pv_IFIT5	XP_011359901.1
Sus scrofa	Ss_IFIT1	AET34760.1
Pig	Ss_IFIT2	XP_001928706.2
	Ss_IFIT3	NP_001191324.1
	Ss_IFIT5	AFN43002.1
Taeniopygia guttata	Tg_IFIT1	XP_004175020.1
Zebra finch	Tg_IFIT5	XP_002188588.2

Species	IFIT	Accession number
Cricetulus griseus	Cg_Ifit1	XP_003514784.1
Chinese hamster	Cg_Ifit1l1	XP_003514788.2
	Cg_Ifit1l2	XP_007634083.2
	Cg_Ifit2	XP_007644639.1
	Cg_Ifit3	XP_007644640.1
Chinchilla lanigera	Cl_Ifit1	XP_005385907.1
Chinchilla	Cl_Ifit1b	XP_005385910.1
	Cl_Ifit2	XP_005385908.1
	Cl_Ifit3	XP_005385909.1
	Cl_Ifit5	XP_005386144.1
Cavia porcellus	Cp_Ifit1b	XP_003473903.1
Guinea pig	Cp_Ifit3	XP_003473600.1
	Cp_Ifit5	XP_003473601.2
Heterocephalus glaber	Hg_Ifit1	XP_004884690.1
Naked mole rat	Hg_Ifit1b	XP_004838536.1
	Hg_Ifit1c	XP_004884677.1
	Hg_Ifit2	XP_004884688.1
	Hg_Ifit3	XP_004838534.1
	Hg_Ifit5	XP_004884679.1
Ictidomys tridecemlineatus	It_Ifit1	XP_005333827.1
Thirteen-lined ground squirrel	It_Ifit1bl1	XP_005333804.1
	It_Ifit1bl2	XP_005333828.1
	It_Ifit1bl3	XP_005333829.1
	It_Ifit2b	XP_005333806.1
	It_Ifit3	XP_005333805.1
	It_Ifit5	XP_005333803.1
Mus musculus	Mm_Ifit1	NP_032357.2
Mouse	Mm_Ifit1b	NP_444447.1
	Mm_Ifit1c	NP_001095075.1
	Mm_Ifit2	NP_032358.1
	Mm_Ifit3	NP_034631.1
	Mm_Ifit3b	NP_001005858.2
Microtus ochrogaster	Mo_Ifit1bl1	XP_005352221.1
Prairie vole	Mo_Ifit1bl2	XP_005352222.1
	Mo_Ifit1bl3	XP_005352304.1
	Mo_Ifit1bl4	XP_005352305.1
	Mo_Ifit2	XP_005372590.1
	Mo_Ifit2b	XP_005352306.1
	Mo_Ifit3	XP_005352220.1
Rattus norvegicus	Rn_Ifit1	XP_001079971.2
Norway rat	Rn_Ifit1l1	NP_064481.1
	Rn_Ifit2	NP_001019924.1
	Rn_Ifit3	NP_001007695.1

Protein accession numbers for IFIT sequences used to make phylogenetic trees, based on nucleotide sequences from Daugherty et al. *(2016)*. Both species and common names are given. Left panel shows mammal sequences used for Figure 1-6. Right panel shows rodent sequences used for Figure 1-6 (mouse and rat) and Figure 5-1.

3 THE HUMAN IFIT COMPLEX

3.1 Background

3.1.1 IFIT protein oligomerisation

Tetratricopeptide repeats (TPRs) are a loosely-conserved 34 amino acid helix-turn-helix motif (Figure 3-1A). They were first identified as important for mediating interactions between cell cycle proteins in yeast *(Sikorski et al., 1990)*. The TPR α-helical bundles form grooves which can accommodate α-helices from protein binding partners *(Das et al., 1998; D'Andrea and Regan, 2003)*. Since IFIT proteins are almost entirely comprised of tandem TPRs *(Smith and Herschman, 1996)*, they therefore have the potential to form multiprotein complexes.

Many IFIT proteins exist as homodimers or higher order oligomers in solution. IFIT2 forms a domain-swapped homodimer by exchange of one and a half TPRs in the N-terminus *(Yang et al., 2012)* (Figure 3-1C). The N-terminal domain of IFIT3 shares 66% amino acid identity with IFIT2 (amino acids 1-180), indicating that IFIT3 could also form domain swapped homodimers (Figure 3-1D). Native gel electrophoresis has shown that IFIT1 and IFIT3 can homooligomerise *(Kumar et al., 2014)*, while X-ray crystallography has demonstrated that IFIT1 forms homodimers via interactions between C-terminal TPRs, in a concentration-dependent manner *(Abbas et al., 2017b)* (Figure 3-1E). The residues involved in IFIT1 dimerisation are conserved in IFIT1, IFIT1B and IFIT3, indicating that they could also mediate heterodimerisation (Figure 3-1B).

In co-immunoprecipitation experiments, Stawowczyk et al *(2011)* showed that IFIT2 could interact with IFIT1 and IFIT3 when overexpressed in HeLa cells. Using glycerol gradient sedimentation of HeLa cytoplasmic lysates, it was shown that IFIT1, IFIT2 and IFIT3 co-migrated at 150-200 kDa, the molecular weight of a trimer or a tetramer. IFIT1 was later

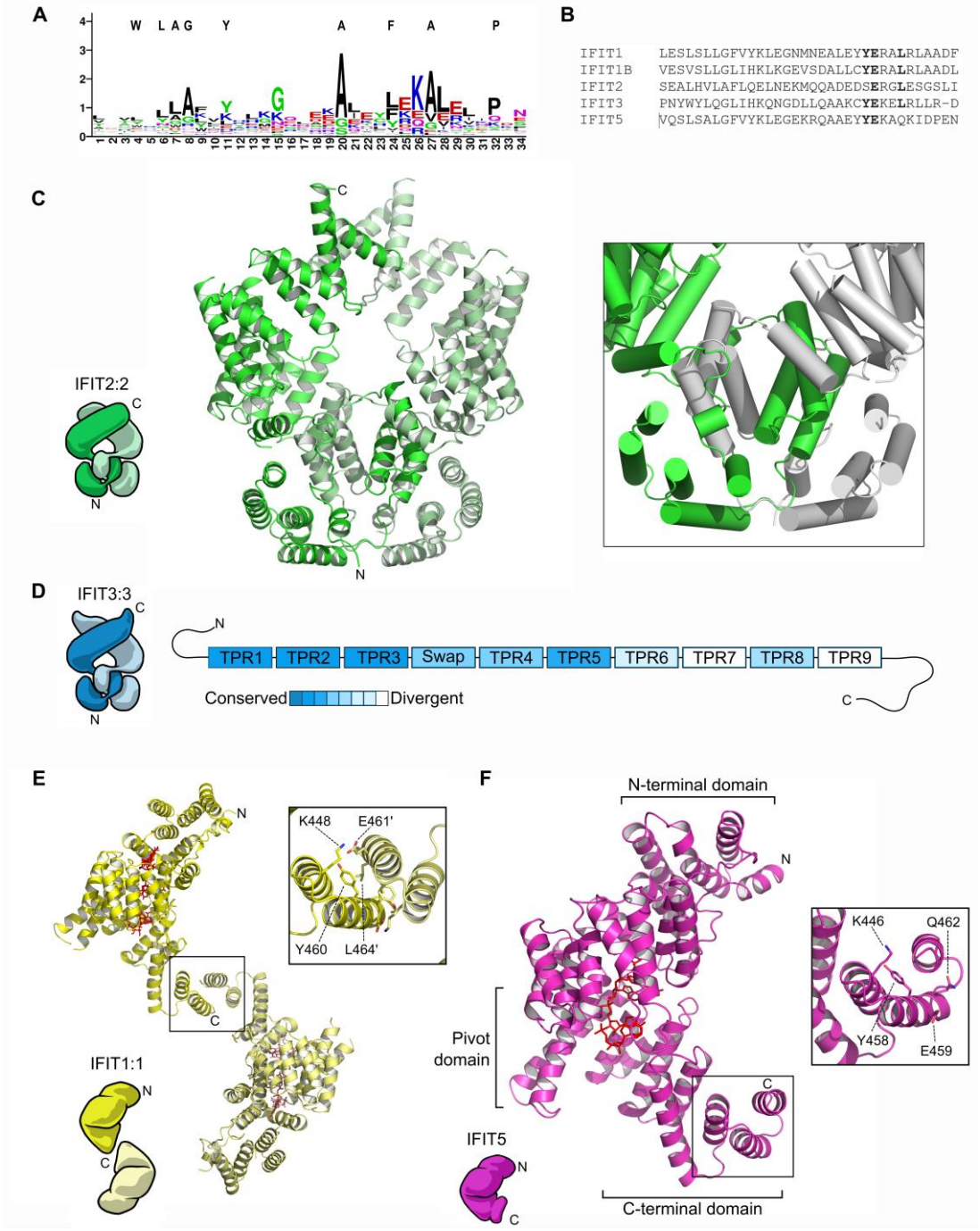

Figure 3-1 Human IFIT proteins form homooligomers.

shown to interact with IFIT2 or IFIT3 in co-precipitation and gel filtration experiments *(Pichlmair et al., 2011)*. By contrast, IFIT5 is monomeric *(Abbas et al., 2013; Feng et al., 2013; Katibah et al., 2013; Kumar et al., 2014)* and does not interact with other IFIT family members *(Pichlmair et al., 2011)* (Figure 3-1F).

Figure 3-1. Human IFIT proteins form homooligomers (cont.).

A. *Consensus sequence of human IFIT protein TPR domains. Sequence alignment was generated in MUSCLE and visualised using WebLogo (Crooks et al., 2004). Typical TPR residues are shown above.* ***B.*** *Alignment of C-terminal TPRs of human IFIT proteins, showing conserved residues involved in IFIT1 homodimerisation in bold.* ***C.*** *Crystal structure of IFIT2 (PDB: 4GIT) and schematic cartoon in green. The domain-swapped dimerisation interface is enlarged in the box.* ***D.*** *Schematic cartoon and domain diagram of IFIT3 in blue, with the regions conserved between IFIT2 and IFIT3 shown in dark blue and divergent regions shown in light blue. TPR motifs are annotated according to Yang et al. (2012) and the putative domain swap region is labelled "Swap".* ***E.*** *Crystal structure of IFIT1 (PDB: 5W5H) and schematic cartoon in yellow. The dimerisation interface is enlarged and key residues labelled. Bound cap0-RNA is shown in red.* ***F.*** *Crystal structure of IFIT5 (PDB: 4HOT) and schematic cartoon in magenta. The C-terminal domain is enlarged and conserved residues are labelled. The final C-terminal helix occludes the dimerisation interface in IFIT5. Adapted from Mears & Sweeney (2018).*

Murine Ifit proteins cannot form the same complexes as human IFITs. Pulldown experiments demonstrated that, while human IFIT1 could co-precipitate with IFIT2 and IFIT3 as previously described, murine Ifit1 precipitated neither murine Ifit2 nor Ifit3 *(Habjan et al., 2013)*. Instead, murine Ifit1 co-precipitated peptides corresponding to Ifit1c, an uncharacterised murine Ifit protein. These putative complexes will be the subject of chapter 6.

3.1.2 Aims

Despite considerable evidence for IFIT protein oligomerisation, the functional significance of these interactions has remained unclear. The aim of this chapter was to reconstitute human IFIT complexes *in vitro*, in order to determine their assembly pathway and examine the influence of IFIT oligomerisation on antiviral function. A better understanding of how human IFIT proteins are regulated is necessary to understand the differences between the human and murine systems, and how the mouse model can be improved to better mimic its human counterpart.

This chapter was undertaken as a collaboration with Dr Renata Fleith, with some experiments performed by Dr Trevor Sweeney and Xin Yun Leong *(Fleith and Mears et al., 2018)*. Experiments performed by these people will be indicated in the text and their data are presented in Appendices A-D.

3.2 Results

3.2.1 SILAC proteomics analysis of IFIT1 and IFIT5 binding partners.

IFIT1 was shown to interact with IFIT2 and IFIT3 in lysates of IFN-stimulated HEK293 cells *(Pichlmair et al., 2011)*. However, a number of other RNA binding proteins were identified in that study, raising the concern that these interactions may have been non-specifically mediated by nucleic acids. Here, an unbiased quantitative mass-spectrometry approach was undertaken in the presence of strong nuclease, to confirm human IFIT proteins could interact directly in cells.

HEK293T cells were passaged in differential-isotope labelled media, to facilitate quantitative proteomic analysis *(Ong et al., 2002)*. Labelled cells were transfected with a plasmid encoding FLAG-tagged IFIT1, FLAG-tagged IFIT5 or an empty vector control. After 24 hours, cells were treated with human IFNα and incubated for a further 16 hours. Cells were lysed in the presence of benzonase nuclease, before precipitation on anti-FLAG affinity resin (Figure 3-2A). Precipitates were combined and sent for liquid chromatography-tandem mass spectrometry analysis (LC-MS/MS) at the proteomics facility at the University of Bristol. Proteomic data analysis was performed by Dr Edward Emmott, consistent with methods outlined previously *(Emmott and Goodfellow, 2014)*.

Consistent with a previous report *(Rabbani et al., 2016)*, IFIT1 was very poorly overexpressed in human cells compared to IFIT5, and was only clearly visible in precipitated samples (Figure 3-2B). However, IFIT1 was still capable of co-precipitating endogenous IFIT2 and IFIT3 (Figure 3-2C), while IFIT5 did not precipitate any other IFIT family members (Figure 3-2D). IFIT2 and IFIT3 were enriched to a similar extent in the IFIT1 pull-downs, supporting a stoichiometric complex *(Pichlmair et al., 2011; Stawowczyk et al., 2011)*. Previously, Pichlmair et al *(2011)* detected peptides corresponding to IFIT1B in IFIT1 and IFIT3 precipitates. However, IFIT1B was not detected in either pulldown in this experiment. This may be due to differences in how the mass spectrometry was carried out, or possibly differences between HEK293 and HEK293T cell lines, the latter of which is known to have lost some innate immune components *(Burdette et al., 2011)*. Owing to the poor overexpression of IFIT1, reliable determination of other IFIT1 binding partners was not possible.

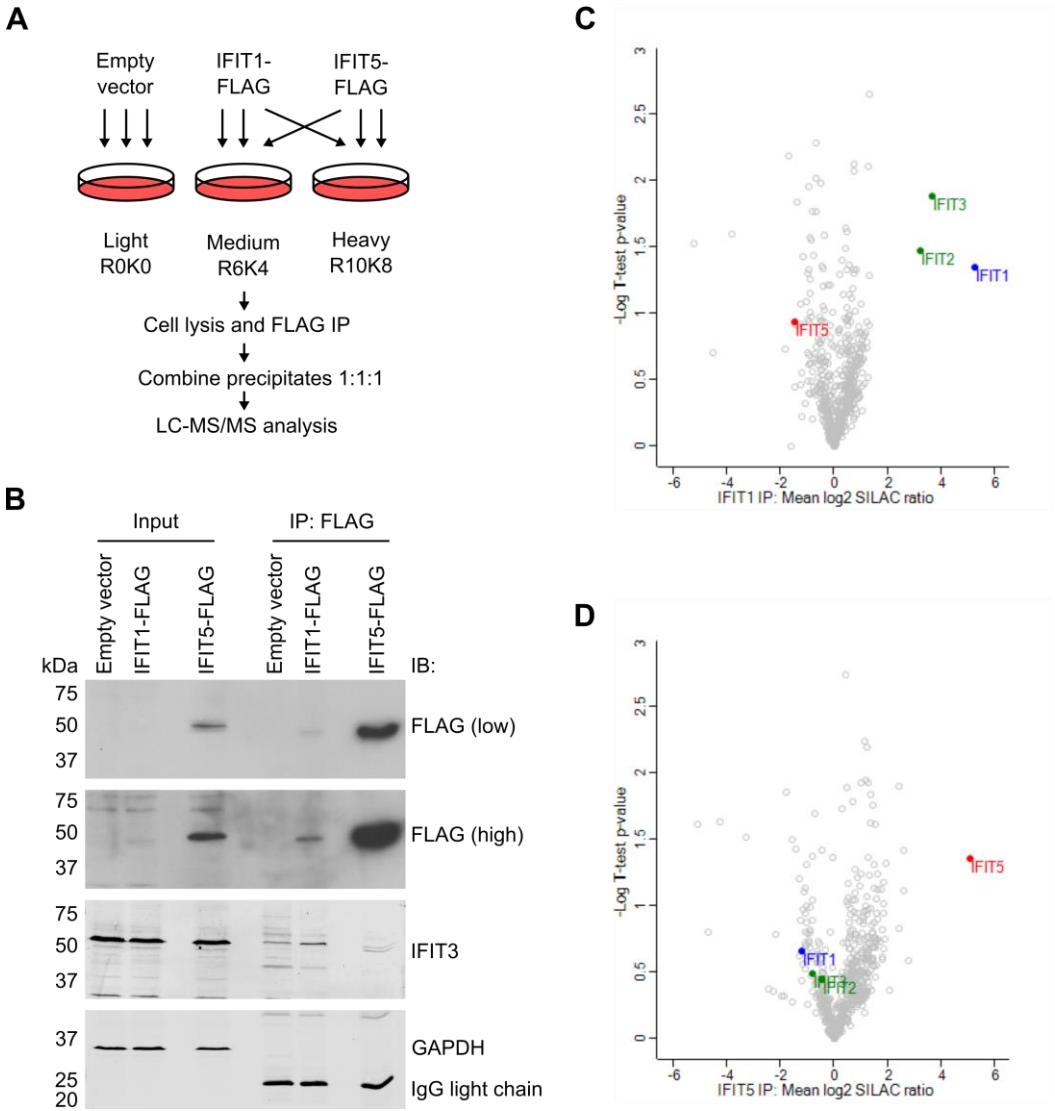

Figure 3-2 IFIT1 interacts with IFIT2 and IFIT3 in human cells.

A. *Strategy for stable-isotope labelling of amino acids in cell culture (SILAC) and immunoprecipitating IFIT1 and IFIT5 interacting partners from HEK293T cells. Medium and heavy labels were swapped in the final experimental replicate to control for any off-target effects of the label.* ***B.*** *Input lysates and immunoprecipitates analysed by western blotting against FLAG, IFIT3 and GAPDH. Top and second panels are different exposures of the same blot to facilitate visualisation of IFIT1. In the bottom panel, the anti-mouse secondary antibody detected IgG from the antibody used for immunoprecipitation.* ***C-D.*** *Volcano plots showing SILAC proteomic data from* ***C.*** *IFIT1 and* ***D.*** *IFIT5 precipitates, expressed as a log_2-fold change over empty vector-transfected cells (SILAC ratio), plotted against statistical significance, determined by pairwise t-test from three replicate experiments. IFIT family members are coloured and labelled.*

3.2.2 *In vitro* reconstitution of human IFIT complexes.

IFIT interaction experiments were performed by Dr Renata Fleith. As such data in this section will be shown in Appendices A and B, and detailed methods can be found in Fleith & Mears et al. *(2018)*. His-tagged human IFIT1, IFIT2 and IFIT3 were recombinantly expressed and purified from bacteria. His-tags were cleaved from IFIT2 and IFIT3, but retained on IFIT1 for later detection. Proteins were incubated together at the temperatures ranging between 4 ˚C to 37 ˚C, then analysed by size exclusion chromatography (SEC) or SEC with in-line multi-angle light scattering (SEC-MALS). Consistent with a recent report *(Abbas et al., 2017b)*, IFIT1 homodimerised in a concentration-dependent manner. IFIT2 was homodimeric, as expected *(Yang et al., 2012)*, with some higher order species, while IFIT3 was homodimeric with a small monomeric population, consistent with previous native gel electrophoresis analysis *(Kumar et al., 2014)*.

IFIT2 was previously shown to interact with IFIT3 in human cells, via TPRs in the N-terminus of IFIT2 *(Stawowczyk et al., 2011)*, in the region responsible for IFIT2 homodimerisation *(Yang et al., 2012)*. When incubated together at 4 ˚C, IFIT2 and IFIT3 did not interact; however, when incubated at 37 ˚C IFIT2 and IFIT3 formed a heterodimer (Appendix B). IFIT2:IFIT3 complexes did not dissociate when re-analysed by SEC-MALS, indicating that this complex is stable. Given that IFIT2 and IFIT3 are co-expressed during the IFN response, at physiological temperatures, IFIT2 and IFIT3 likely exists as a heterodimeric complex in the cell.

By contrast, when incubated together at 4 ˚C, IFIT1 and IFIT3 readily interacted to form a tetrameric complex, containing equimolar IFIT1 and IFIT3. This indicates a preferential, high affinity interaction between these proteins, since no energy input was required to observe an interaction. IFIT1 and IFIT2 only interacted weakly when incubated together at 4 ˚C. When heated to 37 ˚C multiple heterooligomeric species were detected. IFIT1:IFIT2 was primarily tetrameric, but dimeric, trimeric and pentameric species were also detectable. Previous truncation analysis showed that IFIT1 could co-precipitate with both N- and C-terminal truncations of IFIT2 *(Stawowczyk et al., 2011)*. This indicates that the interaction between IFIT1 and IFIT2 may be non-specific or can occur at multiple sites.

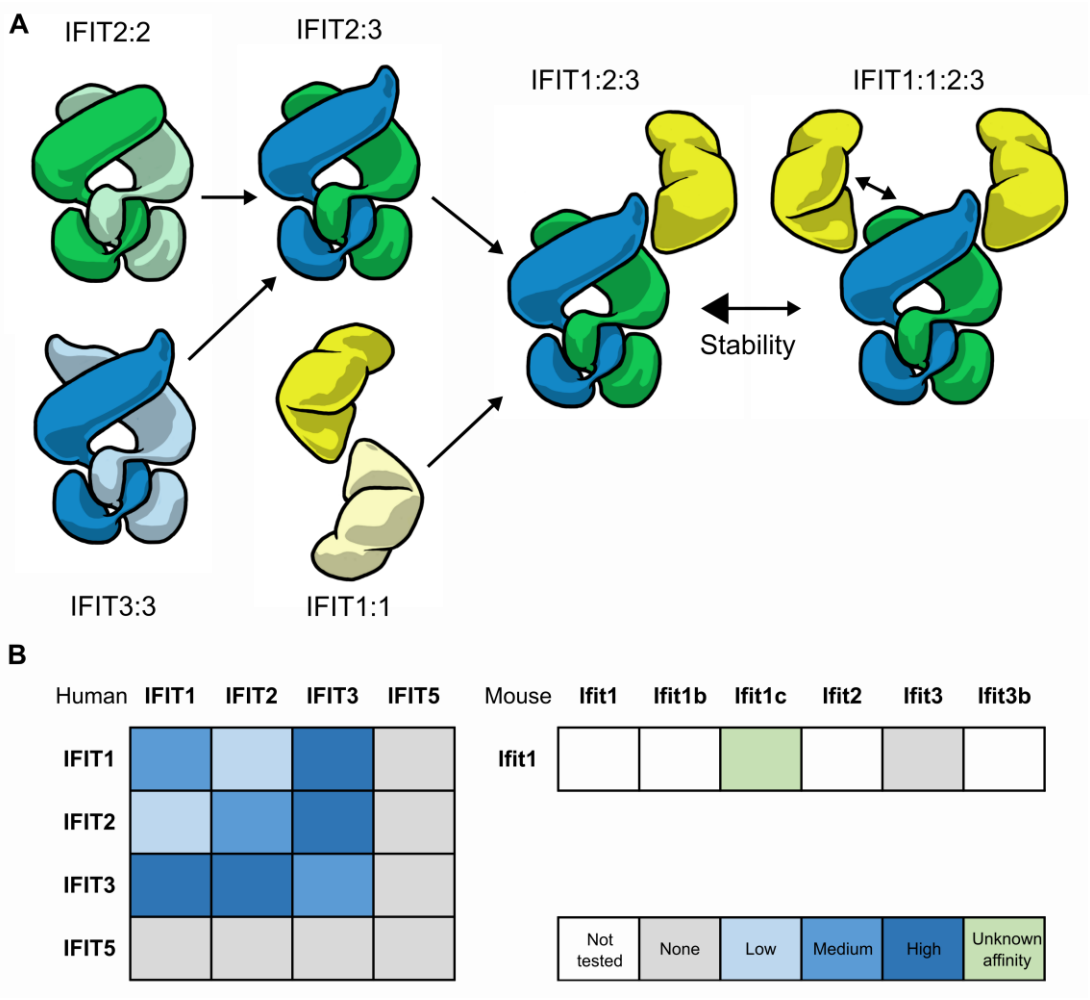

Figure 3-3 Human IFIT complex assembly pathway.

A. *Schematic cartoons showing the IFIT complex assembly pathway, based on gel filtration experiments described in section 3.2.2, presented in Appendices A and B. Weak interactions are indicated by reversible arrows.* ***B.*** *A heatmap showing the relative affinities of human IFIT proteins for each other, with murine Ifit1 as a comparison.*

When IFIT1 was incubated with an equimolar amount of pre-formed IFIT2:IFIT3 heterodimer at 4 °C, a trimeric complex was formed (Appendix B). Given that IFIT1 readily associated with the IFIT2:IFIT3 dimer, without the need for heating, it suggests that IFIT1 associates via an interaction with IFIT3. When the IFIT2:IFIT3 heterodimer was incubated at 30 °C with a two-fold molar excess of IFIT1, a tetrameric complex was formed, with two copies of IFIT1 per IFIT2:IFIT3 dimer. Like the IFIT1:IFIT2 complex, this IFIT1:IFIT2:IFIT3 tetramer was unstable, and tended to precipitate upon freeze-thawing.

A recent report has shown that IFIT1 homodimerises via an interaction between the C-terminal TPRs of each monomer *(Abbas et al., 2017b)*. This region contains a YExxL motif, which is conserved in IFIT1 and IFIT3, but is divergent in IFIT2 (see Figure 3-1B). Murine Ifit3 has been reported to not interact with murine Ifit1 *(Habjan et al., 2013; Johnson et al., 2018)*; in mice Ifit3 has undergone a 3' deletion, which truncates the C-terminus of the protein, including the proposed YExxL interaction motif (discussed further in chapter 6). Therefore, human IFIT1 might interact with human IFIT3 via the C-terminus of both proteins.

To interrogate this putative interaction interface, point mutants were generated of IFIT1 and IFIT3 (see Appendix C). When Y460 or L464 were mutated in the binding motif of IFIT1, homodimerisation was disrupted, consistent with a previous report *(Abbas et al., 2017b)*. Mutation of the YExxL motif in IFIT3 did not affect IFIT3 homodimerisation. Mutating both Y460 and L464 together completely abrogated interaction with IFIT3 and the corresponding double mutant of IFIT3 did not interact with IFIT1. As such, the conserved YExxL motif is necessary for high affinity interaction between IFIT1 and IFIT3.

The complexes purified in this section by Dr Renata Fleith are summarised in Figure 3-3, and were used in subsequent biophysical and biochemical analyses.

3.2.3 Stability of IFIT complexes *in vitro*.

To determine the effect of heterocomplexing on human IFIT stability, proteins and complexes purified in 3.2.1 were analysed by differential scanning fluorimetry. This technique employs a dye which fluoresces in hydrophobic environments when excited at 623nm, but is quenched under aqueous conditions *(Niesen et al., 2007)*. As proteins are unfolded by increasing temperature, the dye can bind to hydrophobic patches within the core of the protein, therefore producing a fluorescent signal with a characteristic sigmoid melt curve. By interpolating this curve, accurate quantification of protein melting temperature is possible. At high temperatures, the unfolded protein begins to aggregate causing a drop off in the signal.

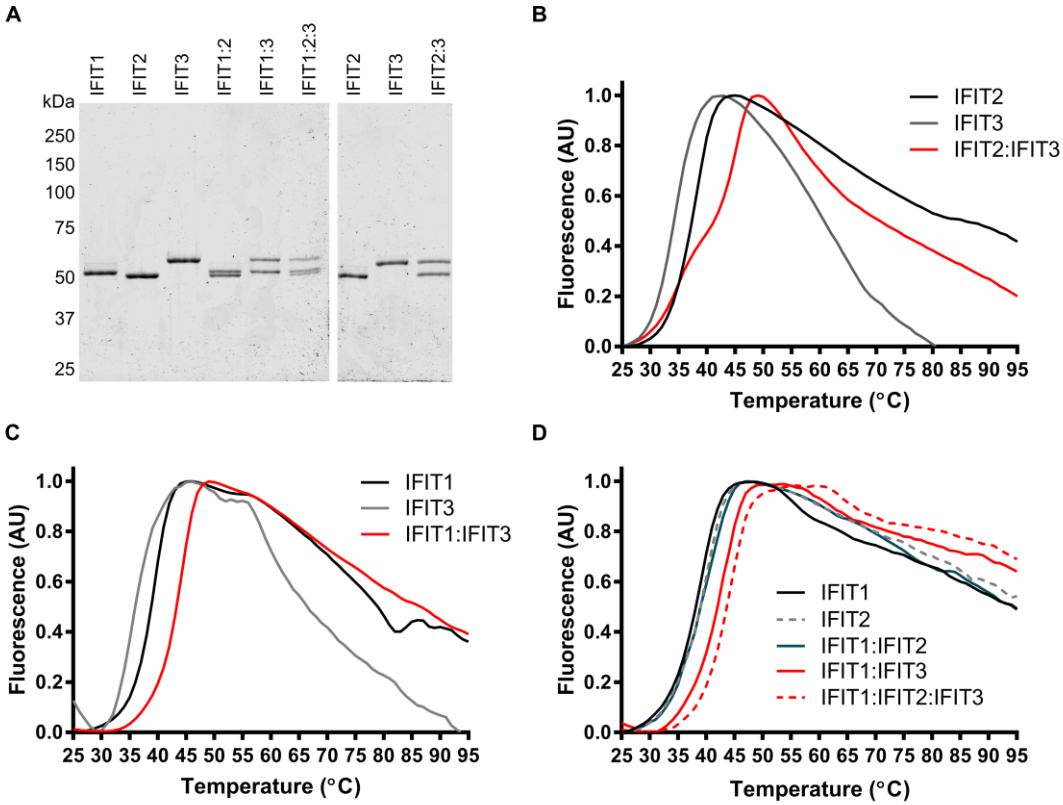

Figure 3-4 IFIT complexes are more stable than individual proteins.

A. *SDS-PAGE of IFIT complexes generated in section 3.2.2.* ***B-D.*** *Differential scanning fluorimetry of the indicated complexes. Results are representative of four experimental replicates. Melting temperatures are given in Table 3-1.*

The same total mass of IFIT proteins or complexes was used in each experiment (Figure 3-4A). Individual IFIT proteins in solution had melting temperatures at or below physiological levels (Figure 3-4, Table 3-1). IFIT3 was particularly unstable, with a melting temperature of < 35 °C. Heterodimerisation of IFIT2 and IFIT3 resulted in a stable complex with a significantly higher melting temperature than either homodimer in isolation (Figure 3-4B). However, the melt curve was biphasic, possibly due to contaminating homodimeric IFIT3, making accurate interpolation of melting temperature impossible. Together with the knowledge that IFIT2 and IFIT3 need to be heated together to observe an interaction, this indicates that partial unfolding of these proteins may be necessary for heterodimerisation, supporting an N-terminal domain-swap model.

IFIT3 also enhanced the stability of IFIT1, with the IFIT1:IFIT3 tetramer and IFIT1:IFIT2:IFIT3 trimer being the most stable complexes analysed (Figure 3-4C-D). By

Table 3-1 Human IFIT complex melting temperatures.

Melting temperatures (Tm) were interpolated from data presented in Figure 3-4. Data were analysed by non-linear regression using the Boltzmann equation, y = LL (UL – LL)/(1 + exp(Tm –x)/a) where LL and UL are lower limit and upper limit respectively. Data represent the mean ± standard deviation of four experimental repeats. For IFIT2:IFIT3 where the melt curve was biphasic, melting temperature was not calculated.

Protein or complex	Tm (°C)
IFIT1	38.1 ± 0.18
IFIT2	38.8 ± 0.18
IFIT3	34.4 ± 0.64
IFIT1:IFIT2	39.0 ± 0.63
IFIT1:IFIT3	41.8 ± 0.90
IFIT1:IFIT2:IFIT3	43.5 ± 0.13

contrast, the IFIT1:IFIT2 complex was just as unstable as its constituent proteins (Figure 3-4D). Melting temperatures of IFIT complexes are shown in Table 3-1. The ready association of IFIT1 and IFIT3, along with its enhanced stability when complexed, indicates that this interaction is thermodynamically preferable.

3.2.3.1 Stability of IFIT complexes in cells.

Given that IFIT1 is physically stabilised by complexing with IFIT3, it was hypothesised that IFIT3 may also enhance IFIT1 expression and stability in cells. The following IFIT1 transfection experiments were performed by Xin Yun Leong and are presented in Appendix D. FLAG-tagged IFITs were overexpressed in HEK293T cells for 24 hours before harvesting for western blot analysis. A plasmid encoding FLAG-IFIT1 was transfected alone, or co-transfected with increasing amounts of FLAG-IFIT2 or FLAG-IFIT3 plasmid. Overexpression of IFIT3 significantly enhanced IFIT1 expression, while IFIT2 only had a marginal effect. IFIT1 expression was not enhanced by IFIT3 when the interaction was disrupted by mutation of either protein. This indicates that the physical association of IFIT1 and IFIT3 is directly necessary for IFIT1 stabilisation, rather than an indirect effect of IFIT3, for example on IFIT1 mRNA expression or stability. Interestingly, expression of the IFIT1 Y460E/L464E double mutant was two-fold higher than wild-type IFIT1, indicating that IFIT1 monomers may be more stable than IFIT1 homodimers.

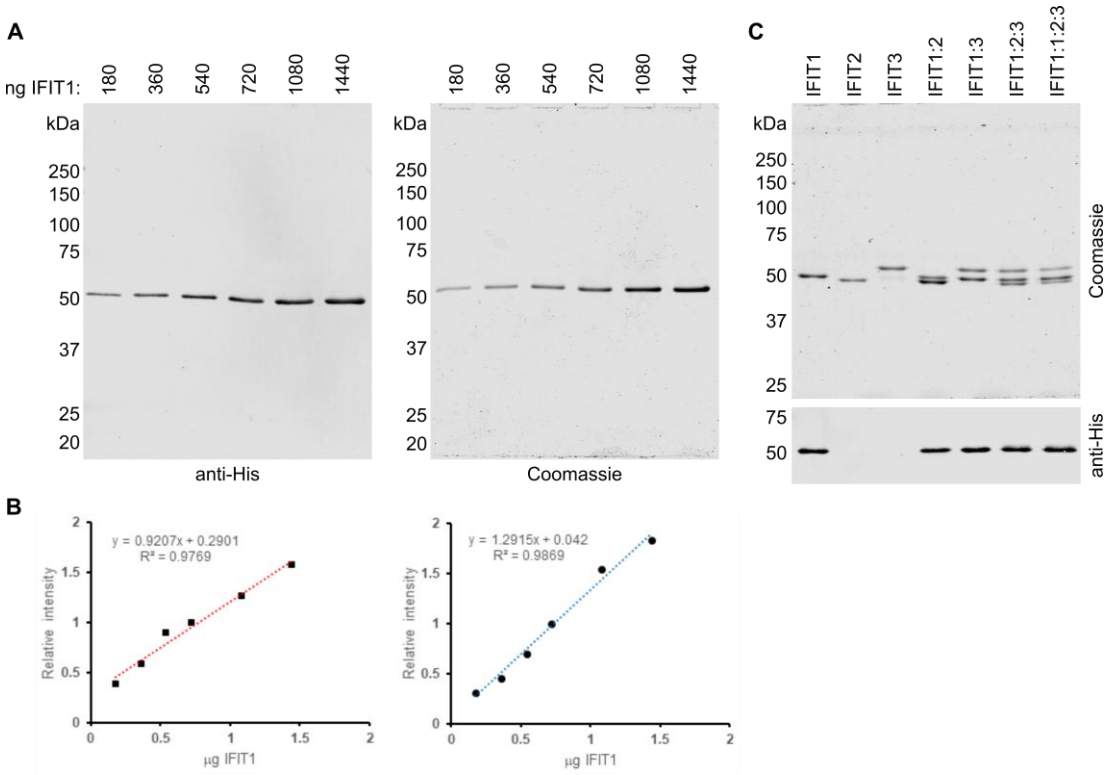

Figure 3-5 Normalisation of IFIT1-containing complexes.

A. *Titration of His-tagged human IFIT1 analysed by western blotting against the His tag or staining with coomassie.* ***B.*** *Quantification of A. measured in ImageJ.* ***C.*** *Coomassie stained SDS-PAGE and anti-His western blot of IFIT complexes generated in section 3.2.2. Concentration of IFIT1 alone or in complexes was normalised based on measurements made within the linear range of the anti-His antibody.*

3.2.4 Translation inhibition by IFIT complexes.

Having established that IFIT3 is necessary for the stability IFIT1, it was then hypothesised that IFIT3 could enhance IFIT1 RNA binding activity. Proteins and complexes purified in 3.2.2 were analysed in an *in vitro* translation system to determine the ability of IFIT1 to inhibit cap0-mRNA translation, alone and in complex with other IFIT family members. Using a cell-free translation system allows direct comparison of controlled quantities of protein and mRNA, without confounding factors such as transfection efficiency, differences in IFIT expression or interference from other ISGs. Therefore, it offers a clean baseline to quantify differences in IFIT1 activity.

The amount of IFIT1 added was normalised by western blotting against the His-tag, within the linear range of the anti-His antibody (Figure 3-5). This ensured that the same molarity

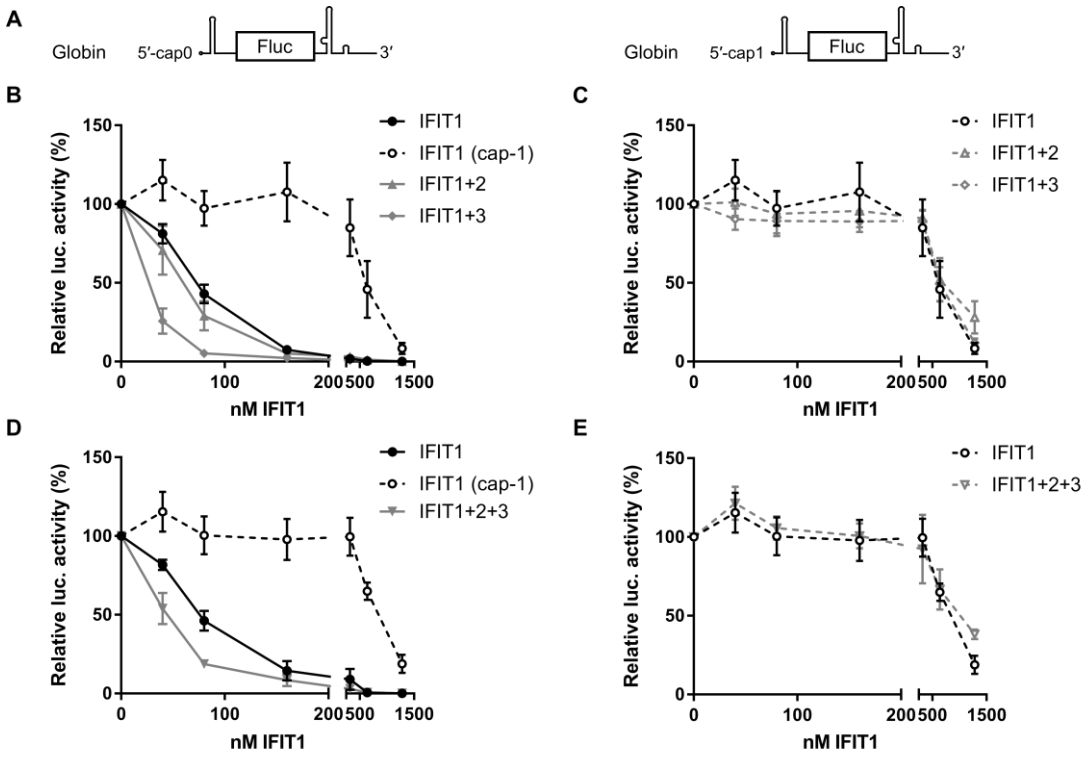

Figure 3-6 IFIT3 enhances translation inhibition of unstructured cap0 RNA by IFIT1.

***A**. Schematic representation of globin-Fluc mRNA. **B-E**. In vitro translation of (**B**,**D**) cap0 or (**C**,**E**) cap1 Globin-Fluc reporter mRNAs in RRL with increasing concentrations of IFIT1 or IFIT1-containing complexes, as indicated. In (**B**) and (**D**), IFIT1 inhibition of cap1-RNA translation is shown as a dashed line, for comparison. Data were normalised to luciferase activity in the absence of IFIT protein and shown as the mean ± the standard error of three experiments. IC_{50} values are listed in Table 3-2.*

of IFIT1 was included in each reaction series. Normalised complexes (Figure 3-5C) were titrated in a buffer containing bovine serum albumin, which acts as a crowding agent to prevent IFIT proteins sticking to the plastic tubes, allowing accurate serial dilution. IFIT1-containing complexes were incubated with an *in vitro* transcribed and capped reporter mRNA, comprising a firefly luciferase (Fluc) open reading frame flanked by the relatively unstructured 5'UTR and 3'UTR of human β-globin (globin-Fluc, Figure 3-6A). Translation was quantified by measurement of luminescence from the Fluc reporter and was normalised to the 'no IFIT' control for each experiment. 50% inhibitory concentration (IC_{50}) values were derived from these experiments by non-linear regression using GraphPad Prism and are presented in Table 3-2.

IFIT1 inhibited translation of the cap0 globin-Fluc reporter in a concentration-dependent manner (Figure 3-6B,D), consistent with a number of previous reports *(Habjan et al., 2013;*

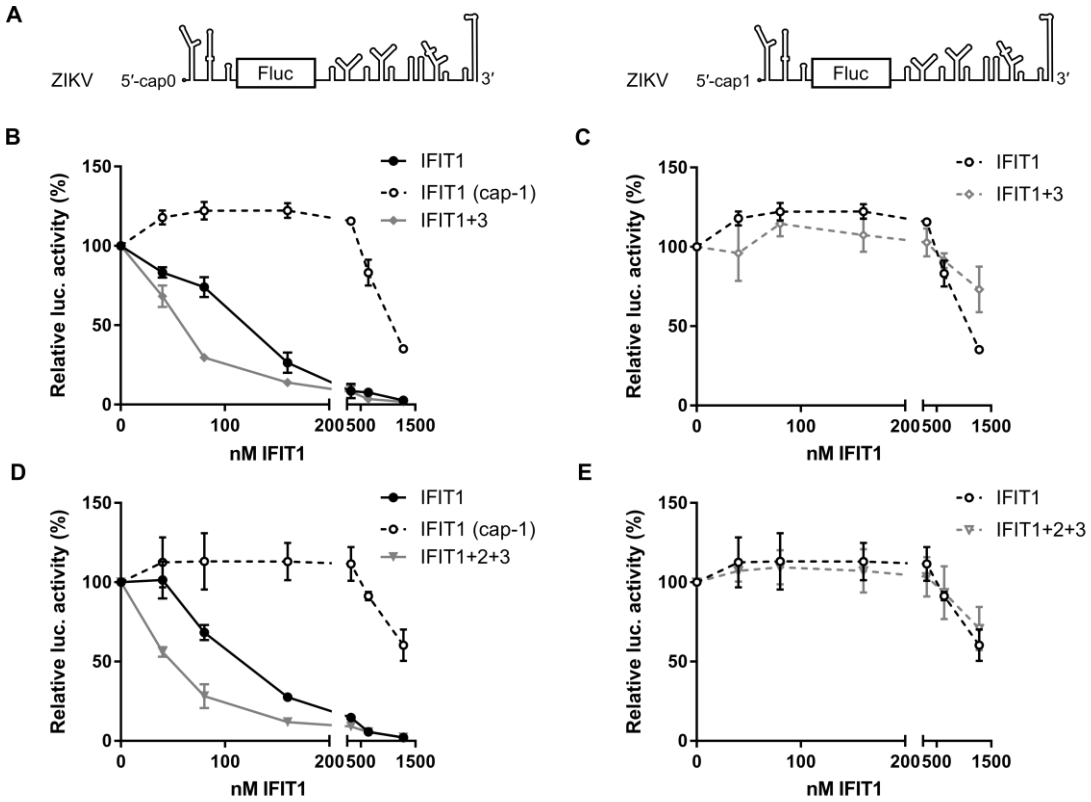

Figure 3-7 IFIT3 enhances translation inhibition of structured cap0 RNA by IFIT1.

A. *Schematic representation of ZIKV-Fluc mRNA.* ***B-E.*** *In vitro translation of of (**B**,**D**) cap0 or (**C**,**E**) cap1 ZIKV-Fluc reporter mRNAs in RRL with increasing concentrations of IFIT1 or IFIT1-containing complexes, as indicated. In (**B**) and (**D**), IFIT1 inhibition of cap1-RNA translation is shown as a dashed line, for comparison. Data were normalised to luciferase activity in the absence of IFIT protein and shown as the mean ± the standard error of three experiments. IC_{50} values are listed in Table 3-2.*

Kumar et al., 2014; Abbas et al., 2017a). The IFIT1:IFIT2 complex had the same activity as IFIT1 alone, indicating that IFIT2 does not regulate IFIT1 activity (Figure 3-6B). Therefore, this complex was not examined further. In contrast, complexing with IFIT3 significantly enhanced IFIT1 activity, decreasing the concentration of IFIT1 required to cause 50% inhibition of reporter expression by two- to three-fold (Figure 3-6B,D and Table 3-2).

It has been shown that secondary structure at the 5' end of mRNA can impact IFIT1 RNA binding *(Hyde et al., 2014; Abbas et al., 2017a)*. Therefore, a second model mRNA was examined, comprising the Fluc open reading frame flanked by 5'UTR and 3'UTR sequences of Zika virus (ZIKV-Fluc), which is much more structured than β-globin (Figure 3-7A). Since flaviviruses lacking 2'-O-methylation are inhibited by IFIT1 *(Daffis et al., 2010; Pinto et al., 2015)*, the cap0 ZIKV-Fluc mRNA represents a relevant model mRNA which is

Table 3-2 Translation inhibition and RNA binding by IFIT proteins and complexes.

50% inhibitory concentrations (IC_{50}) were derived from data presented in Figure 3-6 and Figure 3-7. Data were fit to [Inhibitor] versus normalised response curve (Y = 100)/(1 + (XHillSlope)/(IC50HillSlope)) using the least squares method in GraphPad Prism. Curves were compared by extra sum of squares F-test. RNA binding affinities were derived from data presented in Appendix E. Curves were fitted using the nonlinear Hill equation, $Fraction^{[bound]} = [IFIT1]^h \cdot Fraction^{[bound]}_{max}/([IFIT1]^h + K^h_{1/2,app})$ from data where [IFIT1] was ≥ 10 • [mRNA]. ND, not determined.

		***In vitro* translation in RRL, Figure 3-6 and Figure 3-7**		**Primer extension inhibition, Appendix E**	
Complex	**RNA**	**IC50 (nM IFIT1)**	**p-value (complex vs IFIT1)**	**RNA binding (K1/2app, nM)**	**Hill number**
IFIT1	cap0-globin-Fluc	71 ± 5.9	-	40 ± 1.2	2.8 ± 0.2
IFIT1:IFIT2	cap0-globin-Fluc	58 ± 5.3	0.2798	ND	ND
IFIT1:IFIT3	cap0-globin-Fluc	24 ± 1.2	<0.0001	19 ± 0.8	2.5 ± 0.2
IFIT1:IFIT2:IFIT3	cap0-globin-Fluc	45 ± 2.9	<0.0001	19 ± 0.7	2.0 ± 0.1
IFIT1	cap0-ZIKV-Fluc	112 ± 7.6	-	69 ± 1.8	3.5 ± 0.3
IFIT1:IFIT3	cap0-ZIKV-Fluc	54 ± 3.5	<0.0001	29 ± 1.1	4.1 ± 0.6
IFIT1:IFIT2:IFIT3	cap0-ZIKV-Fluc	46 ± 2.6	<0.0001	58 ± 2.3	3.1 ± 0.3

targeted by IFIT1. Higher concentrations of IFIT1 were necessary to inhibit translation of the cap0 ZIKV reporter, likely owing to the structured nature of the ZIKV 5'UTR (Figure 3-7, Table 3-2). However, IFIT3 still enhanced IFIT1 translation inhibition of this reporter by two fold, both in the context of the IFIT1:IFIT3 tetramer and the IFIT1:IFIT2:IFIT3 trimer (Figure 3-7B,D).

Cap1 versions of the Fluc reporter mRNAs were also examined (Figure 3-6C,E, Figure 3-7C,E). Consistent with previous observations *(Abbas et al., 2017a)*, IFIT1 could inhibit cap1 translation only at concentrations in excess of 1 μM. It has been estimated that 2.4 $x10^6$ copies of IFIT1 were expressed in a single IFN-stimulated HeLa cell *(Pichlmair et al., 2011)* and the average volume of a HeLa cell is approximately 2.6 x 10^3 μm^3 *(Zhao et al., 2008)*. Therefore the concentration of IFIT1 in a single cell at the peak of IFN stimulation is approximately 1.5 μM. As such, IFIT1 may be capable of inhibiting cap1 translation towards the upper limits of IFIT1 expression during the IFN response. Translation inhibition of cap1 mRNA was not affected by complexing with IFIT3 on either reporter construct.

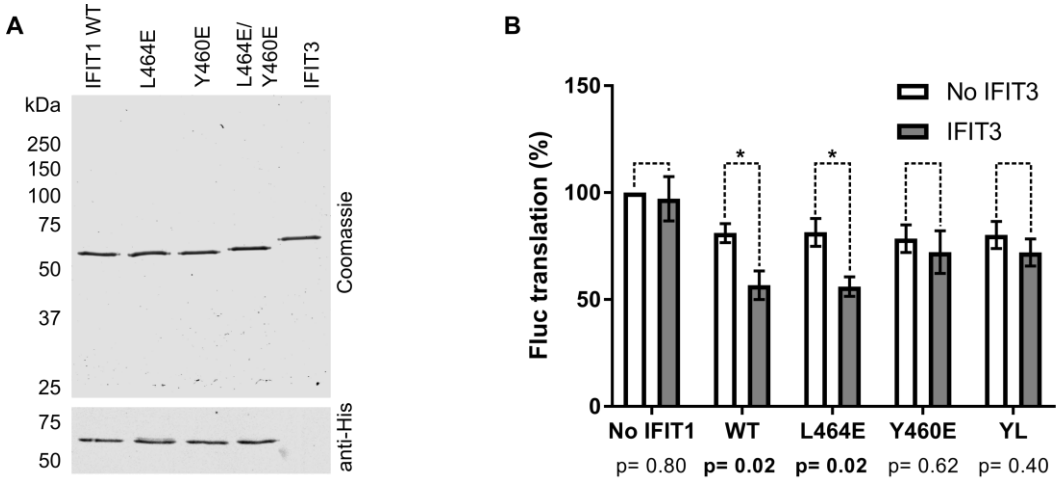

Figure 3-8 Interaction between IFIT1 and IFIT3 is necessary for cofator activity.

***A**. Coomassie and anti-His western blot of wildtype and mutant IFIT1. **B**. Luciferase activity from RRL charged with cap0-Globin-Fluc reporter mRNA with WT or mutant IFIT1 with or without IFIT3, as indicated. Data are normalised to the luciferase activity in the absence of IFIT1 and shown as the mean ± the standard error of three experiments. Statistical analyses were performed by unpaired, two-tailed Student's t-test. P values are indicated and an asterisk indicates statistical significance ($p < 0.05$).*

To determine whether the interaction between IFIT1 and IFIT3 is necessary for the observed stimulation of IFIT1 activity, mutants of IFIT1 which cannot bind IFIT3 were examined (Figure 3-8A). 40 nM wildtype or mutant IFIT1 was incubated with equimolar IFIT3 before addition of cap0-Fluc reporter RNA and RRL as before. IFIT1 alone caused 20% inhibition of translation, which was increased to 40% when IFIT3 was present (Figure 3-8B). Enhancement was also observed for IFIT1 L464E, a mutant which still binds to IFIT3 (see Appendix C). However, when Y460 was mutated or a double mutant (YL) was made, which partially or completely disrupts interaction with IFIT3, translation inhibition was no longer enhanced by addition of IFIT3 (Figure 3-8B). Therefore, IFIT3 can only act as a cofactor for IFIT1 when the two proteins interact directly.

3.2.4.1 Translation inhibition by IFIT complexes in human cells.

For a more physiologically relevant system, the effect of IFIT3 on IFIT1 activity was also examined in human cells. HEK293T cells were transfected with IFIT1 alone, or co-transfected with either wildtype IFIT3 or Y438E/L422E mutant IFIT3, which cannot bind to IFIT1. The expression level of overexpressed FLAG-IFIT1 was equivalent to endogenous IFIT1 expression after 24 hours treatment with type I IFN (Appendix D), ensuring this assay was performed within physiologically relevant parameters. Plasmid concentrations

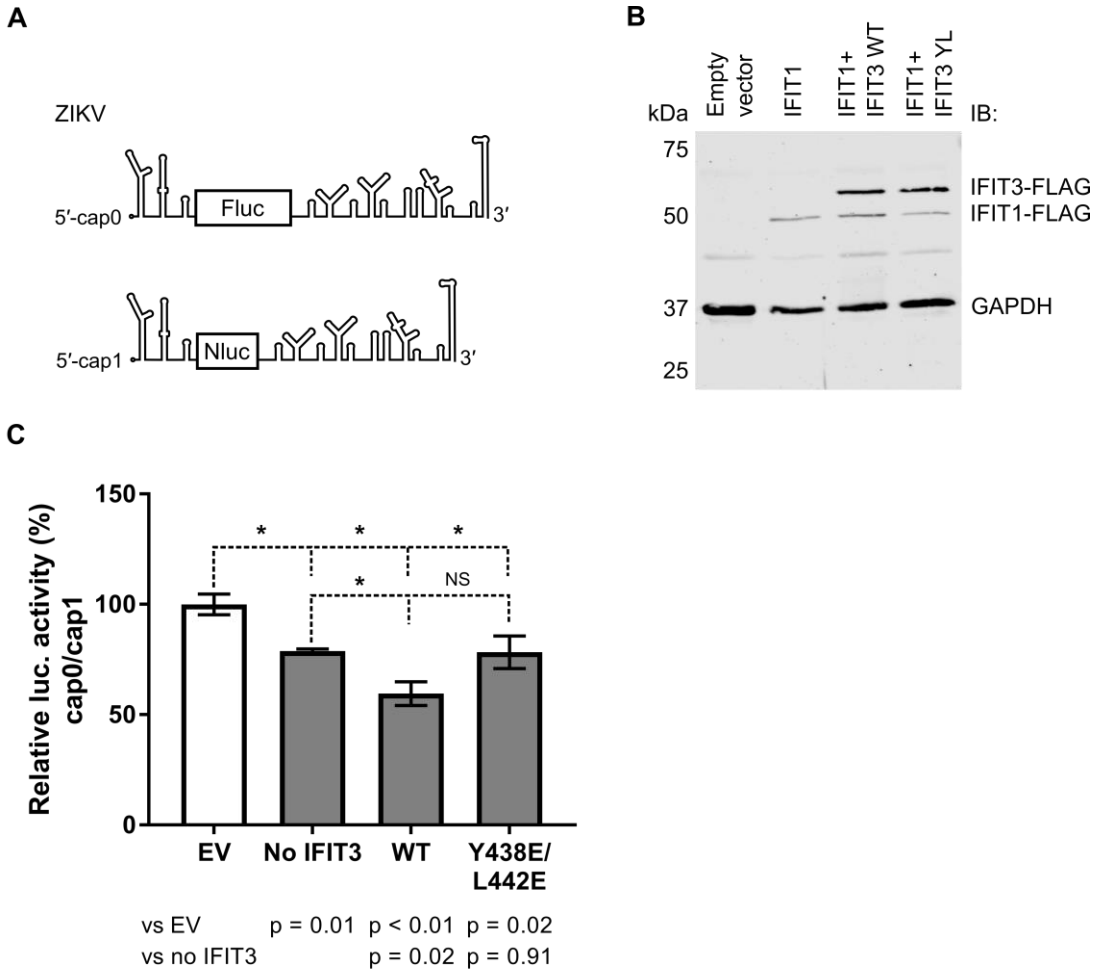

Figure 3-9 IFIT3 enhances IFIT1 activity in human cells.

A. *Schematic representations of reporter mRNAs used in cell-based assays.* ***B.*** *Immunoblotting against FLAG and GAPDH in HEK293T cells overexpressing FLAG-tagged IFIT1 with WT or mutant IFIT3, as indicated.* ***C.*** *Translation of ZIKV reporter mRNAs in HEK293T cells overexpressing IFIT1 with WT or mutant IFIT3. Translation was measured by luciferase activity, expressed as the ratio of Fluc (cap0) over Nluc (cap1) signal, normalised to the empty vector control and shown as the mean ± standard deviation of three biological repeats. Statistical analyses were performed by unpaired, two-tailed Student's t-test. P values are given and an asterisk indicates statistical significance (p < 0.05).*

were adjusted to control for the stabilising effect of IFIT3 on IFIT1 expression, and equal protein was confirmed by western blotting (Figure 3-9B).

After 24 hours, cells were transfected with *in vitro* transcribed and capped ZIKV minigenomes, comprising Fluc or Nanoluciferase (Nluc) reporter genes flanked by the ZIKV 5' and 3'UTRs (Figure 3-9A). Since cap1 ZIKV mRNA is resistant to IFIT1-mediated

translation inhibition, signal from the cap1-ZIKV-Nluc reporter served as an internal control for RNA transfection efficiency, while signal from the cap0-ZIKV-Fluc reporter was used as a readout of IFIT1 activity. Translation was quantified by measuring luminescence from both reporters and expressed as a ratio of Fluc(cap0)/Nluc(cap1), normalised to the empty vector control condition. IFIT1 alone caused a 20% reduction in cap0 translation, while co-expression with wildtype IFIT3 enhanced translation inhibition by 2-fold (Figure 3-9C), consistent with the *in vitro* translation data. Co-expression with mutant IFIT3 had no effect on IFIT1 activity. Therefore in cells, direct interaction with IFIT3 is necessary for translation inhibition by IFIT1.

3.2.4.2 RNA binding by IFIT complexes.

To confirm that IFIT3 can directly enhance IFIT1 RNA binding, a primer extension inhibition approach was undertaken to quantify IFIT1 RNA binding affinity. IFIT RNA binding assays were performed by Dr Trevor Sweeney and are presented in Appendix E. IFIT1 and IFIT1-containing complexes purified in section 3.2.2 were incubated with the model RNAs described above, prior to addition of a radiolabelled primer for reverse transcription. The resultant cDNA products were separated by denaturing PAGE and detected by autoradiography. In the absence of IFIT binding, a full-length cDNA is produced; bound IFIT1 arrests reverse transcriptase producing a cDNA product truncated by 7 nt *(Kumar et al., 2014)*, corresponding to the depth of the IFIT1 RNA binding pocket *(Abbas et al., 2017a)*. Therefore, only specific binding is quantified, which offers an advantage over other methods such as electrophoretic mobility shift assays and filter binding assays. Additionally, the toeprinting approach is performed under equilibrium binding conditions, allowing more accurate determination of binding constants.

As previously reported, IFIT1 bound cap0-globin-Fluc mRNA with high affinity *(Kumar et al., 2014)*. Complexing IFIT1 with IFIT3 or IFIT2:IFIT3 enhanced IFIT1 binding by two fold, consistent with the *in vitro* translation data presented above (see Table 3-2). IFIT1 alone only reached ~80% binding even at the highest concentrations tested, while IFIT3-containing complexes could fully saturate binding. This effect was more pronounced on the more structured ZIKV-Fluc RNA. IFIT1 bound to cap0 ZIKV-Fluc RNA with lower affinity and reached only 60% saturation. Heterocomplexing with IFIT3 again enhanced binding by up to two fold and allowed over 90% binding saturation. This indicates that

IFIT1 in complex with IFIT3 is more stably bound to the 5' end of cap0 RNA, making it more resistant to displacement by reverse transcriptase.

3.3 Conclusions

In this chapter, the reconstituted human IFIT complex was examined in terms of its stability and activity. It has been revealed that IFIT3 interacts with both IFIT1 and IFIT2, acting as a central scaffold for a trimeric complex. Interaction enhanced the thermal stability of all component proteins, indicating that heterocomplexing is a thermodynamically preferable state. IFIT3 was found to be an allosteric activator of IFIT1 cap0 RNA binding, enhancing translation inhibition activity *in vitro* and in cells.

Serendipitously, these findings were independently confirmed in another report, where it was shown that IFIT3 binds to IFIT1 with nanomolar affinity, and this binding enhances IFIT1 binding to cap0 RNA and promotes antiviral activity during infection *(Johnson et al., 2018)*. In that study, a co-crystal structure of IFIT1 in complex with two-and-a-half C-terminal TPRs from IFIT3 was solved, which showed a large buried surface at the binding interface, much larger than that of the IFIT1 homodimer *(Abbas et al., 2017b; Johnson et al., 2018)*. Hydrogen-deuterium exchange assays revealed additional interactions between IFIT3 and the C-terminal domain of IFIT1. This large interaction surface is entropically favourable, compared to IFIT1 homodimers, due to the liberation of solvent from the interaction interface. This is supported by isothermal titration calorimetry experiments in the same study, which showed very low nanomolar affinity between the two proteins *(Johnson et al., 2018)*.

Here it was shown that IFIT3 enhances the biophysical stability of IFIT1, as well as enhancing its expression in human cells when both were transiently overexpressed. Using an inducible IFIT3 expression system, Johnson et al *(2018)* observed that IFIT3 significantly enhanced IFIT1 expression in a dose-dependent manner, increasing the half-life of IFIT1. In the absence of IFIT3, IFIT1 had a half-life of less than two hours, while in transgenic IFIT3-overexpressing cells, IFIT1 was stabilised to over 24 hours $t_{1/2}$. Together with the differential scanning fluorimetry data presented here, this supports a hypothesis whereby the instability of IFIT1 homooligomers promotes their turnover in cells, while the intrinsic physical stability of the IFIT1:IFIT3 complex rescues expression. Like IFIT1,

homodimeric IFIT2 was found to have a low melting temperature and propensity to aggregate. Previously, when overexpressed in human cells, IFIT2 was found shown to form pro-apoptotic aggregates which were cleared in a proteasome-dependent manner *(Chen et al., 2017)*, Therefore, unstable IFIT proteins may be removed from the cell by a generic turnover mechanism. An alternative explanation would be that IFIT1 is specifically targeted for degradation, and IFIT3 conceals a motif on IFIT1 to prevent turnover. Work is ongoing in our laboratory to differentiate these possibilities.

Finally, IFIT3 was shown to enhance translation inhibition by IFIT1 by promoting binding to cap0 RNA, increasing affinity by two to three-fold. Using filter binding assays, Johnson et al *(2018)* reported three-fold higher cap0 binding affinity when IFIT1 was complexed with a C-terminal fragment of IFIT3. In these assays, IFIT3 did not enhance IFIT1 binding to cap1 RNA, consistent with the *in vitro* translation data presented here. Interestingly, they did observe a dramatic reduction in 5'ppp-RNA binding, indicating that IFIT3 has some effect on IFIT1 RNA binding specificity, promoting cap0 recognition over binding to uncapped RNA. Overexpression of IFIT3 in cells promoted restriction of flavivirus replication, including ZIKV and WNV, in viruses lacking 2'-O-methyltransferase activity, supporting the data presented here using cap0 ZIKV model RNAs *(Johnson et al., 2018)*.

While these works have gone some way to understanding how IFIT oligomerisation directly affects their activity, there are still many open questions. The mechanism of IFIT3 cofactor activity remains to be determined. One possibility is that IFIT3 makes additional contacts with the bound RNA, thereby stabilising the interaction. IFIT homooligomers have previously been shown to interact with RNA downstream of the 5' end, indicating that cooperative binding by other units in the complex may contribute to binding avidity *(Kumar et al., 2014)*. However, unlike IFIT2, IFIT3 is not predicted to have a large positively charged nucleic acid binding groove and is not reported to bind to RNA *(Kumar et al., 2014)*. Here when IFIT3 was present no additional reverse transcriptase stops were observed, indicating that IFIT3 does not make contact with the RNA.

Instead, IFIT3 may promote tighter binding of IFIT1 to cap0 mRNA by limiting IFIT1 flexibility, decreasing the off-rate of the RNA to maintain binding. IFIT5 was previously shown to cycle between 'open' and 'closed' conformations upon RNA binding, with the C-terminal domain rotating about the flexible pivot domain to close around the bound RNA

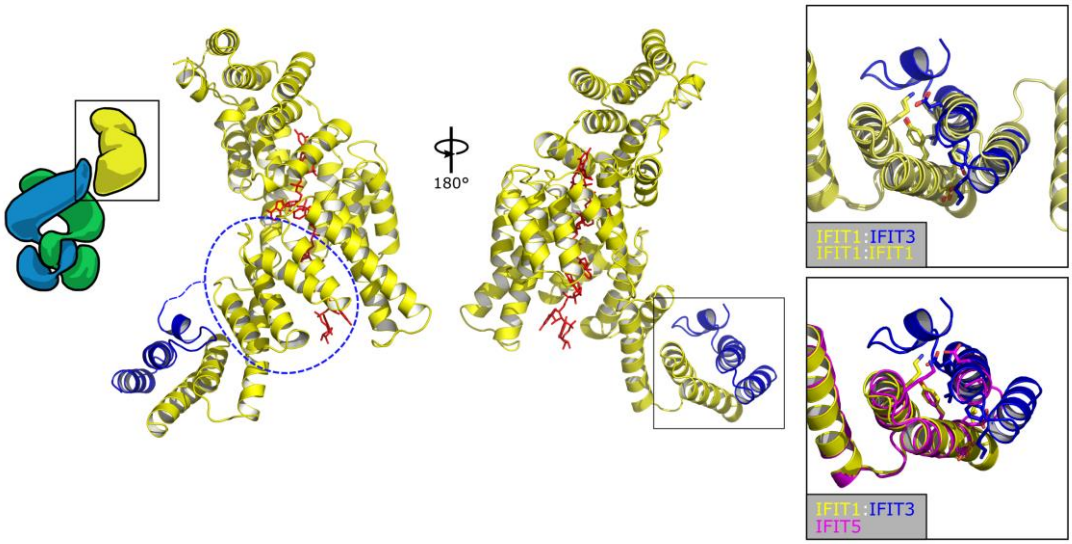

Figure 3-10 The IFIT1:IFIT3 complex.

Crystal structure of IFIT1, yellow, in complex with the C-terminal domain of IFIT3, blue (PDB: 6C6K), with a schematic of the trimeric IFIT1:IFIT2:IFIT3 complex. IFIT3 has an extended C-terminal domain which may make contact with additional regions of the IFIT1 subdomain III, indicated by a blue dashed line. The interface between the two molecules is enlarged on the right, and key residues are shown as sticks. In the upper panel, the IFIT1:IFIT3 complex is superposed with homodimeric IFIT1 (yellow, PDB: 5W5H), illustrating mutually exclusive homo- and hetero-complexes. In the lower panel, the IFIT1:IFIT3 complex is superposed with monomeric IFIT5 (magenta, PDB: 4HOT), which does not interact with IFIT1 or IFIT3, owing to an additional C-terminal α-helix which occludes the YxxxL interaction motif.

strand *(Abbas et al., 2013)*. Hydrogen-deuterium exchange experiments revealed that the extended C-terminal domain of IFIT3 makes contact with the pivot domain of IFIT1, not just the C-terminal interaction interface (Figure 3-10, dashed line) *(Johnson et al., 2018)*. This supports a model by which IFIT3 locks IFIT1 in a closed conformation following RNA binding, to increase binding affinity, and merits further investigation.

It is known that IFIT proteins are not equally expressed during infection. Following different stimuli, the kinetics and magnitude of IFIT expression varies between different family members *(Terenzi et al., 2006)*. Therefore, the composition of the IFIT complex is likely to change over the course of infection, which will contribute to the regulation of its constituent parts. For example, post-translational modification or degradation of IFIT3 may allow for rapid changes in the expression levels of the other two IFIT proteins in the

complex. Promoting IFIT3 expression may therefore be important to sustain antiviral responses.

IFIT5 is monomeric and as such does not benefit from the stabilising and enhancing effects of a cofactor. This is because IFIT5 has an additional C-terminal helix which buries the YExxL motif, preventing homo- or hetero-oligomerisation (Figure 3-10). IFIT5 binds exclusively to 5'ppp RNA *(Pichlmair et al., 2011; Abbas et al., 2013; Feng et al., 2013)*, which is not typically found under normal cellular conditions, rendering IFIT5 a relatively safe protein to overexpress. By contrast IFIT1 binds capped mRNA and is capable of binding to endogenous cap1 RNA at high concentrations *(Abbas et al., 2017a)*. Therefore, IFIT1 has the potential to be highly cytotoxic by shutting off host translation *(Guo et al., 2000b)*. As such, regulation of IFIT1 expression and activity by IFIT3 may be necessary to avoid excessive cell death during infection.

Finally, human IFIT1B has been suggested to lack RNA binding activity, based on overexpression experiments in yeast and mammalian cells *(Daugherty et al., 2016)*. However, IFIT1B is notoriously difficult to express recombinantly *(Kumar et al., 2014)*, indicating it may be highly unstable in the absence of a binding partner. Previously, peptides corresponding to IFIT1B were identified co-precipitating with both IFIT1 and IFIT3, consistent with the shared C-terminal YExxL motif in all three proteins *(Pichlmair et al., 2011)*. It is possible that co-expression with IFIT3 may stabilise IFIT1B expression, allowing the function of IFIT1B to be properly dissected. As discussed in 1.3.1.1, IFIT1B may be expressed in immature immune cells and, since IFIT3 is already known to function in regulating immune cell differentiation *(Huang et al., 2008)*, it is tempting to speculate a role for a complex of IFIT1B and IFIT3 in this process.

For a more detailed discussion of the implications of human IFIT oligomerisation and protein-protein interactions, see Mears & Sweeney *(2018)*.

4 THE MURINE IFIT FAMILY

4.1 Background

4.1.1 Mouse Ifits

While the murine Ifit1 model has been used extensively to study human disease and viral infection, there is little biochemical information specifically on the activity of the murine Ifit family. The function of murine Ifit proteins is often inferred from their human counterparts. As described in section 1.3.4, given the differences between human and murine IFIT protein functions, this assumption is not reliable.

The murine Ifit family lacks a true orthologue of human IFIT1. Instead Ifit1b has been duplicated twice, resulting in three paralogous genes, annotated as Ifit1, Ifit1b and Ifit1c. Ifit1 has been well studied for its sequence and biochemical similarities with human IFIT1, though there are some important functional distinctions. In particular, murine Ifit1 does not bind to cap1 RNA while human IFIT1 can, at high concentrations *(Daugherty et al., 2016; Abbas et al., 2017a)*. The latter two family members, Ifit1b and Ifit1c, have not been characterised. There is mass spectrometry evidence supporting the expression of Ifit1c in stimulated murine cells *(Habjan et al., 2013)*. However, the expression patterns of Ifit1b and Ifit1c remain unknown. Studying these additional murine Ifit family members may address open questions in mouse Ifit biology, including: how do rodents compensate for the loss of IFIT1, the loss of IFIT5 and the truncation of Ifit3? Do these differences significantly impact our ability to interpret data from mouse models when trying to understand human disease?

4.1.2 Aims

The aim of this chapter is to examine the expression patterns of the entire murine Ifit family, including uncharacterised members whose existence is yet to be proven. Then these proteins will be screened for their activity *in vitro*, to determine their function, allowing biochemical characterisation. A detailed understanding of the expression patterns and functions of every member of the murine Ifit family is necessary to examine and improve the mouse model.

4.2 Results

4.2.1 Murine Ifit expression

4.2.1.1 qPCR primers

To examine murine Ifit mRNA expression, specific qPCR primers were designed for two-step Sybr green RT-qPCR (Table 2-3). Ifit1 primers have been published previously *(Tamassia et al., 2008)*. Ifit1b, Ifit1c, Ifit2, Ifit3 and Ifit3b primers were designed within the coding sequence of the second exon, against regions with the highest sequence divergence to ensure their specificity. Since the first exon is very short and highly conserved, designing primers across the exon-exon boundary was not possible. This was particularly challenging for Ifit3 and Ifit3b given the high degree of nucleotide identity between the two sequences. Specificity was verified by PCR against plasmids containing the coding sequence for each Ifit. Each primer pair showed high specificity for their target sequence (Figure 4-1A).

To determine the linear range and the limit of detection, primers were tested against a DNA standard curve. Plasmids containing Ifit coding sequences were linearised by restriction with XhoI and purified by gel extraction followed by ethanol precipitation and 10-fold dilution series were generated from 1 ng (1.5×10^5 plasmid copies) to 10 attograms (1.5 plasmid copies). The qPCR signal, determined by decreasing cycle threshold (CT), correlated well with plasmid DNA concentration ($R^2 > 0.95$) and signal was detectable even at the lowest DNA concentrations tested, indicating a very low limit of detection (Figure 4-1B). The slopes of the standard curve were between -3.6 to -3.1, corresponding to PCR efficiencies of 90% to 106%, within the acceptable range for standard qPCR primers. Together, these validation data indicate that fold-changes in mRNA abundance can be accurately calculated using these primers.

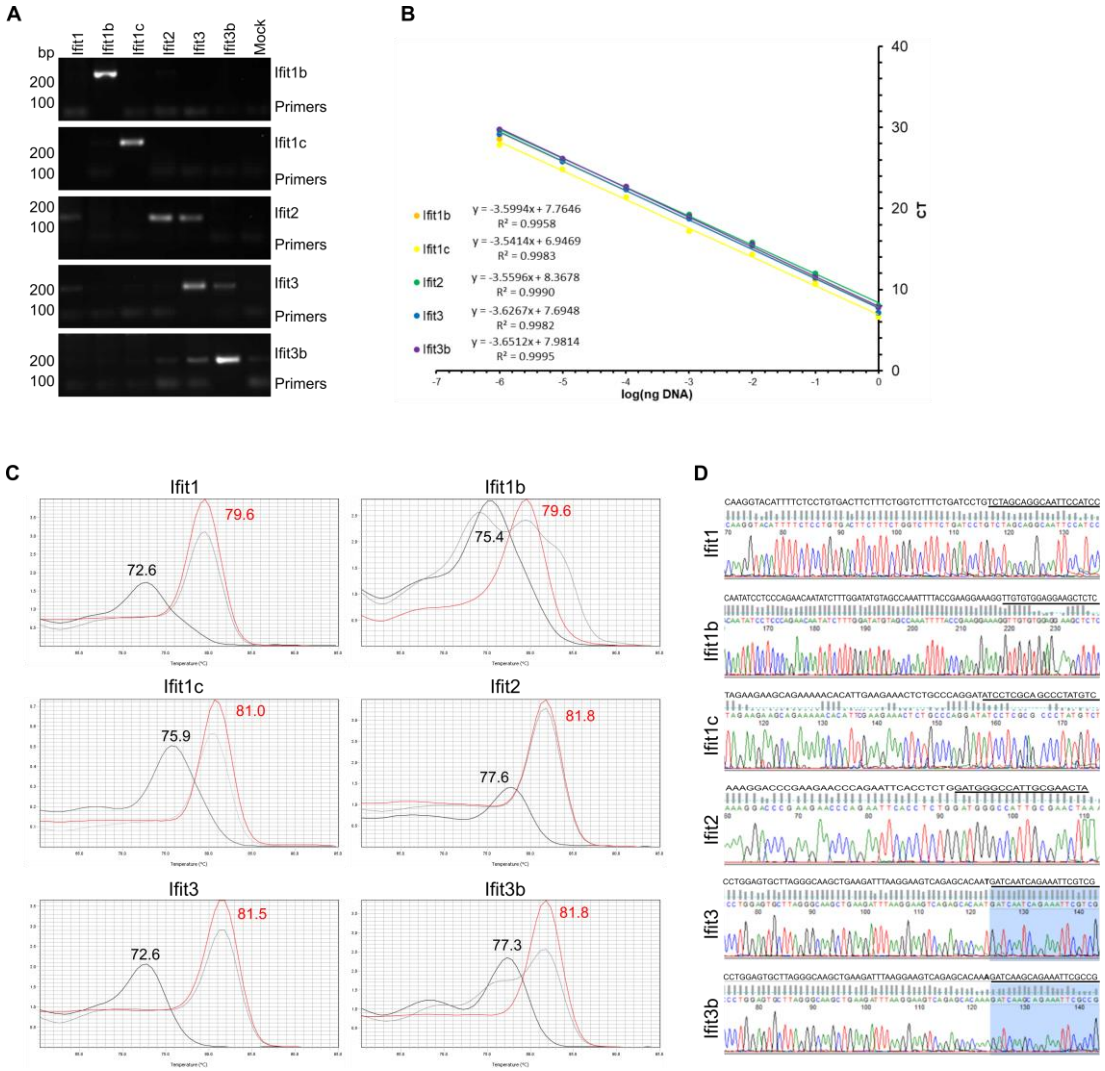

Figure 4-1 Ifit qPCR primer validation.

A. *Specificity of Ifit qPCR primer pairs, tested against plasmids containing Ifit coding sequences.* ***B.*** *Linearity of Ifit amplification, upon 10-fold serial dilutions of linearised plasmids containing Ifit coding sequences. Log_{10}-transformed mass of DNA (ng) was plotted against qPCR cycle threshold (CT) and fit by linear regression. Equations and R^2 values showing linear amplification and goodness of fit are given next to the graph legend.* ***C.*** *Melt curves from qPCR amplification of the indicated Ifit mRNAs, using either cDNA from unstimulated (grey) or IFNβ-stimulated RAW264.7 cells or water (black) as templates.* ***D.*** *Sanger sequencing analysis of RT-qPCR products from stimulated RAW264.7 cells. Reference sequences are given above and primer sequences are underlined.*

Having determined specificity and linearity of signal, primer pairs were tested on endogenous Ifit mRNA. RAW264.7 murine macrophage-like cells were stimulated with IFNβ or transfected with polyI:C, a synthetic immune-stimulatory dsRNA. Cellular RNA

was harvested after 8 hours. Since the Ifit primers were not designed across an exon-exon boundary, RNA was purified twice to minimise genomic DNA carryover. Each Ifit mRNA was detectable in both IFN-treated and polyI:C-stimulated cells. The melting temperature for specific amplification from cellular cDNA was sufficiently different from non-specific signal in the water-only controls (Figure 4-1C).

qPCR products were purified by gel extraction and sent for Sanger sequencing to determine product specificity. Only the target mRNA sequences were detected from each primer pair (Figure 4-1D). In particular, for Ifit3 and Ifit3b there was only a single nucleotide difference between the PCR products from either mRNA. However, there was no evidence of cross-contamination between the PCR products at this position.

4.2.1.2 Antibodies

To confirm Ifit expression at the protein level, it was necessary to identify specific antibodies for each family member (see Table 2-5). Given the high degree of amino acid identity between Ifit3 and Ifit3b (99%), these proteins are impossible to distinguish by western blotting and will be annotated as Ifit3/3b to reflect this. Antibody specificity was tested by western blotting against both recombinantly expressed and purified Ifit proteins (see Figure 4-7) or FLAG-tagged Ifit proteins overexpressed for 24 hours in HEK293T cells. RAW264.7 cells were treated with a high dose of murine IFNβ for 14 hours before harvesting in passive lysis buffer to detect endogenous Ifit expression.

Commercial antibodies were available to detect murine Ifit1, Ifit2 and Ifit3/3b. Anti-Ifit1 (sc-134949, Santa Cruz) specifically detected murine Ifit1 but no other family members, and detected a single band in IFN-treated RAW cells (Figure 4-2A). Anti-human IFIT2 (12604-1-AP, ProteinTech) was cross-reactive for both Ifit2 and Ifit3/3b to approximately the same extent and detected two specific endogenous bands of the correct molecular weight (Figure 4-2A). Additionally, a commercial antibody against human IFIT1 was tested (PA3-848, Pierce). Surprisingly, while murine Ifit1 was weakly detected by this antibody, Ifit1b was detected very strongly (Figure 4-2A). A band of the correct molecular weight was detectable in IFN-stimulated cell lysates. However, this may represent strong detection of lowly expressed Ifit1b, or weak detection of highly expressed Ifit1.

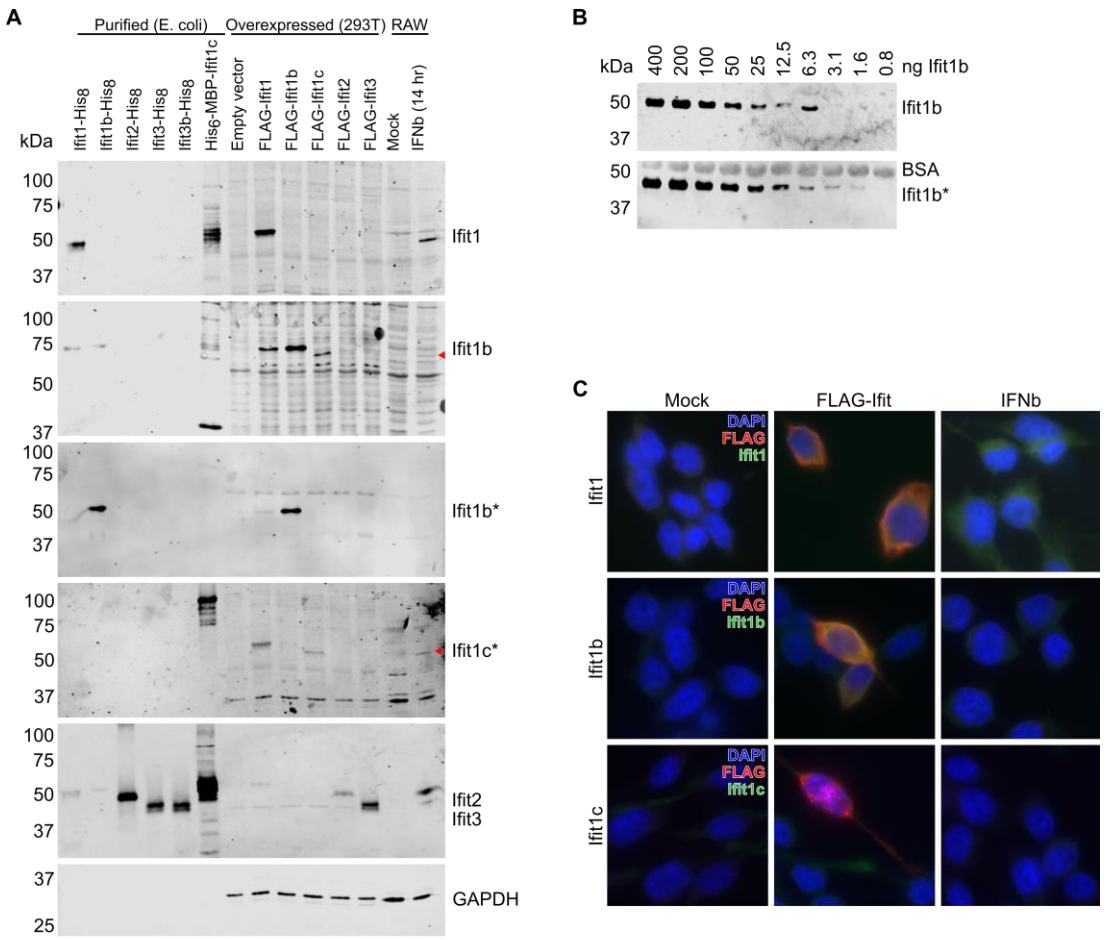

Figure 4-2 Ifit antibody validation.

A. *Western blotting of RAW264.7 cells stimulated with IFNβ for 14 hours alongside recombinant Ifit proteins purified from E. coli or overexpressed in HEK293T cells, probed with antibodies against Ifit1 (Santa-cruz, sc-134949); Ifit1b, using a cross-reactive antibody against human IFIT1 (Pierce, PA3-848); Ifit1b, using a peptide-raised antibody (Eurogentec), indicated by as asterisk; and Ifit1c, using a peptide raised antibody (Eurogentec), indicated by an asterisk; Ifit2 and Ifit3, using a cross-reactive antibody for human IFIT2 (Proteintech, 12604-1-AP). GAPDH is included as a loading control for cell lysates.* ***B.*** *Serial dilution of recombinant Ifit1b protein, to test detection limit of Ifit1b antibodies. In the lower panel, bovine serum albumin (BSA), used to ensure accurate serial dilution, is faintly visible.* ***C.*** *Immunofluorescence of 17C1 cells, either mock treated, transfected with FLAG-Ifit overexpression plasmids or stimulated with IFNβ for 16 hours. Cells were stained with antibodies against FLAG, and Ifit1 (Santa-cruz, sc-134949), Ifit1b (Eurogentec) or Ifit1c (Eurogentec). Cell nuclei were stained with DAPI.*

To detect Ifit1b and Ifit1c with higher sensitivity and specificity, custom antibodies were raised and purified against specific peptides from each protein. These were tested for their specificity and one antibody for each was identified which had little cross-reactivity with

other Ifit family members (Figure 4-2A). Antibody concentrations (25-50 μg/mL) and incubation conditions (overnight at 4 °C in 5 % BSA PBS-T) were optimised for detection of endogenous protein from IFN-treated RAW264.7 cell lysates.

For Ifit1b, the peptide-raised antibody was able to detect as little as 1.6 ng of recombinant protein while the cross-reactive commercial antibody had a limit of detection of 12.5 ng (Figure 4-2B). Therefore, since the peptide-raised antibody could not detect endogenous Ifit1b, it is likely that the commercial antibody may be detecting Ifit1 in stimulated cell lysates. This also indicates that Ifit1b is expressed at less than 160 pg per μg of total protein in the cell lysate. By way of comparison, in IFN-stimulated HeLa cells, human IFIT1 was previously detected at over 200 pg/μg *(Pichlmair et al., 2011)*.

Ifit antibodies were also tested for their ability to detect overexpressed and endogenous proteins by immunofluorescence (Figure 4-2C). Murine 17C1 cells were either transfected with a plasmid encoding FLAG-tagged Ifit1, Ifit1b or Ifit1c, or stimulated with IFNb, then harvested after 16 hours for immunofluorescence microscopy. Endogenous Ifit1 was weakly detected in IFN-stimulated 17C1, though the signal was poor. Ifit1 showed diffuse cytoplasmic localisation, typical of IFIT proteins *(Yu et al., 1997; Guo et al., 2000a; Huang et al., 2008)*. While overexpressed FLAG-Ifit1b was detectable by the custom Ifit1b antibody, neither Ifit1b nor Ifit1c could be detected in IFN-stimulated cells, and the background for these antibodies was very high in mock cells, indicating that they are not suitable for use in immunofluorescence.

4.2.1.3 Induction of Ifit expression in murine cell lines

The expression of murine Ifit1, Ifit2 and Ifit3 have been examined individually and together in various studies *(Bluyssen et al., 1994a; Smith and Herschman, 1996; Terenzi et al., 2005, 2007; Wacher et al., 2007)*. However, to date no study has examined the expression of the entire murine Ifit family in parallel, using quantitative techniques and including the non-canonical family members. To address this, the induction kinetics of murine Ifits were examined under different conditions. Murine embryonic fibroblasts (MEF) (Figure 4-3) and RAW264.7 macrophage-like cells (Figure 4-4) were stimulated with murine IFNβ or transfected with polyI:C. RNA and protein were harvested up to 48 hours post stimulation for RT-qPCR and western blot analyses using the primers and antibodies described above.

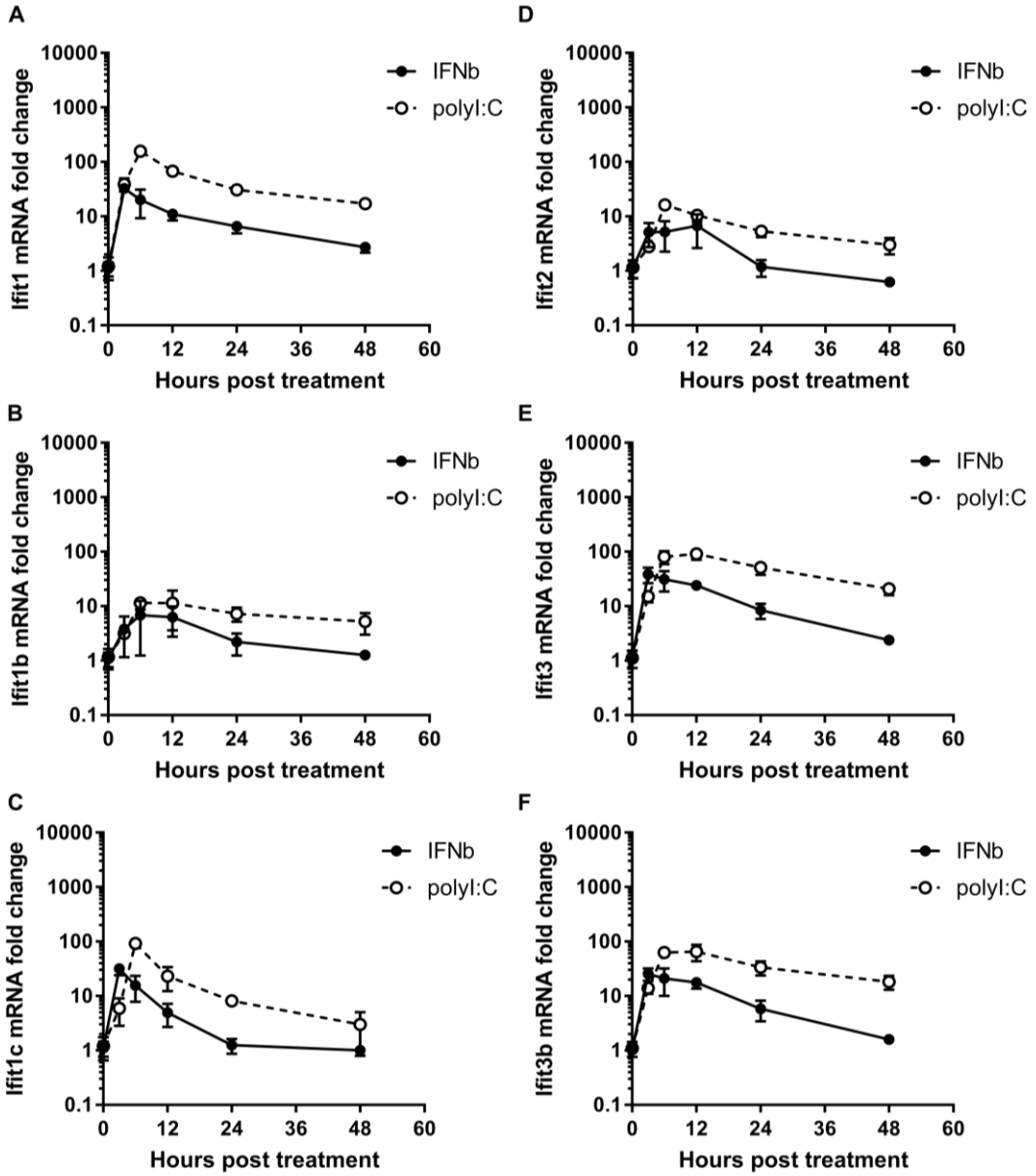

Figure 4-3 Ifit mRNA expression in MEF cells.

A-F. *RT-qPCR analysis of RNA extracted from MEF cells stimulated with IFNβ or transfected with polyI:C over 48 hours, detecting* ***A.*** *Ifit1* ***B.*** *Ifit1b* ***C.*** *Ifit1c* ***D.*** *Ifit2* ***E.*** *Ifit3* ***F.*** *Ifit3b. Graphs show the mean and the standard error of three biological replicates.*

Ifit mRNA expression was rapidly and strongly induced following stimulation, with peak expression 3 to 6 hours post stimulation. Rapid induction following polyI:C is consistent with direct transcription by activated IRF3, as previously reported *(Grandvaux et al., 2002; Terenzi et al., 2005; Daffis et al., 2007)*. Expression decreased between 9-24 hours. Decline was slower in polyI:C-treated cells, compared to IFN-stimulated cells, consistent with secondary IFN signalling induced by dsRNA sensing which maintains the response.

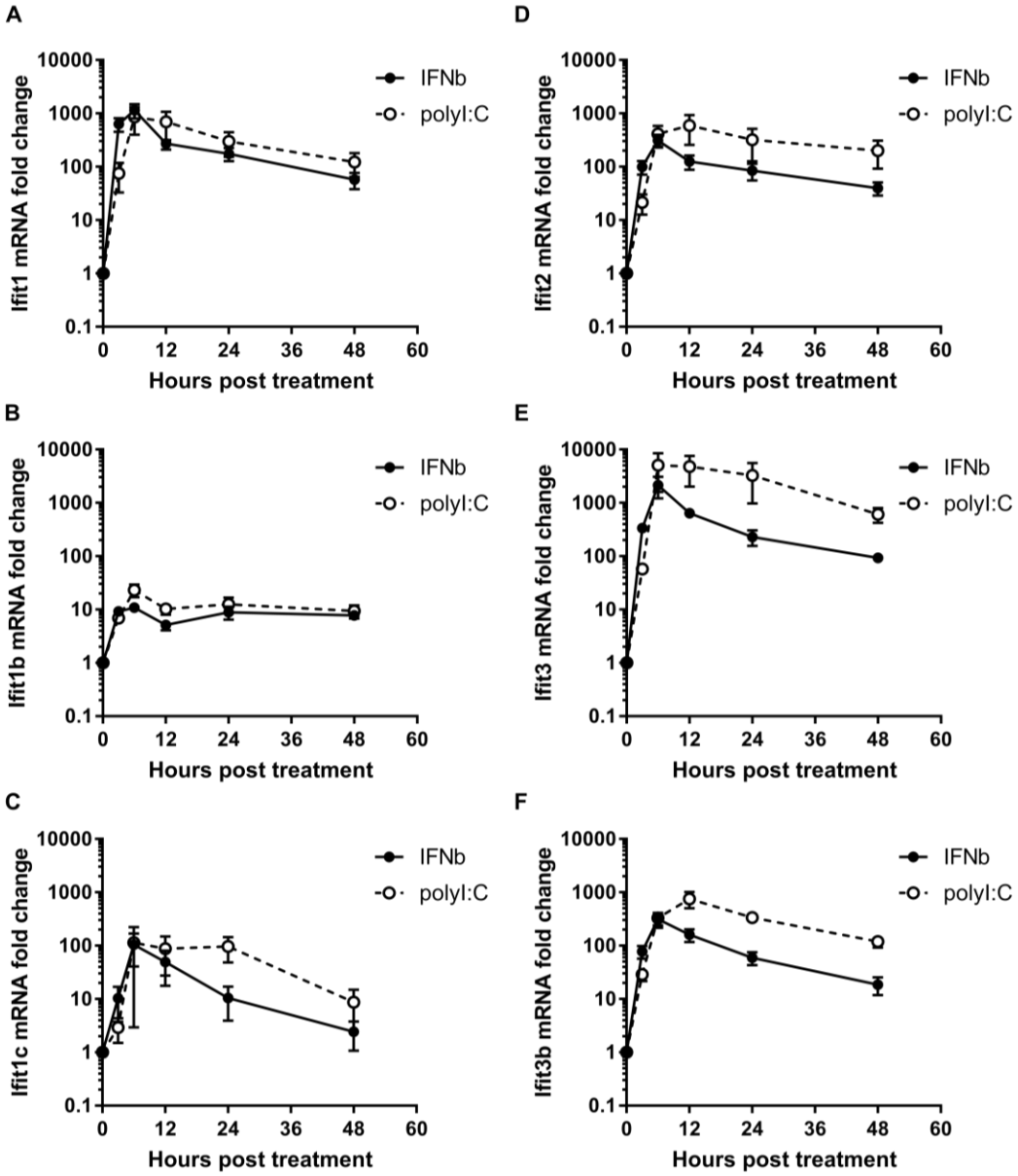

Figure 4-4 Ifit mRNA expression in RAW264.7 cells.

A-F. *RT-qPCR analysis of RNA extracted from RAW264.7 cells stimulated with IFNβ or transfected with polyI:C over 48 hours, detecting* ***A.*** *Ifit1* ***B.*** *Ifit1b* ***C.*** *Ifit1c* ***D.*** *Ifit2* ***E.*** *Ifit3* ***F.*** *Ifit3b. Graphs show the mean and the standard error of two biological replicates.*

Compared to other Ifit family members, Ifit1b was poorly induced at the mRNA level. There was no evidence of high basal Ifit1b expression, since CT values in unstimulated cells were around 28 cycles, similar to the other Ifits; if compared to the cDNA standard curved performed in section4.2.1.1, this corresponds to approximately 150 copies of Ifit1 mRNA. This indicates that Ifit1b is poorly expressed at the mRNA level, compared to other Ifit genes after IFN stimulation.

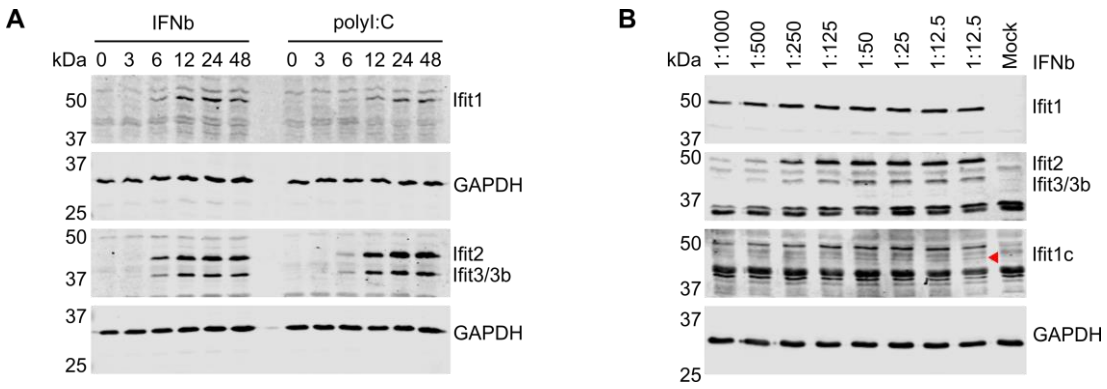

Figure 4-5 Ifit protein expression in murine cells.

A. *Immunoblot analysis of RAW264.7 cells stimulated with IFNβ or transfected with polyI:C over 48 hours. GAPDH is included as a loading control for each membrane tested.* ***B.*** *Immunoblot analysis of 17C1 cells stimulated with increasing doses of IFNβ for 24 hours. GAPDH is included as a loading control for each membrane tested.*

Ifit mRNA expression was generally lower in MEF cells compared to RAW cells (compare Figure 4-3 to Figure 4-4). As such, Ifit proteins were only reliably detected in RAW cell lysates (Figure 4-5A). Ifit1, Ifit2 and Ifit3/3b proteins were detectable 6-12 hours following stimulation, after the peak of mRNA expression, and remained high up to 48 hours. This expression pattern is highly consistent with previous studies *(Terenzi et al., 2005, 2007)*. Unfortunately, Ifit1b and Ifit1c were not detectable, presumably because their expression was lower than the limit of detection for the antibodies.

Ifit protein expression was also examined in 17C1 cells, a fibroblast cell line derived from immortalised Swiss 3T3 cells *(Sturman and Takemoto, 1972)*. These cells do not respond to viral infection *(Irigoyen et al., 2016)*, indicating that they may have impaired immune signalling pathways. Therefore, to determine whether these cells can respond to type I IFN, an IFNβ titration was performed. Ifit1, Ifit2 and Ifit3/3b expression was detectable even when cells were stimulated with low concentrations of IFNβ, and increased in a dose-dependent manner (Figure 4-5B). Ifit1c expression was only detectable when cells were stimulated with a high concentration of IFNβ, while Ifit1b could not be detected.

4.2.1.4 Activity of Ifit promoters

To determine why Ifit1b is apparently so poorly expressed compared to other murine Ifit family members, the activity of its promoter was investigated. Ifit1 has two well-defined

tandem interferon stimulated response elements (ISRE) within 100 bp of the transcription start site (TSS) (Figure 4-6A-B). Similarly, the Ifit1c promoter contains one ISRE, also proximal to the TSS, and a second ISRE-like sequence further upstream. For Ifit1b, there are two annotated TSSs: one proximal to the coding sequence of Ifit1b (Ifit1b_2) and one

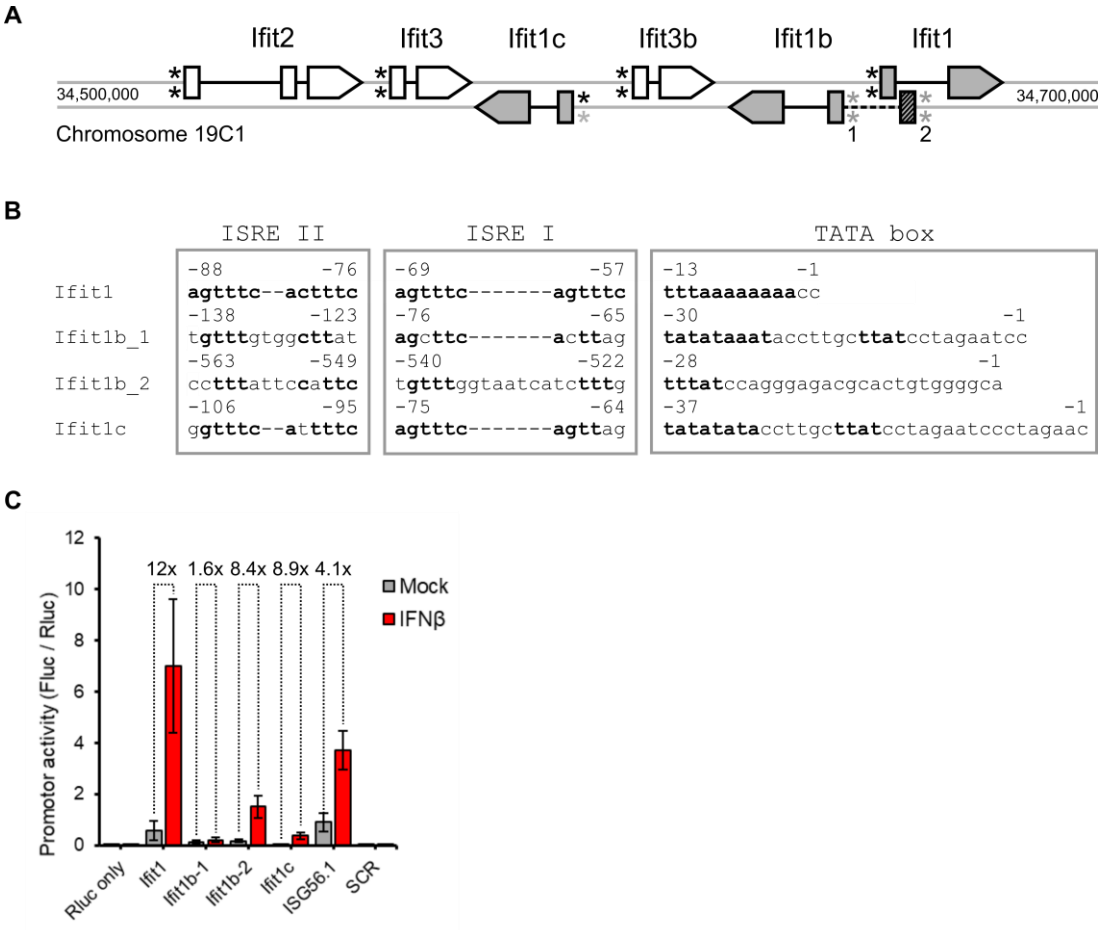

Figure 4-6 Ifit promoter activity.

A. *Schematic of the murine Ifit locus. Exons are shown as boxes with arrows indicating the direction of the reading frame. Introns indicated by solid black lines. In Ifit1b, two transcription start sites are annotated, the longer of which is represented by a dotted black line and hashed box. Black stars represent canonical ISRE sequences, while grey stars represent non-canonical ISRE-like sequences.* ***B.*** *Promoters for Ifit1, Ifit1b (both downstream, Ifit1b_1, and upstream, Ifit1b_2, transcription start sites) and Ifit1c. Numbers indicate the distance from the transcription start site. ISRE, interferon-stimulated response element. Nucleotides which are conserved with respect to Ifit1 are shown in bold.* ***C.*** *Promoter-driven firefly luciferase (Fluc) activity in 17C1 cells stimulated with IFNβ, normalised to constitutive Renilla luciferase (Rluc) activity. Data represent the mean ± the standard error of three biological repeats. The human IFIT1 promoter (ISG56.1) is included as a positive control (White et al., 2016). A scrambled (SCR) promoter sequence is included as a negative control.*

several kilobases upstream (Ifit1b_1), overlapping the Ifit1 promoter region (Figure 4-6A). Both contain poorly conserved ISRE-like sequences, with the Ifit1b_2 promoter more closely resembling the structure of that of Ifit1 (Figure 4-6B).

Constructs were designed to express firefly luciferase (Fluc) under the control of these promoters. These comprised 0.8-1 kb of sequence upstream of the transcription start site (TSS) for each gene, which were determined from their respective mRNA sequences (Ifit1: NM_008331.3, Ifit1b_1: NM_001362130.1, Ifit1b_2: NM_053217.2, Ifit1c: NM_001110517.1). A control plasmid was also generated with 1 kb of scrambled DNA sequence upstream of the Fluc mRNA (SCR), which should not act as a promoter. Promoter plasmids were co-transfected into 17C1 cells alongside a constitutive Renilla luciferase (Rluc) plasmid. After 4 hours, cells were treated with IFNβ to stimulate promoter activity, then harvested after 24 hours to determine luciferase expression. Luciferase activity was normalised to the Rluc control for each condition. RAW264.7 cells were not used for this assay, since DNA transfection itself activated an interferon response.

As expected, luciferase production from the Ifit1 promoter was strongly stimulated by treatment with IFNβ (Figure 4-6C). The upstream Ifit1b_1 promoter weakly drove Fluc expression but was not IFN responsive, while the downstream Ifit1b_2 promoter was slightly stimulated in response to IFNβ. Similarly, the Ifit1c promoter showed a small degree of upregulation when cells were treated with IFNβ. Therefore the lower expression of Ifit1b and Ifit1c at the mRNA level, described above, may be due to weakly IFN-sensitive promoter sequences.

4.2.2 Purification of recombinant Ifit proteins

In order to biochemically characterise the murine Ifit family, each protein was purified recombinantly. Murine Ifit proteins were expressed with a C-terminal His_8-tag in bacteria and purified as described in Materials and Methods. Inclusion of a low concentration of imidazole (5 mM) in the binding buffer during Ni-NTA affinity chromatography resulted in sufficiently high purity proteins which did not require further purification steps. When 1 μg of protein was analysed by SDS-PAGE, no additional bands were visible, indicative of >95% purity (Figure 4-7A).

While most Ifit family members expressed and purified well, Ifit1c-His_8 was expressed poorly and remained in the insoluble fraction following cell lysate clarification, indicating protein misfolding or aggregation. Recovery of Ifit1c from the insoluble fraction by denaturation and refolding was not successful. Therefore, to boost expression and solubility, N-terminal His-GST- and His-MBP-tagged constructs were generated. While the GST-tag rescued Ifit1c expression, allowing a small amount of soluble protein to be purified, addition of an N-terminal GST-tag affected the expression of other murine Ifit proteins. For example, GST-tagged Ifit1 had a tendency to precipitate out of solution and, when analysed by gel filtration, produced two peaks, neither of which were the expected size of either a monomer or dimer of GST-Ifit1. As GST is a homodimer in solution, it may induce aggregation of proteins which are themselves multimeric *(Reuten et al., 2016)*. Since IFIT proteins are known to self-associate, as discussed in the previous chapter, the addition of the GST-tag could cross-link Ifit oligomers, promoting aggregation and precipitation.

Therefore, MBP-tagged constructs were generated allowing successful expression and purification of Ifit1c, though the final yield and purity of MBP-Ifit1c was still much lower than other MBP-Ifit proteins. For example, 0.5 mg MBP-Ifit1c required preparation from 16 L of E coli. MBP-Ifit1c was additionally purified by size-exclusion chromatography which improved purity, though residual contaminant bands were still present (Figure 4-7). These are likely degradation products since they can be detected by both Ifit1c and His antibodies.

To improve the expression of Ifit1c, the C-terminal domain was expressed in isolation, containing 1 to 3 C-terminal TPRs, with or without terminal linker regions. The shortest Ifit1c truncations produced the highest yields, but eluted as multiple peaks when analysed by SEC, indicating the protein is flexible or heterogeneously folded. Therefore, while it is still very poorly expressed in *E. coli*, the longest Ifit1c truncation (henceforth referred to as $Ifit1c_{CTD}$) was chosen for further experiments and will be used in chapter 6. MBP-tagged Ifit1 and Ifit1b were also generated as controls.

For downstream experiments, proteins were normalised by western blotting against the His-tag (Figure 4-7A). Signal was weaker for MBP-tagged proteins, which are 6x-His-tagged, rather than 8x-His-tagged, which may reduce antibody binding.

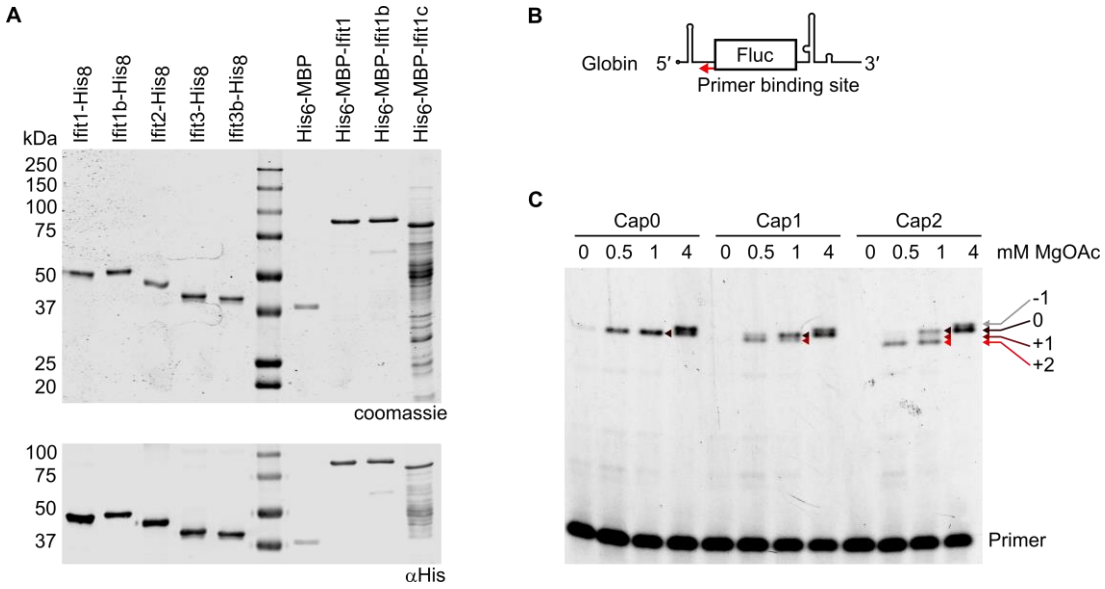

Figure 4-7 Purified Ifit proteins and model RNA.

A. *SDS-PAGE (upper panel) and anti-His (lower panel) western blot of recombinant Ifit proteins used in this study.* ***B.*** *Schematic representation of globin-Fluc mRNA with a red arrow indicating the reverse transcription (RT) primer binding site for primer extension analysis.* ***C.*** *Primer extension analysis of capped globin-Fluc mRNAs at different concentrations of MgOAc. At lower Mg^{2+} concentrations, additional stops are visible corresponding to 2'O-methylation of the first and second nucleotides, indicated with arrowheads. At high Mg^{2+} concentrations an additional band is seen at the -1 position, consistent with terminal transferase activity of the reverse transcriptase.*

4.2.3 Translation inhibition by murine Ifit proteins

To screen for RNA binding specificity, an *in vitro* translation approach was taken using a similar experimental setup as section 3.2.3. Firefly luciferase (Fluc) flanked by the 5' and 3'UTRs of the human β-globin mRNA (globin-Fluc) was transcribed and capped *in vitro*. Cap2 mRNA was generated from cap1 templates using a recombinant cap2 methyltransferase.

To verify that capped transcripts were properly modified, a variant primer extension inhibition assay was used, based on the propensity for reverse transcriptase to terminate at methylated nucleotides *(Zamudio et al., 2009)*, dependent on magnesium ion concentration. Reverse transcription was carried out using avian myoblastosis virus reverse transcriptase in the presence of a range of magnesium concentrations (Figure

4-7B-C). At high Mg^{2+} concentrations, full-length signal was present for all mRNAs, as well as a proportion of 1 nt longer cDNAs, consistent with low level terminal transferase activity of highly processive reverse transcriptase. At lower Mg^{2+} concentrations, 1 or 2 nt shorter cDNA products were present for cap1 and cap2 RNA, respectively. At very low Mg^{2+} concentrations, only the lower band was detectable for methylated RNA, but not for cap0 RNA. This indicates high cap methylation efficiency, since no residual full-length signal was detectable.

A high concentration (0.5 μM) of each Ifit protein was incubated with *in vitro* transcribed and capped globin-Fluc mRNA with different methylation states: cap0, cap1 or cap2 (Figure 4-8A-B). Uncapped RNA was also tested, however, since uncapped RNA translates very poorly, the signal from the luciferase reporter was typically 1000-fold lower than capped mRNA translation. As some murine Ifit proteins had a tendency to precipitate at 37 ˚C, Ifit proteins were preincubated with RNA at 30 ˚C. Translation was monitored by measuring luminescence from the Fluc reporter, normalised to the no Ifit or MBP only controls, depending on the experiment.

Ifit1 strongly inhibited the translation of cap0 RNA (Figure 4-8C), but did not inhibit the translation of cap1 or cap2 RNA, consistent with previous reports *(Habjan et al., 2013; Kimura et al., 2013; Daugherty et al., 2016)*. Translation from the uncapped reporter was not reproducibly inhibited by Ifit1. A previous report showed that Ifit1 was capable of partially inhibiting the translation of uncapped mRNA *(Pichlmair et al., 2011)*, but only at 100-fold higher concentrations than those tested here, far in excess of physiological Ifit expression levels. Ifit2, Ifit3 and Ifit3b did not inhibit translation of any of the RNAs tested, consistent with their human counterparts *(Pichlmair et al., 2011; Yang et al., 2012; Kumar et al., 2014)*. Intriguingly, Ifit1b inhibited the translation of cap1 RNA, but not cap0 or cap2 (Figure 4-8C). Unlike Ifit1, which completely inhibited cap0 translation, Ifit1b inhibited cap1 RNA by 80%. This indicates that Ifit1b either has lower affinity for cap1 RNA than Ifit1 does for cap0, or it cannot saturate binding under these conditions.

MBP-tagged Ifit1 and Ifit1b behaved similarly to their His-tagged counterparts (Figure 4-8D). MBP-Ifit1 inhibited cap0 translation and MBP-Ifit1b inhibited cap1 translation, though inhibition was not as strong as the His-tagged proteins. Additionally, MBP-tagged Ifit proteins appeared to be less specific than the His-tagged versions, since MBP-Ifit1 was

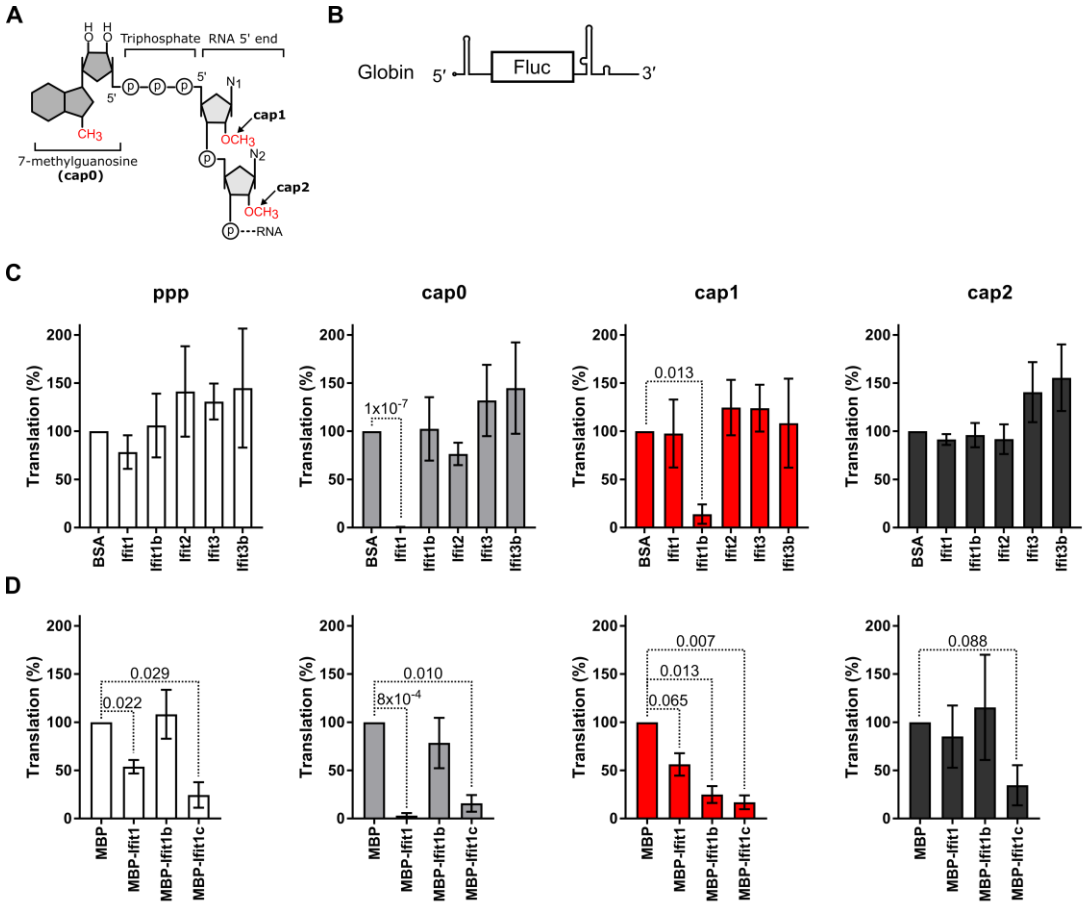

Figure 4-8 Translation inhibition by murine Ifit proteins

A. *Schematic of the mRNA 5′ cap.* ***B.*** *Schematic representation of model globin-Fluc mRNA.* ***C-D.*** *In vitro translation of differentially capped globin-Fluc reporter mRNAs by (**C**) His-tagged or (**D**) MBP-tagged Ifit proteins, normalised to the BSA-only or MBP controls, respectively. Data are shown as the mean and the standard error of three experiments. Data were compared to the BSA or MBP-only controls by pairwise two-tailed t-tests and p values < 0.1 are shown.*

found to be slightly inhibitory to cap1 translation. It is possible that the large MBP-tag may interfere with conformation or flexibility of N-terminus of the Ifit proteins, thereby disrupting RNA binding.

MBP-tagged IfitIc caused general inhibition of translation of all mRNAs tested (Figure 4-8D). While this could be due to genuine broad-spectrum RNA binding, it is difficult to draw too many conclusions given the poor quality of the recombinant protein. Since the protein was of low purity, MBP-IfitIc was tested for RNase activity, but was found not to degrade RNA. Owing to its low stability MBP-IfitIc may precipitate during the reaction, which could cause the RNA to come out of solution preventing its translation. A previous

report showed that Ifit1c in cell lysates could not precipitate with cap-RNA beads on its own, indicating that it may lack intrinsic RNA binding activity *(Habjan et al., 2013)*. However, without a way to express Ifit1c recombinantly, this remains uncertain.

4.3 Conclusions

To date, a comprehensive study of the expression pattern and function of all members of the murine Ifit family has not been carried out. In this chapter, Ifit expression was examined in different murine cell lines by quantitative PCR and, where possible, western blotting. All Ifit family members were found to be upregulated in response to type I IFN and dsRNA in both fibroblasts and macrophage cell lines. The rapid and potent induction of Ifit expression following stimulation is consistent with previous reports of Ifit1, Ifit2 and Ifit3 expression in murine cells *(Bluyssen et al., 1994a; Smith and Herschman, 1996; Terenzi et al., 2005, 2007)*.

Historically, Ifit1b and Ifit1c have not been examined in detail. These genes are particularly challenging to study, since they share high nucleotide identity with each other (85%), as well as sharing significant similarity with Ifit1 (52% and 54%, respectively). As such, these genes are difficult to differentiate at both the mRNA and protein level. In methods such as RNA sequencing and mass spectrometry, which often discard redundant reads or peptides to avoid skew, Ifit1b and Ifit1c may have been overlooked in the past. Here, this presented a problem for sensitive immunoblotting, since antibodies which detected Ifit1b tended to cross-react with Ifit1c or Ifit1, and vice versa. Ifit1b and Ifit1c could be differentiated at the mRNA level, but specific antibodies for Ifit1b and Ifit1c were not sufficiently sensitive to reliably pick up endogenous protein.

Ifit1b was found to be poorly upregulated in response to type I IFN. This is at least partly due to lower activity from the promoter regions upstream of either of Ifit1b's transcription start sites, which contain poorly conserved ISRE-like elements. Interestingly, the region 100 nt immediately upstream of the murine Ifit1b transcription start site is very similar to the same region upstream of human IFIT1B. Similar cryptic ISRE-like sequences can be seen in the human IFIT1B promoter region, indicating that these genes may share expression kinetics.

The reason for the poor upregulation of Ifit1b and Ifit1c, relative to the other murine Ifit family members, is still unclear. Here, it was revealed that Ifit1b can specifically inhibit the translation of cap1 mRNA. As such, Ifit1b has the capacity to inhibit cellular translation, making overexpression of Ifit1b potentially toxic. Therefore, the cell may purposely downregulate Ifit1b expression, to prevent translation shut off. Unfortunately, the activity of Ifit1c could not be determined, owing to difficulty expressing and purifying the protein recombinantly.

Previous work showed that, at high concentrations, Ifit2 could inhibit translation from an uncapped reporter mRNA *in vitro (Hui et al., 2005)*. However, at the concentrations tested here, which more closely reflect physiological expression levels, Ifit2 had no effect on translation of an unstructured reporter mRNA, regardless of 5' cap. Similarly, murine Ifit3 and Ifit3b did not inhibit translation of any of the RNAs tested. The mRNA encoding these proteins was strongly upregulated very early following stimulation of IFN or dsRNA, indicating that they, like Ifit1, are necessary in the early stages of an antiviral response. Therefore, Ifit2, Ifit3 and Ifit3b likely play important roles in different branches of the innate immune response, other than translation inhibition. This is discussed in more detail in chapter 7.

5 The activity of murine Ifit1b

5.1 Background

5.1.1 IFIT1B-like proteins

While some rodents maintain IFIT1 and IFIT5, in mice and other small rodents, including other model species such as rat and hamster, both of these genes have been lost *(Daugherty et al., 2016)*. These species encode at least two copies of Ifit1b, which may functionally compensate for the loss of IFIT1 and IFIT5 orthologues (Figure 5-1). IFIT1B is conserved in all mammals (see Figure 1-6), but despite this, there is little data on the function of IFIT1B-like proteins.

In mice there are three IFIT1B-like genes: Ifit1, Ifit1b and Ifit1c. While Ifit1 is known to bind to cap0 RNA and inhibit its translation *(Habjan et al., 2013; Kimura et al., 2013; Daugherty et al., 2016)*, a finding which was confirmed in chapter 4, the functions of murine Ifit1b and Ifit1c have not been examined. Murine Ifit1b was hypothesised to be non-functional, owing to a number of substitutions in the N-terminal domain which could interfere with cap binding *(Abbas et al., 2017a)*. In particular, the small hydrophobic residues in the cap-binding loop of human IFIT1, which coordinate the cap, are substituted for large, charged side chains in murine Ifit1b. Additional substitutions are present within the RNA binding channel, in particular surrounding the 2'-hydroxyl of the first ribose. Despite this, in

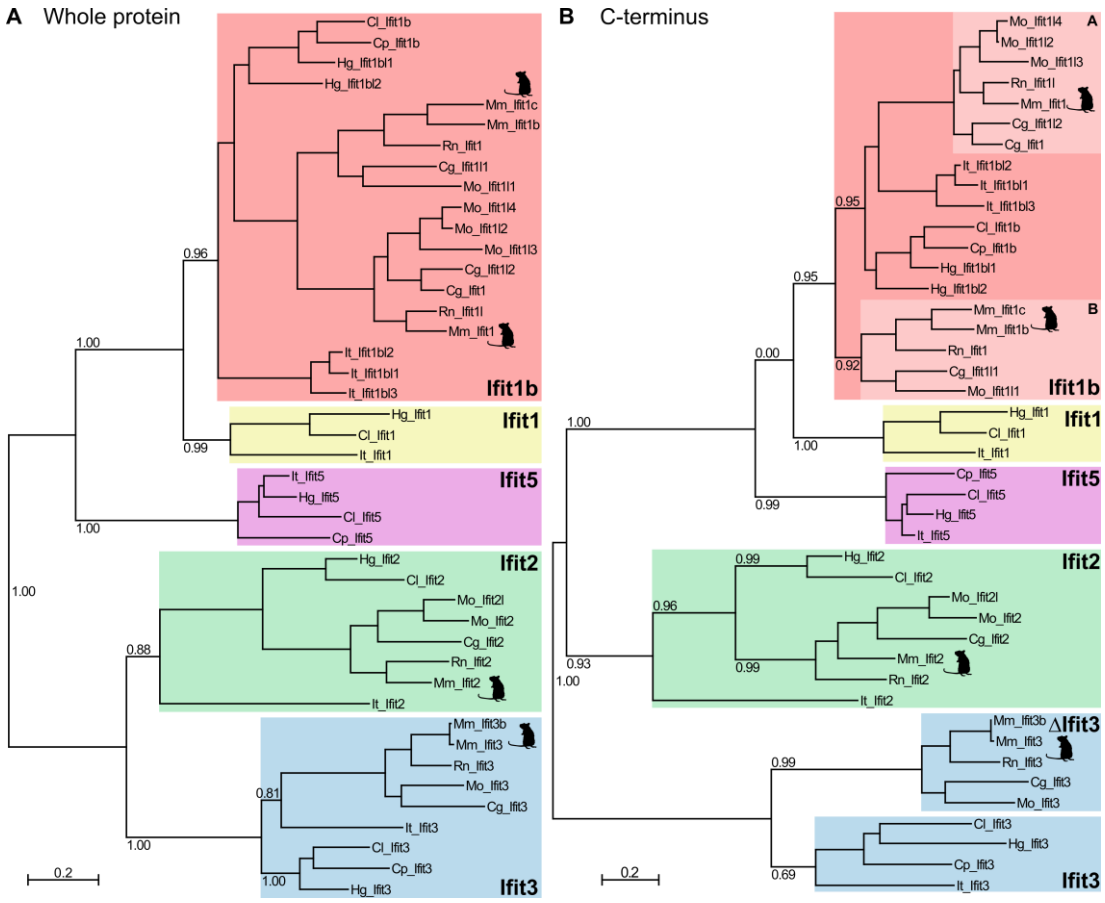

Figure 5-1 Phylogeny of rodent Ifit proteins

*Maximum-likelihood phylogenetic tree, constructed as in Figure 1-6, using (**A**) whole protein or (**B**) C-terminal sequence alignments of Ifits from eight different rodent species (Cg, Chinese hamster; Cl, chinchilla; Cp, guinea pig; Hg, naked mole rat; It, thirteen-lined ground squirrel; Mm, house mouse; Mo, prairie vole; Rn, Norway rat). Bootstrap supports are shown for major branches. Scale bars represent amino acid substitutions per position.*

chapter 4 it was demonstrated that not only is Ifit1b expressed in murine cells, but it can specifically inhibit the translation of cap1 mRNA *in vitro*.

5.1.2 Aims

The aim of this chapter is to characterise murine Ifit1b, using different biochemical and biophysical approaches. The RNA binding capacity of Ifit1b will be dissected to determine how it achieves specific cap1 binding on different RNA substrates. This activity will also be examined in cell culture, to determine what impact Ifit1b has on viral and host translation. This aims to expand our knowledge of the function of IFIT1B-like proteins in different species and give insights into how the rodent lineage has compensated for the loss of IFIT1 during their evolution.

5.2 Results

5.2.1 Translation inhibition by Ifit1b

To examine Ifit1b activity in more detail, three model mRNAs were used comprising an Fluc reporter coding sequence flanked by the 5' and 3'UTRs of β-globin (globin-Fluc), as a representative unstructured cellular mRNA; mouse hepatitis virus (MHV), as a moderately unstructured viral mRNA; and ZIKV, as a structured viral mRNA (Figure 5-2B). Coronaviruses, including MHV, and flaviviruses, including ZIKV, encode their own 2'-O-methyltransferase, so the viral mRNA is naturally cap1. These reporter mRNAs therefore simulate wildtype viral mRNA.

Serial dilutions of Ifit1b were incubated with Fluc mRNAs bearing differentially methylated 5' caps, as described in section 4.2.3, and luciferase activity was used to monitor translation. Ifit1 was included as a positive control and, as expected, caused a dose-dependent inhibition of cap0 globin-Fluc mRNA translation (IC_{50} = 102 nM, Figure 5-2C). Ifit1b inhibited cap1 translation at low concentrations, comparable to inhibition of cap0 RNA by Ifit1 (IC_{50} = 152 nM, Figure 5-2C). However, even at the highest concentrations tested, Ifit1b did not completely saturate inhibition. Ifit1b only weakly inhibited cap0 and cap2 translation (IC_{50} ~ 675 nM and 825 nM, respectively).

MHV-Fluc mRNA was slightly more susceptible to translation inhibition by Ifit proteins, with 1.5-fold lower concentrations required to cause a 50% reduction in translation (IC_{50} Ifit1-cap0 = 68 nM, Ifit1b-cap1 = 101 nM, Figure 5-2D). Inhibition of the cap0-MHV reporter by Ifit1b was similar to the inhibition of the cap0-globin reporter (IC_{50} ~ 690 nM). However, inhibition of cap2-MHV mRNA was greater (IC_{50} = 238 nM), indicating that the mRNA sequence or structure may alter cap-binding specificity, as well as affinity.

By contrast, ZIKV-Fluc mRNA was resistant to both Ifit1 and Ifit1b, even at micromolar concentrations (Figure 5-2D). The highest concentrations of Ifit1 or Ifit1b tested caused ~50% translation inhibition on the cap0-ZIKV or cap1-ZIKV reporters, respectively. In chapter 3 it was shown that human IFIT1 could completely inhibit the translation of cap0-ZIKV mRNA at nanomolar concentrations, and could inhibit cap1 ZIKV translation at micromolar concentrations (see Figure 3-7). Therefore, the inability of murine Ifit proteins

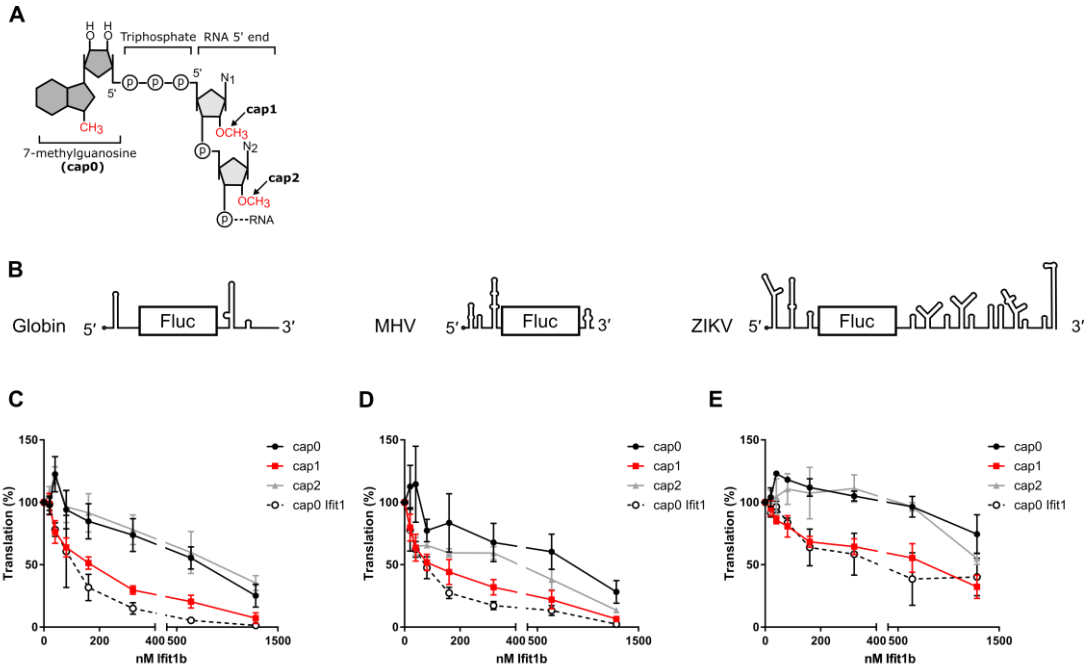

Figure 5-2 Ifit1b inhibits the translation of unstructured cap1 mRNA.

A. *Schematic of the mRNA 5' cap.* ***B.*** *Schematics of the reporter mRNAs used for in vitro translation.* ***C-E.*** *In vitro translation of differentially capped* ***C.*** *globin-Fluc,* ***D.*** *MHV-Fluc or* ***E.*** *ZIKV-Fluc, in RRL with increasing concentrations of Ifit1b (solid lines) or Ifit1 (dashed lines). Data were normalised to luciferase activity in the absence of IFIT protein and shown as the mean ± the standard error of at least three experiments. IC_{50} values are listed in Table 5-1.*

to inhibit the translation of the same reporter mRNA is quite surprising. This may be due to the high degree of secondary RNA structure at the very 5' end of the ZIKV genome. However, rodents are not natural hosts of flaviviruses; as such murine Ifit proteins may not be under selective pressure to recognise their RNA.

5.2.1.1 Effect of Ifit overexpression on murine hepatitis virus infection.

Since Ifit1b could inhibit the translation of a model MHV mRNA, it was then tested for its ability to inhibit MHV infection in murine cells. 17Cl cells are permissive for MHV infection *(Sturman and Takemoto, 1972)* but do not produce interferon in response to infection *(Irigoyen et al., 2016)*. This provides an even baseline for comparing the direct effect of overexpressed Ifit proteins on viral infection, since there should not be confounding effects from other ISGs. Cells were either treated with IFNβ or transfected with plasmids encoding FLAG-tagged murine Ifit1, Ifit1b and Ifit1c for 16 hours before infection with MHV at a multiplicity of infection (MOI) of 3 PFU/cell. Cells on coverslips were harvested after 8 hours for immunofluorescence, staining for dsRNA, indicative of

Table 5-1 Translation inhibition by Ifit1b.

Concentration of Ifit that reduced translation from the reporter RNA by 50% (IC_{50}) ± standard error. Data were fitted to [Inhibitor] versus normalised response curve (Y = 100)/(1 + (XHillSlope)/(IC50HillSlope)) using the least squares method in GraphPad Prism. For Ifit1 RNA binding, data were fitted using the non-linear Hill equation: $Fraction^{[bound]} = [Ifit1]^h \cdot Fraction^{[bound]}_{max}/([Ifit1]^h + K^h_{1/2,app})$. Data are the mean ± standard deviation of at least three experiments.

		***In vitro* translation in RRL, Figure 5-2**	**Primer extension inhibition, Figure 5-5**	
Ifit	**RNA**	**IC_{50} (nM Ifit) in RRL)**	**RNA binding (K1/2app, nM)**	**Hill number**
Ifit1b	cap0-globin-Fluc	675 ± 129		
Ifit1b	cap1-globin-Fluc	152 ± 18.1		
Ifit1b	cap2-globin-Fluc	826 ± 183		
Ifit1	cap0-globin-Fluc	102 ± 14.5	79 ± 9.3	1.3 ± 0.1
Ifit1b	cap0-MHV-Fluc	690 ± 233		
Ifit1b	cap1-MHV-Fluc	101 ± 17.9		
Ifit1b	cap2-MHV-Fluc	238 ± 50.1		
Ifit1	cap0-MHV-Fluc	68 ± 9.5		

viral replication complexes *(Weber et al., 2006)*. Surrounding cells from the same well were lysed for immunoblotting, to monitor expression of N protein, the viral nucleocapsid produced late in infection.

N protein expression was reduced in cells overexpressing Ifit1, Ifit1b or Ifit1c, compared to mock transfected cells. Similarly, fewer cells were positive for dsRNA in cells expressing Ifit1b or Ifit1c, indicating lower viral replication. While this may indicate that all three Ifit proteins are antiviral during MHV infection, transfection efficiency in these cells was quite poor and Ifit1c expression was particularly low. Therefore, it is more like that transfection of l7C1 cells makes them less susceptible to infection, for example due to cytotoxic effects of the transfection reagent. Previous reports overexpressing human IFIT proteins have seen similar generic inhibitory effects on infection *(Ishida et al., 2019; Wichit et al., 2019)*, indicating that IFIT overexpression may be an inappropriate system to study IFIT-virus interactions.

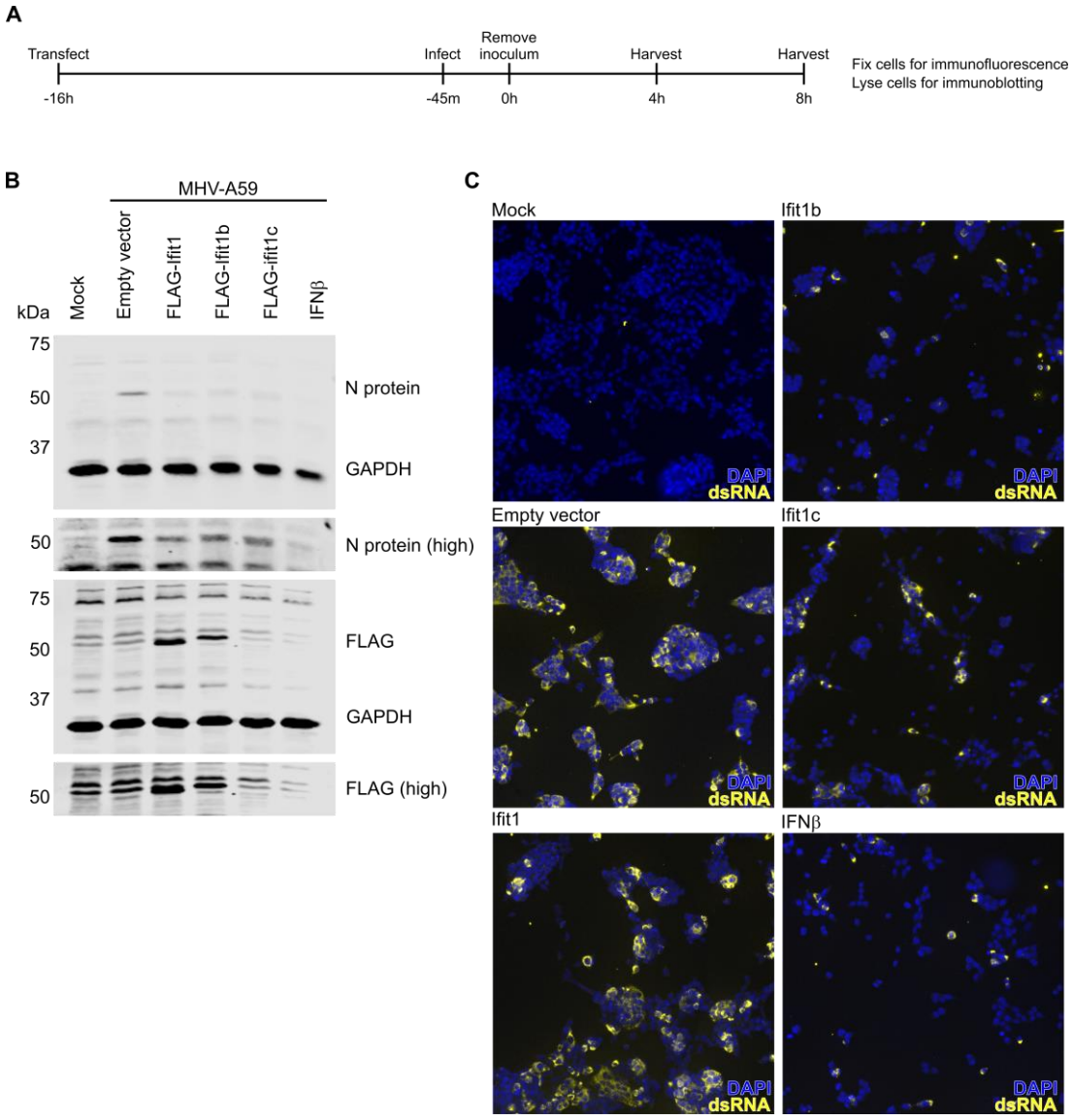

Figure 5-3 Effect of Ifit proteins on coronavirus infection in murine cells.

A. *Schematic of experimental design. 17C1 cells were transfected with Ifit expression plasmids, then infected with MHV strain A59 at an MOI of 3 PFU/cell, and harvested at the indicated times.* ***B.*** *Immunoblotting of MHV-infected cell lysates after 8 hours. GAPDH is included as a loading control for each membrane.* ***C.*** *Immunofluorescence of MHV-infected cells at 8 hours post infection, stained for double-stranded RNA (dsRNA, yellow). Cell nulcei are stained with DAPI (blue). Data are representative of two independent experiments.*

As expected, pre-treating cells with IFNβ greatly reduced viral replication and protein expression compared to untreated cells. Therefore, using this as a baseline, Ifit genes could be stably knocked-down to see whether this recovers viral infection. This would provide a more relevant assay system, since Ifit proteins would be expressed at endogenous levels, while avoiding artefacts introduced by transfection and overexpression.

5.2.1.2 Ifit1b regulation of host translation

Since Ifit1b can inhibit translation of cap1 mRNA, it was hypothesised that Ifit1b would be capable of inhibiting host translation. To investigate this, a puromycylation labelling approach was taken *(Schmidt et al., 2009)*. Puromycin is an antibiotic which mimics the structure of aminoacylated tRNA and is thus incorporated into the nascent polypeptide chain during elongation, resulting in premature chain termination. When mammalian cells are treated with low concentrations of puromycin, it is stochastically incorporated towards the C-terminus of nascent polypeptides. Using antibodies raised against puromycin, these labelled proteins can be detected by western blotting and immunofluorescence microscopy, thereby allowing visualisation of the nascent proteome of the treated cell.

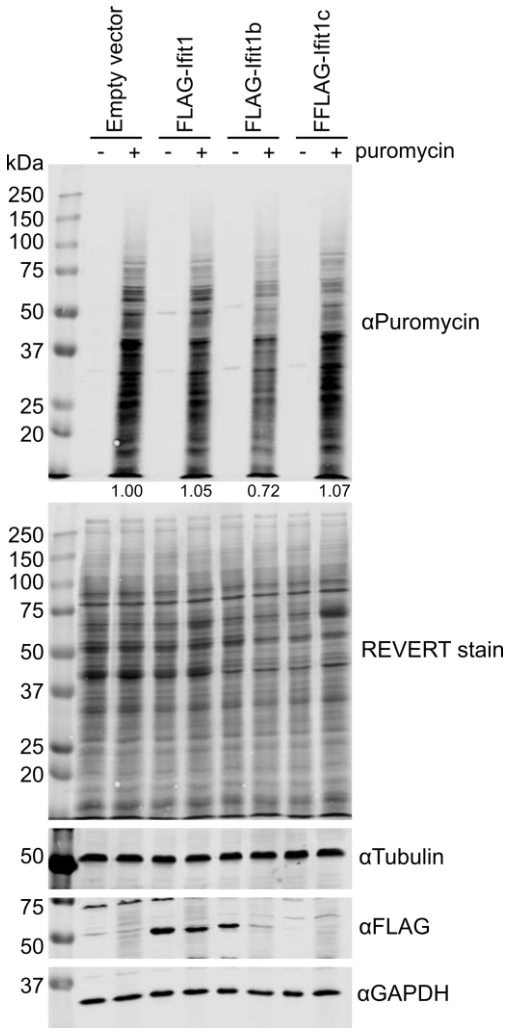

Figure 5-4 Ifit1b inhibits a proportion of cellular translation.

Immunoblot analysis of 17C1 cells transfected with FLAG-Ifit1, FLAG-Ifit1b or FLAG-Ifit1c for 16 hours and labelled with puromycin for 4 hours. Quantification of puromycin signal intensity, normalised to tubulin and shown as a proportion of the empty vector control, is shown under the top panel.

Murine 17C1 fibroblast cells were transfected with FLAG-tagged Ifit1, Ifit1b or Ifit1c for 16 hours, before treatment with 5 μg/mL puromycin for a further 4 hours. Cell lysates were separated by SDS-PAGE and transferred to nitrocellulose membranes, which were stained with REVERT total protein stain to ensure an equal quantity of lysate was loaded in each well (Figure 5-4). Membranes were then analysed by immunoblotting, using a monoclonal antibody against puromycin, which was generated by Dr Jia Lu. Cells overexpressing Ifit1b showed a 30% reduction in puromycin incorporation, compared to the empty vector control, indicating that Ifit1b can indeed inhibit a proportion of cellular translation (Figure 5-4). Cells overexpressing Ifit1 and Ifit1c showed similar levels of incorporation, compared to empty vector-transfected cells, indicating little effect on cellular translation. However, the expression level of Ifit1c was very poor, consistent with its instability *in vitro*. Therefore, without stabilising Ifit1c expression, it still remains unclear whether Ifit1c impacts global translation rate.

5.2.2 Ifit1b RNA binding

To examine the RNA binding activity of Ifit1b in more detail, a toeprinting approach was taken. This assay has previously been used to characterise RNA binding by human and rabbit IFITs, including cap1 binding by rabbit IFIT1B *(Kumar et al., 2014)*. First, to establish that the assay was functional, increasing concentrations of recombinant Ifit1 were incubated with cap0 globin-Fluc mRNA and reverse transcription was carried out using a fluorescent Cy5-labelled primer. Ifit1 bound to cap0 RNA in a dose-dependent manner, as evident by the increase in toeprint signal, with an affinity of 76 nM (Figure 5-5A-B, Table 5-1). Ifit1 did not produce a toeprint on cap1 RNA.

Ifit1 has also been reported to bind to uncapped RNA with high affinity *(Pichlmair et al., 2011)*. Therefore, a toeprint assay was also performed on uncapped globin-Fluc RNA, using a radioactive ^{32}P-labelled primer for increased sensitivity. Human IFIT5 was included as a positive control, since this was previously shown to bind uncapped RNA in this assay system *(Kumar et al., 2014)*. However, Ifit1 only produced a very weak toeprint on uncapped RNA (Figure 5-5C), supporting much higher affinity for cap0-RNA compared to 5'ppp-RNA binding.

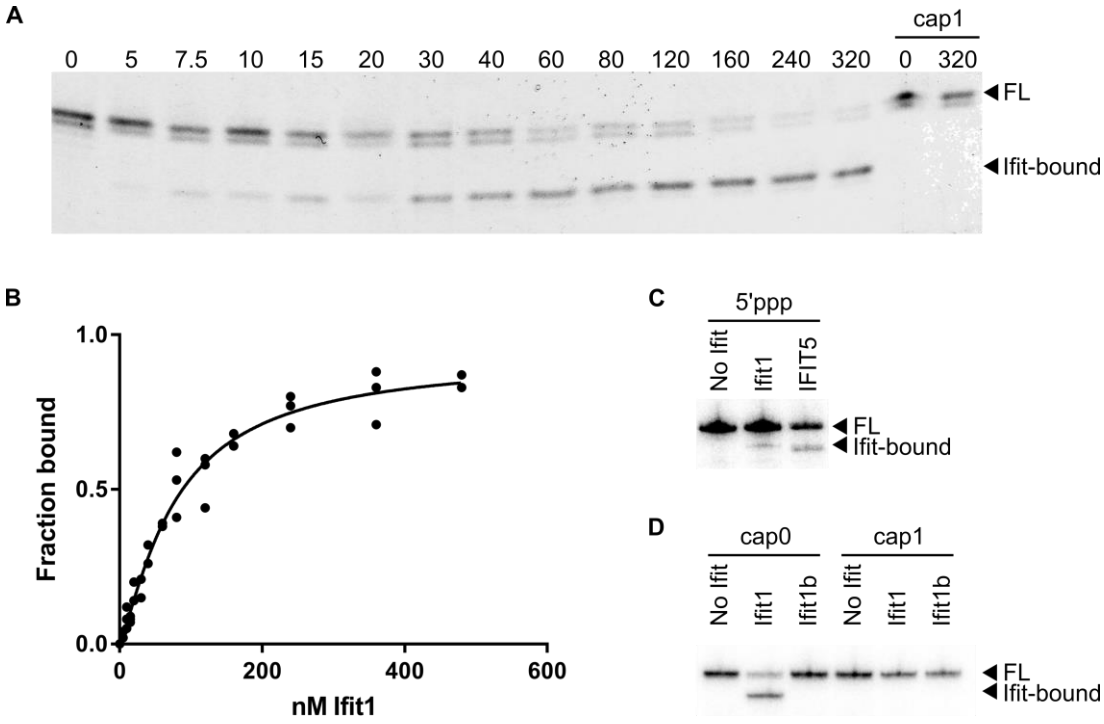

Figure 5-5 RNA binding by Ifit1 and Ifit1b.

A. *Primer extension analysis of murine Ifit1 bound to cap0-globin-Fluc RNA. The full length (FL) and 7 nt-truncated cDNA products produced by Ifit1 binding are indicated.* ***B.*** *Graph showing the fraction of RNA bound at increasing Ifit1 concentrations. Curve is representative of three separate experiments. Dissociation constants ($K_{1/2,app}$) and Hill coefficients (h) are listed in Table 5-1.* ***C.*** *Primer extension analysis of murine Ifit1 and human IFIT5 on uncapped globin-Fluc RNA.* ***D.*** *Primer extension analysis of murine Ifit1 and Ifit1b on cap0 and cap1-globin-Fluc RNA.*

Finally, recombinant Ifit1 or Ifit1b were incubated with cap0 or cap1 globin-Fluc RNA and reverse transcription was carried out, using a ^{32}P-labelled primer. As before, Ifit1 produced a toeprint on cap0 but not cap1 RNA. However, unexpectedly, Ifit1b was incapable of producing a toeprint on cap1 RNA, even at high concentrations (Figure 5-5D).

5.2.2.1 Differential scanning fluorimetry RNA binding assay

As an alternative approach, a thermal stability assay was developed to examine Ifit1b-RNA binding, adapted from the assay described in 3.2.3. Binding to a substrate can increase the thermal stability of proteins, resulting in an increase in a melting temperature which correlates with its binding kinetics *(Niesen et al., 2007)*. Human IFIT5 is known to change conformation upon RNA binding to a more rigid, closed structure *(Abbas et al., 2013)*, indicating that RNA binding alters IFIT flexibility. Therefore, it was reasoned that RNA

binding may alter the kinetics of IFIT unfolding, which could then be quantified by measuring differences in melting temperature.

For this assay, an RNA oligonucleotide was used, derived from the first 25 nucleotides of the human β-globin 5'UTR (globin25), which is predicted to be unstructured (Figure 5-6A). A short RNA was chosen to minimise any non-specific stabilising effects from the body of the RNA interacting with the IFIT protein, independently of the 5' end. This RNA was transcribed *in vitro*, using a modified protocol in which the NTP concentrations were optimised to reduce spurious T7 transcription products *(Triana-Alonso et al., 1995; Rong et al., 1998)*. This involved a 10-fold reduction in the ATP and UTP in the reaction, with a concomitant reduction in Mg^{2+} ions, and a high concentration of both template DNA and T7 RNA polymerase. RNA was purified by S75 size exclusion chromatography to remove residual nucleotides and small molecule contaminants, following both transcription and capping, resulting in highly pure RNA species (Figure 5-6B, left panel). When resolved by high percentage denaturing PAGE, capped transcripts were retarded by one nucleotide, which confirmed high capping efficiency (Figure 5-6B, right panel). To improve specificity, a low concentration of heterogeneous yeast tRNA was included in the binding reaction as a blocking agent.

Increasing concentrations of cap0 RNA resulted in a dose-dependent stabilisation of Ifit1, as expected, while cap1 RNA did not stabilise Ifit1, but actually slightly reduced Ifit1 melting temperature (Figure 5-6C,E). Consistent with the translation inhibition assays, Ifit1b was stabilised in a dose-dependent manner by cap1-globin25 RNA, indicative of binding (Figure 5-6D,F). Stabilisation by cap0-globin25 RNA was lower, supporting specific binding to cap1 RNA over cap0. Although this clearly shows RNA binding and specificity, accurate interpolation of binding affinity was not possible from these data.

5.2.2.2 Ifit1b RNA binding specificity determinants

To investigate the mode of RNA binding by Ifit1b, the thermofluor assay system was used to examine the effect of point mutations on cap0 and cap1 RNA binding. Mutants were purified and normalised by immunoblotting against the C-terminal His_8 tag (Figure 5-7A-B). A two-fold molar excess of cap0 or cap1 RNA was mixed with wildtype or mutant Ifit1b, before analysis.

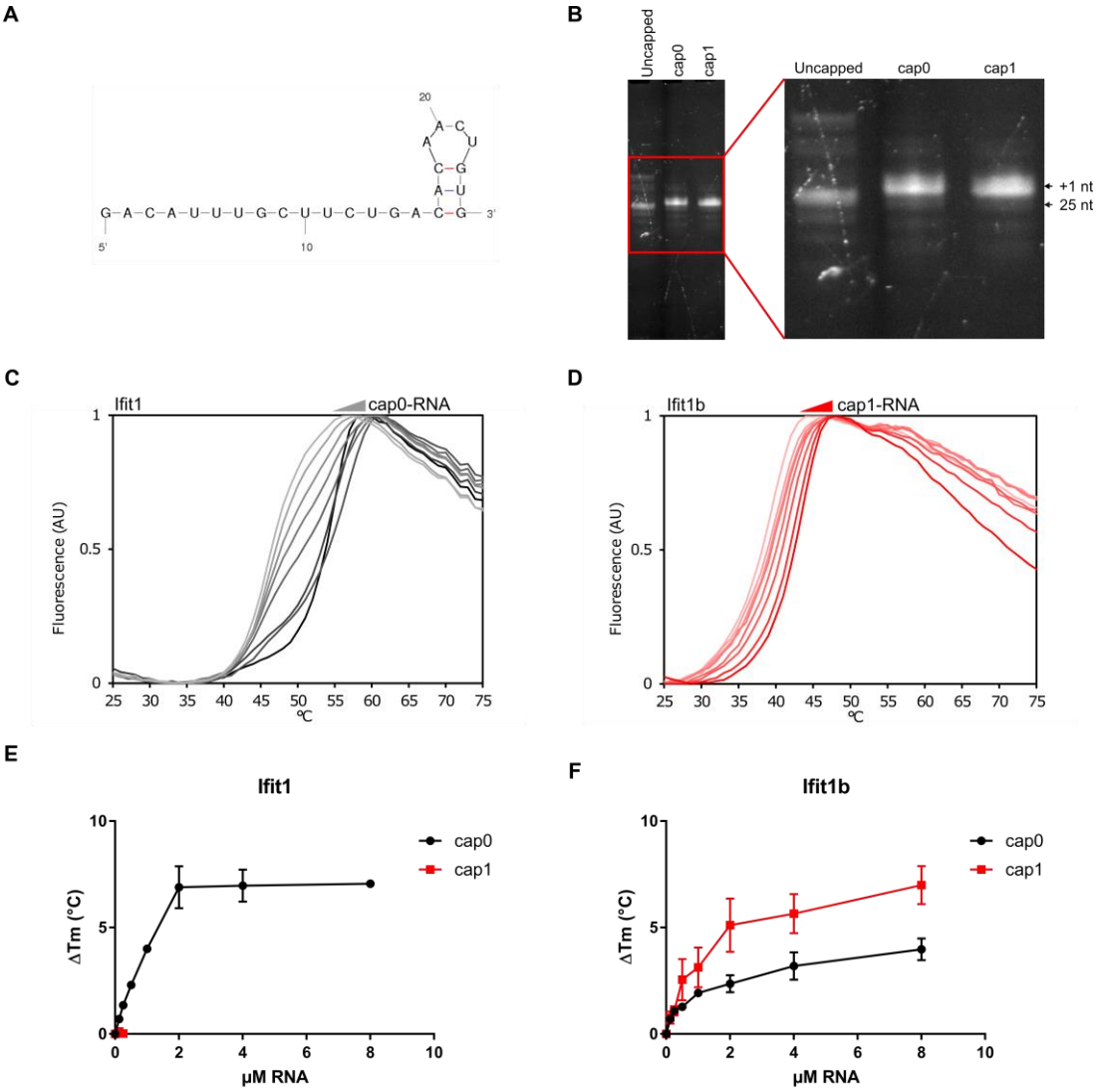

Figure 5-6 Thermal stability RNA binding assay.

A. *Secondary structure prediction of the first 25 nt of the β-globin 5'UTR (globin25) RNA, calculated in Mfold (Zuker, 2003).* ***B.*** *Denaturing PAGE analysis of uncapped, cap0 and cap1 globin25 RNA.* ***C-F.*** *Differential scanning fluorimetry analysis of Ifit1 or Ifit1b with increasing concentrations of cap0 or cap1 globin25 RNA.* ***C-D.*** *Melt curves of (**C**) Ifit1 and (**D**) Ifit1b with increasing concentrations of cap0 (grey) or cap1 (red) globin25 RNA, respectively.* ***E-F.*** *Quantification of (**C-D**), showing the difference in melting temperature (ΔTm) from the protein without RNA. To determine Tm, data were analysed by non-linear regression using the Boltzmann equation, y = LL (UL – LL)/(1 + exp(Tm –x)/a) where LL and UL are lower limit and upper limit respectively.*

First, the N-terminal domain of Ifit1b was investigated (Figure 5-7A). Mutation of a conserved tryptophan residue, W144, which is necessary for cap guanosine coordination

by human IFIT1 *(Abbas et al., 2017a)*, reduced stabilisation of Ifit1b by cap1 RNA back to background levels (Figure 5-7C). However, mutation of the charged residues in the cap-binding loop, which were hypothesised to inhibit RNA binding, had little effect on cap1 RNA binding. Mutation of E50 to alanine or glutamine only slightly reduced cap1 RNA binding, while mutation of R54 to alanine or leucine reduced stabilisation by cap1 RNA by about half. Mutation of both E50 and R54 to the equivalent residues in Ifit1 (glutamine and leucine, respectively) restored cap1 binding back to wildtype levels (Figure 5-7C). Previously, in human IFIT1, mutation of these residues to alanine only slightly reduced cap0-RNA binding *(Abbas et al., 2017a)*, indicating that they contribute to stable cap binding but their exact identity is not critical. Together this indicates that Ifit1b likely engages the cap using the conserved tryptophan residue but the other face of the cap-guanosine residue is coordinated non-specifically, in this case by long, polar side-chains in the cap-binding loop.

Next, mutations were made within the RNA binding channel to investigate how Ifit1b achieves specific cap1 RNA binding. In the structure of human IFIT1, the residues immediately proximate to the ribose 2'-hydroxyl group are Y157 and R187 (Figure 5-7D). These side-chains may sterically hinder binding to 2'-O-methylated RNA. In murine Ifit1b the tyrosine is conserved at position 162, but the arginine residue is substituted for H192. Therefore, H192 was investigated for its contribution to RNA methylation sensing, by mutation to alanine, arginine or glutamate. Mutation to alanine reduced stabilisation by cap1 RNA by half, while mutation to glutamate had no effect on cap1-RNA binding. However, H192E increased stabilisation of Ifit1b by cap0 RNA by two-fold, indicating that H192 may indeed play a role in discriminating RNA methylation (Figure 5-7C). Mutation of H192 to arginine, mimicking human IFIT1 and murine Ifit1, abrogated RNA binding entirely. However, Ifit1b H192R was less stable than wildtype Ifit1b and ran faster on SDS-PAGE despite have the same mass (Figure 5-7B). This indicates that H192R may disrupt the correct folding of Ifit1b, accounting for the loss of RNA binding activity.

None of the mutants tested could reverse the cap binding specificity of Ifit1b, to promote cap0 binding over cap1. This indicates that other residues, or indeed the overall geometry of the RNA binding channel, are necessary for cap1 discrimination. Larger panels of mutants, or ideally structural information, will be necessary to determine exactly how Ifit1b can sense cap1 over cap0.

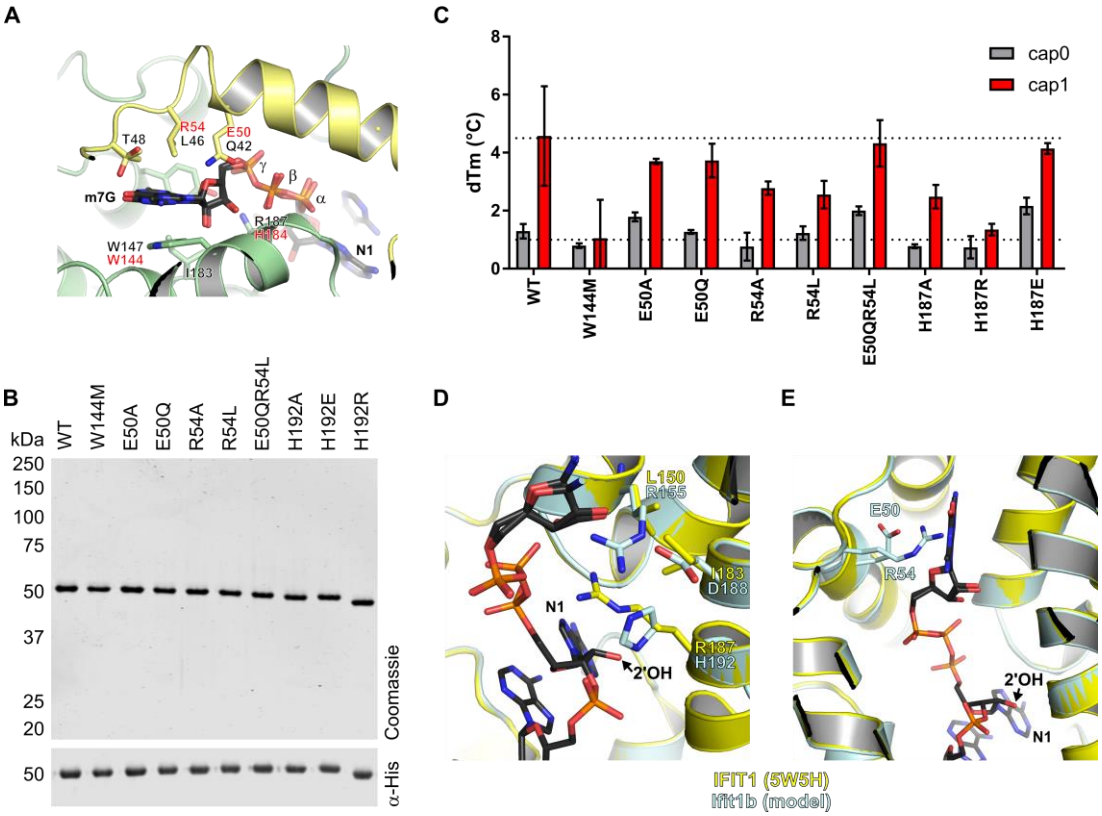

Figure 5-7 Mutational analysis of Ifit1b RNA binding.

A. *Cap-binding residues in human IFIT1 (PDB: 5W5H), coloured by subdomain, as in Figure 1-4. Key side-chains are shown as sticks and their equivalents in murine Ifit1b are labelled in red.* ***B.*** *Coomassie-stained SDS-PAGE (upper panel) and anti-His western blot (lower panel) of wildtype (WT) and mutant Ifit1b.* ***C.*** *Thermal shift assay of 2 μM WT and mutant Ifit1b with 4 μM cap0 or cap1 RNA, showing the difference in melting temperature (dTm) between protein only and protein with RNA. To determine Tm, data were analysed by non-linear regression using the Boltzmann equation, y = LL (UL – LL)/(1 + exp(Tm –x)/a) where LL and UL are lower limit and upper limit respectively. Data represent the mean and the standard deviation of three experimental replicates.* ***D.*** *Structural model of Ifit1b based on the structure of human IFIT1 (PDB: 5W5H), showing the position of residues which impact cap0 binding by Ifit1b (cyan) superimposed with human IFIT1 (yellow), in relation to the 2'-hydroxyl group (2'OH) on the first ribonucleotide (N1). RNA is shown as black sticks.*

5.2.3 Structural modelling of rodent Ifit1b-like proteins

In the absence of structural data, structural modelling of Ifit1b proteins from different rodents can give insights into their potential function and mechanism of action. Models were generated for mouse, rat and hamster (Figure 5-8 and Appendix F), using SWISS-MODEL *(Waterhouse et al., 2018)*, based on the structure of human IFIT1 (PDB: 5W5H)

(Abbas et al., 2017b). It is important to note that interpretation of structural models is constrained by the structure upon which the model is based. While the overall architecture of a model can be examined, molecular details, such as the exact position and rotations of side-chains, cannot be inferred.

The positively charged RNA binding channel formed in the groove between the N- and C-terminal domains, which allows IFIT1 and IFIT5 to bind ssRNA, was maintained in all rodent Ifit models. Hamster Ifit1-like2 which has a hydrophobic patch at the mouth of the channel that may prevent RNA binding (see Appendix F). Murine Ifit1c has bulky side chains in the N-terminal domain, which appear to close off the end of the RNA binding channel and may prevent cap binding, similar to human IFIT5 (see Figure 1-3, Figure 5-8). Murine Ifit1-like proteins (clade A, Figure 5-8) maintained the cap-binding pocket present in human IFIT1, but had a slightly negative charge indicating that they may engage the cap in a different way to human IFIT1, consistent with their divergent evolutionary trajectories *(Daugherty et al., 2016)*.

Murine Ifit1b maintained a similar overall charge profile to human IFIT1, despite the substitutions in the cap-binding pocket and RNA binding channel described above. However, Ifit1b was found to have an acidic patch in the C-terminal domain (Figure 5-8). The positively-charged C-terminus in human IFIT1 engages the RNA substrate *(Abbas et al., 2017a; Johnson et al., 2018)* and is necessary for optimal RNA binding *(Kumar et al., 2014)*. Therefore, an acidic C-terminal domain could electrostatically interfere with RNA binding, which may explain why Ifit1b struggles to bind structured mRNAs and fails to saturate inhibition of translation even on unstructured targets. It may also account for the lack of a toeprint when Ifit1b was analysed by primer extension inhibition, since without stabilisation by the C-terminal domain, Ifit1b may not bind strongly enough to resist displacement by the reverse transcriptase. Mutating this patch to reverse its charge could therefore be used to improve Ifit1b RNA binding affinity.

5.3 Conclusions

In this chapter, the activity of murine Ifit1b was characterised *in vitro* and in cells. Ifit1b was found to have remarkable specificity for cap1-mRNA over cap0 or cap2, and inhibited translation of cap1 mRNA at nanomolar concentrations. Previously IFIT proteins have

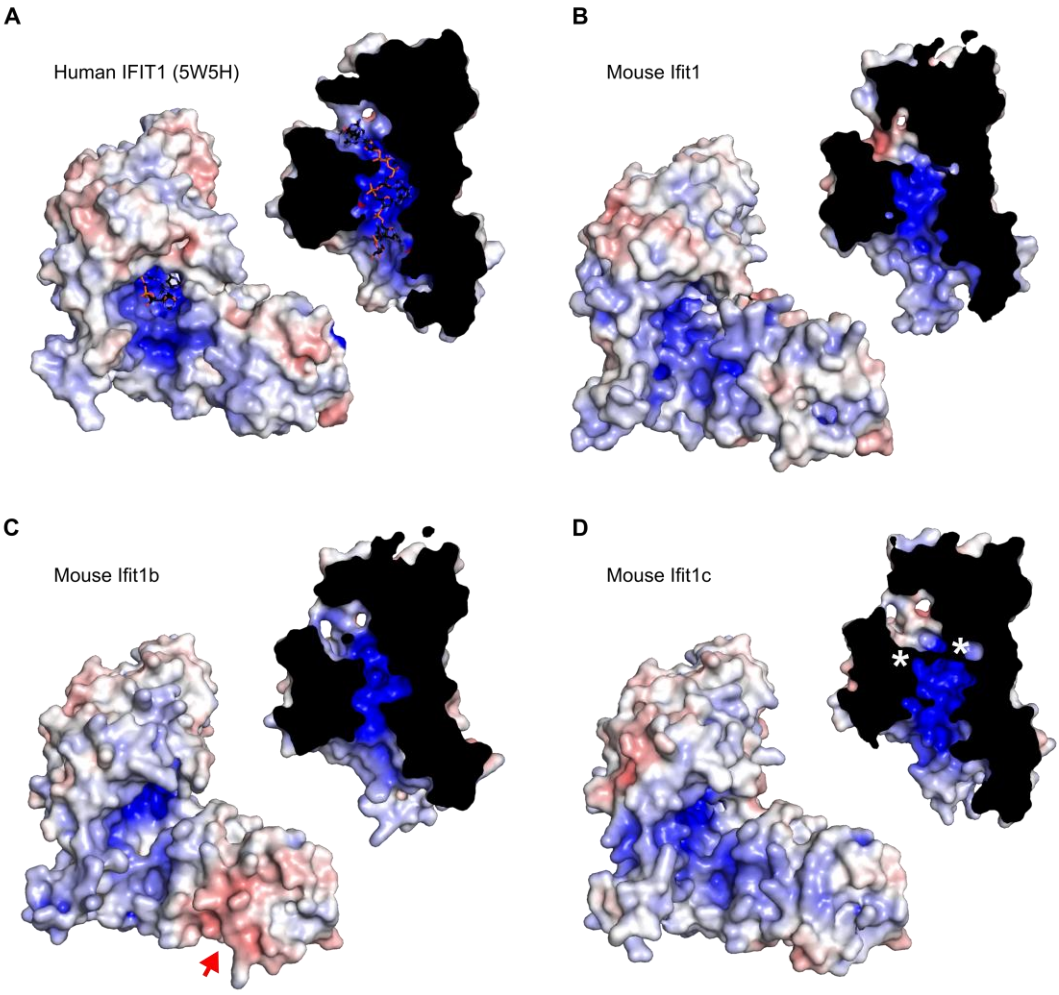

Figure 5-8 Structural modelling of rodent Ifit proteins.

*Structural models of **B.** murine Ifit1 **C.** murine Ifit1b and **D.** murine Ifit1c, based on **A.** the X-ray crystal structure of human IFIT1 (PDB: 5W5H). Models are coloured by surface electrostatic potential from negative (-10 kTe^{-1}; red) to positive (+10 kTe^{-1}; blue), via white (hydrophobic), generated in APBS using PDB2PQR (Dolinsky et al., 2004). White asterisks indicate where residues may occlude the RNA binding channel. Red arrows indicate acidic patches, which could interfere with RNA binding.*

been identified which preferentially bind to uncapped RNA *(Abbas et al., 2013; Feng et al., 2013; Katibah et al., 2013; Kumar et al., 2014)* or cap0 RNA *(Habjan et al., 2013; Kumar et al., 2014; Abbas et al., 2017a)*. Rabbit IFIT1B has been described to bind both cap0 and cap1 RNA very strongly, with slightly higher affinity for cap0 *(Kumar et al., 2014)*. Murine Ifit1b is the first example of an IFIT protein which binds very poorly to cap0 RNA, but strongly to cap1 RNA.

This distinction between cap0 and cap1 RNA is not made by other cap-binding proteins. Mammalian eIF4E, for example, binds to cap0 and cap1 mRNAs with comparable affinity *(Niedzwiecka et al., 2002; Kumar et al., 2014)*. Interestingly, eIF4E from trypanosomatid parasites, which is larger than mammalian eIF4E, does sense 2'-O-methylation on host mRNAs. The structure of *Trypanosoma cruzi* eIF4E5 in complex with cap4 mRNA, a methylation status unique to trypanosomes in which the first 4 nucleotides are 2'-O-methylated, shows specific hydrophobic contacts between the protein and the RNA methyl groups, accounting for the increased affinity for cap4 over cap0 RNA *(Reolon et al., 2019)*. In these parasites, cap4 methylation is linked to high translation efficiency *(Zamudio et al., 2009)*, presumably by increasing initiation or recycling rates.

The mechanism of cap1 discrimination by Ifit1b remains uncertain. It is possible that, like trypanosome eIF4E, specific contacts are made with the methyl group itself which stabilises the Ifit1b-RNA complex, allowing preferential binding to cap1 over cap0. While no mutants were identified here which could switch the cap binding specificity of Ifit1b from cap1 to cap0, three mutants were identified here which slightly increased cap0 RNA binding: H192E, E50A and E50Q/R54L.

Histidine-192 is predicted to be in close proximity to the 2'-O-methyl group on the first ribose (Figure 5-7D). In human IFIT1, this residue is an arginine which reaches up to coordinate the triphosphate moiety with its positively-charged head group, while sterically occluding cap1 binding with the base of the side chain (Figure 5-7A,D). Since R187 is critical for triphosphate binding in human IFIT1, mutation of this residue completely abrogates cap0-RNA binding *(Abbas et al., 2017a)*. However in Ifit1b, H192 is likely not involved in triphosphate binding since it could be mutated to alanine without affecting cap1-RNA binding. Mutation to arginine, however, completely disrupts RNA binding, probably by interfering with stable folding. Structural modelling of Ifit1b positions charged side chains R155 and D188 in close proximity to H192, which may clash with the introduction of an arginine residue. Interestingly, R155 was modelled close to the triphosphate moiety and may contribute to its coordination in a way analogous to R187 in human IFIT1 (Figure 5-7D).

E50 and R54 reside in the cap-binding loop, distal to the first ribonucleotide (Figure 5-7E). Therefore, their contribution to cap1 sensing is unclear. Previously, mutation of an N-

terminal glutamate residue in human IFIT5 was found to alter cap-RNA binding specificity, promoting cap1 binding *(Katibah et al., 2014)*. Therefore, it is possible that mutation of charged residues in the N-terminal domain may alter the conformation of the RNA binding pocket and indirectly affect RNA binding specificity.

The binding affinity of Ifit1 for cap0-RNA was determined by primer extension inhibition, and was comparable to the affinity of human IFIT1 for cap0-RNA determined in an equivalent assay system *(Kumar et al., 2014; Fleith and Mears et al., 2018)* (Appendix E, Table 3-2). The Hill coefficient for Ifit1 binding to cap0 RNA was 1.4, indicating a slight positive cooperativity in binding. Human IFIT1 was previously found to have Hill coefficients of 1.6 *(Kumar et al., 2014)* and 2.8 *(Fleith and Mears et al., 2018)* on comparable substrates, indicating moderate to strong positive binding cooperativity. As such, RNA binding by one molecule in the IFIT1 homodimer may promote binding by the second molecule.

While the toeprint assay has been valuable in determining binding affinities for different IFIT family members, the stringency of the technique has its limitations. For example, murine Ifit1, which has high reported affinity for uncapped RNA *(Pichlmair et al., 2011)*, produced only a weak toeprint on uncapped globin-Fluc mRNA. Human IFIT5 was capable of forming a stronger toeprint but still did not saturate binding, despite very high affinity for 5'ppp-RNA *(Abbas et al., 2013)*, consistent with a previous report *(Kumar et al., 2014)*. It is possible that IFIT proteins bound to uncapped RNA may be more susceptible to displacement by reverse transcriptase, compared to binding capped RNA.

Ifit1b did not form a toeprint on cap1 RNA when assayed by primer extension inhibition. Ifit1b had a tendency to precipitate in buffers containing magnesium salts, used in both the translation and primer extension assays. The induction of protein aggregation by divalent cations, particularly Mg^{2+}, has been documented *(Silman et al., 1965; Zhu and Damodaran, 1994; Haque and Aryana, 2002)*. Therefore, under these conditions, Ifit1b may be artificially destabilised, preventing accurate determination of RNA binding. To circumvent this problem, a thermal stability assay was developed to quantify RNA binding, using highly pure RNA oligonucleotides with different 5' caps. In this assay, Ifit1b was shown to be stabilised by cap1 RNA in a dose-dependent manner, but was not stabilised to the same extent by cap0 RNA, supporting specific cap1 binding.

While quantification of binding affinity was not possible using this assay, since it does not give information about the proportion of unbound RNA and protein, it allowed direct comparison of a panel of Ifit1b mutants in parallel, since it is performed in a 96-well plate format. Therefore, provided sufficient substrate can be generated, this assay can be adapted for high throughput screening of binding mutants. This has the added benefit of simultaneously identifying destabilising mutations, which can be easily identified by drastic decreases in melting temperature.

6 MURINE IFIT COMPLEXES

6.1 Background

6.1.1 Murine Ifit complexes

In chapter 3, the importance of heterocomplex formation was demonstrated for the regulation of human IFIT1. As discussed in chapter 3, in humans IFIT1, IFIT2 and IFIT3 form a multifunctional heterotrimeric complex, in which IFIT3 is a central scaffold which regulates the activity and stability of both IFIT1 and IFIT2 *(Stawowczyk et al., 2011; Fleith and Mears et al., 2018; Johnson et al., 2018)*. Since Ifit1, Ifit2 and Ifit3 are conserved in mice, an analogous complex was thought to also form in murine cells *(Pichlmair et al., 2011)*.

Mass spectrometry co-precipitation experiments demonstrated that murine Ifit1 does not bind to Ifit2 or Ifit3 *(Habjan et al., 2013)*. Rather, Ifit1 precipitated peptides corresponding to the uncharacterised protein Ifit1c. Later, *in vitro* pulldown assays showed that neither human IFIT1 nor murine Ifit1 could co-precipitate murine Ifit3 *(Johnson et al., 2018)*. In mice and other small rodents, Ifit3 has undergone a 3' deletion, likely resulting from an unsuccessful genetic recombination event *(Daugherty et al., 2016)*. Thus, Ifit3 lacks the C-terminal YExxL motif to allow Ifit1 binding (Figure 6-1). This truncation coincides with the loss of IFIT1 and IFIT5 orthologues from these rodents (see Figure 5-1). As such, loss of IFIT1 and IFIT5 may be coincident with a restructuring of the IFIT complex.

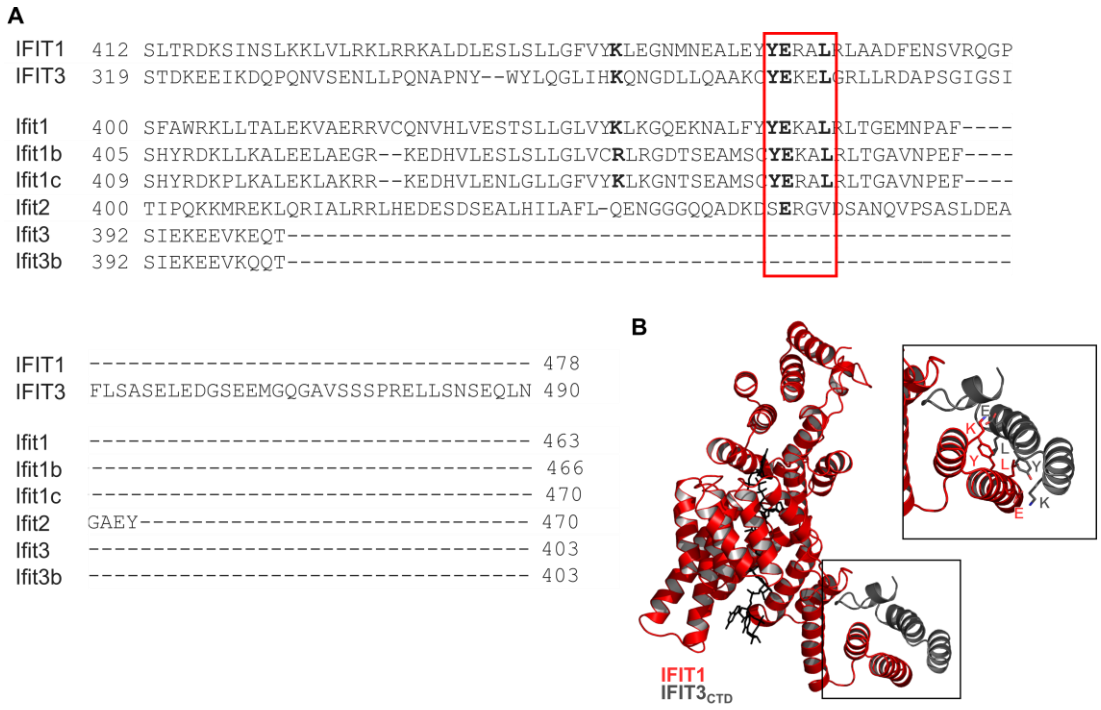

Figure 6-1 Sequence alignment of human IFIT and murine Ifit C-terminal domains.

A. *Sequences aligned in MUSCLE, showing the YExxL interaction motif (red box), which mediates interaction between human IFIT1 and IFIT3 (uppercase labels), and its conservation in murine Ifit proteins (lowercase labels).* ***B.*** *Structure of human IFIT1 (red) in complex with a C-terminal fragment of IFIT3 (IFIT3$_{CTD}$, grey) (PDB: 6C6K), demonstrating the position of the emboldened residues from (**A**).*

The C-terminal YExxL interaction motif, and many of the surrounding residues, is conserved in murine Ifit1, Ifit1b and Ifit1c (Figure 6-1). This suggests that these Ifit proteins in mouse should form homodimers, like human IFIT1 *(Abbas et al., 2017b)*, but may also be capable of heterodimerisation. Whether Ifit heterocomplexes can form in mice, and whether these complexes have any functional significance, has not been examined.

6.1.2 Aims

The aim of this chapter is to examine murine Ifit-Ifit interactions, to determine which complexes can form and what impact heterocomplex formation has on Ifit function. Heterocomplexes will be examined biochemically, to determine the impact of protein-protein interactions on the affinity and specificity of Ifit1 or Ifit1b for different mRNAs. Complexes will also be examined in terms of their stability both *in vitro* and in cells, to

determine whether one of the murine Ifit proteins can act as a functional analogue of human IFIT3 to stabilise the expression of another. Together, this will begin to reveal how murine Ifit proteins are regulated, what their role is in infection, and how this differs from, or potentially parallels, the human IFIT family.

6.2 Results

6.2.1 Oligomeric state of murine Ifits in solution.

Murine Ifit1 and Ifit1b were examined to determine their oligomeric state. When analysed by size exclusion chromatography (SEC), Ifit1 and Ifit1b eluted at 12.4-12.8 mL (Figure 6-2A-B), the expected elution volume for a ~100 kDa, dimeric species, when compared to a BSA standard. Dimeric human IFIT1 was previously shown to elute at ~12.5 mL, while monomeric mutants eluted at ~14.5 mL, on an equivalent column *(Abbas et al., 2017b)*. A mutant of Ifit1b was generated which contained mutations in the C-terminal domain to disrupt homodimerisation (M449E/L465E, Ifit1b-ML). Ifit1b-ML eluted at 14.4 mL, the expected elution volume of a monomer. This indicates that wildtype Ifit1b, and by inference Ifit1, is indeed dimeric in solution (Figure 6-2B).

To confirm this, wildtype Ifit1b was examined by SEC coupled with multi angle light scattering (MALS). SEC-MALS determines the molecular weight of protein species as they elute off the gel filtration column *(Some et al., 2019)*. The molecular weight of Ifit1b in solution was 110 kDa, which corresponds to a dimer (Figure 6-2C-E). This was found at 0.5 mg/mL and 2 mg/mL, indicating that Ifit1b dimers are quite stable, since they neither dissociate at low concentrations nor aggregate at high concentrations. By contrast, human IFIT1 was previously shown to homodimerise in a concentration-dependent manner and typically started to dissociate at 0.5 mg/mL *(Abbas et al., 2017b; Fleith and Mears et al., 2018)*. As such, it is likely that Ifit1 and Ifit1b both exist as dimeric species in solution. Ifit1c, and its truncations, typically eluted in the void fraction when purified by SEC, indicating that Ifit1c forms aggregates, consistent with its poor stability.

6.2.2 Co-precipitation of murine Ifit proteins

Since murine Ifit1 and Ifit1b eluted at very similar volumes when analysed by SEC, it was not possible to differentiate homodimeric and heterodimeric species using this technique.

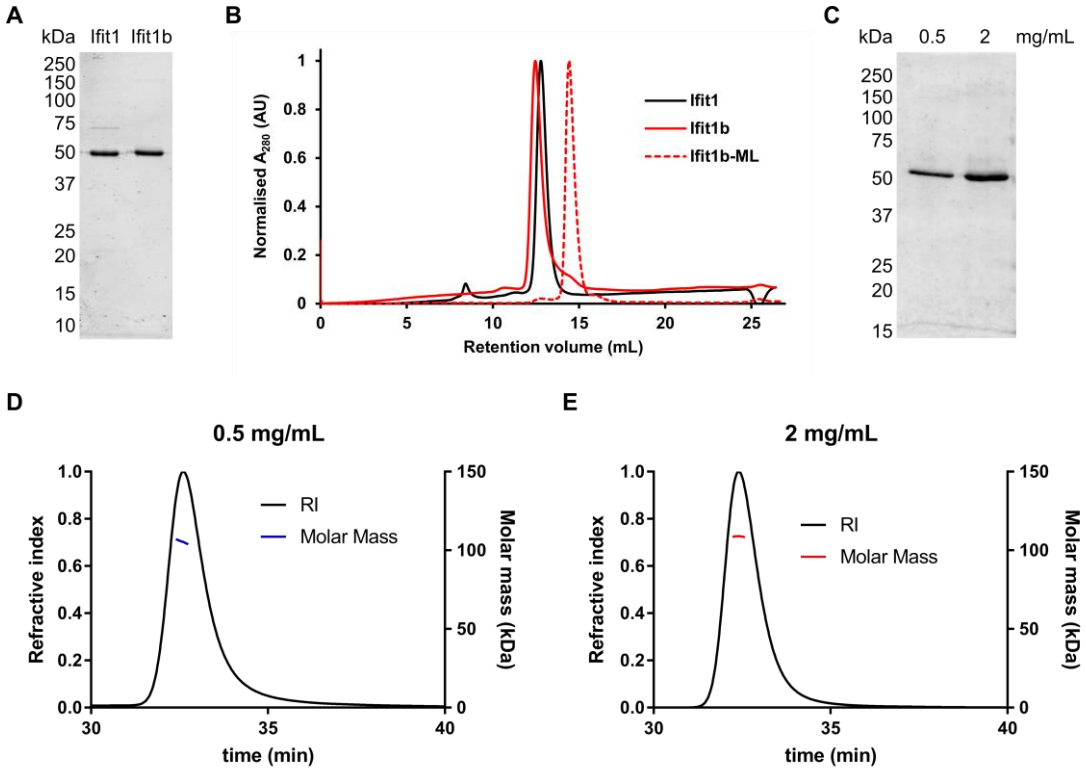

Figure 6-2 Murine Ifit1 and Ifit1b are homodimeric in solution.

A. *SDS-PAGE of recombinant Ifit1 and Ifit1b.* ***B.*** *Gel filtration analysis of Ifit1 (black), Ifit1b (red) and Ifit1b M449E/L465E (Ifit1b-ML, dashed red line), on a Superdex 200 Increase 10/300 column. For comparison, the peak maximum for each UV trace was set to 1.* ***C.*** *Recombinant Ifit1b inputs for size exclusion chromatography (SEC) with inline multi-angle light scattering (MALS) analysis.* ***D-E.*** *SEC-MALS of Ifit1b inject at the indicated concentrations on a Superdex 200 Increase 10/300 column. Normalized differential refractive index is shown as a black line on the left y-axis. Calculated molecular masses (kDa) of eluting species are shown as blue or red lines on the right y-axis.*

Therefore, to investigate which murine Ifit proteins can interact, an *in vitro* co-precipitation assay was used, similar to that employed by Johnson et al *(2018)* for the interrogation of human IFIT interactions. Equimolar MBP-tagged bait and His-tagged prey proteins were incubated together at 30˚C for one hour, before precipitation on amylose resin. Ifit3 was included as a negative control in each experiment and, consistent with a recent report *(Johnson et al., 2018)*, did not co-precipitate with any of the baits tested.

MBP-Ifit1 precipitated both Ifit1 and Ifit1b, while MBP-Ifit1b precipitated both Ifit1b and Ifit1 (Figure 6-3A-B). This confirms that, not only can these proteins interact with themselves, likely as homodimers, but they can also heterodimerise. MBP alone did not

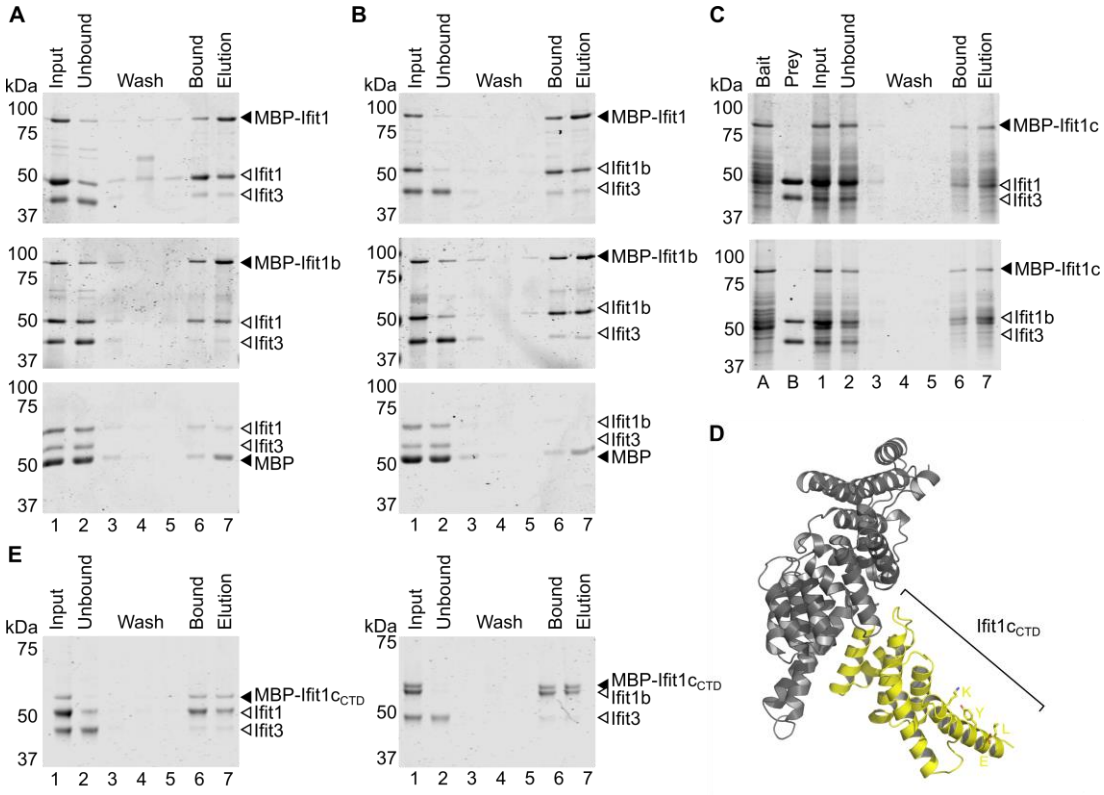

Figure 6-3 Murine Ifit1b-like proteins interact with each other but not with Ifit3.

A-C, E. *Co-precipitation of Ifit1, Ifit1b, Ifit1c (full-length or C-terminal domain, CTD), and Ifit3. MBP-tagged bait, or MBP alone, was incubated with prey proteins (lane 1) before binding to amylose resin. Unbound proteins were washed away (lanes 2-5) and bound proteins remained on the beads (lane 6). Bound proteins were eluted in maltose-containing buffer (lane 7). For clarity, in panel (**C**) bait and prey proteins are also shown separately (lanes A and B).* ***D.*** *Model of Ifit1c based on human IFIT1 (PDB: 5W5H) generated in SWISS-MODEL, with the C-terminal domain (CTD) in yellow.*

pull down any Ifit proteins tested, except for a trace amount of Ifit1 (Figure 6-3A-B). Since Ifit1 had a tendency to precipitate during this assay, this likely represents nonspecific binding of Ifit1 to the MBP or to the beads themselves.

To test whether Ifit1 or Ifit1b could interact with Ifit1c, full-length MBP-tagged Ifit1c was first used as bait. Despite the degradation products present in the recombinant MBP-Ifit1c, Ifit1b was clearly visible in the precipitate, indicative of an interaction (Figure 6-3C). However, owing to the presence of a contaminant band in Ifit1c at the same molecular weight as Ifit1, this interaction was more difficult to confirm. To circumvent this, a

truncated MBP-tagged Ifit1c construct was generated, containing the three most C-terminal TPRs (MBP-Ifit1c$_{CTD}$, amino acids 338-470, Figure 6-3D), which allowed purification of clean recombinant Ifit1c for use as bait. Ifit1 and Ifit1b both precipitated with MBP-Ifit1c$_{CTD}$, while Ifit3 did not. Therefore, Ifit1c can specifically form complexes with both Ifit1 and Ifit1b via its C-terminal domain (Figure 6-3E).

6.2.2.1 Competitive co-precipitation of Ifit proteins

Since Ifit1, Ifit1b and Ifit1c can all interact with one-another, presumably via the same motif, it is unclear whether one complex will form preferentially over the others. As such, the relative affinity of these interactions was investigated by competitive co-precipitation experiments. MBP-tagged Ifits were used as bait, and incubated with prey protein at 30 °C before binding to amylose resin, as previously. Beads were then washed with increasing concentrations of a competitor prey protein, with the expectation that higher affinity interactions should displace lower affinity ones. This may result in one prey being replaced by the other, or both preys washing off as a complex together.

When Ifit1b partially displaced Ifit1 bound to MBP-Ifit1, while Ifit1b was unable to displace Ifit1 bound to MBP-Ifit1b (Figure 6-4A). Similarly, Ifit1 could partially displace Ifit1b bound to MBP-Ifit1b, while Ifit1 could not displace a complex of MBP-Ifit1 and Ifit1b (Figure 6-4B). Together, this indicates that a heterocomplex of Ifit1 and Ifit1b is preferable over a homocomplex. Ifit1 bound stably to MBP-Ifit1c$_{CTD}$ and was not displaced by increasing concentrations of Ifit1b. However, Ifit1b was partially displaced by Ifit1 when the reciprocal experiment was performed (Figure 6-4C). This indicates that the interaction between Ifit1c and Ifit1 may be slightly stronger than between Ifit1c and Ifit1b. However, in the previous experiments with MBP only, a little Ifit1 co-precipitated non-specifically with the beads, possibly due to precipitation of Ifit1 during the assay.

Therefore, to investigate this further, MBP-Ifit1c$_{CTD}$ was incubated together with both Ifit1 and Ifit1b, at different temperatures. When incubated together on ice MBP-Ifit1c$_{CTD}$ coprecipitated both Ifit1 and Ifit1b, to a similar extent (Figure 6-4D). Since this interaction occurred even at low temperatures, it indicates that heterocomplexing is preferential and high affinity. Slightly more Ifit1 coprecipitated when the proteins were incubated at 30 °C, which may be indicative of aggregation, rather than true preferential interaction (Figure

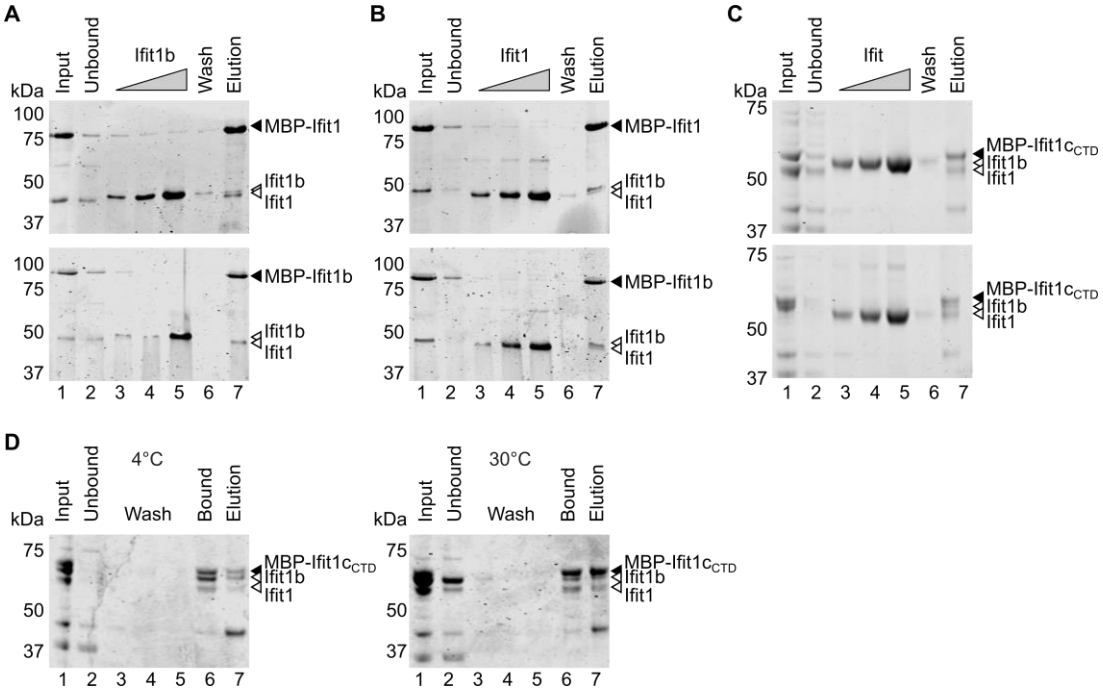

Figure 6-4 Ifit proteins preferentially heterooligomerise.

A-C. *Co-precipitation of Ifit1, Ifit1b and the C-terminal domain of Ifit1c (Ifit1c$_{CTD}$). MBP-tagged bait was incubated with prey protein (lane 1) before binding to amylose resin. Unbound proteins were washed away (lane 2) and resin was washed with an increasing concentration of competitor prey protein (lanes 3-5). Resin was washed again (lane 6) before elution in maltose-containing buffer (lane 7).* ***D.*** *Co-precipitation of Ifit1, Ifit1b and MBP-Ifit1c$_{CTD}$ (lane 1), incubated together at 4 ˚C (left panel) or at 30 ˚C (right panel) before binding to amylose resin. Unbound proteins were washed away (lanes 2-5) and bound proteins remained on the beads (lane 6). Bound proteins were eluted in maltose-containing buffer (lane 7).*

6-4D). Therefore, these experiments indicate that Ifit1c can interact with both Ifit1 and Ifit1b to a similar extent, and these interactions are preferential over homodimerisation.

6.2.3 Stability of Ifit complexes *in vitro*

To investigate whether these interactions were functionally significant, the thermal stability of the Ifit proteins and complexes was analysed by differential scanning fluorimetry. Full length Ifit1c could not be used due to the high degree of contaminants present. Therefore, the C-terminal fragment of Ifit1c was analysed. Ifit1c$_{CTD}$ was expressed without an MBP tag, since MBP is very stable and would interfere with the melt curve

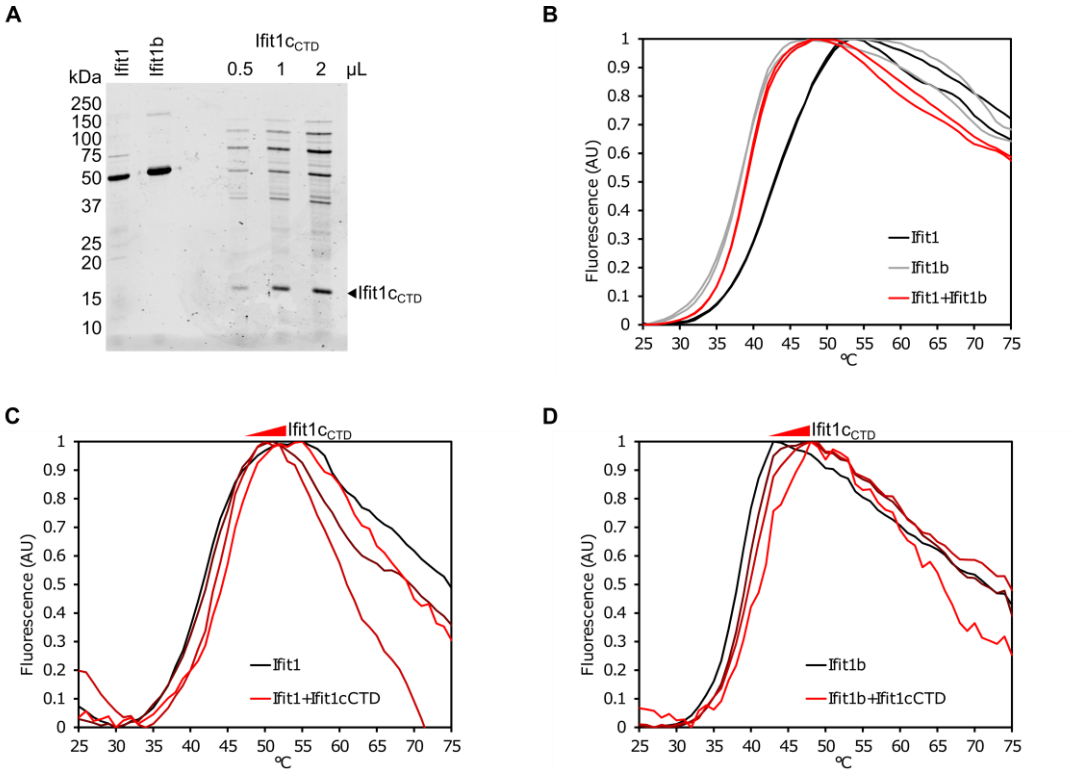

Figure 6-5 Heterocomplexing increases Ifit stability *in vitro*.

A. *SDS-PAGE of Ifit proteins used for thermal stability analysis.* ***B-D.*** *Differential scanning fluorimetry of Ifit proteins alone or in combination, as indicated. In (**C**) and (**D**), lighter shades of red indicate increasing concentrations of Ifit1c$_{CTD}$. Results are representative of at least two experimental replicates. CTD, C-terminal domain. Data are representative of at least two experimental repeats.*

analysis, though the yield and purity of Ifit1c$_{CTD}$ was poorer without the tag (Figure 6-5A). Ifit proteins were incubated alone or in combination for 30 minutes on ice, then assayed for thermal stability, as previously.

Murine Ifit proteins alone were typically unstable, with melting temperatures at or around physiological temperature (Figure 6-5 and Table 6-1). When Ifit1 and Ifit1b were mixed together, the melt curve was intermediate between the melting temperatures of the constituent proteins, indicating that this interaction does not provide any stability to either protein (Figure 6-5B). Ifit1c$_{CTD}$ alone was very unstable and, in most cases, did not produce a quantifiable melt curve at all. However, when either Ifit1 or Ifit1b was mixed with increasing concentrations of Ifit1c$_{CTD}$, melting temperature increased by up to 3 ˚C (Figure 6-5C-D).

Table 6-1 Melting temperatures of Ifit proteins and complexes.

Melting temperatures (Tm) were interpolated from data presented in Figure 6-5. Data were analysed by non-linear regression using the Boltzmann equation, y = LL (UL – LL)/(1 + exp(Tm –x)/a) where LL and UL are lower limit and upper limit respectively.

Protein or complex	Tm (°C)
Ifit1	41.9
Ifit1 + Ifit1c$_{CTD}$	44.4
Ifit1b	38.3
Ifit1b + Ifit1c$_{CTD}$	41.0

6.2.3.1 Ifit complex expression in cells

Ifit heterocomplexes were examined in mouse cells, to determine if co-expression of different murine Ifit proteins can stabilise their expression, as previously observed for human IFIT complexes. Murine 17C1 cells were seeded onto coverslips, then transfected with expression plasmids for eGFP, eGFP-Ifit1b or FLAG-Ifit1c, or co-transfected with eGFP or eGFP-Ifit1b and FLAG-Ifit1c (Figure 6-6A). After 24 hours, cells on coverslips were washed and stained for FLAG, as described in section 2.5, while surrounding cells from the same well were harvested for western blotting. Plasmids expressing an eGFP-Ifit1 fusion protein were also generated but, surprisingly, did not express in either murine or human cells, despite having the same plasmid backbone. The reason for this is unclear.

When eGFP-Ifit1b was expressed alone, it showed diffuse cytoplasmic localisation, typical of IFIT proteins *(Guo et al., 2000a; Huang et al., 2008)*. However, when FLAG-Ifit1c was expressed alone, it often showed punctate staining throughout the cytoplasm, with few cells showing diffuse localisation (Figure 6-6C). When FLAG-Ifit1c was co-transfected with eGFP-Ifit1b, both proteins were expressed in the cytoplasm with a similar localisation pattern. In some cells, Ifit1c no longer formed puncta, but instead showed a more diffuse localisation, similar to eGFP-Ifit1b (Figure 6-6D, see Appendix G). This apparent relocalisation did not occur in cells co-transfected with FLAG-Ifit1c and eGFP.

However, co-transfection efficiency was very low, so it was rare to observe cells expressing both proteins to a high level. Therefore, co-expression plasmids were generated, comprising eGFP-Ifit1b followed by FLAG-tagged Ifit1c in the same open reading frame,

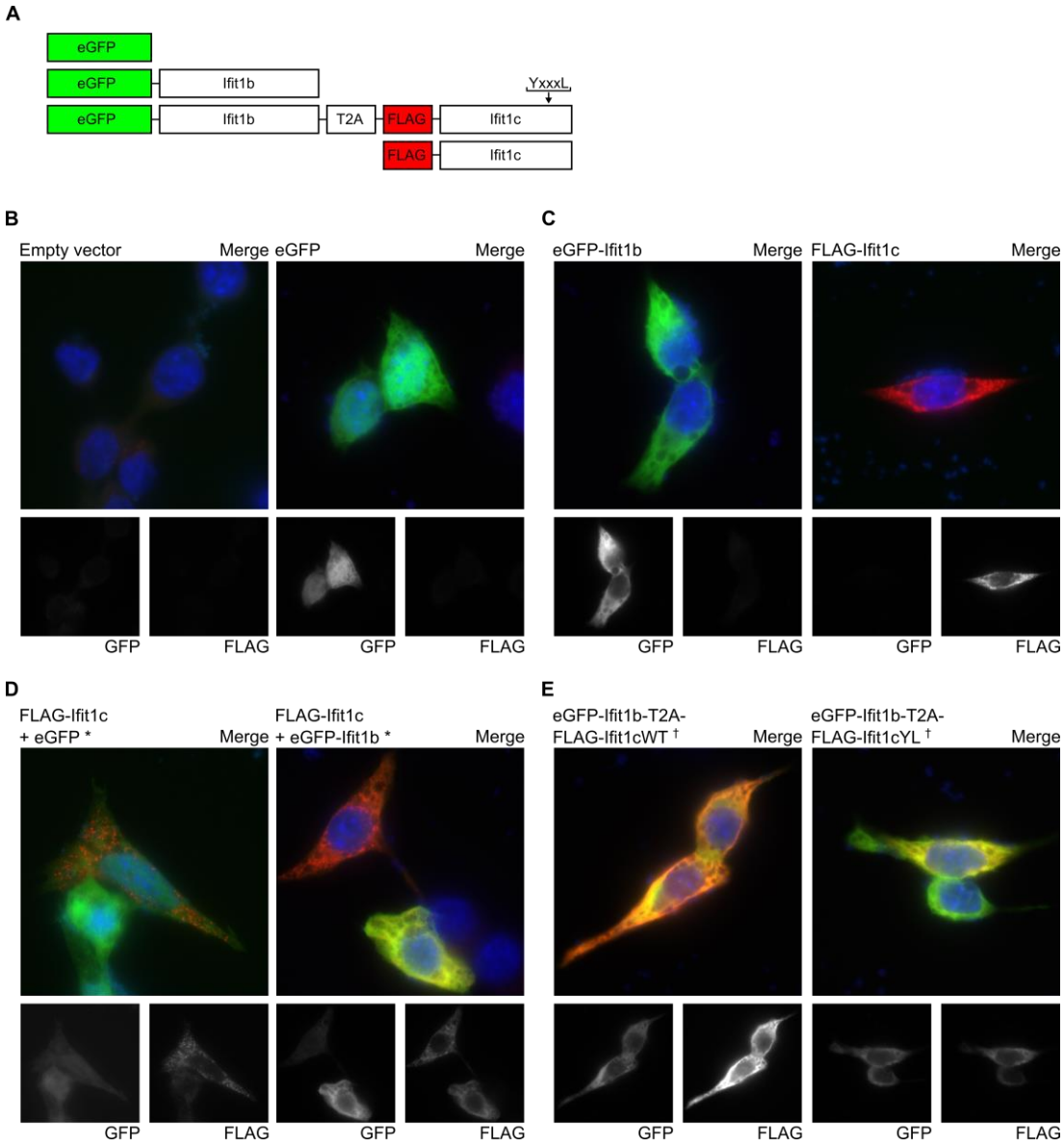

Figure 6-6 Ifit1b and Ifit1c co-localise in murine cells.

A. *Schematic of cellular expression constructs for Ifit fusion proteins.* ***B-E.*** *Immunofluorescence microscopy of murine 17C1 cells, 24 hours after transfection with (**B**) control plasmids, (**C**) eGFP-Ifit1b or FLAG-Ifit1c expression plasmids, (**D**) eGFP or GFP-Ifit1b with FLAG-Ifit1c or (**E**) eGFP-Ifit1b-FLAG-Ifit1c coexpression plasmids. T2A, thosea asigna virus 2A stop-go sequence. WT, wildtype. YL, Y456E/L460E mutant Ifit1c. Asterisks indicate where expression plasmids were cotransfected, while daggers show where proteins were co-expressed from a single transfected plasmid.*

separated by the 2A stop-go sequence from thosea asigna virus *(Liu et al., 2017)* (Figure 6-6A). This allows stoichiometric co-expression of both proteins, since the stop-go sequence prompts the ribosome to skip a peptide bond during elongation *(Donnelly et al., 2001; Atkins et al., 2007)*. Ifit1c in these constructs was either wildtype, or contained point

mutations in the C-terminal YxxxL motif, which should disrupt interaction with other Ifit proteins (YL).

When wildtype FLAG-Ifit1c was co-expressed with eGFP-Ifit1b, both proteins colocalised in the cytoplasm and very few cells showed punctate staining for Ifit1c (Figure 6-6E). Ifit1c expression also appeared to be higher, evident from the brighter fluorescence in the red channel (see Appendix G). When YxxxL interaction mutant FLAG-Ifit1c was co-expressed with eGFP-Ifit1b, cells still expressed both signals in the cytoplasm. However, co-localisation of the two signals was not as consistent as for wildtype Ifit1c and many cells still showed punctate FLAG staining (Figure 6-6D). This supports the observation that interaction between Ifit1b and Ifit1c may relocalise Ifit1c from cytoplasmic puncta. Ifit1c signal was also generally lower when the YxxxL motif was mutated, indicating that expression may be reduced in these cells, compared to wildtype Ifit1c co-expressed with Ifit1b.

To test whether co-expression indeed affects steady state Ifit expression, cell lysates from the same experiments were examined by immunoblotting. FLAG-Ifit1c alone was poorly expressed, indicative of instability at the protein level (Figure 6-7), as was previously observed for human IFIT1 (see Figure 3-2). When FLAG-Ifit1c was co-transfected with eGFP, both proteins were expressed more poorly than when transfected alone, consistent with the poor transfection efficiency observed in microscopy. FLAG-Ifit1c expression was slightly higher when co-transfected with eGFP-Ifit1b, relative to co-transfection with eGFP.

Ifit1c expression was strongly enhanced when co-expressed with eGFP-Ifit1b from the same plasmid (Figure 6-7). Expression of wildtype Ifit1c was 2.5-fold higher upon co-expression with Ifit1b. eGFP-Ifit1b expression was not significantly affected by co-expression with wildtype Ifit1c. When the YxxxL motif in Ifit1c was mutated, Ifit1c-YL expression was similar to Ifit1c expression without Ifit1b (Figure 6-7), indicating that interaction between Ifit1b and Ifiit1c is necessary for stabilisation. Expression of eGFP-Ifit1b was slightly reduced upon co-expression with Ifit1c-YL, when compared to co-expression with wildtype Ifit1c.

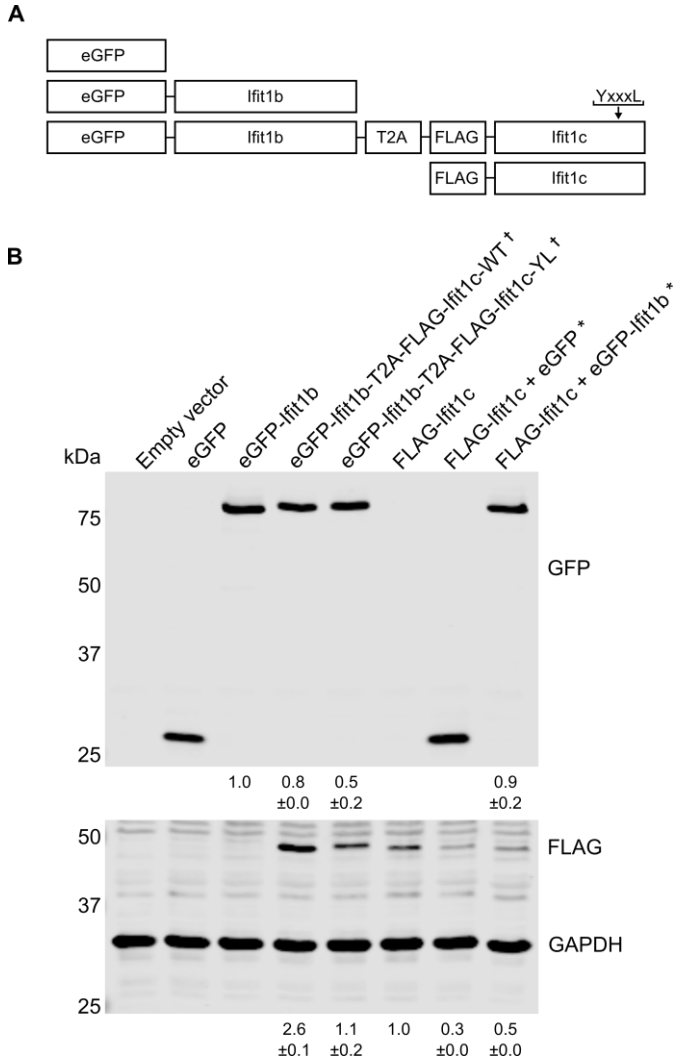

Figure 6-7 Ifit1b enhances Ifit1c expression in murine cells.

A. *Schematic of cellular expression constructs for Ifit fusion proteins.* ***B.*** *Western blot analysis of murine 17C1 cells transfected with Ifit1b expression plasmids, with or without coexpression of Ifit1c, after 24 hours. T2A, thosea asigna virus 2A stop-go sequence. WT, wildtype. YL, Y456E/L460E mutant Ifit1c. Asterisks indicate where expression plasmids were cotransfected, while daggers show where proteins were co-expressed from a single transfected plasmid. Quantification of GFP or FLAG signal is shown under each panel, normalised to GAPDH and expressed as fold increase over eGFP-Ifit1b or FLAG-Ifit1c alone. Data represent the mean ± the standard error of two biological repeats.*

6.2.4 Translation inhibition by Ifit complexes

To determine the activity of Ifit1c-containing complexes, the translation inhibition activity of purified complexes was analysed *in vitro*. Increasing concentrations of Ifit1 or Ifit1b were incubated with cap0 or cap1 Fluc reporter mRNAs (Figure 6-8), respectively, in a reaction containing RRL with or without the addition of 500 nM MBP-Ifit1c$_{CTD}$. Luciferase signal

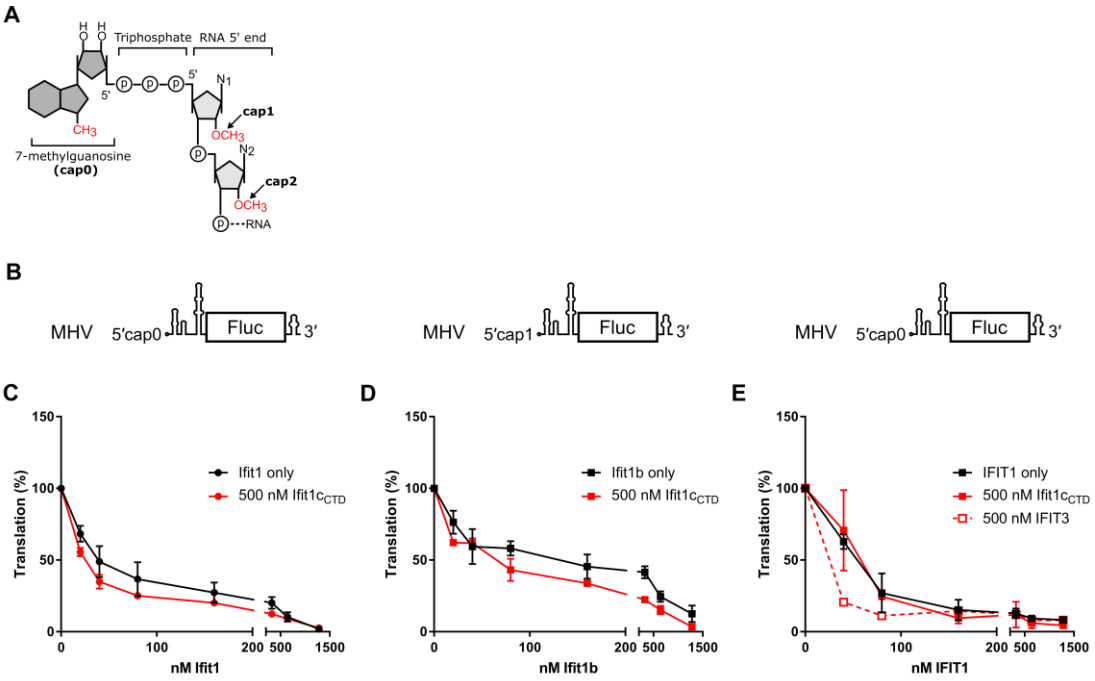

Figure 6-8 Ifit1c enhances translation inhibition by Ifit1 and Ifit1b *in vitro*.

A. *Schematic of the mRNA 5' cap and* ***B.*** *model RNAs used for translation assays.* ***C-E.*** *In vitro translation of MHV-Fluc reporter mRNAs in RRL with increasing concentrations of (**C**) Ifit1, (**D**) Ifit1b or (**E**) human IFIT1, in the presence or absence of 500 nM Ifit1c$_{CTD}$. Data were normalised to luciferase activity in the absence of IFIT protein and shown as the mean ± the standard error of three experiments.*

was measured, as previously, and normalised to the buffer only or MBP-Ifit1c$_{CTD}$ only condition for each titration series, to eliminate any effect of MBP-Ifit1c$_{CTD}$ alone on translation.

Inclusion of Ifit1c$_{CTD}$ in the translation reaction decreased the concentration of Ifit1l required to cause a 50% decrease in translation (IC$_{50}$) from cap0 MHV-Fluc reporter mRNA by 2-fold (Figure 6-8A and Table 6-2). Similarly, addition of Ifit1c$_{CTD}$ decreased the IC$_{50}$ of Ifit1b on cap1 MHV-Fluc mRNA by 2-fold (Figure 6-8B and Table 6-2). Ifit1c$_{CTD}$ also enhanced translation inhibition by Ifit1b at higher concentrations, allowing almost complete inhibition of translation. However, when Ifit1c$_{CTD}$ was added to a translation reaction with human IFIT1, inhibition of cap0 MHV-Fluc mRNA was similar to human IFIT1 alone (Figure 6-8C and Table 6-2). When human IFIT3 was added to the RRL master mix, human IFIT1 activity was enhanced, as expected. Together this indicates that Ifit1c can specifically act as a cofactor for both Ifit1 and Ifit1b to enhance their translation inhibition activity.

Table 6-2 Translation inhibition by Ifit complexes.

Concentration of Ifit that reduced translation from the reporter RNA by 50% (IC_{50}) ± standard error. Mouse Ifit proteins are shown in lowercase while human IFIT1 is shown in uppercase. To calculate the Ifit concentration at which translation was inhibited by 50%, data were fit to [Inhibitor] versus normalised response curve (Y = 100)/(1 + (XHillSlope)/(IC50HillSlope)) using the least squares method in GraphPad Prism. IC_{50} values are listed in Table 6-2.

Ifit	RNA	IC_{50} (nM Ifit in RRL)	p-value (Ifit only vs Ifit1c$_{CTD}$)
Ifit1	cap0-MHV-Fluc	44.36 ± 6.7	-
Ifit1 + Ifit1c$_{CTD}$	cap0-MHV-Fluc	22.45 ± 2.1	0.0015
Ifit1b	cap1-MHV-Fluc	115.9 ± 21.1	-
Ifit1b + Ifit1c$_{CTD}$	cap1-MHV-Fluc	56.52 ± 5.7	0.0012
IFIT1	cap0-MHV-Fluc	49.84 ± 7.3	-
IFIT1 + Ifit1c$_{CTD}$	cap0-MHV-Fluc	55.02 ± 7.1	0.5044

The effect of Ifit1c on Ifit1b activity was also investigated in murine cells, by overexpression followed by infection with mouse hepatitis virus. However, as discussed in chapter 5, the overexpression system is not optimal for studying the influence of Ifit proteins on viral infection, since transfection or overexpression appeared to reduce the susceptibility of l7C1 cells to infection. Previously, Johnson et al. *(2018)* used an inducible expression system to determine the effect of IFIT3 on the ability of IFIT1 to restrict viral infection. A similar system could be employed with Ifit1c, since it would allow fine-tuned protein overexpression and, as such, allow expression at levels which still permit viral infection. This would also circumvent the need for transfection entirely, which is poor in l7C1 cells, allowing a more homogeneous population of cells to be studied. Ideally, gene editing could be used to introduce mutations into endogenous Ifit genes, to disrupt heterodimerisation. While potentially laborious, this would give the clearest indication of the effect of Ifit complexes during infection.

6.3 Conclusions

In this chapter, murine Ifit complexes were examined in terms of their composition and activity. Ifit1, Ifit1b and Ifit1c all share a C-terminal YExxL motif and were found to interact with one another both *in vitro* and in cells. *In vitro*, Ifit1c was shown to enhance stability

of Ifit1 and Ifit1b, while Ifit1b stimulated Ifit1c expression in murine cells. Ifit1c was also found to act as a cofactor for Ifit1 and Ifit1b, promoting translation inhibition *in vitro*.

As discussed in chapter 3, in humans IFIT3 stabilises IFIT1 and enhances its RNA binding activity, possibly by altering the flexibility of IFIT1 via interactions between the long C-terminal domain of IFIT3 and the pivot domain of IFIT1. In mice, Ifit1c lacks an extended C-terminal domain (see Figure 6-1), but nevertheless enhanced stability and translation inhibition of both Ifit1 and Ifit1b, acting in an analogous fashion to human IFIT3. Structural modelling predicts that Ifit1c has a positively charged C-terminal domain, which is not present in human IFIT3 (Figure 6-9). In murine Ifit complexes, this domain in Ifit1c may provide an additional RNA binding surface, increasing the avidity of binding by Ifit1 or Ifit1b.

In humans, because of the long C-terminal domain in IFIT3, the IFIT1:IFIT3 interaction interface has a larger buried surface area than IFIT1 homodimers *(Abbas et al., 2017b; Johnson et al., 2018)*. As such, interaction between IFIT1 and IFIT3 is entropically favourable compared to IFIT1 homodimerisation, driving the high affinity between the two proteins. By contrast, the C-terminal domains of murine Ifit proteins are similar in length and are well conserved that the amino acid level (see Figure 6-1). Therefore, it remains to be determined why Ifit1, Ifit1b and Ifit1c have a propensity to heterodimerise, rather than remain as homodimers. A more complete structural understanding of both the human and murine IFIT complexes will be necessary to answer these questions fully.

Recently, mouse Ifit3 was shown to not interact with human IFIT1 *(Johnson et al., 2018)*, since it is C-terminally truncated and lacks the YExxL interaction motif, a finding that was recapitulated here. That study also found that a chimeric protein in which the C-terminal domain of human IFIT3 was added to the end of murine Ifit3 could interact with human IFIT1, but could not interact with murine Ifit1 *(Johnson et al., 2018)*. Therefore, while this motif appears necessary for interaction between IFIT proteins, it is not sufficient to mediate that interaction. Consistently, here it was found that the YExxL motif itself is not sufficient for cofactor activity, since the translation inhibition by human IFIT1 was not enhanced by Ifit1c *in vitro*. Therefore, interactions with surrounding residues, or the 3D presentation of the motif, may be important for specific IFIT-IFIT interactions within species or lineages. Mutants in and around the YExxL motif will be necessary to confirm

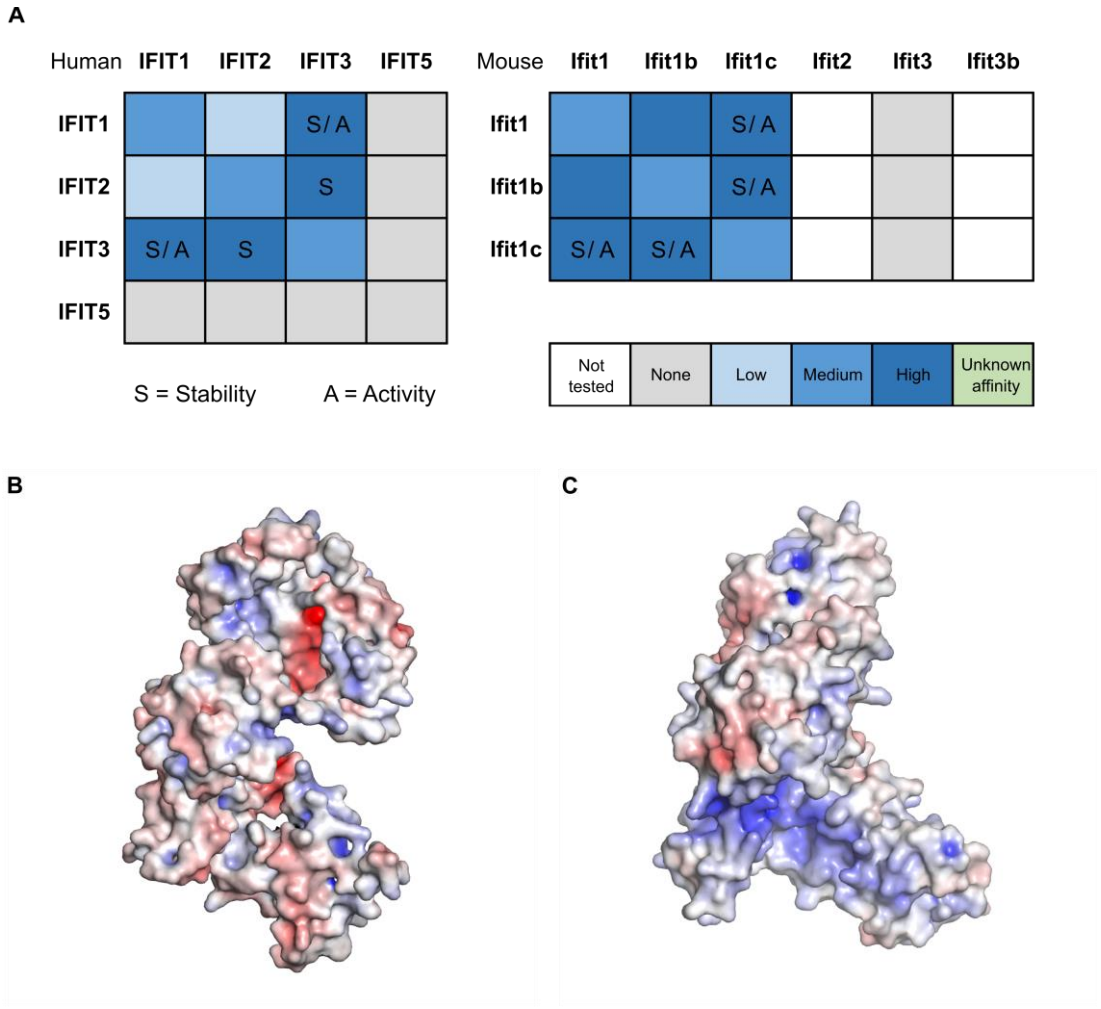

Figure 6-9 Murine Ifit heterocomplexes.

A. *Summary of murine Ifit heterocomplexes and the effect of heterocomplex formation on Ifit stability and activity, with human IFIT complexes for comparison.* ***B-C****. Structural models of (****B****) human IFIT3 based on human IFIT2 (PDB: 4GIT) or (****C****) murine Ifit1c based on human IFIT1 (PDB: 5W5H), coloured by electrostatic potential from negative (-10 kTe^{-1}; red) to positive (+10 kTe^{-1}; blue), via hydrophobic (white), generated in APBS using PDB2PQR (Dolinsky et al., 2004).*

this motif is important for interaction and evaluate which other residues contribute to stabilising murine Ifit heterocomplexes.

Like human IFIT complexes, interaction between murine Ifit proteins was shown to increase their thermal stability, suggesting heterocomplexing is a thermodynamically preferable state. Ifit1c was the most unstable murine Ifit tested and, as discussed in chapter 4, the full-length protein was recalcitrant to recombinant expression; even the C-terminal

domain in isolation was challenging to express and purify. This is especially surprising given that Ifit1b, with which Ifit1c shares 87% similarity, expresses very well in bacteria and can be prepared to very high concentration and purity. Ifit1c expression in murine cells was significantly enhanced by co-expression with Ifit1b, only when the C-terminal YExxL motif was intact. Instability in the absence of a binding partner may be a mechanism to regulate Ifit1c expression at the protein level, in contrast to Ifit1b which is regulated at the mRNA level.

Stabilising Ifit1c expression in this way opens up new avenues for interrogating its function. Constructs can be generated in which Ifit1b lacks RNA binding activity, allowing potential RNA binding by Ifit1c to be investigated. Preliminary trials using bacterial co-expression vectors has shown that co-expression with either Ifit1 or Ifit1b improves both yield and purity of Ifit1c, though it is still prone to degradation. Therefore, co-expression in mammalian cells may provide a route for purification of stable recombinant Ifit1c-containing complexes for examination *in vitro*.

7 SUMMARY

Interferons developed early in vertebrate evolution to coordinate innate immunity and the burgeoning adaptive immune response *(Secombes and Zou, 2017)*. The IFN gene programme includes hundreds of antiviral proteins, providing a primary barrier against viral infection, during which time an adaptive response can be mounted. Host restriction factors exert strong selective pressures on viruses to maintain mechanisms to evade or counteract restriction, which can come at the cost of optimal replication.

7.1 RNA binding by human and murine IFIT proteins

IFIT proteins are a class of ISG which are as ancient as interferon itself *(Liu et al., 2013)*. In humans, IFIT1 and IFIT5 are well-characterised RNA binding proteins, which serve as dual effector-sensors of non-self RNA in the cytoplasm. Human IFIT1 binds to cap0 RNA with high affinity *(Kumar et al., 2014; Abbas et al., 2017a)* and, in so doing, exerts strong selective pressure on viruses which replicate in the cytoplasm to maintain mechanisms to evade IFIT1 recognition. Some viruses, including flaviviruses and coronaviruses, achieve IFIT1 evasion by encoding a viral 2'-O-methyltransferase to modify their capped RNA to cap1 *(Daffis et al., 2010; Züst et al., 2011, 2013; Menachery et al., 2014, 2017)*. However, at high concentrations IFIT1 is also capable of inhibiting cap1 RNA translation *(Abbas et al., 2017a)* and as such confers some protection against cap1 viruses in the cytoplasm *(Daugherty et al., 2016; Johnson et al., 2018)*.

In mice, Ifit1 binds to cap0 RNA with high affinity *(Habjan et al., 2013; Kimura et al., 2013)*, but cannot bind to cap1 RNA *(Daugherty et al., 2016)*, findings that were recapitulated in

this thesis. Here, Ifit1b was found to bind cap1 RNA with high specificity and inhibit its translation at nanomolar concentrations. However, while Ifit1 was highly expressed in stimulated mouse cells, Ifit1b was poorly upregulated owing at least in part to weak promoter activity. In this way, mouse cells may achieve the same balance between cap0 and cap1 binding as human cells. In humans a single highly-expressed protein, IFIT1, regulates cap0 versus cap1-RNA translation inhibition at the level of binding affinity; in mice, cap0 and cap1-RNA binding by Ifit proteins is regulated at the mRNA level, by differential induction of Ifit1 and Ifit1b expression, respectively. As such, murine Ifit1 and Ifit1b together can inhabit the same functional niche as human IFIT1.

Alphaviruses have a very stable stem loop at the immediate 5' end of the genome and were previously shown to be impervious to binding by Ifit1, conferring resistance to type I IFN *in vivo (Hyde et al., 2014; Reynaud et al., 2015)*. Destabilising this RNA secondary structure confers susceptibility to restriction by Ifit1 *(Hyde et al., 2014)*. Flaviviruses, including Zika virus (ZIKV), have a comparable stable stem loop at the very 5' end of their genomes *(Gebhard et al., 2011)*. Here, it was found that murine Ifit1 and Ifit1b could not inhibit translation from a ZIKV reporter mRNA, even at micromolar concentrations. Human IFIT1 effectively inhibited translation of the same ZIKV reporter construct at nanomolar concentrations. Therefore, this has identified a key difference in the ability of human and murine IFIT proteins to bind to structured substrates. Such differences in the ability of human IFIT1 and murine Ifits to bind RNA with strong 5' structure may have implications for vaccine development.

Despite this, there has been some success with IFIT1-sensitive vaccine strains in murine models. 2'-O-methyltransferase mutants of flaviviruses and coronaviruses are highly attenuated *in vivo* and vaccination with these viruses can protect mice from challenge with virulent strains *(Daffis et al., 2010; Szretter et al., 2012; Li et al., 2013; Züst et al., 2013; Menachery et al., 2014, 2017)*. Protection was shown in a rhesus macaque model of dengue virus infection *(Züst et al., 2013)*, indicating that the results in mouse models are indeed applicable to primates. Knockout of murine Ifit1 could partially restore virulence in these models *(Daffis et al., 2010; Szretter et al., 2012; Menachery et al., 2014, 2017)*, indicating that murine Ifit1 can indeed mediate antiviral activity against cap0 virus strains *in vivo*, even those with strong 5' RNA structure. However, Ifit1 knockout did not restore attenuation of cap0 WNV strain in some tissues and in primary cultures derived from knockout mice *(Szretter et al., 2012)*. The viral loads in the central nervous system, for

example, were unaffected by Ifit1 knockout *(Szretter et al., 2012)*, even though Ifit1 was previously found to be expressed throughout the brain following WNV infection *(Wacher et al., 2007)*. Differences in the expression or activity of IFIT proteins in different tissues between humans and mice may have major implications for the safety and efficacy of a cap0 WNV vaccine strain. Reconstituting these mice with a humanised IFIT gene cassette would be necessary to determine whether these vaccine strains are genuinely sensitive to IFIT1-mediated restriction in the brain.

7.1.1 Modulation of host translation by IFIT proteins

Human IFIT1 was previously shown to inhibit up to ~40% of cellular translation when overexpressed in human cells *(Guo et al., 2000b)*. Treatment of cells with type I IFN similarly caused 40% translation inhibition, possibly via the action of IFIT1 *(Guo et al., 2000b)*. A recent report has using mass spectrometry to quantify the proportion of cellular transcripts with different 5' caps has found that the vast majority of caps were 2'-O-methylated at the first nucleotide, and cap0 structures were not detected, in a number of human and mouse cell lines and primary tissues *(Wang et al., 2019)*. Therefore, translation inhibition by IFIT proteins is unlikely to be through inhibition of cap0 transcripts, since these are not abundant in the cell. Consistently here murine Ifit1, which is specific for cap0 RNA, did not inhibit cellular translation when overexpressed in mouse cells, while Ifit1b inhibited translation by ~30%. Those transcripts which avoid inhibition are likely to be either highly structured or cap2 modified, thus escaping Ifit1b binding.

As discussed in chapter 4, the endogenous expression level of Ifit1b is very low, much lower than overexpressed protein. Therefore, the transcriptional repression of Ifit1b expression may serve to prevent dramatic host translation inhibition following IFN stimulation. Whether endogenous Ifit1b plays a role in fine-tuning translation during the innate response remains to be determined. In the future, RNA pulldowns, mass spectrometric analysis of nascent proteins, or ribosome profiling of Ifit1b-expressing cells, could give insights into which mRNAs are bound and inhibited by Ifit1b, to determine the effect of Ifit1b on the antiviral gene programme.

7.2 IFIT complexes and protein-protein interactions

While the tetratricopeptide (TPR) repeat motifs in IFIT proteins facilitate binding to RNA, TPRs are a canonical protein-protein interaction motif *(D'Andrea and Regan, 2003)*. Here, in chapters 3 and 6, human and murine IFIT proteins were found to form defined heterocomplexes which regulated their stability and function.

In humans, the regulation of IFIT1 is intrinsically linked to the activity of the IFIT2:IFIT3 complex, via interactions between IFIT1 and IFIT3. As such, these three proteins are co-regulated: the expression level of one member of the complex may have profound implications for the stability or activity of another complex member. In mice, on the other hand, Ifit1/Ifit1b activity is decoupled from the Ifit2:Ifit3 complex and its associated functions. These subtle differences in the co-regulation of human IFIT1 and murine Ifit1/Ifit1b are unlikely to have drastic implications for determining whether a vaccine works or not. However, they may limit the degree of molecular detail that can be extracted from a mouse study into host-virus interactions.

IFIT proteins are also known to interact with other cellular proteins, to regulate different stages of the antiviral response. IFIT3 has been shown to potentiate signalling downstream of nucleic acid sensing and to enhance type I IFN production during viral infection. The N-terminal domain of IFIT3 was found to interact with both MAVS and its downstream kinase TBK1 *(Liu et al., 2011)*. Binding by IFIT3 enhanced recruitment of TBK1 to MAVS, consequently enhancing phosphorylation of IRF3 and transcription of type I IFNs *(Liu et al., 2011; Hou et al., 2016)*. IFIT3 was also found to interact with both TBK1 and STING, and potentiated DNA sensing in the cytoplasm *(Wang et al., 2018)*. An acidic motif in the N-terminal domain of IFIT3 was identified, which bound to the positively-charged N-terminus of TBK1 *(Liu et al., 2011)*. These residues are maintained in murine Ifit3, though any role for Ifit3 in innate signalling in mouse cells has not been established.

IFIT3 interacts with IFIT2 via the N-terminal domain of IFIT2 *(Stawowczyk et al., 2011)* which, as discussed in chapter 3, may involve an N-terminal domain swap between IFIT2 and IFIT3 *(Fleith and Mears et al., 2018)*. The acidic motif responsible for interaction between IFIT3 and TBK1 is within this N-terminal domain, close to the putative domain swap site. Therefore, the effect of IFIT2:IFIT3 heterodimerisation on IFIT3's described role in innate immune signalling warrants further investigation (see Appendix H).

IFIT1 has been found to promote type I IFN expression in response to alphavirus infection, thereby limiting virus spread *(Reynaud et al., 2015)*. Similarly, IFIT1 depletion was shown to decrease IFN production in human macrophages, in both artificially stimulated and infected cells *(John et al., 2018)*. A similar phenotype was observed in murine macrophages, indicating that murine Ifit1 may share this function *(John et al., 2018)*. Consistently, knockout of murine Ifit1 in a macrophage cell line reduced cytoplasmic dsRNA sensing (Appendix J) and promoted replication of murine norovirus (Appendix K), indicating that murine Ifit1 may restrict viral infection by synergising type I IFN induction *(Mears et al., 2019)*.

However, a previous study found that IFIT1 downregulates production of type I IFN, by binding to STING *(Li et al., 2009)*. STING has been shown to synergise the interaction between the MAVS complex and the downstream kinase TBK1, potentiating IRF3 phosphorylation *(Zhong et al., 2008)*. IFIT1 binding occludes the interaction between STING and MAVS/TBK1. IFIT1 therefore inhibited STING-mediated enhancement of this signalling pathway, inhibiting production of type I IFN in response to infection *(Li et al., 2009)*. As such, IFIT1 and IFIT3 appear to have diametrically opposing roles in IFN induction: IFIT1 breaks the interaction between MAVS and TBK1 while IFIT3 enhances it. Therefore, the effect of an IFIT1:IFIT3 heterocomplex on MAVS signalling is still unclear (see Appendix H).

In addition to regulating innate immune signalling, IFIT proteins have been implicated in modulating apoptosis (summarised in Appendix I). Overexpression of IFIT2 was shown to activate apoptosis in a number of human cell lines *(Stawowczyk et al., 2011; Chen et al., 2017)* and has been particularly investigated for its ability to induce cancer cell death *(Lai et al., 2013; Feng et al., 2014; Wang et al., 2016; Jia et al., 2017; Ohsugi et al., 2017; Tang et al., 2017; Zhang et al., 2017b)*. Interestingly, overexpression of IFIT3 was shown to ameliorate IFIT2-dependent apoptosis *(Stawowczyk et al., 2011)*, while knockdown of IFIT3 potentiated apoptosis induced by dengue virus infection *(Hsu et al., 2013)*. Therefore, it is possible that the IFIT2:IFIT3 interaction acts a regulatory complex to prevent unfettered cell death during the antiviral response. Since the molecular details of IFIT2-dependent apoptosis are unclear, it is difficult to postulate whether this role may be conserved in murine Ifit2.

Murine Ifit2 has been implicated in regulating the inflammatory response during fungal infection *in vivo*. Ifit2 downregulated production of reactive oxygen species by binding to a $p67^{phox}$, a positive regulator of NADPH oxidase activity *(Stawowczyk et al., 2018)*. Human IFIT2 was also shown to interact with $p67^{phox}$, indicating that this function may be shared in both species *(Stawowczyk et al., 2018)*. While these proteins are also localised to the outer mitochondrial membrane, a link with apoptosis induction in mice was not established.

Murine Ifit2 and Ifit3, whose N-terminal domains are well-conserved, have also been shown to interact in primary mouse cells *(Siegfried et al., 2013)*, indicating that they may indeed form an equivalent heterocomplex to their human counterparts. Ifit3b differs from Ifit3 by only five amino acids; two of these substitutions are situated within the putative domain-swap region in the N-terminal domain, indicating that they could have implications for heterodimerisation, either between Ifit3 and Ifit3b, or with Ifit2. The impact of murine Ifit2/Ifit3/Ifit3b, individually or in complex, on murine innate immune signalling requires clarification.

7.3 Concluding remarks

Overall, this study has provided insights into the expression, function and regulation of the murine Ifit family and their role in antiviral defence. Ifit1b was identified as a novel cap1-RNA binding protein which may functionally compensate for the loss of IFIT1 in mice and other rodents. Ifit1c was found to functionally mimic human IFIT3 by acting as a cofactor to stimulate the activity of other Ifit family members. As such, Ifit1, Ifit1b and Ifit1c together can be considered as a functional unit which mimics the action of human IFIT1, a valuable consideration for the design of future mouse experiments.

8 References

Abbas, Y. M., **Pichlmair, A.**, **Górna, M. W.**, **Superti-Furga, G.** and **Nagar, B.** (2013) 'Structural basis for viral 5'-PPP-RNA recognition by human IFIT proteins.', *Nature*, 494(7435), pp. 60–4, doi:10.1038/nature11783.

Abbas, Y. M., **Laudenbach, B. T.**, **Martínez-Montero, S.**, **Cencic, R.**, **Habjan, M.**, **Pichlmair, A.**, **Damha, M. J.**, **Pelletier, J.** and **Nagar, B.** (2017a) 'Structure of human IFIT1 with capped RNA reveals adaptable mRNA binding and mechanisms for sensing N1 and N2 ribose 2'-O methylations', *Proceedings of the National Academy of Sciences*, 114(11), pp. E2106–E2115, doi:10.1073/pnas.1612444114.

Abbas, Y. M., **Martínez-montero, S.**, **Cencic, R.**, **Pelletier, J.** and **Peter, D.** (2017b) 'A conserved homo-dimerization interface in human IFIT1 provides insights into IFIT interactome assembly', *bioRxiv*, 152850, doi:https://doi.org/10.1101/152850.

Andrejeva, J., **Norsted, H.**, **Habjan, M.**, **Thiel, V.**, **Goodbourn, S.** and **Randall, R. E.** (2013) 'ISG56/IFIT1 is primarily responsible for interferon-induced changes to patterns of parainfluenza virus type 5 transcription and protein synthesis', *Journal of General Virology*, 94(Pt_1), pp. 59–68, doi:10.1099/vir.0.046797-0.

Atkins, J. F., **Wills, N. M.**, **Loughran, G.**, **Wu, C.-Y.**, **Parsawar, K.**, **Ryan, M. D.**, **Wang, C.-H.** and **Nelson, C. C.** (2007) 'A case for "StopGo": reprogramming translation to augment codon meaning of GGN by promoting unconventional termination (Stop) after addition of glycine and then allowing continued translation (Go).', *RNA (New York, N.Y.)*, 13(6), pp. 803–10, doi:10.1261/rna.487907.

Baltimore, D. (1971) 'Expression of animal virus genomes.', *Bacteriological reviews*, 35(3), pp. 235–41.

Bandyopadhyay, S. K., **Kalvakolanu, D. V** and **Sen, G. C.** (1990) 'Gene induction by interferons: functional complementation between trans-acting factors induced by alpha interferon and gamma

interferon.', *Molecular and cellular biology*, 10(10), pp. 5055–5063, doi:10.1128/mcb.10.10.5055.

Barreau, C., **Paillard, L.** and **Osborne, H. B.** (2005) 'AU-rich elements and associated factors: Are there unifying principles?', *Nucleic Acids Research*, pp. 7138–7150, doi:10.1093/nar/gki1012.

Berchtold, S., **Manncke, B.**, **Klenk, J.**, **Geisel, J.**, **Autenrieth, I. B.** and **Bohn, E.** (2008) 'Forced IFIT-2 expression represses LPS induced TNF-alpha expression at posttranscriptional levels.', *BMC immunology*, 9, p. 75, doi:10.1186/1471-2172-9-75.

Bluyssen, H. A., **Vlietstra, R. J.**, **Faber, P. W.**, **Smit, E. M.**, **Hagemeijer, A.** and **Trapman, J.** (1994a) 'Structure, chromosome localization, and regulation of expression of the interferon-regulated mouse Ifi54/Ifi56 gene family.', *Genomics*, 24(1), pp. 137–48, doi:10.1006/geno.1994.1591.

Bluyssen, H. A., **Vlietstra, R. J.**, **van der Made, A.** and **Trapman, J.** (1994b) 'The interferon-stimulated gene 54 K promoter contains two adjacent functional interferon-stimulated response elements of different strength, which act synergistically for maximal interferon-alpha inducibility.', *European journal of biochemistry*, 220(2), pp. 395–402, doi:10.1111/j.1432-1033.1994.tb18636.x.

Bogorad, A. M., **Lin, K. Y.** and **Marintchev, A.** (2017) 'Novel mechanisms of eIF2B action and regulation by eIF2 phosphorylation', *Nucleic Acids Research*. Oxford University Press, 45(20), pp. 11962–11979, doi:10.1093/nar/gkx845.

Brown, C. J., **Verma, C. S.**, **Walkinshaw, M. D.** and **Lane, D. P.** (2009) 'Crystallization of eIF4E complexed with eIF4GI peptide and glycerol reveals distinct structural differences around the cap-binding site', *Cell Cycle*, 8(12), pp. 1905–1911, doi:10.4161/cc.8.12.8742.

Brown, R. S., **Dewan, J. C.** and **Klug, A.** (1985) 'Crystallographic and biochemical investigation of the lead(II)-catalyzed hydrolysis of yeast phenylalanine tRNA.', *Biochemistry*, 24(18), pp. 4785–801, doi:10.1021/bi00339a012.

Buggele, W. A. and **Horvath, C. M.** (2013) 'MicroRNA profiling of Sendai virus-infected A549 cells identifies miR-203 as an interferon-inducible regulator of IFIT1/ISG56.', *Journal of virology*, 87(16), pp. 9260–70, doi:10.1128/jvi.01064-13.

Burdette, D. L., **Monroe, K. M.**, **Sotelo-Troha, K.**, **Iwig, J. S.**, **Eckert, B.**, **Hyodo, M.**, **Hayakawa, Y.** and **Vance, R. E.** (2011) 'STING is a direct innate immune sensor of cyclic di-GMP', *Nature*. Nature Publishing Group, 478(7370), pp. 515–518, doi:10.1038/nature10429.

Carlos, T. S., **Young, D. F.**, **Schneider, M.**, **Simas, J. P.** and **Randall, R. E.** (2009) 'Parainfluenza virus 5 genomes are located in viral cytoplasmic bodies whilst the virus dismantles the interferon-induced antiviral state of cells', *Journal of General Virology*, 90(9), pp. 2147–2156, doi:10.1099/vir.0.012047-0.

Cate, J. H. D. (2017) 'Human eIF3: from "blobology" to biological insight.', *Philosophical transactions of the Royal Society of London. Series B, Biological sciences*, 372(1716), doi:10.1098/rstb.2016.0176.

Chavali, P. L., **Stojic, L.**, **Meredith, L. W.**, **Joseph, N.**, **Nahorski, M. S.**, **Sanford, T. J.**, **Sweeney, T. R.**, **Krishna, B. A.**, **Hosmillo, M.**, **Firth, A. E.**, **Bayliss, R.**, **Marcelis, C. L.**, **Lindsay, S.**, **Goodfellow, I.**, **Woods, C. G.** and **Gergely, F.** (2017) 'Neurodevelopmental protein Musashi-1 interacts with the Zika genome and promotes viral replication.', *Science (New York, N.Y.)*,

357(6346), pp. 83–88, doi:10.1126/science.aam9243.

Chebath, J., **Merlin, G.**, **Metz, R.**, **Benech, P.** and **Revel, M.** (1983) 'Interferon-induced 56,000 Mr protein and its mRNA in human cells: molecular cloning and partial sequence of the cDNA.', *Nucleic Acids Research*, 11(5), pp. 1213–26, doi:10.1093/nar/11.5.1213.

Chen, L., **Liu, S.**, **Xu, F.**, **Kong, Y.**, **Wan, L.**, **Zhang, Y.** and **Zhang, Z.** (2017) 'Inhibition of Proteasome Activity Induces Aggregation of IFIT2 in the Centrosome and Enhances IFIT2-Induced Cell Apoptosis', *International Journal of Biological Sciences*, 13(3), pp. 383–390, doi:10.7150/ijbs.17236.

Cho, H., **Shrestha, B.**, **Sen, G. C.** and **Diamond, M. S.** (2013) 'A role for Ifit2 in restricting West Nile virus infection in the brain.', *Journal of virology*, 87(15), pp. 8363–71, doi:10.1128/jvi.01097-13.

Cho, S., **Cheng, T.** and **Kazazian, H. H.** (1978) 'Characterization of 5'-terminal methylation of human alpha- and beta-globin mRNAs.', *The Journal of biological chemistry*, 253(16), pp. 5558–61.

Cleaves, G. R. and **Dubin, D. T.** (1979) 'Methylation status of intracellular dengue type 2 40 S RNA.', *Virology*, 96(1), pp. 159–65, doi:10.1016/0042-6822(79)90181-8.

Coley, S. E., **Lavi, E.**, **Sawicki, S. G.**, **Fu, L.**, **Schelle, B.**, **Karl, N.**, **Siddell, S. G.** and **Thiel, V.** (2005) 'Recombinant Mouse Hepatitis Virus Strain A59 from Cloned, Full-Length cDNA Replicates to High Titers In Vitro and Is Fully Pathogenic In Vivo', *Journal of Virology*, 79(5), pp. 3097–3106, doi:10.1128/jvi.79.5.3097-3106.2005.

Colonno, R. J. and **Pang, R. H. L.** (1982) 'Induction of unique mRNAs by human interferons.', *The Journal of Biological Chemistry*, 257(16), pp. 9234–7.

Cowling, V. H. (2010) 'Regulation of mRNA cap methylation', *Biochemical Journal*, 425(2), pp. 295–302, doi:10.1042/bj20091352.

Crooks, G. E., **Hon, G.**, **Chandonia, J.** and **Brenner, S. E.** (2004) 'WebLogo: a sequence logo generator.', *Genome Research*, 14(6), pp. 1188–90, doi:10.1101/gr.849004.

D'Andrea, L. D. and **Regan, L.** (2003) 'TPR proteins: the versatile helix.', *Trends in Biochemical Sciences*, 28(12), pp. 655–62, doi:10.1016/j.tibs.2003.10.007.

Daffis, S., **Samuel, M. A.**, **Keller, B. C.**, **Gale, M.** and **Diamond, M. S.** (2007) 'Cell-Specific IRF-3 Responses Protect against West Nile Virus Infection by Interferon-Dependent and -Independent Mechanisms', *PLoS Pathogens*, 3(7), p. e106, doi:10.1371/journal.ppat.0030106.

Daffis, S., **Szretter, K. J.**, **Schriewer, J.**, **Li, J.**, **Youn, S.**, **Errett, J.**, **Lin, T.-Y. Y.**, **Schneller, S.**, **Zust, R.**, **Dong, H.**, **Thiel, V.**, **Sen, G. C.**, **Fensterl, V.**, **Klimstra, W. B.**, **Pierson, T. C.**, **Buller, R. M.**, **Gale Jr, M.**, ... **Diamond, M. S.** (2010) '2'-O methylation of the viral mRNA cap evades host restriction by IFIT family members', *Nature*. Nature Publishing Group, 468(7322), pp. 452–456, doi:10.1038/nature09489.

Dai, Q., **Moshitch-Moshkovitz, S.**, **Han, D.**, **Kol, N.**, **Amariglio, N.**, **Rechavi, G.**, **Dominissini, D.** and **He, C.** (2017) 'Nm-seq maps 2'-O-methylation sites in human mRNA with base precision', *Nature Methods*, 14(7), pp. 695–698, doi:10.1038/nmeth.4294.

Das, A. K., **Cohen, P. W.** and **Barford, D.** (1998) 'The structure of the tetratricopeptide repeats of protein phosphatase 5: implications for TPR-mediated protein-protein interactions.', *The EMBO*

journal, 17(5), pp. 1192–9, doi:10.1093/emboj/17.5.1192.

Daugherty, M. D., **Schaller, A. M.**, **Geballe, A. P.** and **Malik, H. S.** (2016) 'Evolution-guided functional analyses reveal diverse antiviral specificities encoded by IFIT1 genes in mammals', *eLife*, 5, pp. 1–22, doi:10.7554/elife.14228.

Der, S. D., **Zhou, A.**, **Williams, B. R.** and **Silverman, R. H.** (1998) 'Identification of genes differentially regulated by interferon alpha, beta, or gamma using oligonucleotide arrays.', *Proceedings of the National Academy of Sciences of the United States of America*, 95(26), pp. 15623–8, doi:10.1073/pnas.95.26.15623.

Devarkar, S. C., **Wang, C.**, **Miller, M. T.**, **Ramanathan, A.**, **Jiang, F.**, **Khan, A. G.**, **Patel, S. S.** and **Marcotrigiano, J.** (2016) 'Structural basis for m7G recognition and 2′-O-methyl discrimination in capped RNAs by the innate immune receptor RIG-I', *Proceedings of the National Academy of Sciences*, 113(3), pp. 596–601, doi:10.1073/pnas.1515152113.

Diamond, M. S. and **Farzan, M.** (2013) 'The broad-spectrum antiviral functions of IFIT and IFITM proteins', *Nature Reviews Immunology*. Nature Publishing Group, 13(1), pp. 46–57, doi:10.1038/nri3344.

Dolinsky, T. J., **Nielsen, J. E.**, **McCammon, J. A.** and **Baker, N. A.** (2004) 'PDB2PQR: an automated pipeline for the setup of Poisson-Boltzmann electrostatics calculations.', *Nucleic Acids Research*, 32(Web Server issue), pp. W665-7, doi:10.1093/nar/gkh381.

Donnelly, M. L. L., **Luke, G.**, **Mehrotra, A.**, **Li, X.**, **Hughes, L. E.**, **Gani, D.** and **Ryan, M. D.** (2001) 'Analysis of the aphthovirus 2A/2B polyprotein "cleavage" mechanism indicates not a proteolytic reaction, but a novel translational effect: A putative ribosomal "skip"', *Journal of General Virology*, 82(5), pp. 1013–1025, doi:10.1099/0022-1317-82-5-1013.

Dörner, T. and **Radbruch, A.** (2007) 'Antibodies and B Cell Memory in Viral Immunity', *Immunity*, 27(3), pp. 384–392, doi:10.1016/j.immuni.2007.09.002.

Douam, F., **Soto Albrecht, Y. E.**, **Hrebikova, G.**, **Sadimin, E.**, **Davidson, C.**, **Kotenko, S. V** and **Ploss, A.** (2017) 'Type III Interferon-Mediated Signaling Is Critical for Controlling Live Attenuated Yellow Fever Virus Infection In Vivo.', *mBio*, 8(4), pp. 1–22, doi:10.1128/mbio.00819-17.

Dubin, D. T. and **Stollar, V.** (1975) 'Methylation of sindbis virus "26S" messenger RNA', *Biochemical and Biophysical Research Communications*, 66(4), pp. 1373–1379, doi:10.1016/0006-291x(75)90511-2.

Edgar, R. C. (2004) 'MUSCLE: multiple sequence alignment with high accuracy and high throughput.', *Nucleic Acids Research*, 32(5), pp. 1792–7, doi:10.1093/nar/gkh340.

Egloff, M.-P., **Decroly, E.**, **Malet, H.**, **Selisko, B.**, **Benarroch, D.**, **Ferron, F.** and **Canard, B.** (2007) 'Structural and Functional Analysis of Methylation and 5′-RNA Sequence Requirements of Short Capped RNAs by the Methyltransferase Domain of Dengue Virus NS5', *Journal of Molecular Biology*, 372(3), pp. 723–736, doi:10.1016/j.jmb.2007.07.005.

Emmott, E. and **Goodfellow, I.** (2014) 'Identification of Protein Interaction Partners in Mammalian Cells Using SILAC-immunoprecipitation Quantitative Proteomics', *Journal of Visualized Experiments*, (89), p. e51656, doi:10.3791/51656.

Feng, F., **Yuan, L.**, **Wang, Y. E.**, **Crowley, C.**, **Lv, Z.**, **Li, J.**, **Liu, Y.**, **Cheng, G.**, **Zeng, S.** and **Liang, H.** (2013) 'Crystal structure and nucleotide selectivity of human IFIT5/ISG58.', *Cell research*, 23(8), pp. 1055–8, doi:10.1038/cr.2013.80.

Feng, Q., **Hato, S. V.**, **Langereis, M. A.**, **Zoll, J.**, **Virgen-Slane, R.**, **Peisley, A.**, **Hur, S.**, **Semler, B. L.**, **van Rij, R. P.** and **van Kuppeveld, F. J. M.** (2012) 'MDA5 detects the double-stranded RNA replicative form in picornavirus-infected cells.', *Cell reports*, 2(5), pp. 1187–96, doi:10.1016/j.celrep.2012.10.005.

Feng, X., **Wang, Y.**, **Ma, Z.**, **Yang, R.**, **Liang, S.**, **Zhang, M.**, **Song, S.**, **Li, S.**, **Liu, G.**, **Fan, D.** and **Gao, S.** (2014) 'MicroRNA-645, up-regulated in human adencarcinoma of gastric esophageal junction, inhibits apoptosis by targeting tumor suppressor IFIT2', *BMC Cancer*, 14(1), pp. 1–12, doi:10.1186/1471-2407-14-633.

Fensterl, V., **White, C. L.**, **Yamashita, M.** and **Sen, G. C.** (2008) 'Novel Characteristics of the Function and Induction of Murine p56 Family Proteins', *Journal of Virology*, 82(22), pp. 11045–11053, doi:10.1128/jvi.01593-08.

Fensterl, V. and **Sen, G. C.** (2011) 'The *ISG56/IFIT1* Gene Family', *Journal of Interferon & Cytokine Research*, 31(1), pp. 71–78, doi:10.1089/jir.2010.0101.

Fensterl, V., **Wetzel, J. L.**, **Ramachandran, S.**, **Ogino, T.**, **Stohlman, S. A.**, **Bergmann, C. C.**, **Diamond, M. S.**, **Virgin, H. W.** and **Sen, G. C.** (2012) 'Interferon-Induced Ifit2/ISG54 Protects Mice from Lethal VSV Neuropathogenesis', *PLoS Pathogens*. Edited by J. Hiscott, 8(5), p. e1002712, doi:10.1371/journal.ppat.1002712.

Fensterl, V. and **Sen, G. C.** (2015) 'Interferon-Induced Ifit Proteins: Their Role in Viral Pathogenesis', *Journal of Virology*. Edited by S. P. Goff, 89(5), pp. 2462–2468, doi:10.1128/jvi.02744-14.

Ferguson, B. J., **Benfield, C. T. O.**, **Ren, H.**, **Lee, V. H.**, **Frazer, G. L.**, **Strnadova, P.**, **Sumner, R. P.** and **Smith, G. L.** (2013) 'Vaccinia virus protein N2 is a nuclear IRF3 inhibitor that promotes virulence.', *The Journal of general virology*, 94(Pt 9), pp. 2070–81, doi:10.1099/vir.0.054114-0.

Fleith, R. C., **Mears, H. V**, **Leong, X. Y.**, **Sanford, T. J.**, **Emmott, E.**, **Graham, S. C.**, **Mansur, D. S.** and **Sweeney, T. R.** (2018) 'IFIT3 and IFIT2/3 promote IFIT1-mediated translation inhibition by enhancing binding to non-self RNA', *Nucleic Acids Research*, 46(10), pp. 5269–5285, doi:10.1093/nar/gky191.

Gebhard, L. G., **Filomatori, C. V.** and **Gamarnik, A. V.** (2011) 'Functional RNA elements in the dengue virus genome.', *Viruses*, 3(9), pp. 1739–56, doi:10.3390/v3091739.

Gouy, M., **Guindon, S.** and **Gascuel, O.** (2010) 'SeaView version 4: A multiplatform graphical user interface for sequence alignment and phylogenetic tree building.', *Molecular Biology and Evolution*, 27(2), pp. 221–4, doi:10.1093/molbev/msp259.

Grandvaux, N., **Servant, M. J.**, **TenOever, B.**, **Sen, G. C.**, **Balachandran, S.**, **Barber, G. N.**, **Lin, R.** and **Hiscott, J.** (2002) 'Transcriptional Profiling of Interferon Regulatory Factor 3 Target Genes: Direct Involvement in the Regulation of Interferon-Stimulated Genes', *Journal of Virology*, 76(11), pp. 5532–5539, doi:10.1128/jvi.76.11.5532-5539.2002.

Gross, J. D., **Moerke, N. J.**, **von der Haar, T.**, **Lugovskoy, A. A.**, **Sachs, A. B.**, **McCarthy, J. E. G.** and **Wagner, G.** (2003) 'Ribosome loading onto the mRNA cap is driven by conformational coupling between eIF4G and eIF4E.', *Cell*, 115(6), pp. 739–50, doi:10.1016/s0092-8674(03)00975-9.

Grüner, S., **Peter, D.**, **Weber, R.**, **Wohlbold, L.**, **Chung, M.-Y.**, **Weichenrieder, O.**, **Valkov, E.**, **Igreja, C.** and **Izaurralde, E.** (2016) 'The Structures of eIF4E-eIF4G Complexes Reveal an Extended Interface to Regulate Translation Initiation.', *Molecular cell*, 64(3), pp. 467–479, doi:10.1016/j.molcel.2016.09.020.

Guindon, S., **Dufayard, J.-F.**, **Lefort, V.**, **Anisimova, M.**, **Hordijk, W.** and **Gascuel, O.** (2010) 'New algorithms and methods to estimate maximum-likelihood phylogenies: assessing the performance of PhyML 3.0.', *Systematic Biology*, 59(3), pp. 307–21, doi:10.1093/sysbio/syq010.

Guinn, Z., **Brown, D. M.** and **Petro, T. M.** (2017) 'Activation of IRF3 contributes to IFN-γ and ISG54 expression during the immune responses to B16F10 tumor growth.', *International immunopharmacology*, 50, pp. 121–129, doi:10.1016/j.intimp.2017.06.016.

Guo, J., **Peters, K. L.** and **Sen, G. C.** (2000a) 'Induction of the human protein P56 by interferon, double-stranded RNA, or virus infection', *Virology*, 267(2), pp. 209–219, doi:10.1006/viro.1999.0135.

Guo, J., **Hui, D. J.**, **Merrick, W. C.** and **Sen, G. C.** (2000b) 'A new pathway of translational regulation mediated by eukaryotic initiation factor 3.', *The EMBO Journal*, 19(24), pp. 6891–9, doi:10.1093/emboj/19.24.6891.

Guo, J. and **Sen, G. C.** (2000) 'Characterization of the interaction between the interferon-induced protein P56 and the Int6 protein encoded by a locus of insertion of the mouse mammary tumor virus.', *Journal of Virology*, 74(4), pp. 1892–9, doi:10.1128/jvi.74.4.1892-1899.2000.

Habjan, M., **Hubel, P.**, **Lacerda, L.**, **Benda, C.**, **Holze, C.**, **Eberl, C. H.**, **Mann, A.**, **Kindler, E.**, **Gil-Cruz, C.**, **Ziebuhr, J.**, **Thiel, V.** and **Pichlmair, A.** (2013) 'Sequestration by IFIT1 Impairs Translation of 2′O-unmethylated Capped RNA', *PLoS Pathogens*, 9(10), p. e1003663, doi:10.1371/journal.ppat.1003663.

Haque, Z. Z. and **Aryana, K. J.** (2002) 'Effect of Copper, Iron, Zinc and Magnesium Ions on Bovine Serum Albumin Gelation', *Food Science and Technology Research*, 8(1), pp. 1–3, doi:10.3136/fstr.8.1.

Harwig, A., **Landick, R.** and **Berkhout, B.** (2017) 'The battle of RNA synthesis: Virus versus host', *Viruses*, 9(10), pp. 1–18, doi:10.3390/v9100309.

Hashimoto, S. I. and **Green, M.** (1976) 'Multiple methylated cap sequences in adenovirus type 2 early mRNA.', *Journal of virology*, 20(2), pp. 425–35.

Heckle, W. L., **Fenton, R. G.**, **Wood, T. G.**, **Merkel, C. G.** and **Lingrel, J. B.** (1977) 'Methylated nucleosides in globin mRNA from mouse nucleated erythroid cells.', *The Journal of Biological Chemistry*, 252(5), pp. 1764–70.

Hefti, E., **Bishop, D. H.**, **Dubin, D. T.** and **Stollar, V.** (1975) '5' nucleotide sequence of sindbis viral RNA.', *Journal of Virology*, 17(1), pp. 149–59.

Henras, A. K., **Plisson-Chastang, C.**, **O'Donohue, M. F.**, **Chakraborty, A.** and **Gleizes, P. E.** (2015) 'An overview of pre-ribosomal RNA processing in eukaryotes', *Wiley Interdisciplinary*

Reviews: RNA, 6(2), pp. 225–242, doi:10.1002/wrna.1269.

Hinnebusch, A. G. (2017) 'Structural Insights into the Mechanism of Scanning and Start Codon Recognition in Eukaryotic Translation Initiation.', *Trends in biochemical sciences*, 42(8), pp. 589–611, doi:10.1016/j.tibs.2017.03.004.

Hou, Z., **Zhang, J.**, **Han, Q.**, **Su, C.**, **Qu, J.**, **Xu, D.**, **Zhang, C.** and **Tian, Z.** (2016) 'Hepatitis B virus inhibits intrinsic RIG-I and RIG-G immune signaling via inducing miR146a', *Scientific Reports*, 6(1), p. 26150, doi:10.1038/srep26150.

Hsu, Y.-L., **Shi, S.-F.**, **Wu, W.-L.**, **Ho, L.-J.** and **Lai, J.-H.** (2013) 'Protective roles of interferon-induced protein with tetratricopeptide repeats 3 (IFIT3) in dengue virus infection of human lung epithelial cells.', *PloS one*, 8(11), p. e79518, doi:10.1371/journal.pone.0079518.

Hu, W., **Niu, G.**, **Li, H.**, **Gao, H.**, **Kang, R.**, **Chen, X.** and **Lin, L.** (2016) 'The association between expression of IFIT1 in podocytes of MRL/lpr mice and the renal pathological changes it causes: An animal study.', *Oncotarget*, 7(47), pp. 76464–76470, doi:10.18632/oncotarget.13045.

Huang, C., **Lewis, C.**, **Borg, N. A.**, **Canals, M.**, **Diep, H.**, **Drummond, G. R.**, **Goode, R. J.**, **Schittenhelm, R. B.**, **Vinh, A.**, **Zhu, M.**, **Kemp-Harper, B.**, **Kleifeld, O.** and **Stone, M. J.** (2018) 'Proteomic Identification of Interferon-Induced Proteins with Tetratricopeptide Repeats as Markers of M1 Macrophage Polarization.', *Journal of proteome research*, 17(4), pp. 1485–1499, doi:10.1021/acs.jproteome.7b00828.

Huang, X., **Shen, N.**, **Bao, C.**, **Gu, Y.**, **Wu, L.** and **Chen, S.** (2008) 'Interferon-induced protein IFIT4 is associated with systemic lupus erythematosus and promotes differentiation of monocytes into dendritic cell-like cells', *Arthritis Research and Therapy*, 10(4), p. R91, doi:10.1186/ar2475.

Hui, D. J., **Bhasker, C. R.**, **Merrick, W. C.** and **Sen, G. C.** (2003) 'Viral Stress-inducible Protein p56 Inhibits Translation by Blocking the Interaction of eIF3 with the Ternary Complex eIF2·GTP·Met-tRNA i', *Journal of Biological Chemistry*, 278(41), pp. 39477–39482, doi:10.1074/jbc.m305038200.

Hui, D. J., **Terenzi, F.**, **Merrick, W. C.** and **Sen, G. C.** (2005) 'Mouse p56 Blocks a Distinct Function of Eukaryotic Initiation Factor 3 in Translation Initiation', *Journal of Biological Chemistry*, 280(5), pp. 3433–3440, doi:10.1074/jbc.m406700200.

Hwang, J., **Sato, H.**, **Tang, Y.**, **Matsuda, D.** and **Maquat, L. E.** (2010) 'UPF1 association with the cap-binding protein, CBP80, promotes nonsense-mediated mRNA decay at two distinct steps.', *Molecular Cell*, 39(3), pp. 396–409, doi:10.1016/j.molcel.2010.07.004.

Hyde, J. L., **Gardner, C. L.**, **Kimura, T.**, **White, J. P.**, **Liu, G.**, **Trobaugh, D. W.**, **Huang, C.**, **Tonelli, M.**, **Paessler, S.**, **Takeda, K.**, **Klimstra, W. B.**, **Amarasinghe, G. K.** and **Diamond, M. S.** (2014) 'A viral RNA structural element alters host recognition of nonself RNA.', *Science*, 343(6172), pp. 783–7, doi:10.1126/science.1248465.

Imaizumi, T., **Murakami, K.**, **Ohta, K.**, **Seki, H.**, **Matsumiya, T.**, **Meng, P.**, **Hayakari, R.**, **Xing, F.**, **Aizawa-Yashiro, T.**, **Tatsuta, T.**, **Yoshida, H.** and **Kijima, H.** (2013) 'MDA5 and ISG56 mediate CXCL10 expression induced by Toll-like receptor 4 activation in U373MG human astrocytoma cells', *Neuroscience Research*. Elsevier Ireland Ltd and Japan Neuroscience Society, 76(4), pp. 195–206,

doi:10.1016/j.neures.2013.05.002.

Imaizumi, T., **Numata, A.**, **Yano, C.**, **Yoshida, H.**, **Meng, P.**, **Hayakari, R.**, **Xing, F.**, **Wang, L.**, **Matsumiya, T.**, **Tanji, K.**, **Tatsuta, T.**, **Murakami, M.** and **Tanaka, H.** (2014) 'ISG54 and ISG56 are induced by TLR3 signaling in U373MG human astrocytoma cells: Possible involvement in CXCL10 expression', *Neuroscience Research*. Elsevier Ireland Ltd and Japan Neuroscience Society, 84, pp. 34–42, doi:10.1016/j.neures.2014.03.001.

Imaizumi, T., **Yoshida, H.**, **Hayakari, R.**, **Xing, F.**, **Wang, L.**, **Matsumiya, T.**, **Tanji, K.**, **Kawaguchi, S.**, **Murakami, M.** and **Tanaka, H.** (2016) 'Interferon-stimulated gene (ISG) 60, as well as ISG56 and ISG54, positively regulates TLR3/IFN-β/STAT1 axis in U373MG human astrocytoma cells', *Neuroscience Research*. Elsevier Ireland Ltd and Japan Neuroscience Society, 105, pp. 35–41, doi:10.1016/j.neures.2015.09.002.

Irigoyen, N., **Firth, A. E.**, **Jones, J. D.**, **Chung, B. Y. W.**, **Siddell, S. G.** and **Brierley, I.** (2016) 'High-Resolution Analysis of Coronavirus Gene Expression by RNA Sequencing and Ribosome Profiling.', *PLoS pathogens*, 12(2), p. e1005473, doi:10.1371/journal.ppat.1005473.

Isaacs, A. and **Lindenmann, J.** (1957) 'Virus interference. I. The interferon.', *Proceedings of the Royal Society of London. Series B, Biological sciences*, 147(927), pp. 258–67, doi:10.1089/jir.1987.7.429.

Ishida, Y., **Kakuni, M.**, **Bang, B.-R.**, **Sugahara, G.**, **Lau, D. T.-Y.**, **Tateno-Mukaidani, C.**, **Li, M.**, **Gale, M.** and **Saito, T.** (2019) 'Hepatic IFN-Induced Protein with Tetratricopeptide Repeats Regulation of HCV Infection.', *Journal of Interferon & Cytokine Research*, 39(3), pp. 133–146, doi:10.1089/jir.2018.0103.

Izaurralde, E., **Lewis, J.**, **McGuigan, C.**, **Jankowska, M.**, **Darzynkiewicz, E.** and **Mattaj, I. W.** (1994) 'A nuclear cap binding protein complex involved in pre-mRNA splicing', *Cell*, 78(4), pp. 657–668, doi:10.1016/0092-8674(94)90530-4.

Jaafar, Z. A., **Oguro, A.**, **Nakamura, Y.** and **Kieft, J. S.** (2016) 'Translation initiation by the hepatitis C virus IRES requires eIF1A and ribosomal complex remodeling.', *eLife*, 23(5), pp. 1–23, doi:10.7554/elife.21198.

Jackson, R. J., **Hellen, C. U. T.** and **Pestova, T. V.** (2010) 'The mechanism of eukaryotic translation initiation and principles of its regulation', *Nature Reviews Molecular Cell Biology*, 11(2), pp. 113–127, doi:10.1038/nrm2838.

Jia, H., **Song, L.**, **Cong, Q.**, **Wang, J.**, **Xu, H.**, **Chu, Y.**, **Li, Q.**, **Zhang, Y.**, **Zou, X.**, **Zhang, C.**, **Chin, Y. E.**, **Zhang, X.**, **Li, Z.**, **Zhu, K.**, **Wang, B.**, **Peng, H.** and **Hou, Z.** (2017) 'The LIM protein AJUBA promotes colorectal cancer cell survival through suppression of JAK1/STAT1/IFIT2 network', *Oncogene*, 36(19), pp. 2655–2666, doi:10.1038/onc.2016.418.

Jiang, Z., **Su, C.** and **Zheng, C.** (2016) 'Herpes Simplex Virus 1 Tegument Protein UL41 Counteracts IFIT3 Antiviral Innate Immunity', *Journal of Virology*, 90(24), pp. 11056–11061, doi:10.1128/jvi.01672-16.

John, S. P., **Sun, J.**, **Carlson, R. J.**, **Cao, B.**, **Bradfield, C. J.**, **Song, J.**, **Smelkinson, M.** and **Fraser, I. D. C.** (2018) 'IFIT1 Exerts Opposing Regulatory Effects on the Inflammatory and Interferon Gene

Programs in LPS-Activated Human Macrophages', *Cell Reports*, 25(1), pp. 95-106.e6, doi:10.1016/j.celrep.2018.09.002.

Johnson, B., **VanBlargan, L. A.**, **Xu, W.**, **White, J. P.**, **Shan, C.**, **Shi, P.-Y.**, **Zhang, R.**, **Adhikari, J.**, **Gross, M. L.**, **Leung, D. W.**, **Diamond, M. S.** and **Amarasinghe, G. K.** (2018) 'Human IFIT3 Modulates IFIT1 RNA Binding Specificity and Protein Stability', *Immunity*, 48(3), pp. 487-499.e5, doi:10.1016/j.immuni.2018.01.014.

Kashiwagi, K., **Ito, T.** and **Yokoyama, S.** (2017) 'Crystal structure of eIF2B and insights into eIF2-eIF2B interactions.', *The FEBS Journal*, 284(6), pp. 868–874, doi:10.1111/febs.13896.

Katibah, G. E., **Lee, H. J.**, **Huizar, J. P.**, **Vogan, J. M.**, **Alber, T.** and **Collins, K.** (2013) 'tRNA binding, structure, and localization of the human interferon-induced protein IFIT5.', *Molecular Cell*, 49(4), pp. 743–50, doi:10.1016/j.molcel.2012.12.015.

Katibah, G. E., **Qin, Y.**, **Sidote, D. J.**, **Yao, J.**, **Lambowitz, A. M.** and **Collins, K.** (2014) 'Broad and adaptable RNA structure recognition by the human interferon-induced tetratricopeptide repeat protein IFIT5', *Proceedings of the National Academy of Sciences*, 111(33), pp. 12025–12030, doi:10.1073/pnas.1412842111.

Kawasaki, T. and **Kawai, T.** (2014) 'Toll-like receptor signaling pathways.', *Frontiers in Immunology*, 5(5625), p. 461, doi:10.3389/fimmu.2014.00461.

Kieft, J. S., **Zhou, K.**, **Jubin, R.** and **Doudna, J. A.** (2001) 'Mechanism of ribosome recruitment by hepatitis C IRES RNA.', *RNA*, 7(2), pp. 194–206, doi:10.1017/s1355838201001790.

Kimura, T., **Katoh, H.**, **Kayama, H.**, **Saiga, H.**, **Okuyama, M.**, **Okamoto, T.**, **Umemoto, E.**, **Matsuura, Y.**, **Yamamoto, M.** and **Takeda, K.** (2013) 'Ifit1 Inhibits Japanese Encephalitis Virus Replication through Binding to 5' Capped 2'-O Unmethylated RNA', *Journal of Virology*, 87(18), pp. 9997–10003, doi:10.1128/jvi.00883-13.

Konarska, M. M., **Padgett, R. A.** and **Sharp, P. A.** (1984) 'Recognition of cap structure in splicing in vitro of mRNA precursors', *Cell*, 38(3), pp. 731–736, doi:10.1016/0092-8674(84)90268-x.

Kondili, M., **Roux, M.**, **Vabret, N.** and **Bailly-Bechet, M.** (2016) 'Innate immune system activation by viral RNA: How to predict it?', *Virology*. Elsevier, 488, pp. 169–78, doi:10.1016/j.virol.2015.11.007.

Koonin, E. V. and **Moss, B.** (2010) 'Viruses know more than one way to don a cap.', *Proceedings of the National Academy of Sciences of the United States of America*, 107(8), pp. 3283–4, doi:10.1073/pnas.0915061107.

Korneeva, N. L., **Lamphear, B. J.**, **Hennigan, F. L. C.** and **Rhoads, R. E.** (2000) 'Mutually cooperative binding of eukaryotic translation initiation factor (eIF) 3 and eIF4A to human eIF4G-1.', *The Journal of Biological Chemistry*, 275(52), pp. 41369–76, doi:10.1074/jbc.m007525200.

Kotenko, S. V., **Gallagher, G.**, **Baurin, V. V.**, **Lewis-Antes, A.**, **Shen, M.**, **Shah, N. K.**, **Langer, J. A.**, **Sheikh, F.**, **Dickensheets, H.** and **Donnelly, R. P.** (2003) 'IFN-lambdas mediate antiviral protection through a distinct class II cytokine receptor complex.', *Nature Immunology*, 4(1), pp. 69–77, doi:10.1038/ni875.

Kowalinski, E., **Lunardi, T.**, **McCarthy, A. A.**, **Louber, J.**, **Brunel, J.**, **Grigorov, B.**, **Gerlier, D.**

and **Cusack, S.** (2011) 'Structural Basis for the Activation of Innate Immune Pattern-Recognition Receptor RIG-I by Viral RNA', *Cell*. Elsevier Inc., 147(2), pp. 423–435, doi:10.1016/j.cell.2011.09.039.

Kumar, B. V., **Connors, T. J.** and **Farber, D. L.** (2018) 'Human T Cell Development, Localization, and Function throughout Life', *Immunity*. Elsevier Inc., 48(2), pp. 202–213, doi:10.1016/j.immuni.2018.01.007.

Kumar, P., **Hellen, C. U. T.** and **Pestova, T. V.** (2016) 'Toward the mechanism of eIF4F-mediated ribosomal attachment to mammalian capped mRNAs', *Genes & Development*, 30(13), pp. 1573–1588, doi:10.1101/gad.282418.116.

Kumar, P., **Sweeney, T. R.**, **Skabkin, M. a**, **Skabkina, O. V**, **Hellen, C. U. T.** and **Pestova, T. V** (2014) 'Inhibition of translation by IFIT family members is determined by their ability to interact selectively with the 5'-terminal regions of cap0-, cap1- and 5'ppp- mRNAs', *Nucleic Acids Research*, 42(5), pp. 3228–3245, doi:10.1093/nar/gkt1321.

Kusari, J. and **Sen, G. C.** (1986) 'Regulation of synthesis and turnover of an interferon-inducible mRNA.', *Molecular and Cellular Biology*, 6(6), pp. 2062–7, doi:10.1128/mcb.6.6.2062.updated.

Kyrieleis, O. J. P., **Chang, J.**, **de la Peña, M.**, **Shuman, S.** and **Cusack, S.** (2014) 'Crystal Structure of Vaccinia Virus mRNA Capping Enzyme Provides Insights into the Mechanism and Evolution of the Capping Apparatus', *Structure*, 22(3), pp. 452–465, doi:10.1016/j.str.2013.12.014.

Lai, K. C., **Liu, C. J.**, **Chang, K. W.** and **Lee, T. C.** (2013) 'Depleting IFIT2 mediates atypical PKC signaling to enhance the migration and metastatic activity of oral squamous cell carcinoma cells', *Oncogene*, 32(32), pp. 3686–3697, doi:10.1038/onc.2012.384.

Lama, D., **Pradhan, M. R.**, **Brown, C. J.**, **Eapen, R. S.**, **Joseph, T. L.**, **Kwoh, C.-K.**, **Lane, D. P.** and **Verma, C. S.** (2017) 'Water-Bridge Mediates Recognition of mRNA Cap in eIF4E.', *Structure*, 25(1), pp. 188–194, doi:10.1016/j.str.2016.11.006.

Langberg, S. R. and **Moss, B.** (1981) 'Post-transcriptional modifications of mRNA. Purification and characterization of cap I and cap II RNA (nucleoside-2'-)-methyltransferases from HeLa cells.', *The Journal of Biological Chemistry*, 256(19), pp. 10054–60.

Lee, A. S. Y., **Kranzusch, P. J.**, **Doudna, J. A.** and **Cate, J. H. D.** (2016) 'eIF3d is an mRNA cap-binding protein that is required for specialized translation initiation', *Nature*, 536(7614), pp. 96–99, doi:10.1038/nature18954.

LeFebvre, A. K., **Korneeva, N. L.**, **Trutschl, M.**, **Cvek, U.**, **Duzan, R. D.**, **Bradley, C. A.**, **Hershey, J. W. B.** and **Rhoads, R. E.** (2006) 'Translation initiation factor eIF4G-1 binds to eIF3 through the eIF3e subunit', *Journal of Biological Chemistry*, 281(32), pp. 22917–22932, doi:10.1074/jbc.m605418200.

Levy, D., **Larner, A.**, **Chaudhuri, A.**, **Babiss, L. E.** and **Darnell, J. E.** (1986) 'Interferon-stimulated transcription: isolation of an inducible gene and identification of its regulatory region.', *Proceedings of the National Academy of Sciences of the United States of America*, 83(23), pp. 8929–33, doi:10.1073/pnas.83.23.8929.

Lewis, J. D. and **Izaurralde, E.** (1997) 'The role of the cap structure in RNA processing and nuclear export', *European Journal of Biochemistry*, 247(2), pp. 461–469, doi:10.1111/j.1432-1033.1997.00461.x.

Li, J.-J., **Wang, Y.**, **Yang, C.-W.**, **Ran, J.-S.**, **Jiang, X.-S.**, **Du, H.-R.**, **Hu, Y.-D.** and **Liu, Y.-P.** (2017) 'Genotypes of IFIH1 and IFIT5 in seven chicken breeds indicated artificial selection for commercial traits influenced antiviral genes.', *Infection, Genetics and Evolution*, 56, pp. 54–61, doi:10.1016/j.meegid.2017.10.019.

Li, S.-H., **Dong, H.**, **Li, X.-F.**, **Xie, X.**, **Zhao, H.**, **Deng, Y.-Q.**, **Wang, X.-Y.**, **Ye, Q.**, **Zhu, S.-Y.**, **Wang, H.-J.**, **Zhang, B.**, **Leng, Q.-B.**, **Zuest, R.**, **Qin, E.-D.**, **Qin, C.-F.** and **Shi, P.-Y.** (2013) 'Rational Design of a Flavivirus Vaccine by Abolishing Viral RNA 2'-O Methylation', *Journal of Virology*, 87(10), pp. 5812–5819, doi:10.1128/jvi.02806-12.

Li, Y., **Li, C.**, **Xue, P.**, **Zhong, B.**, **Mao, A.**, **Ran, Y.**, **Chen, H.**, **Wang, Y.**, **Yang, F.** and **Shu, H.-B.** (2009) 'ISG56 is a negative-feedback regulator of virus-triggered signaling and cellular antiviral response.', *Proceedings of the National Academy of Sciences of the United States of America*, 106(19), pp. 7945–50, doi:10.1073/pnas.0900818106.

Liu, J. and **Jia, G.** (2014) 'Methylation Modifications in Eukaryotic Messenger RNA', *Journal of Genetics and Genomics*. Elsevier Limited and Science Press, 41(1), pp. 21–33, doi:10.1016/j.jgg.2013.10.002.

Liu, X.-Y. X.-Y., **Chen, W.**, **Wei, B. B.**, **Shan, Y.-F.** and **Wang, C.** (2011) 'IFN-Induced TPR Protein IFIT3 Potentiates Antiviral Signaling by Bridging MAVS and TBK1', *The Journal of Immunology*, 187(5), pp. 2559–2568, doi:10.4049/jimmunol.1100963.

Liu, Y., **Zhang, Y.-B.**, **Liu, T.-K.** and **Gui, J.-F.** (2013) 'Lineage-Specific Expansion of IFIT Gene Family: An Insight into Coevolution with IFN Gene Family', *PLoS ONE*, 8(6), p. e66859, doi:10.1371/journal.pone.0066859.

Liu, Z., **Chen, O.**, **Wall, J. B. J.**, **Zheng, M.**, **Zhou, Y.**, **Wang, L.**, **Ruth Vaseghi, H.**, **Qian, L.** and **Liu, J.** (2017) 'Systematic comparison of 2A peptides for cloning multi-genes in a polycistronic vector.', *Scientific reports*, 7(1), p. 2193, doi:10.1038/s41598-017-02460-2.

Loo, Y.-M. and **Gale, M.** (2011) 'Immune signaling by RIG-I-like receptors.', *Immunity*, 34(5), pp. 680–92, doi:10.1016/j.immuni.2011.05.003.

Ma, X., **Helgason, E.**, **Phung, Q. T.**, **Quan, C. L.**, **Iyer, R. S.**, **Lee, M. W.**, **Bowman, K. K.**, **Starovasnik, M. A.** and **Dueber, E. C.** (2012) 'Molecular basis of Tank-binding kinase 1 activation by transautophosphorylation.', *Proceedings of the National Academy of Sciences of the United States of America*, 109(24), pp. 9378–83, doi:10.1073/pnas.1121552109.

Magor, K. E., **Miranzo Navarro, D.**, **Barber, M. R. W.**, **Petkau, K.**, **Fleming-Canepa, X.**, **Blyth, G. A. D.** and **Blaine, A. H.** (2013) 'Defense genes missing from the flight division', *Developmental & Comparative Immunology*. Elsevier Ltd, 41(3), pp. 377–388, doi:10.1016/j.dci.2013.04.010.

Maquat, L. E., **Tarn, W.-Y.** and **Isken, O.** (2010) 'The pioneer round of translation: features and functions.', *Cell*, 142(3), pp. 368–74, doi:10.1016/j.cell.2010.07.022.

Marintchev, A. and **Wagner, G.** (2005) 'eIF4G and CBP80 share a common origin and similar domain organization: Implications for the structure and function of eIF4G', *Biochemistry*, 44(37), pp. 12265–12272, doi:10.1021/bi051271v.

Mazza, C., **Ohno, M.**, **Segref, A.**, **Mattaj, I. W.** and **Cusack, S.** (2001) 'Crystal structure of the

human nuclear cap binding complex', *Molecular Cell*, 8(2), pp. 383–396, doi:10.1016/s1097-2765(01)00299-4.

McCartney, S. A., **Thackray, L. B.**, **Gitlin, L.**, **Gilfillan, S.**, **Virgin, H. W.**, **Virgin Iv, H. W.** and **Colonna, M.** (2008) 'MDA-5 recognition of a murine norovirus.', *PLoS pathogens*, 4(7), p. e1000108, doi:10.1371/journal.ppat.1000108.

McCracken, S., **Fong, N.**, **Rosonina, E.**, **Yankulov, K.**, **Brothers, G.**, **Siderovski, D.**, **Hessel, A.**, **Foster, S.**, **Shuman, S.** and **Bentley, D. L.** (1997) '5'-Capping enzymes are targeted to pre-mRNA by binding to the phosphorylated carboxy-terminal domain of RNA polymerase II', *Genes and Development*, 11(24), pp. 3306–3318, doi:10.1101/gad.11.24.3306.

McNab, F., **Mayer-Barber, K.**, **Sher, A.**, **Wack, A.** and **O'Garra, A.** (2015) 'Type I interferons in infectious disease', *Nature Reviews Immunology*. Nature Publishing Group, 15(2), pp. 87–103, doi:10.1038/nri3787.

Mears, H. V., **Emmott, E.**, **Chaudhry, Y.**, **Hosmillo, M.**, **Goodfellow, I. G.** and **Sweeney, T. R.** (2019) 'Ifit1 regulates norovirus infection and enhances the interferon response in murine macrophage-like cells', *Wellcome Open Research*, 4, p. 82, doi:10.12688/wellcomeopenres.15223.1.

Mears, H. V and **Sweeney, T. R.** (2018) 'Better together: the role of IFIT protein-protein interactions in the antiviral response.', *The Journal of General Virology*, 99(11), pp. 1463–1477, doi:10.1099/jgv.0.001149.

Menachery, V. D., **Yount, B. L.**, **Josset, L.**, **Gralinski, L. E.**, **Scobey, T.**, **Agnihothram, S.**, **Katze, M. G.** and **Baric, R. S.** (2014) 'Attenuation and restoration of severe acute respiratory syndrome coronavirus mutant lacking 2'-O-methyltransferase activity.', *Journal of virology*, 88(8), pp. 4251–64, doi:10.1128/jvi.03571-13.

Menachery, V. D., **Gralinski, L. E.**, **Mitchell, H. D.**, **Dinnon, K. H.**, **Leist, S. R.**, **Yount, B. L.**, **Graham, R. L.**, **McAnarney, E. T.**, **Stratton, K. G.**, **Cockrell, A. S.**, **Debbink, K.**, **Sims, A. C.**, **Waters, K. M.** and **Baric, R. S.** (2017) 'Middle East Respiratory Syndrome Coronavirus Nonstructural Protein 16 Is Necessary for Interferon Resistance and Viral Pathogenesis', *mSphere*, 2(6), pp. e00346-17, doi:10.1128/msphere.00346-17.

Meyer, K. D., **Patil, D. P.**, **Zhou, J.**, **Zinoviev, A.**, **Skabkin, M. A.**, **Elemento, O.**, **Pestova, T. V.**, **Qian, S. B.** and **Jaffrey, S. R.** (2015) '5′ UTR m6A Promotes Cap-Independent Translation', *Cell*, 163(4), pp. 999–1010, doi:10.1016/j.cell.2015.10.012.

Niedzwiecka, A., **Marcotrigiano, J.**, **Stepinski, J.**, **Jankowska-Anyszka, M.**, **Wyslouch-Cieszynska, A.**, **Dadlez, M.**, **Gingras, A. C.**, **Mak, P.**, **Darzynkiewicz, E.**, **Sonenberg, N.**, **Burley, S. K.** and **Stolarski, R.** (2002) 'Biophysical studies of eIF4E cap-binding protein: Recognition of mRNA 5′ cap structure and synthetic fragments of eIF4G and 4E-BP1 proteins', *Journal of Molecular Biology*, 319(3), pp. 615–635, doi:10.1016/s0022-2836(02)00328-5.

Niesen, F. H., **Berglund, H.** and **Vedadi, M.** (2007) 'The use of differential scanning fluorimetry to detect ligand interactions that promote protein stability', *Nature Protocols*, 2(9), pp. 2212–2221, doi:10.1038/nprot.2007.321.

Niikura, T., **Hirata, R.** and **Weil, S. C.** (1997) 'A novel interferon-inducible gene expressed during

myeloid differentiation', *Blood Cells, Molecules and Diseases*, 23(3), pp. 337–349, doi:10.1006/bcmd.1997.0151.

Norbury, C. J. (2010) '3′ uridylation and the regulation of RNA function in the cytoplasm', *Biochemical Society Transactions*, 38(4), pp. 1150–1153, doi:10.1042/bst0381150.

Ogino, T. and **Green, T. J.** (2019) 'Transcriptional control and mRNA capping by the GDP polyribonucleotidyltransferase domain of the rabies virus large protein', *Viruses*, 11(6), doi:10.3390/v11060504.

Ohsugi, T., **Yamaguchi, K.**, **Zhu, C.**, **Ikenoue, T.** and **Furukawa, Y.** (2017) 'Decreased expression of interferon-induced protein 2 (IFIT2) by Wnt/β-catenin signaling confers anti-apoptotic properties to colorectal cancer cells.', *Oncotarget*, 8(59), pp. 100176–100186, doi:10.18632/oncotarget.22122.

Ong, S.-E., **Blagoev, B.**, **Kratchmarova, I.**, **Kristensen, D. B.**, **Steen, H.**, **Pandey, A.** and **Mann, M.** (2002) 'Stable isotope labeling by amino acids in cell culture, SILAC, as a simple and accurate approach to expression proteomics.', *Molecular & Cellular Proteomics : MCP*, 1(5), pp. 376–86, doi:10.1074/mcp.m200025-mcp200.

Pennock, N. D., **White, J. T.**, **Cross, E. W.**, **Cheney, E. E.**, **Tamburini, B. A.** and **Kedl, R. M.** (2013) 'T cell responses: Naïve to memory and everything in between', *American Journal of Physiology - Advances in Physiology Education*, 37(4), pp. 273–283, doi:10.1152/advan.00066.2013.

Perry, R. P. and **Kelley, D. E.** (1976) 'Kinetics of formation of 5′ terminal caps in mRNA', *Cell*, 8(3), pp. 433–442, doi:10.1016/0092-8674(76)90156-2.

Perry, R. P., **Kelley, D. E.**, **Friderici, K.** and **Rottman, F.** (1975) 'The methylated constituents of L cell messenger RNA: Evidence for an unusual cluster at the 5′ terminus', *Cell*, 4(4), pp. 387–394, doi:10.1016/0092-8674(75)90159-2.

Perry, R. P. and **Scherrer, K.** (1975) 'The methylated constituents of globin mRNA.', *FEBS letters*, 57(1), pp. 73–8, doi:10.1016/0014-5793(75)80155-4.

Perwitasari, O., **Cho, H.**, **Diamond, M. S.** and **Gale, M.** (2011) 'Inhibitor of κB Kinase ϵ (IKKϵ), STAT1, and IFIT2 Proteins Define Novel Innate Immune Effector Pathway against West Nile Virus Infection', *Journal of Biological Chemistry*, 286(52), pp. 44412–44423, doi:10.1074/jbc.m111.285205.

Pestova, T. V, **Hellen, C. U.** and **Shatsky, I. N.** (1996) 'Canonical eukaryotic initiation factors determine initiation of translation by internal ribosomal entry.', *Molecular and Cellular Biology*, 16(12), pp. 6859–6869, doi:10.1128/mcb.16.12.6859.

Phizicky, E. M. and **Hopper, A. K.** (2015) 'tRNA processing, modification, and subcellular dynamics: Past, present, and future', *RNA*, 21(4), pp. 483–485, doi:10.1261/rna.049932.115.

Pichlmair, A., **Schulz, O.**, **Tan, C. P.**, **Näslund, T. I.**, **Liljeström, P.**, **Weber, F.** and **Reis e Sousa, C.** (2006) 'RIG-I-mediated antiviral responses to single-stranded RNA bearing 5'-phosphates.', *Science (New York, N.Y.)*, 314(5801), pp. 997–1001, doi:10.1126/science.1132998.

Pichlmair, A., **Lassnig, C.**, **Eberle, C.-A.**, **Górna, M. W.**, **Baumann, C. L.**, **Burkard, T. R.**, **Bürckstümmer, T.**, **Stefanovic, A.**, **Krieger, S.**, **Bennett, K. L.**, **Rülicke, T.**, **Weber, F.**, **Colinge, J.**, **Müller, M.** and **Superti-Furga, G.** (2011) 'IFIT1 is an antiviral protein that recognizes 5′-

triphosphate RNA', *Nature Immunology*, 12(7), pp. 624–630, doi:10.1038/ni.2048.

Pietilä, M. K., **Hellström, K.** and **Ahola, T.** (2017) 'Alphavirus polymerase and RNA replication', *Virus Research*. Elsevier B.V., 234, pp. 44–57, doi:10.1016/j.virusres.2017.01.007.

Pingale, K. D., **Kanade, G. D.** and **Karpe, Y. A.** (2019) 'Hepatitis E virus polymerase binds to IFIT1 to protect the viral RNA from IFIT1-mediated translation inhibition.', *The Journal of general virology*, 100(3), pp. 471–483, doi:10.1099/jgv.0.001229.

Pinto, A. K., **Williams, G. D.**, **Szretter, K. J.**, **White, J. P.**, **Proença-Módena, J. L.**, **Liu, G.**, **Olejnik, J.**, **Brien, J. D.**, **Ebihara, H.**, **Mühlberger, E.**, **Amarasinghe, G.**, **Diamond, M. S.** and **Boon, A. C. M.** (2015) 'Human and Murine IFIT1 Proteins Do Not Restrict Infection of Negative-Sense RNA Viruses of the Orthomyxoviridae, Bunyaviridae, and Filoviridae Families', *Journal of Virology*, 89(18), pp. 9465–9476, doi:10.1128/jvi.00996-15.

Platanias, L. C. (2005) 'Mechanisms of type-I- and type-II-interferon-mediated signalling.', *Nature reviews. Immunology*, 5(5), pp. 375–86, doi:10.1038/nri1604.

Plotch, S. J., **Bouloy, M.** and **Krug, R. M.** (1979) 'Transfer of 5'-terminal cap of globin mRNA to influenza viral complementary RNA during transcription in vitro.', *Proceedings of the National Academy of Sciences of the United States of America*, 76(4), pp. 1618–22, doi:10.1073/pnas.76.4.1618.

Rabbani, M. A. G., **Ribaudo, M.**, **Guo, J.** and **Barik, S.** (2016) 'Identification of Interferon-Stimulated Gene Proteins That Inhibit Human Parainfluenza Virus Type 3.', *Journal of virology*, 90(24), pp. 11145–11156, doi:10.1128/jvi.01551-16.

Ray, D., **Shah, A.**, **Tilgner, M.**, **Guo, Y.**, **Zhao, Y.**, **Dong, H.**, **Deas, T. S.**, **Zhou, Y.**, **Li, H.** and **Shi, P.-Y.** (2006) 'West Nile Virus 5'-Cap Structure Is Formed by Sequential Guanine N-7 and Ribose 2'-O Methylations by Nonstructural Protein 5', *Journal of Virology*, 80(17), pp. 8362–8370, doi:10.1128/jvi.00814-06.

Raychoudhuri, A., **Shrivastava, S.**, **Steele, R.**, **Kim, H.**, **Ray, R.** and **Ray, R. B.** (2011) 'ISG56 and IFITM1 Proteins Inhibit Hepatitis C Virus Replication', *Journal of Virology*, 85(24), pp. 12881–12889, doi:10.1128/jvi.05633-11.

Reolon, L. W., **Vichier-Guerre, S.**, **de Matos, B. M.**, **Dugué, L.**, **Assunção, T. R. da S.**, **Zanchin, N. I. T.**, **Pochet, S.** and **Guimarães, B. G.** (2019) 'Crystal structure of the Trypanosoma cruzi EIF4E5 translation factor homologue in complex with mRNA cap-4.', *Nucleic Acids Research*, 47(11), pp. 5973–5987, doi:10.1093/nar/gkz339.

Reuten, R., **Nikodemus, D.**, **Oliveira, M. B.**, **Patel, T. R.**, **Brachvogel, B.**, **Breloy, I.**, **Stetefeld, J.** and **Koch, M.** (2016) 'Maltose-binding protein (MBP), a secretion-enhancing tag for mammalian protein expression systems', *PLoS ONE*, 11(3), pp. 1–15, doi:10.1371/journal.pone.0152386.

Reynaud, J. M., **Kim, D. Y.**, **Atasheva, S.**, **Rasalouskaya, A.**, **White, J. P.**, **Diamond, M. S.**, **Weaver, S. C.**, **Frolova, E. I.** and **Frolov, I.** (2015) 'IFIT1 Differentially Interferes with Translation and Replication of Alphavirus Genomes and Promotes Induction of Type I Interferon', *PLoS Pathogens*, 11(4), p. e1004863, doi:10.1371/journal.ppat.1004863.

Roeder, R. G. (1991) 'The complexities of eukaryotic transcription initiation: regulation of preinitiation complex assembly.', *Trends in Biochemical Sciences*, 16(11), pp. 402–8,

doi:10.1016/0968-0004(91)90164-q.

Rong, M., **Durbin, R. K.** and **McAllister, W. T.** (1998) 'Template strand switching by T7 RNA polymerase', *Journal of Biological Chemistry*, 273(17), pp. 10253–10260, doi:10.1074/jbc.273.17.10253.

Rose, J. K. (1975) 'Heterogeneous 5'-terminal structures occur on vesicular stomatitis virus mRNAs.', *The Journal of Biological Chemistry*, 250(20), pp. 8098–104.

Saikia, P., **Fensterl, V.** and **Sen, G. C.** (2010) 'The Inhibitory Action of P56 on Select Functions of E1 Mediates Interferon's Effect on Human Papillomavirus DNA Replication', *Journal of Virology*, 84(24), pp. 13036–13039, doi:10.1128/jvi.01194-10.

Samarajiwa, S. A., **Forster, S.**, **Auchettl, K.** and **Hertzog, P. J.** (2009) 'INTERFEROME: the database of interferon regulated genes.', *Nucleic acids research*, 37(Database issue), pp. D852-7, doi:10.1093/nar/gkn732.

Santhakumar, D., **Rohaim, M. A. M. S.**, **Hussein, H. A.**, **Hawes, P.**, **Ferreira, H. L.**, **Behboudi, S.**, **Iqbal, M.**, **Nair, V.**, **Arns, C. W.** and **Munir, M.** (2018) 'Chicken Interferon-induced Protein with Tetratricopeptide Repeats 5 Antagonizes Replication of RNA Viruses', *Scientific Reports*, 8(1), p. 6794, doi:10.1038/s41598-018-24905-y.

Sanz, M. A., **González Almela, E.** and **Carrasco, L.** (2017) 'Translation of Sindbis Subgenomic mRNA is Independent of eIF2, eIF2A and eIF2D.', *Scientific reports*. Nature Publishing Group, 7(October 2016), p. 43876, doi:10.1038/srep43876.

Schmeisser, H., **Mejido, J.**, **Balinsky, C. A.**, **Morrow, A. N.**, **Clark, C. R.**, **Zhao, T.** and **Zoon, K. C.** (2010) 'Identification of alpha interferon-induced genes associated with antiviral activity in Daudi cells and characterization of IFIT3 as a novel antiviral gene.', *Journal of Virology*, 84(20), pp. 10671–10680, doi:10.1128/jvi.00818-10.

Schmidt, E. K., **Clavarino, G.**, **Ceppi, M.** and **Pierre, P.** (2009) 'SUnSET, a nonradioactive method to monitor protein synthesis', *Nature Methods*, 6(4), pp. 275–277, doi:10.1038/nmeth.1314.

Schuberth-Wagner, C., **Ludwig, J.**, **Bruder, A. K.**, **Herzner, A.-M.**, **Zillinger, T.**, **Goldeck, M.**, **Schmidt, T.**, **Schmid-Burgk, J. L.**, **Kerber, R.**, **Wolter, S.**, **Stümpel, J.-P.**, **Roth, A.**, **Bartok, E.**, **Drosten, C.**, **Coch, C.**, **Hornung, V.**, **Barchet, W.**, ... **Schlee, M.** (2015) 'A Conserved Histidine in the RNA Sensor RIG-I Controls Immune Tolerance to N1-2'O-Methylated Self RNA.', *Immunity*, 43(1), pp. 41–51, doi:10.1016/j.immuni.2015.06.015.

Scott, I. (2010) 'The role of mitochondria in the mammalian antiviral defense system', *Mitochondrion*. Mitochondria Research Society, 10(4), pp. 316–320, doi:10.1016/j.mito.2010.02.005.

Secombes, C. J. and **Zou, J.** (2017) 'Evolution of interferons and interferon receptors', *Frontiers in Immunology*, 8(MAR), pp. 2–11, doi:10.3389/fimmu.2017.00209.

Shaw, G. and **Kamen, R.** (1986) 'A conserved AU sequence from the 3′ untranslated region of GM-CSF mRNA mediates selective mRNA degradation', *Cell*, 46(5), pp. 659–667, doi:10.1016/0092-8674(86)90341-7.

Siegfried, A., **Berchtold, S.**, **Manncke, B.**, **Deuschle, E.**, **Reber, J.**, **Ott, T.**, **Weber, M.**, **Kalinke, U.**, **Hofer, M. J.**, **Hatesuer, B.**, **Schughart, K.**, **Gailus-Durner, V.**, **Fuchs, H.**, **Hrabe de Angelis,**

M., **Weber, F.**, **Hornef, M. W.**, **Autenrieth, I. B.** and **Bohn, E.** (2013) 'IFIT2 is an effector protein of type I IFN-mediated amplification of lipopolysaccharide (LPS)-induced TNF-α secretion and LPS-induced endotoxin shock.', *Journal of immunology*, 191(7), pp. 3913–21, doi:10.4049/jimmunol.1203305.

Sikorski, R. S., **Boguski, M. S.**, **Goebl, M.** and **Hieter, P.** (1990) 'A repeating amino acid motif in CDC23 defines a family of proteins and a new relationship among genes required for mitosis and RNA synthesis', *Cell*, 60(2), pp. 307–317, doi:10.1016/0092-8674(90)90745-z.

Silman, N., **Artman, M.** and **Engelberg, H.** (1965) 'Effect of magnesium and spermine on the aggregation of bacterial and mammalian ribosomes', *BBA Section Nucleic Acids And Protein Synthesis*, 103(2), pp. 231–240, doi:10.1016/0005-2787(65)90164-4.

Skabkin, M. A., **Skabkina, O. V.**, **Dhote, V.**, **Komar, A. A.**, **Hellen, C. U. T.** and **Pestova, T. V.** (2010) 'Activities of Ligatin and MCT-1/DENR in eukaryotic translation initiation and ribosomal recycling', *Genes and Development*, 24(16), pp. 1787–1801, doi:10.1101/gad.1957510.

Smith, J. B. and **Herschman, H. R.** (1996) 'The glucocorticoid attenuated response genes GARG-16, GARG-39, and GARG-49/IRG2 encode inducible proteins containing multiple tetratricopeptide repeat domains.', *Archives of Biochemistry and Biophysics*, 330(2), pp. 290–300, doi:10.1006/abbi.1996.0256.

Soday, L., **Lu, Y.**, **Albarnaz, J. D.**, **Davies, C. T. R.**, **Antrobus, R.**, **Smith, G. L.** and **Weekes, M. P.** (2019) 'Quantitative Temporal Proteomic Analysis of Vaccinia Virus Infection Reveals Regulation of Histone Deacetylases by an Interferon Antagonist', *Cell Reports*, 27(6), pp. 1920-1933.e7, doi:10.1016/j.celrep.2019.04.042.

Some, D., **Amartely, H.**, **Tsadok, A.** and **Lebendiker, M.** (2019) 'Characterization of Proteins by Size-Exclusion Chromatography Coupled to Multi-Angle Light Scattering (SEC-MALS).', *Journal of Visualized Experiments : JoVE*, (148), pp. 1–9, doi:10.3791/59615.

Stawowczyk, M., **Van Scoy, S.**, **Kumar, K. P.** and **Reich, N. C.** (2011) 'The interferon stimulated gene 54 promotes apoptosis.', *The Journal of Biological Chemistry*, 286(9), pp. 7257–66, doi:10.1074/jbc.m110.207068.

Stawowczyk, M., **Naseem, S.**, **Montoya, V.**, **Baker, D. P.**, **Konopka, J.** and **Reich, N. C.** (2018) 'Pathogenic Effects of IFIT2 and Interferon-β during Fatal Systemic Candida albicans Infection.', *mBio*, 9(2), pp. 1–17, doi:10.1128/mbio.00365-18.

Stegelmeier, A. A., **van Vloten, J. P.**, **Mould, R. C.**, **Klafuric, E. M.**, **Minott, J. A.**, **Wootton, S. K.**, **Bridle, B. W.** and **Karimi, K.** (2019) 'Myeloid Cells during Viral Infections and Inflammation.', *Viruses*, 11(2), p. E168, doi:10.3390/v11020168.

Sturman, L. S. and **Takemoto, K. K.** (1972) 'Enhanced growth of a murine coronavirus in transformed mouse cells.', *Infection and Immunity*, 6(4), pp. 501–7.

Sun, C., **Querol-Audí, J.**, **Mortimer, S. A.**, **Arias-Palomo, E.**, **Doudna, J. A.**, **Nogales, E.** and **Cate, J. H. D.** (2013) 'Two RNA-binding motifs in eIF3 direct HCV IRES-dependent translation', *Nucleic Acids Research*, 41(15), pp. 7512–7521, doi:10.1093/nar/gkt510.

Szretter, K. J., **Daniels, B. P.**, **Cho, H.**, **Gainey, M. D.**, **Yokoyama, W. M.**, **Gale, M.**, **Virgin, H.**

W., **Klein, R. S.**, **Sen, G. C.** and **Diamond, M. S.** (2012) '2'-O methylation of the viral mRNA cap by West Nile virus evades ifit1-dependent and -independent mechanisms of host restriction in vivo.', *PLoS pathogens*, 8(5), p. e1002698, doi:10.1371/journal.ppat.1002698.

Tamassia, N., **Le Moigne, V.**, **Rossato, M.**, **Donini, M.**, **McCartney, S.**, **Calzetti, F.**, **Colonna, M.**, **Bazzoni, F.** and **Cassatella, M. A.** (2008) 'Activation of an Immunoregulatory and Antiviral Gene Expression Program in Poly(I:C)-Transfected Human Neutrophils', *The Journal of Immunology*, 181(9), pp. 6563–6573, doi:10.4049/jimmunol.181.9.6563.

Tang, W.-G., **Hu, B.**, **Sun, H.-X.**, **Sun, Q.-M.**, **Sun, C.**, **Fu, P.-Y.**, **Yang, Z.-F.**, **Zhang, X.**, **Zhou, C.-H.**, **Fan, J.**, **Ren, N.** and **Xu, Y.** (2017) 'Long non-coding RNA00364 represses hepatocellular carcinoma cell proliferation via modulating p-STAT3-IFIT2 signaling axis', *Oncotarget*, 8(60), pp. 102006–102019, doi:10.18632/oncotarget.22039.

Terenzi, F., **Pal, S.** and **Sen, G. C.** (2005) 'Induction and mode of action of the viral stress-inducible murine proteins, P56 and P54', *Virology*, 340(1), pp. 116–124, doi:10.1016/j.virol.2005.06.011.

Terenzi, F. and **Saikia, P.** (2008) 'Interferon-inducible protein, P56, inhibits HPV DNA replication by binding to the viral protein E1', *EMBO Journal*, 27(24), pp. 3311–3321, doi:10.1038/emboj.2008.241.

Terenzi, F., **Hui, D. J.**, **Merrick, W. C.** and **Sen, G. C.** (2006) 'Distinct Induction Patterns and Functions of Two Closely Related Interferon-inducible Human Genes, ISG54 and ISG56', *Journal of Biological Chemistry*, 281(45), pp. 34064–34071, doi:10.1074/jbc.m605771200.

Terenzi, F., **White, C.**, **Pal, S.**, **Williams, B. R. G.** and **Sen, G. C.** (2007) 'Tissue-Specific and Inducer-Specific Differential Induction of ISG56 and ISG54 in Mice', *Journal of Virology*, 81(16), pp. 8656–8665, doi:10.1128/jvi.00322-07.

Triana-Alonso, F. J., **Dabrowski, M.**, **Wadzack, J.** and **Nierhaus, K. H.** (1995) 'Self-coded 3'-extension of run-off transcripts produces aberrant products during in vitro transcription with T7 RNA polymerase', *Journal of Biological Chemistry*, pp. 6298–6307, doi:10.1074/jbc.270.11.6298.

Uchiyama, R., **Chassaing, B.**, **Zhang, B.** and **Gewirtz, A. T.** (2015) 'MyD88-mediated TLR signaling protects against acute rotavirus infection while inflammasome cytokines direct Ab response', *Innate Immunity*, 21(4), pp. 416–428, doi:10.1177/1753425914547435.

Uhlén, M., **Fagerberg, L.**, **Hallström, B. M.**, **Lindskog, C.**, **Oksvold, P.**, **Mardinoglu, A.**, **Sivertsson, Å.**, **Kampf, C.**, **Sjöstedt, E.**, **Asplund, A.**, **Olsson, I. M.**, **Edlund, K.**, **Lundberg, E.**, **Navani, S.**, **Szigyarto, C. A. K.**, **Odeberg, J.**, **Djureinovic, D.**, ... **Pontén, F.** (2015) 'Tissue-based map of the human proteome', *Science*, 347(6220), p. 1260419, doi:10.1126/science.1260419.

Ullah, M. O., **Ve, T.**, **Mangan, M.**, **Alaidarous, M.**, **Sweet, M. J.**, **Mansell, A.** and **Kobe, B.** (2013) 'The TLR signalling adaptor TRIF/TICAM-1 has an N-terminal helical domain with structural similarity to IFIT proteins', *Acta Crystallographica Section D Biological Crystallography*, 69(12), pp. 2420–2430, doi:10.1107/s0907444913022385.

Valášek, L., **Nielsen, K. H.** and **Hinnebusch, A. G.** (2002) 'Direct eIF2-eIF3 contact in the multifactor complex is important for translation initiation in vivo.', *The EMBO journal*, 21(21), pp. 5886–98, doi:10.1093/emboj/cdf563.

Valášek, L. S., **Zeman, J.**, **Wagner, S.**, **Beznosková, P.**, **Pavlíková, Z.**, **Mohammad, M. P.**, **Hronová, V.**, **Herrmannová, A.**, **Hashem, Y.** and **Gunišová, S.** (2017) 'Embraced by eIF3: structural and functional insights into the roles of eIF3 across the translation cycle.', *Nucleic Acids Research*, 45(19), pp. 10948–10968, doi:10.1093/nar/gkx805.

Varela, M., **Diaz-Rosales, P.**, **Pereiro, P.**, **Forn-Cuní, G.**, **Costa, M. M.**, **Dios, S.**, **Romero, A.**, **Figueras, A.** and **Novoa, B.** (2014) 'Interferon-Induced Genes of the Expanded IFIT Family Show Conserved Antiviral Activities in Non-Mammalian Species', *PLoS ONE*. Edited by V. Thiel, 9(6), p. e100015, doi:10.1371/journal.pone.0100015.

de Veer, M. J., **Sim, H.**, **Whisstock, J. C.**, **Devenish, R. J.** and **Ralph, S. J.** (1998) 'IFI60/ISG60/IFIT4, a new member of the human IFI54/IFIT2 family of interferon-stimulated genes.', *Genomics*, 54(2), pp. 267–77, doi:10.1006/geno.1998.5555.

te Velthuis, A. J. W., **Long, J. C.**, **Bauer, D. L. V.**, **Fan, R. L. Y.**, **Yen, H. L.**, **Sharps, J.**, **Siegers, J. Y.**, **Killip, M. J.**, **French, H.**, **Oliva-Martín, M. J.**, **Randall, R. E.**, **de Wit, E.**, **van Riel, D.**, **Poon, L. L. M.** and **Fodor, E.** (2018) 'Mini viral RNAs act as innate immune agonists during influenza virus infection', *Nature Microbiology*, 3(11), pp. 1234–1242, doi:10.1038/s41564-018-0240-5.

Ventoso, I., **Sanz, M. A.**, **Molina, S.**, **Berlanga, J. J.**, **Carrasco, L.** and **Esteban, M.** (2006) 'Translational resistance of late alphavirus mRNA to eIF2α phosphorylation: A strategy to overcome the antiviral effect of protein kinase PKR', *Genes and Development*, 20(1), pp. 87–100, doi:10.1101/gad.357006.

Villa, N., **Do, A.**, **Hershey, J. W. B.** and **Fraser, C. S.** (2013) 'Human eukaryotic initiation factor 4G (eIF4G) protein binds to eIF3c, -d, and -e to promote mRNA recruitment to the ribosome', *Journal of Biological Chemistry*, 288(46), pp. 32932–32940, doi:10.1074/jbc.m113.517011.

Wacher, C., **Muller, M.**, **Hofer, M. J.**, **Getts, D. R.**, **Zabaras, R.**, **Ousman, S. S.**, **Terenzi, F.**, **Sen, G. C.**, **King, N. J. C.** and **Campbell, I. L.** (2007) 'Coordinated Regulation and Widespread Cellular Expression of Interferon-Stimulated Genes (ISG) ISG-49, ISG-54, and ISG-56 in the Central Nervous System after Infection with Distinct Viruses', *Journal of Virology*, 81(2), pp. 860–871, doi:10.1128/jvi.01167-06.

Walker, A. P. and **Fodor, E.** (2019) 'Interplay between Influenza Virus and the Host RNA Polymerase II Transcriptional Machinery', *Trends in Microbiology*. The Authors, 27(5), pp. 398–407, doi:10.1016/j.tim.2018.12.013.

Wang, J., **Alvin Chew, B. L.**, **Lai, Y.**, **Dong, H.**, **Xu, L.**, **Balamkundu, S.**, **Cai, W. M.**, **Cui, L.**, **Liu, C. F.**, **Fu, X.-Y.**, **Lin, Z.**, **Shi, P.-Y.**, **Lu, T. K.**, **Luo, D.**, **Jaffrey, S. R.** and **Dedon, P. C.** (2019) 'Quantifying the RNA cap epitranscriptome reveals novel caps in cellular and viral RNA', *Nucleic Acids Research*. Oxford University Press, pp. 1–16, doi:10.1093/nar/gkz751.

Wang, J., **Dai, M.**, **Cui, Y.**, **Hou, G.**, **Deng, J.**, **Gao, X.**, **Liao, Z.**, **Meng, Y.**, **Wu, L.**, **Yao, C.**, **Wang, Y.**, **Qian, J.**, **Guo, Q.**, **Ding, H.**, **Qu, B.**, **Shen, N.**, **Wang, J.**, ... **Shen, N.** (2018) 'Elevated IFIT3 Contributes to Abnormal Overactive cGAS-STING Signaling in Human Systemic Lupus Erythematosus Monocytes', *Arthritis & Rheumatology*, doi:10.1002/art.40576.

Wang, Y., **Zhang, L.**, **Zheng, X.**, **Zhong, W.**, **Tian, X.**, **Yin, B.**, **Tian, K.** and **Zhang, W.** (2016)

'Long non-coding RNA LINC00161 sensitises osteosarcoma cells to cisplatin-induced apoptosis by regulating the miR-645-IFIT2 axis', *Cancer Letters*, 382(2), pp. 137–146, doi:10.1016/j.canlet.2016.08.024.

Waterhouse, A., **Bertoni, M.**, **Bienert, S.**, **Studer, G.**, **Tauriello, G.**, **Gumienny, R.**, **Heer, F. T.**, **De Beer, T. A. P.**, **Rempfer, C.**, **Bordoli, L.**, **Lepore, R.** and **Schwede, T.** (2018) 'SWISS-MODEL: Homology modelling of protein structures and complexes', *Nucleic Acids Research*, 46(W1), pp. W296–W303, doi:10.1093/nar/gky427.

Wathelet, M., **Moutschen, S.**, **Defilippi, P.**, **Cravador, A.**, **Collet, M.**, **Huez, G.** and **Content, J.** (1986) 'Molecular cloning, full-length sequence and preliminary characterization of a 56-kDa protein induced by human interferons.', *European Journal of Biochemistry*, 155(1), pp. 11–7, doi:10.1111/j.1432-1033.1986.tb09452.x.

Weber, F., **Wagner, V.**, **Rasmussen, S. B.**, **Hartmann, R.** and **Paludan, S. R.** (2006) 'Double-stranded RNA is produced by positive-strand RNA viruses and DNA viruses but not in detectable amounts by negative-strand RNA viruses.', *Journal of virology*, 80(10), pp. 5059–64, doi:10.1128/jvi.80.10.5059-5064.2006.

Wei, C. M., **Gershowitz, A.** and **Moss, B.** (1975) 'Methylated nucleotides block 5′ terminus of HeLa cell messenger RNA', *Cell*, 4(4), pp. 379–386, doi:10.1016/0092-8674(75)90158-0.

Wei, C. M. and **Moss, B.** (1974) 'Methylation of newly synthesized viral messenger RNA by an enzyme in vaccinia virus.', *Proceedings of the National Academy of Sciences of the United States of America*, 71(8), pp. 3014–8, doi:10.1073/pnas.71.8.3014.

Werner, M., **Purta, E.**, **Kaminska, K. H.**, **Cymerman, I. A.**, **Campbell, D. A.**, **Mittra, B.**, **Zamudio, J. R.**, **Sturm, N. R.**, **Jaworski, J.** and **Bujnicki, J. M.** (2011) '2′-O-ribose methylation of cap2 in human: function and evolution in a horizontally mobile family', *Nucleic Acids Research*, 39(11), pp. 4756–4768, doi:10.1093/nar/gkr038.

White, C. L., **Kessler, P. M.**, **Dickerman, B. K.**, **Ozato, K.** and **Sen, G. C.** (2016) 'Interferon Regulatory Factor 8 (IRF8) Impairs Induction of Interferon Induced with Tetratricopeptide Repeat Motif (IFIT) Gene Family Members', *Journal of Biological Chemistry*, 291(26), pp. 13535–13545, doi:10.1074/jbc.m115.705467.

Wichit, S., **Hamel, R.**, **Zanzoni, A.**, **Diop, F.**, **Cribier, A.**, **Talignani, L.**, **Diack, A.**, **Ferraris, P.**, **Liegeois, F.**, **Urbach, S.**, **Ekchariyawat, P.**, **Merits, A.**, **Yssel, H.**, **Benkirane, M.** and **Missé, D.** (2019) 'SAMHD1 Enhances Chikungunya and Zika Virus Replication in Human Skin Fibroblasts', *International Journal of Molecular Sciences*, 20(7), p. 1695, doi:10.3390/ijms20071695.

Williams, B. R. (1999) 'PKR; a sentinel kinase for cellular stress.', *Oncogene*, 18(45), pp. 6112–20, doi:10.1038/sj.onc.1203127.

Xiao, S., **Li, D.**, **Zhu, H.**, **Song, M.**, **Pan, X.**, **Jia, P.**, **Peng, L.**, **Dou, A.**, **Chen, G.**, **Chen, S.**, **Chen, Z.** and **Tong, J.** (2006) 'RIG-G as a key mediator of the antiproliferative activity of interferon-related pathways through enhancing p21 and p27 proteins', *Proceedings of the National Academy of Sciences*, 103(44), pp. 16448–16453.

Xu, N., **Chen, C. Y.** and **Shyu, A. B.** (1997) 'Modulation of the fate of cytoplasmic mRNA by AU-

rich elements: key sequence features controlling mRNA deadenylation and decay.', *Molecular and Cellular Biology*, 17(8), pp. 4611–4621, doi:10.1128/mcb.17.8.4611.

Yang, N. S., **Manning, R. F.** and **Patrick Gage, L.** (1976) 'The blocked and methylated 5′ terminal sequence of a specific cellular messenger: the mRNA for silk fibroin of bombyx mori', *Cell*, 7(3), pp. 339–347, doi:10.1016/0092-8674(76)90163-x.

Yang, Z., **Liang, H.**, **Zhou, Q.**, **Li, Y.**, **Chen, H.**, **Ye, W.**, **Chen, D.**, **Fleming, J.**, **Shu, H.** and **Liu, Y.** (2012) 'Crystal structure of ISG54 reveals a novel RNA binding structure and potential functional mechanisms', *Cell Research*, 22(9), pp. 1328–1338, doi:10.1038/cr.2012.111.

Young, D. F., **Andrejeva, J.**, **Li, X.**, **Inesta-Vaquera, F.**, **Dong, C.**, **Cowling, V. H.**, **Goodbourn, S.** and **Randall, R. E.** (2016) 'Human IFIT1 Inhibits mRNA Translation of Rubulaviruses but Not Other Members of the Paramyxoviridae Family', *Journal of Virology*. Edited by ., 90(20), pp. 9446–9456, doi:10.1128/jvi.01056-16.

Yu, M., **Tong, J. H.**, **Mao, M.**, **Kan, L. X.**, **Liu, M. M.**, **Sun, Y. W.**, **Fu, G.**, **Jing, Y. K.**, **Yu, L.**, **Lepaslier, D.**, **Lanotte, M.**, **Wang, Z. Y.**, **Chen, Z.**, **Waxman, S.**, **Wang, Y. X.**, **Tan, J. Z.** and **Chen, S. J.** (1997) 'Cloning of a gene (RIG-G) associated with retinoic acid-induced differentiation of acute promyelocytic leukemia cells and representing a new member of a family of interferon-stimulated genes.', *Proceedings of the National Academy of Sciences of the United States of America*, 94(14), pp. 7406–11, doi:10.1073/pnas.94.14.7406.

Zamudio, J. R., **Mittra, B.**, **Campbell, D. A.** and **Sturm, N. R.** (2009) 'Hypermethylated cap 4 maximizes Trypanosoma brucei translation', *Molecular Microbiology*, 72(5), pp. 1100–1110, doi:10.1111/j.1365-2958.2009.06696.x.

Zhang, B., **Liu, X.**, **Chen, W.** and **Chen, L.** (2013) 'IFIT5 potentiates anti-viral response through enhancing innate immune signaling pathways', *Acta Biochimica et Biophysica Sinica*, 45(10), pp. 867–874, doi:10.1093/abbs/gmt088.

Zhang, L., **Wang, B.**, **Li, L.**, **Qian, D.**, **Yu, H.**, **Xue, M.**, **Hu, M.** and **Song, X.** (2017a) 'Antiviral effects of IFIT1 in human cytomegalovirus-infected fetal astrocytes', *Journal of Medical Virology*, 89(4), pp. 672–684, doi:10.1002/jmv.24674.

Zhang, Y., **Kong, Y.**, **Liu, S.**, **Zeng, L.**, **Wan, L.** and **Zhang, Z.** (2017b) 'Curcumin induces apoptosis in human leukemic cell lines through an IFIT2-dependent pathway', *Cancer Biology & Therapy*, 18(1), pp. 43–50, doi:10.1080/15384047.2016.1276129.

Zhao, L., **Sukstanskii, A. L.**, **Kroenke, C. D.**, **Song, J.**, **Piwnica-Worms, D.**, **Ackerman, J. J. H.** and **Neil, J. J.** (2008) 'Intracellular water specific MR of microbead-adherent cells: HeLa cell intracellular water diffusion.', *Magnetic Resonance in Medicine*, 59(1), pp. 79–84, doi:10.1002/mrm.21440.

Zhong, B., **Yang, Y.**, **Li, S.**, **Wang, Y.-Y.**, **Li, Y.**, **Diao, F.**, **Lei, C.**, **He, X.**, **Zhang, L.**, **Tien, P.** and **Shu, H.-B.** (2008) 'The Adaptor Protein MITA Links Virus-Sensing Receptors to IRF3 Transcription Factor Activation', *Immunity*, 29(4), pp. 538–550, doi:10.1016/j.immuni.2008.09.003.

Zhou, X., **Michal, J. J.**, **Zhang, L.**, **Ding, B.**, **Lunney, J. K.**, **Liu, B.** and **Jiang, Z.** (2013) 'Interferon induced IFIT family genes in host antiviral defense.', *International journal of biological sciences*,

9(2), pp. 200–8, doi:10.7150/ijbs.5613.

Zhu, H. and **Damodaran, S.** (1994) 'Effects of Calcium and Magnesium Ions on Aggregation of Whey Protein Isolate and Its Effect on Foaming Properties', *Journal of Agricultural and Food Chemistry*, 42(4), pp. 856–862, doi:10.1021/jf00040a003.

Zlotnik, A. and **Yoshie, O.** (2000) 'Chemokines: a new classification system and their role in immunity.', *Immunity*, 12(2), pp. 121–7.

Zuker, M. (2003) 'Mfold web server for nucleic acid folding and hybridization prediction', *Nucleic Acids Research*, 31(13), pp. 3406–3415, doi:10.1093/nar/gkg595.

Züst, R., **Dong, H.**, **Li, X.-F.**, **Chang, D. C.**, **Zhang, B.**, **Balakrishnan, T.**, **Toh, Y.-X.**, **Jiang, T.**, **Li, S.-H.**, **Deng, Y.-Q.**, **Ellis, B. R.**, **Ellis, E. M.**, **Poidinger, M.**, **Zolezzi, F.**, **Qin, C.-F.**, **Shi, P.-Y.** and **Fink, K.** (2013) 'Rational Design of a Live Attenuated Dengue Vaccine: 2′-O-Methyltransferase Mutants Are Highly Attenuated and Immunogenic in Mice and Macaques', *PLoS Pathogens*, 9(8), p. e1003521, doi:10.1371/journal.ppat.1003521.

Züst, R., **Cervantes-Barragan, L.**, **Habjan, M.**, **Maier, R.**, **Neuman, B. W.**, **Ziebuhr, J.**, **Szretter, K. J.**, **Baker, S. C.**, **Barchet, W.**, **Diamond, M. S.**, **Siddell, S. G.**, **Ludewig, B.** and **Thiel, V.** (2011) 'Ribose 2'-O-methylation provides a molecular signature for the distinction of self and non-self mRNA dependent on the RNA sensor Mda5', *Nature Immunology*, 12(2), pp. 137–143, doi:10.1038/ni.1979.

9 APPENDICES

"But I am very poorly today and very stupid and hate everybody and everything"

- CHARLES DARWIN

APPENDIX A: STRUCTURAL DETAILS OF IFIT-RNA INTERACTIONS.

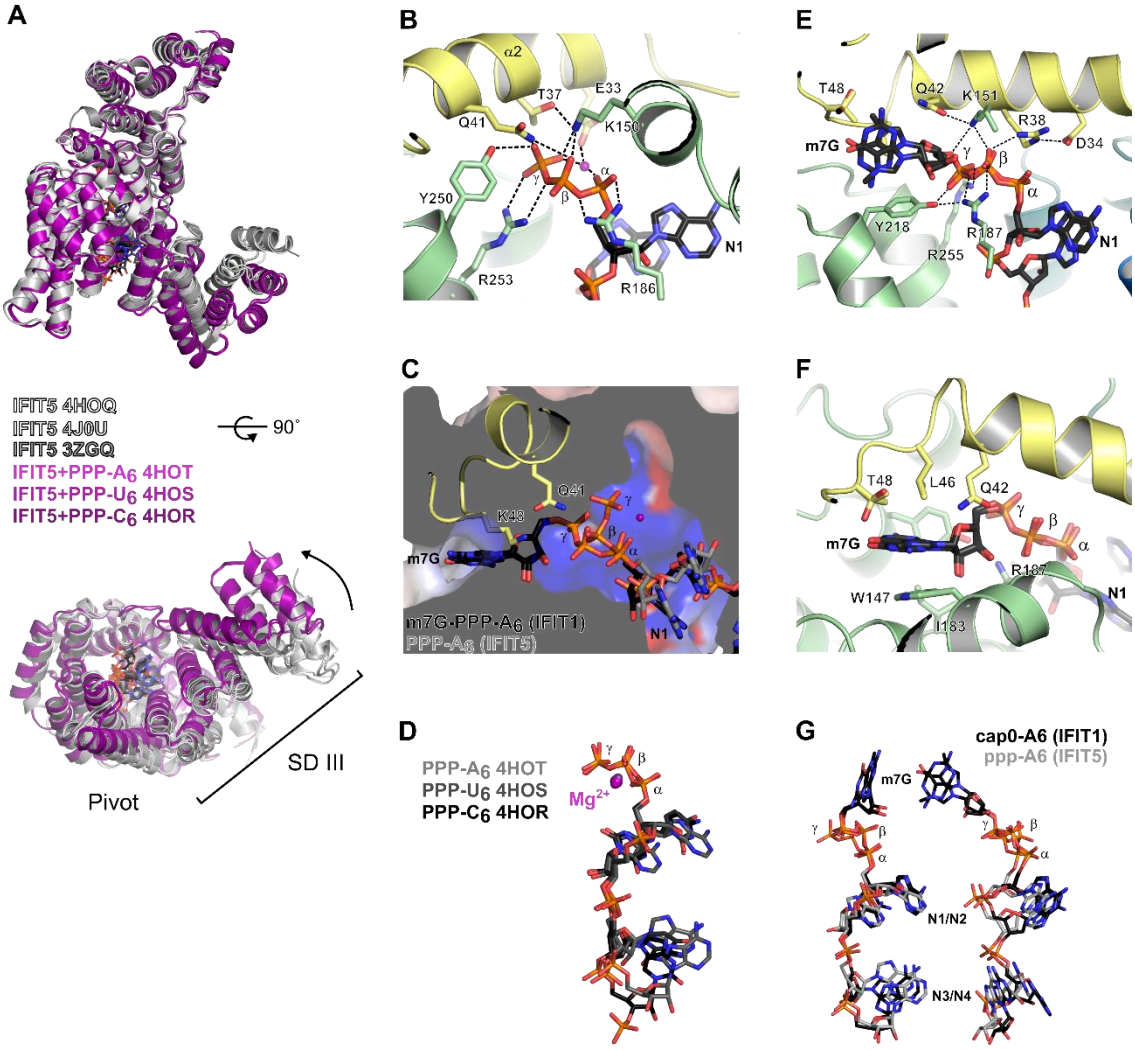

A. Cartoon representation of IFIT5, showing superposed apo (white/grey) and holo (magenta) states. Subdomain III (SD III) rotates about the RNA-binding channel upon ligand binding, creating a 'closed' conformation. **B.** Cartoon representation of IFIT5 residues interacting with the 5'ppp moiety, coloured by subdomain. Key side-chains are shown as sticks. RNA is shown as black sticks and hydrogen bonds are shown as dashed lines. **C.** Surface representation of the IFIT5 triphosphate binding channel, superimposed with cap0-oligo(A). Residues which occlude cap binding are shown as sticks. **D.** Superposition of oligo(A), oligo(U) and oligo(C) in complex with IFIT5. A metal ion, likely Mg^{2+}, involved in coordinating the α and γ phosphates, is shown as a magenta sphere. **E-F.** Cartoon representation of IFIT1 residues interacting with the (**E**) 5'ppp moiety and (**F**) m7G cap, coloured by subdomain. Key side-chains are shown as sticks. RNA is shown as black sticks and hydrogen bonds are shown as dashed lines. **G.** Overlay of oligo(A) bound by IFIT1 (black) or IFIT5 (grey). The gamma phosphate is held in a bent conformation by IFIT5 compared to the extended conformation in IFIT1.

APPENDIX B: SEC AND SEC-MALS ANALYSIS OF HUMAN IFIT COMPLEXES.

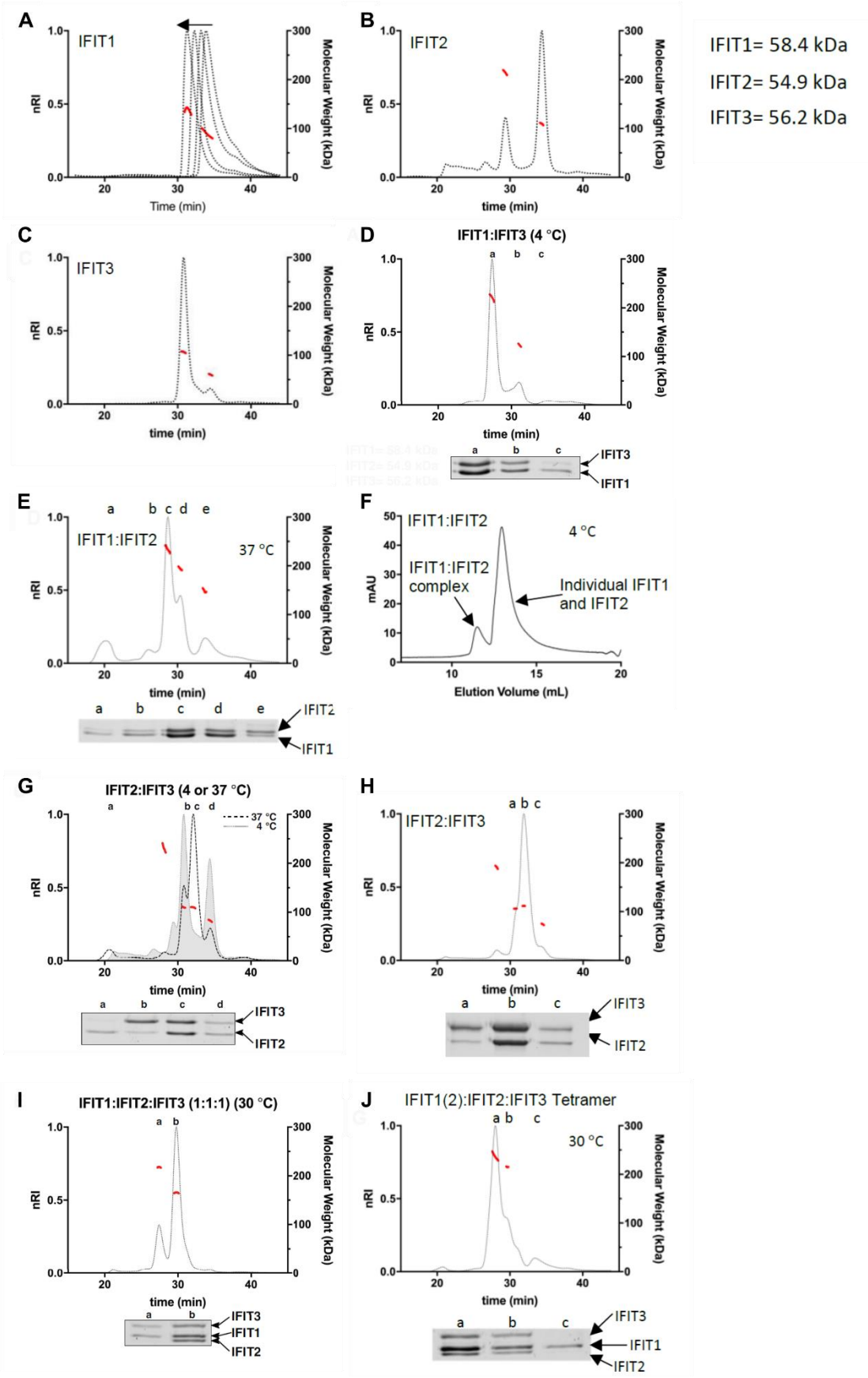

From Fleith and Mears et al. *(2018)*. These experiments were performed by Dr Renata Fleith.
A-C. SEC-MALS analysis of individual IFIT proteins on a Superdex 200 increase 10/300 column: (**A**) IFIT1 (0.5, 1, 2.8 or 8 mg/ml, arrow indicates earlier elution of peak with increasing amount of IFIT1 loaded onto column), (**B**) IFIT2 (1 mg/ml), (**C**) IFIT3 (1 mg/ml). **D,E,G-J.** SEC-MALS analysis of assembled IFIT complexes, formed at the indicated temperatures: (**D**) IFIT1:IFIT3, (**E-F**) IFIT1:IFIT2, (**G**) IFIT2:IFIT3, (**F**) peak fractions from **G** reanalysed by SEC, (**I**) the IFIT2:IFIT3 complex shown in **G** was incubated with equimolar IFIT1, (**J**) the IFIT2:IFIT3 complex shown in **G** was incubated with a two-fold molar excess of IFIT1. While the most abundant IFIT1:IFIT2 complex form is likely tetrameric, the presence of several overlapping peaks precludes reliable determination of specific molecular mass and hence oligomeric state. Normalized differential refractive index (nRI) is shown as dotted or broken lines on the left y-axis. Calculated molecular masses (kDa) of eluting species are shown as solid, red lines on the right y-axis. Gel insets below each trace show SDS-PAGE analysis of each run. Protein gel lanes and corresponding peaks are indicated by lower case letters. The positions of IFIT1, IFIT2 and IFIT3 on the protein gels are indicated. The calculated molecular masses of individual IFITs are: 6xHis-IFIT1- 58.4 kDa, IFIT2- 54.9 kD and IFIT3- 56.2 kDa.

APPENDIX C: MUTATION OF THE YXXXL MOTIF IN HUMAN IFIT1 AND IFIT3 DISRUPTS INTERACTION.

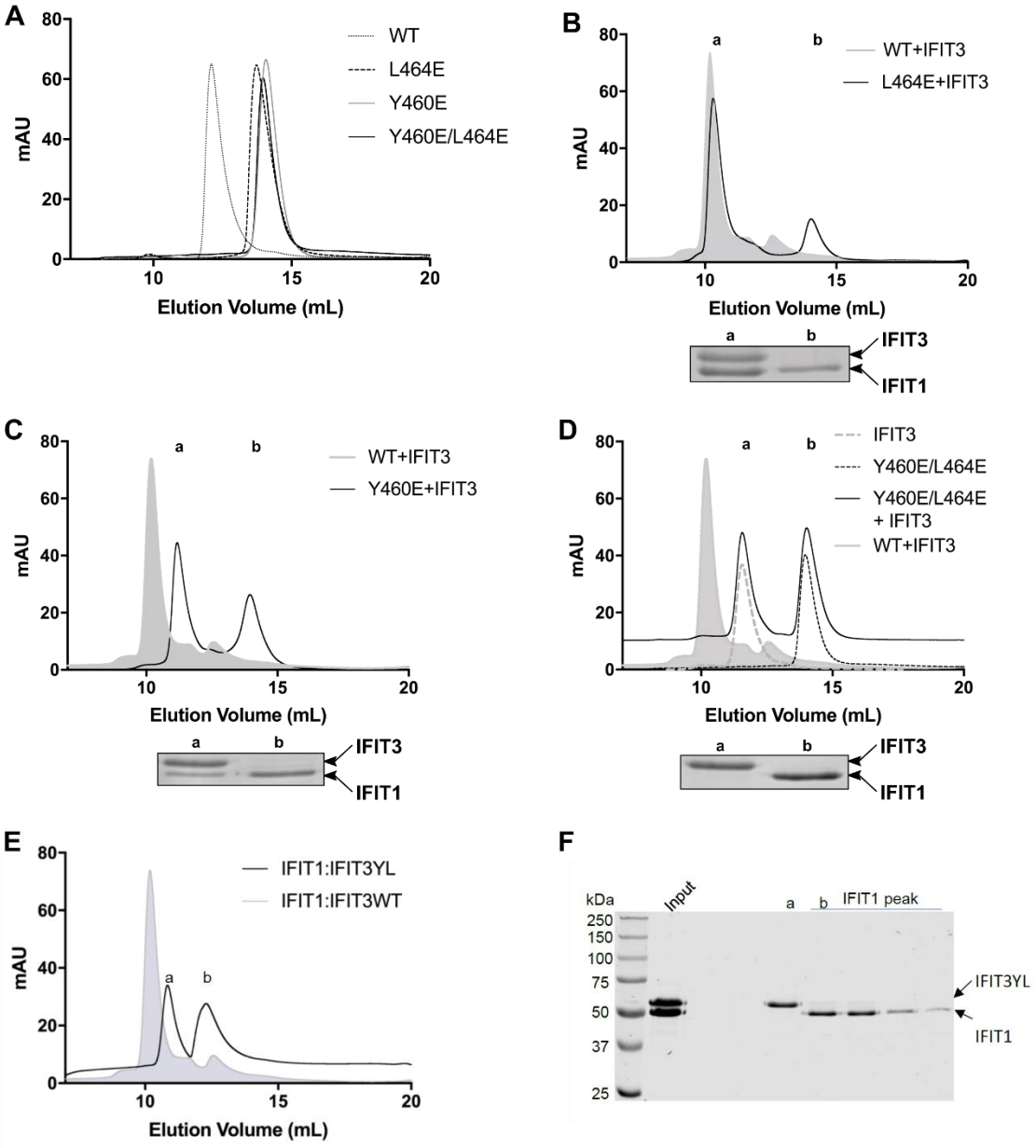

From Fleith and Mears et al. *(2018)*. These experiments were performed by Dr Renata Fleith.

A-D. UV280 absorbance traces of SEC analysis (Superdex S200 Increase 10/300 column) of wild type (WT) and mutant IFIT1 alone or incubated with IFIT3. **B-D.** Gel insets below each trace show SDS-PAGE analysis of each run. Protein gel lanes and corresponding peaks are indicated by lower case letters. The position of IFIT1 and IFIT3 on the protein gels is indicated. The Y460E/L464E+IFIT3 trace in (**D**) is adjusted by +10 milli absorbance units (mAU) for clarity. The elution profile of WT IFIT1+IFIT3 is shown in grey shadow for reference. **E.** Purified WT IFIT1 and IFIT3-Y438E/L442E (IFIT3YL) were preincubated for 1 hour at 4 ˚C and loaded onto a Superdex200 10/300 Increase size exclusion column. The elution profile of WT IFIT1+IFIT3 is shown in grey shadow for reference. **F.** Analysis of the peak fractions from **E** by SDS-PAGE.

APPENDIX D: HUMAN IFIT3 PROMOTES IFIT1 STABILITY IN CELLS.

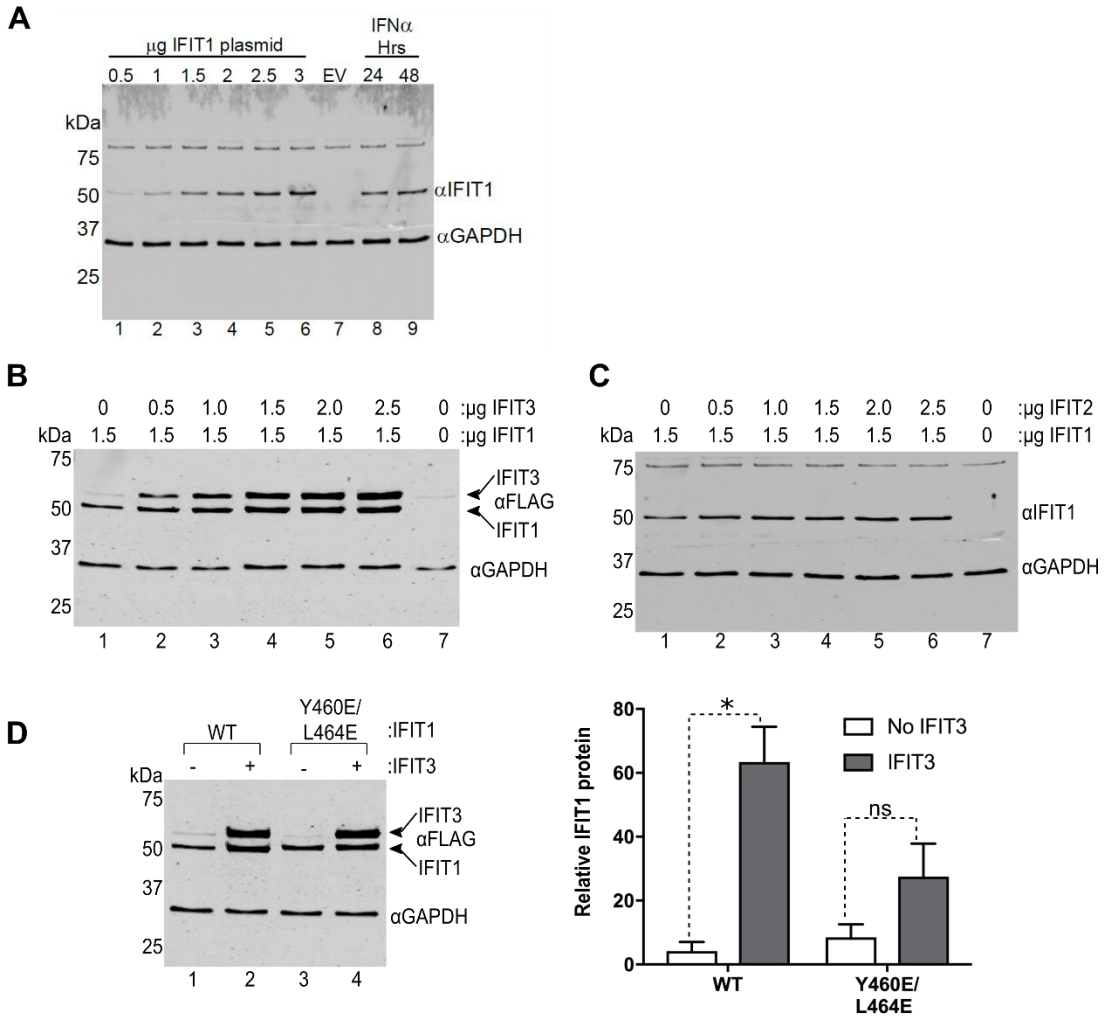

From Fleith and Mears et al. *(2018)*. These experiments were performed by Xin Yun Leong.

A. HEK293T cells were transfected with empty vector (EV) or increasing amounts of FLAG-tagged IFIT1 for 24 hrs (Lanes 1-7). Empty vector was added to normalise the amount of DNA transfected. HEK293T cells were separately treated with 1000 U/mL human IFN-α for 24 or 48 hrs (Lanes 8 and 9). **B,C.** HEK293T cells were transfected with the indicated amounts of plasmid encoding FLAG-tagged versions of IFIT1, IFIT2 and IFIT3, for 24 hours. The blots shown are representative of three separate experiments. **C.** HEK293T cells were transfected with 1.5 μg of FLAG-tagged wild type (WT) or mutant IFIT1 and 1.5 μg of FLAG-tagged IFIT3 or empty vector as indicated, for 24 hours. The graph on right shows the quantification of the IFIT1 protein expression relative to GAPDH probed as a loading control. Data represent the mean ± the standard deviation of three biological repeats.

APPENDIX E: HUMAN IFIT3 ENHANCES RNA BINDING BY IFIT1.

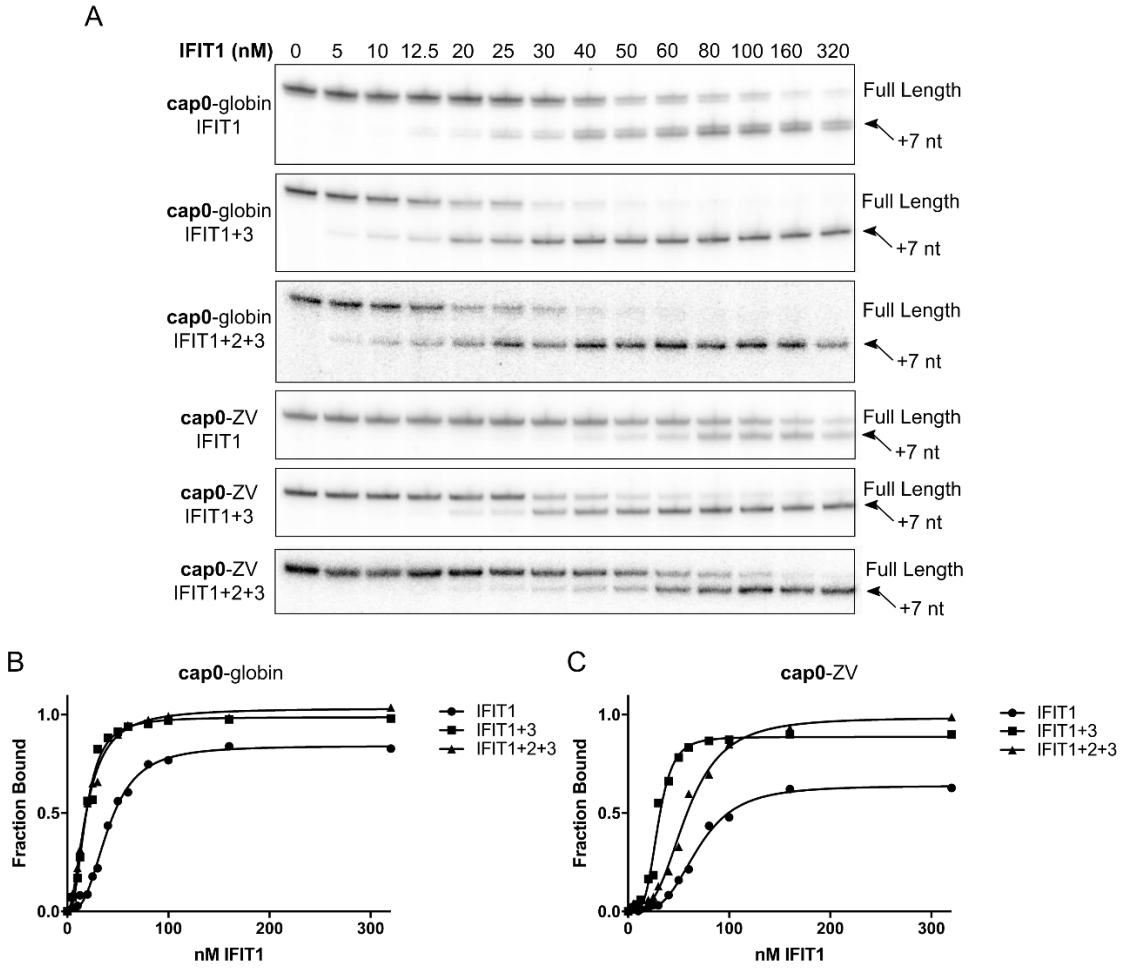

From Fleith and Mears et al. *(2018)*. These experiments were performed by Dr Trevor Sweeney.

A. Toeprinting analysis of the interaction of IFIT1 and IFIT1-containing complexes with cap0 RNA. The full length and 7 nucleotide (nt) truncated cDNA product produced by IFIT1 binding are indicated. Protein complexes and RNAs are the same as those used in Figure 3. **B,C.** Graphs represent fraction of RNA bound by IFIT1 and IFIT1-containing complexes at varying IFIT1 concentrations, representative of three separate experiments. $K_{1/2,app}$ and Hill coefficients (*h*) are listed in Table 3-2.

APPENDIX F: STRUCTURAL MODELS OF RODENT IFIT PROTEINS.

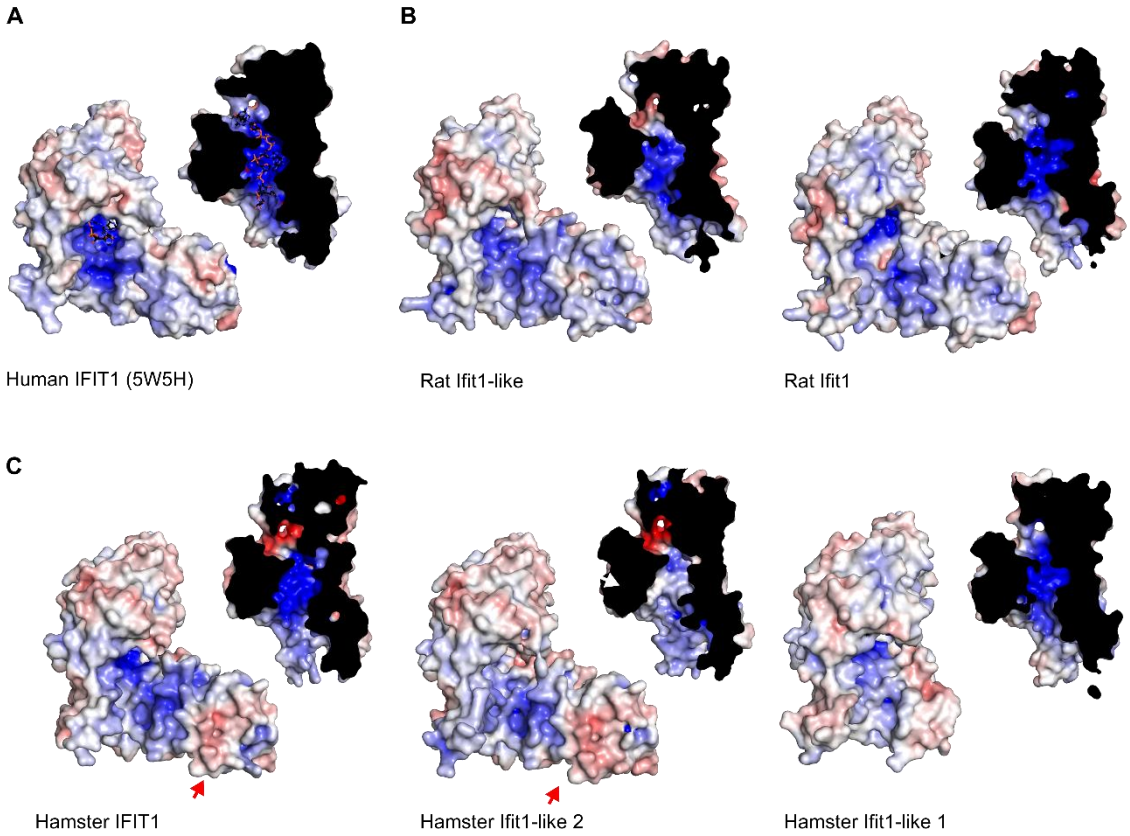

Structural models of **B.** rat and **C.** hamster Ifit1b-like proteins, based on **A.** the X-ray crystal structure of human IFIT1 (PDB: 5W5H). Models are coloured by surface electrostatic potential from negative (-10 kTe^{-1}; red) to positive (+10 kTe^{-1}; blue), via white (hydrophobic), generated in APBS using PDB2PQR *(Dolinsky et al., 2004)*. Red and white arrows indicate acidic and hydrophobic patches, respectively, which could interfere with RNA binding.

APPENDIX G: LOCALISATION OF IFIT COMPLEXES IN MURINE CELLS.

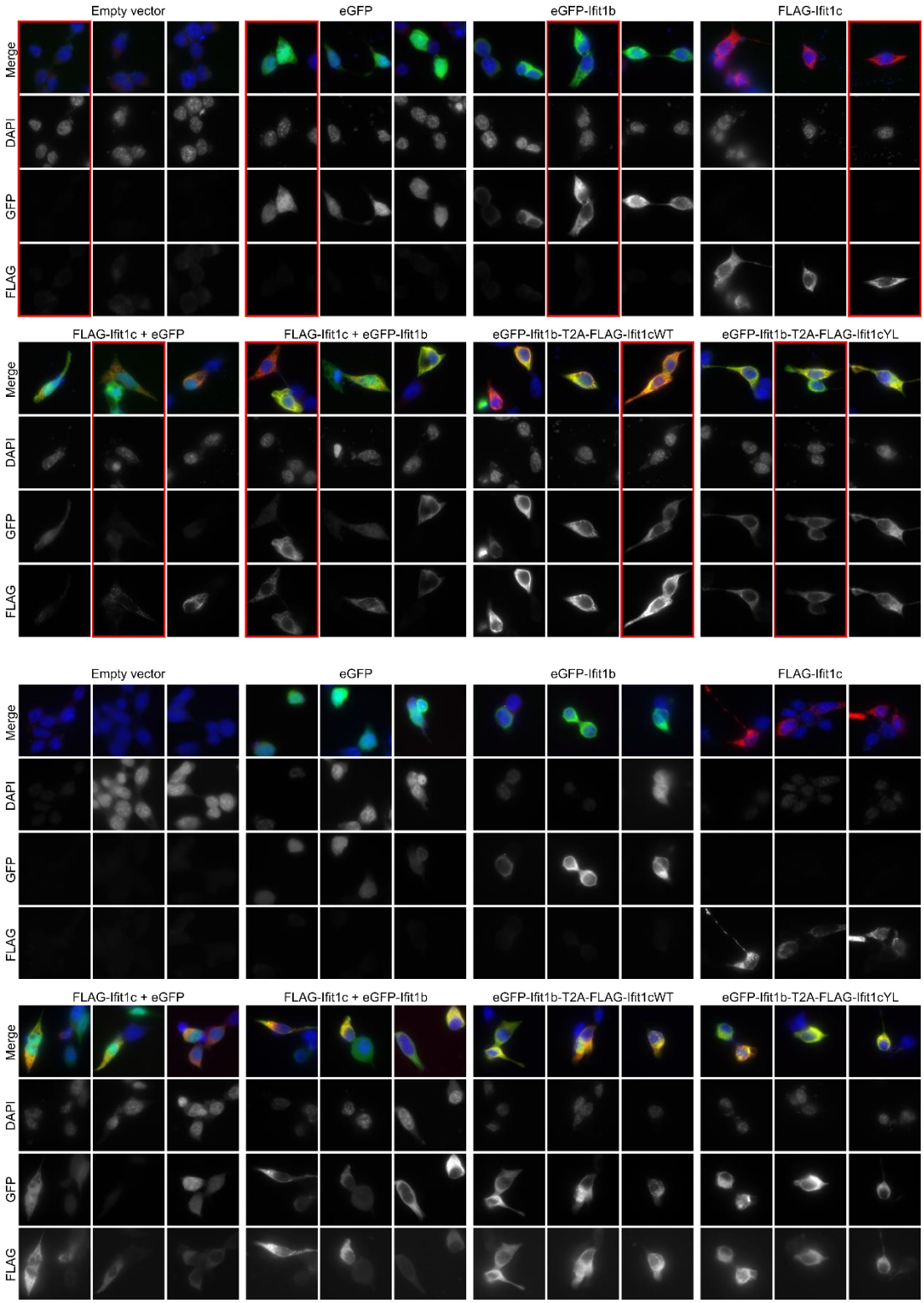

A-B. Immunofluorescence microscopy showing three fields of view each from two independent experiments (**A** and **B**), of murine l7C1 cells transfected with Ifit1b expression plasmids, with or without coexpression of Ifit1c, after 24 hours. T2A, thosea asigna virus 2A stop-go sequence. WT, wildtype. YL, Y456E/L460E mutant Ifit1c. Asterisks indicate where expression plasmids were cotransfected, while daggers show where proteins were co-expressed from a single transfected plasmid. Panels used in Figure 6-6 are boxed in red.

APPENDIX H: HUMAN IFIT PROTEINS REGULATE INNATE IMMUNE SIGNALLING.

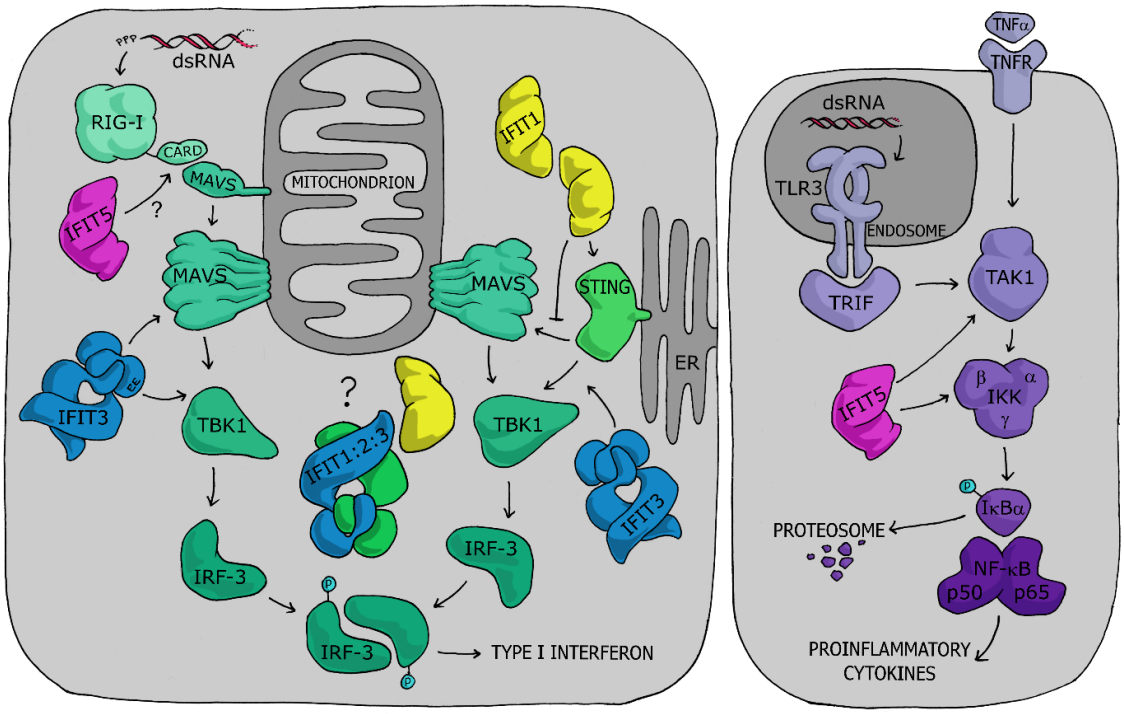

From Mears and Sweeney *(2018)*.

Schematic showing the pathways that IFIT family members modulate during innate immune signalling. The question mark highlights the unknown role of the entire IFIT1:IFIT2:IFIT3 complex in this process, compared to individual components.

APPENDIX I: HUMAN IFIT2 AND IFIT3 MODULATE APOPTOSIS AND CELL PROLIFERATION.

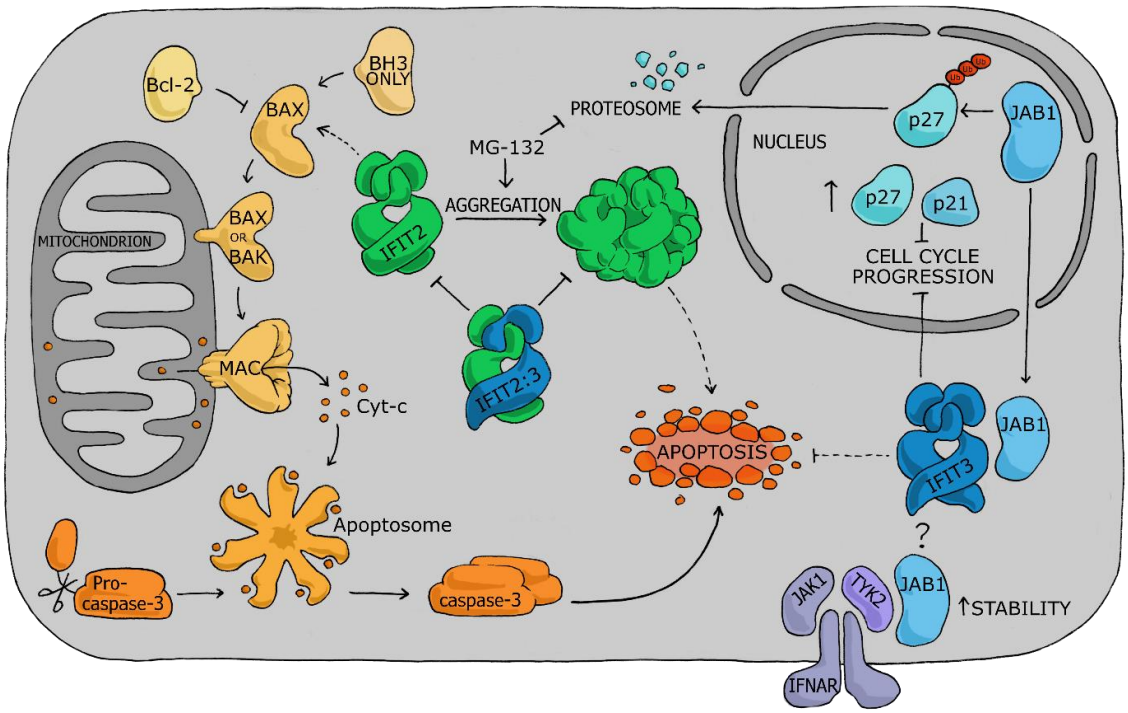

From Mears and Sweeney *(2018)*.

IFIT2 and IFIT3 modulate apoptosis and cell proliferation. Schematic showing the pathways with which IFIT2 and IFIT3 interact to modulate apoptosis and cell cycle progression. 1-3

APPENDIX J: MURINE IFIT1 DECREASES MURINE NOROVIRUS REPLICATION IN RAW264.7 CELLS.

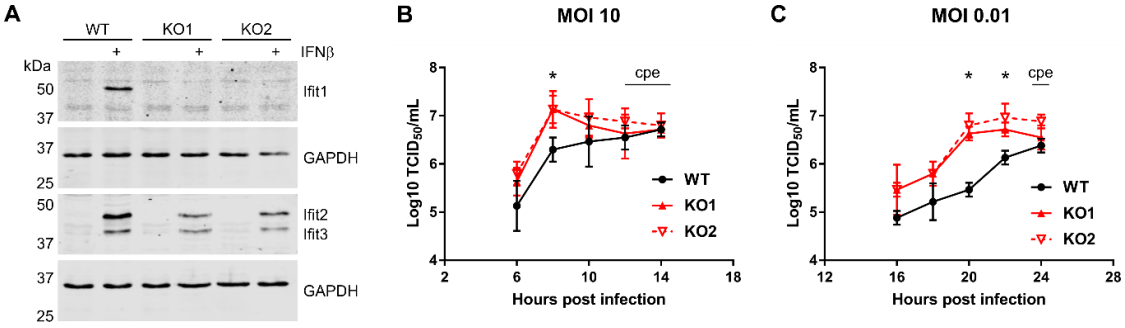

From Mears et al. *(2019)*.

A. Ifit1 knockout RAW264.7 cells were generated by CRISPR-Cas9 gene editing by Dr Edward Emmott. Cells were stimulated with IFNβ for 12 hours then analysed by western blotting against Ifit1 and Ifit2/Ifit3. GAPDH was included as a loading control for each membrane. **B,C.** Infection of wild-type (WT) and Ifit1 knockout (KO) RAW264.7 cells at (**B**) high or (**C**) low multiplicity of infection (MOI) with murine norovirus (MNV-1). Viral titres were determined by 50% tissue culture infectious dose ($TCID_{50}$) in BV2 cells and expressed as log10-transformed values. At late time points, indicated, severe cytopathic effect (cpe) was visible. Graphs show the mean and the standard error of three biological replicates. Titres were compared between WT and KO cells for each time point by two-tailed Student's t-test. Asterisks indicate that a statistically significant difference ($p < 0.05$) was observed for both KO cell lines.

APPENDIX K: MURINE IFIT1 PROMOTES TYPE I IFN EXPRESSION AFTER CYTOPLASMIC RNA SENSING.

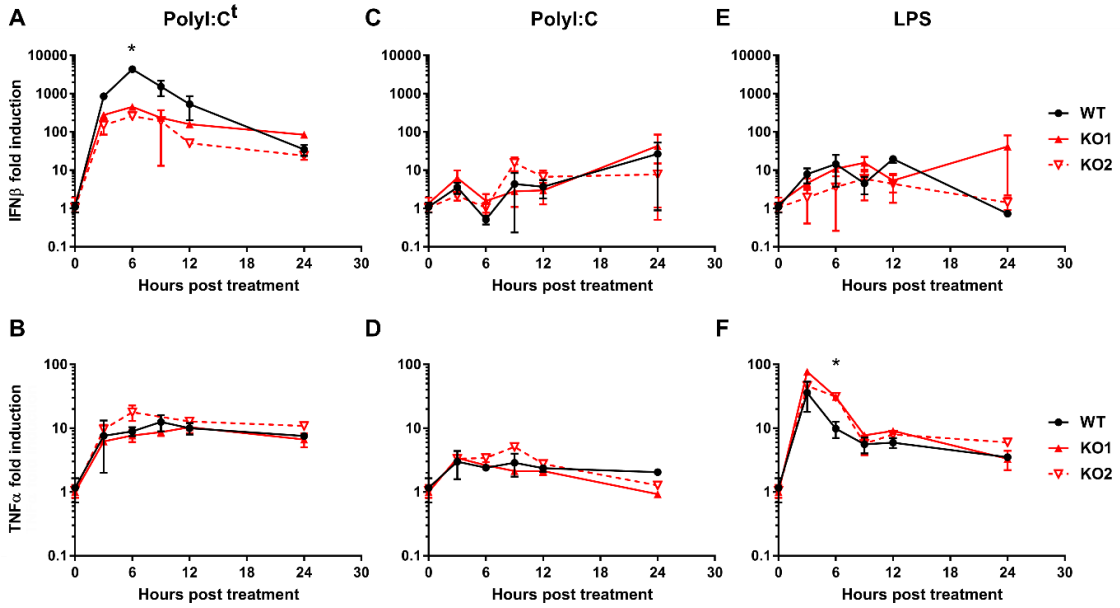

From Mears et al. *(2019)*.

A–F. Wild-type (WT) and Ifit1 knockout (KO) RAW264.7 cells were stimulated with (**A,B**) 2 µg transfected polyI:C (polyI:C^t), or treated with (**C,D**) 1 µg/mL polyI:C or (**E,F**) 10 ng/mL lipopolysaccharide (LPS) in the cell culture medium. RNA was extracted and analysed by RT-qPCR for IFNβ (**A,C,E**) and TNFα (**B,D,F**) mRNA, expressed as fold induction over untreated cells, normalised against GAPDH ($2^{-\Delta\Delta Cq}$). Graphs show the mean and the standard error of three biological replicates. Fold induction was compared between WT and KO cells for each time point by two-tailed Student's t-test. Asterisks indicate that a statistically significant difference ($p < 0.05$) was observed for both KO cell lines.